Lateglacial and early holocene environmental changes along the Northwest European continental margin

Patricia Helen Ranner

Lateglacial and Early Holocene Environmental Changes along the Northwest European Continental Margin

By

Patricia Helen Ranner B.Sc.

Department of Biological and Biomedical Sciences

University of Durham

2005

This Thesis is submitted in partial fulfilment of the requirements for the degree of Doctor of Philosophy

Declaration

The material contained within this thesis has not previously been submitted for a degree at the University of Durham or any other university. The research reported within this thesis had been conducted by the author unless indicated otherwise.

Acknowledgements

I would like to thank my supervisors Professor Brian Huntley and Dr Judy Allen for their relentless support throughout this project. Their enthusiasm and spirit have prevailed.

Thank you to Scottish Natural Heritage and Mr J Clark, Eriboll Lodge, for permission to core at Lochan An Druim in Spring 1999, and to the coring team B Huntley, J P Huntley, A L Huntley, J R P Huntley, V Kay and J R M Allen.

Thank you also to the Norwegian coring team of 2001, B Huntley, J R M Allen, A J Long, A Dean, D Wisheart.

I feel very priviledged to have been supported on this project by a University of Durham Millenium Studentship, without which this opportunity would not have been possible.

NERC supported the electron microprobe analysis performed at the University of Edinburgh, and I am very grateful for the help and support of Anthony Newton and Peter Hill during my visit to the facility.

Radiocarbon dating was supported using funds from the Royal Society-Wolfson Foundation 'Research Merit Award' held by B Huntley, and NERC (Allocation number 931.0901).

John Corr from Leeds University came up trumps in identifying some Lateglacial 'junk'; thank you for introducing me to dinoflagellate cysts. Thanks also to Jonathan Holmes for help with ostracods, and to Jerry Lloyd for help with foraminifera.

Finally, thank you to my enduring family. To David, for his love, support and sacrifice through these years of research, and to Alison, Michael and Helena who are my inspiration.

This work is dedicated to Peter who leant on the wind....

Contents

List of Abbreviations IX

List of Figures XI

List of Tables XVI

List of Plates XIX

List of Appendices XX

Abstract 1

Chapter 1 Introduction 2

1.1 Introduction 3

1.2 Aims 5

1.3 A Guide to the Thesis 5

Chapter 2 Background to the Study 7

2.1 Introduction 8

2.1.1 The Natural Variability of Climate 8

2.1.2 Quaternary Climate 9

2.2 The Background to the Present Study 10

2.2.1 North Atlantic Deep Water (NADW) 10

2.2.2 The Migrating North Atlantic Polar Front (NAPF) 11

2.2.3 The Gulf Stream 13

2.2.4 Deglaciation and Relative Sea-level History 16

2.3 Developing Palaeoenvironmental Histories 19

2.3.1 Pollen as a Climate Proxy 19

2.3.1.1 Pollen Analysis 19

2.3.2 Developing Chronologies 21

2.3.2.1 Greenland Ice-core Chronology 22

2.3.2.2 Radiocarbon Dating 23

2.3.2.3 Tephrochronology 26

2.3.3	Other Palaeoenvironmental Evidence	28
2.3.4	Making Correlations	30
2.3.4.1	Palynological Profiles	30
2.3.4.2	The Greenland Ice-core Records	31
2.3.4.3	The Marine Sedimentary Record	31
2.3.4.3.1	The Lateglacial and Early Holocene Marine Sedimentary Record in the North Atlantic	33
2.3.4.4	Reconstructing Palaeoenvironments	36
Chapter 3	**The Study Sites**	**38**
3.1	Introduction	39
3.2	Lochan An Druim	40
3.2.1	Location	40
3.2.2	Geology and Vegetation	41
3.2.3	Climate	41
3.2.4	Deglaciation and Relative Sea-level History Summary	43
3.2.5	Tephrochronology	43
3.2.6	Previous Palynological Studies	43
3.3	Nikkupierjav'ri	46
3.3.1	Location	46
3.3.2	Geology and Vegetation	47
3.3.3	Climate	48
3.3.4	Deglaciation and Relative Sea-level History Summary	49
3.3.5	Isolation Basin Characteristics	50
3.3.6	Tephrochronology	50
3.3.7	Previous Palynological Studies	50

Chapter 4 **Methods and Data Analyses** **53**

4.1 Fieldwork 54

4.2 Laboratory Analyses 58

4.2.1 Lithostratigraphy 58

4.2.2 Sub-sampling Methods 58

4.2.3 Analytical Methods 58

4.2.3.1 Estimate of the Organic Content of the Sub-samples 59

4.2.3.2 Preparation of Sub-samples for Radiocarbon Dating 59

4.2.3.3 Pollen Preparation Techniques and Identification 60

4.2.3.4 Cryptotephra Preparation Techniques and Identification 63

4.3 Data Analyses 65

4.3.1 Descriptions of the Pollen Zones 66

4.3.2 Systematic - Quantitative Analyses 67

4.3.3 Land - Sea - Ice Correlations 70

Chapter 5 **72**

The Lateglacial and early Holocene Palaeovegetation and Palaeoenvironment at Lochan An Druim in northwest Scotland

5.1 Results 73

5.1.1 Sediment Stratigraphy 73

5.1.2 Radiocarbon Chronology 75

5.1.3 Tephrochronology 77

5.1.4 The Age-Depth Model 89

5.1.5 Correlation with Greenland Ice Record 92

5.1.6 Pollen Analyses 92

5.1.7 Pollen Influx 94
5.1.8 Descriptions of the Pollen Zones 95
5.1.9 Macrofossil Analyses 95
5.1.10 Systematic - Quantitative Analyses 101
5.1.10.1 Palaeobiome Reconstructions 101
5.1.10.2 Palaeoclimate Reconstructions 105
5.2 The Palaeoenvironment at Lochan An Druim 113

Chapter 6 **123**
The Lateglacial and early Holocene Palaeovegetation and Palaeoenvironment at Nikkupierjav'ri in Northern Finnmark

6.1 Results 124
6.1.1 Sediment Stratigraphy 124
6.1.2 Radiocarbon Chronology 127
6.1.3 Tephrochronology 130
6.1.4 Age-Depth Model 130
6.1.5 Correlations with Greenland Ice Record 133
6.1.6 Pollen Analyses 135
6.1.7 Pollen Influx 136
6.1.8 Descriptions of the Pollen Zones 137
6.1.9 Macrofossil Analyses 137
6.1.10 Systematic - Quantitative Analyses 144
6.1.10.1 Palaeobiome Reconstructions 144
6..1.10.2 Palaeoclimate Reconstructions 145
6.2 The Palaeoenvironment at Nikkupierjav'ri 151

Chapter 7 Synthesis **156**

Appendix I **163**

Appendix II **164**

Appendix III 166

Appendix IV 167

References 168

List of Abbreviations

ka BP	10^3 calendar years before present
^{14} C ka BP	10^3 radiocarbon years before present
BD	Below Datum
BP	Before Present = AD 1950 (calib.)
NADW	North Atlantic Deep Water
NAPF	North Atlantic Polar Front
GTC	Global Thermohaline Circulation
NATC	North Atlantic Thermohaline Circulation
IPCC	Intergovernmental Panel on Climate Change
D/O events	Dansgaard - Oeschger Events
GRIP	Greenland Ice-core Project
GISP2	Greenland Ice Sheet Project 2
NGRIP	North Greenland Ice-core Project
GI	Greenland Interstadial
GS	Greenland Stadial
SST	Sea Surface Temperature
SSS	Sea Surface Salinity
LGM	Last Glacial Maximum
CLIMAP	Climate Long- range Investigation, Mapping And Prediction
SPECMAP	Spectral Mapping
EPILOG	Environmental Processes of the Ice-age: Land, Oceans, Glaciers
BIS	Barents Ice Sheet
BIIS	British and Irish Ice Sheet
SIS	Scandinavian Ice Sheet
RSL	Relative Sea Level
OD	Ordnance Datum
SD	Standard Deviation
SE	Standard Error

Delta R	Marine reservoir Correction
PFT	Plant Functional Type
Polypodiaecae-type	sensu (Moore et al., 1991)
Polypodium spp	sensu (Moore et al., 1991)
Km	Kilometre
m	Metre
IRD	Ice Rafted Debris
WDS	Wavelength Dispersive Spectrometry
BD	Below Datum
LPAZ	Local Pollen Assemblage Zone
GDD5	Growing Degree Days above 5°C
MTCO	Mean Temperature of the Coldest Month
AET/PET	Actual Evapotranspiration / Potential Evapotranspiration
UTM	Universal Transverse Mercator (grid zones)
AP	Arboreal Pollen
NAP	Non Arboreal Pollen
N	Refractive Index
PDB	PeeDee Belemnite
DCA	Detrended Correspondence Analysis
LOI	Loss On Ignition
AMS	Accelerator Mass Spectrometry
TAS	Total Alkali vs. Silica

List of Figures

Figure 1 12

A chart of the North Atlantic showing the position of the NAPF and the limits of winter sea ice during, and immediately prior to the last glacial - interglacial transition (based on Ruddiman and McIntyre (1981) from Lowe and Walker (1997, p351): 1) *ca* 20 -19 ka BP; 2) 19-15.5 ka BP; 3) 15.5-13 ka BP; 4) 13-11.5 ka BP). Thin lines represent the pronounced thermal gradient to the south of the Polar Front; the dashed line marked PIL shows the approximate southern limit of the pack ice at the present day.

Figure 2 15

A: Map of northwest Europe showing the location of the two study sites with respect to the approximate ice fronts for the Weichselian LGM and for the Younger Dryas, for the British and Irish, Scandinavian, and Barents Sea ice sheets. The hatched lines suggest some uncertainty regarding the maximum extent, particularly in northwest Scotland and northern Norway (adapted from Mangerud (1991), Mangerud et al. (1996) and Landvik (1998)). The warm and cold surface currents and the approximate location of the Vøring Plateau are shown. Coring sites for the marine records discussed in the text are indicated.

B: Map of the northwest European continental margin indicating the relative positions of the palynological studies discussed in this study and the locations of the weather stations referenced: 1 The Isle of Skye; 2 The Isle of Mull; 3 The Western Isles; 4 Shetland; 5 Abernethy Forest; 6 Morrone; 7 Lochan An Druim; 8 Rogaland Area; 9 Sunnmøre Area, Kråkenes and Lerstadvatn; 10 Andøya; 11 Lake Ifjord; 12 Nikkupierjav'ri; 13 Østervatnet; 14 The North Timan Ridge; 15 Vadsø weather station; and 16 Stornoway weather station.

Figure 3 23

The solid line shows the $\delta^{18}O$ curve as measured in the GRIP Greenland ice core with the chronology of the Lateglacial following Björck et al. (1998) and the chronozones of Mangerud *et al* (1974) (GI = Greenland Interstadial; GS = Greenland stadial).

Figure 4 40

Location of Lochan An Druim beside Loch Eriboll in northwest Scotland

Figure 5 46

Location of Nikkupierjav'ri on Varangerhalvøya, northern Finnmark, Norway

Figure 6 57

Details of core locations: (A) Lochan An Druim (based on the Ordnance Survey Landranger 9 1:50000 scale); and (B) Nikkupierjav'ri (based on Topografisk Hovedkartserie – M711 1:50000 scale).

Figure 7 63

Illustration of the sampling pattern used to remove sub-samples for cryptotephra analysis.

Figure 8 78

Graph of the number of shards of cryptotephra per drop (tephra float from $5cm^3$ wet sediment in $0.5cm^3$ distilled water).

Figure 9 81

Two examples of major element bi-plots for the micro-tephra horizons S13, S21 and S30, showing the relationship between: a) magnesium and calcium ratios; and b) potassium and total iron ratios.

Figure 10 82

A model based on Le Maitre (1989) using a plot of potassium against silica to characterise the micro-tephra horizons S13, S21 and S30.

Figure 11 84

A ternary diagram of the ratio of calcium oxide (wt %), potassium oxide (wt %) and total iron oxide (wt %), to compare the S21 and S30 horizons with the Vedde Ash and Borrobol Tephras. The fields are defined by data from Tephrabase (http://www.geo.ed.ac.uk/tephraexe/ 19.08.05).

Figure 12 86

A ternary diagram of potassium oxide (wt %), calcium oxide (wt %) and total iron oxide (wt %), comparing data for the three known early Holocene silicic Icelandic tephras with high potassium (Lairg B (Dugmore et al., 1995), Snn (Boygle, 1999) and Hovsdalur (Wastegård, 2002)) with the data for the cryptotephra from horizon S13.

Figure 13 88

A TAS plot showing the geochemical evolutionary trends of three of the most active Icelandic volcanic systems (modelled by Haflidason et al (2000), after Jakobsson (1979) and Oskarsson et al (1985), and the proximity in character of the three tephra horizons S13, S21 and S30.

Figure 14 91

Age-depth model for Lochan An Druim using a third order polynomial (y = 12778.69x3 - 439890.75x2 + 5049058.30x - 19311069.03, R2 = 0.9997507938) for the lower sections (10.84 - 12.07 m) and two linear segments for the uppermost section (10.56 - 10.84 m), with mean sediment accumulation rates for each gradient section.

Figure 15 93

Lochan An Druim: Relative abundance pollen data for the most common taxa, rare taxa mentioned in the text, and totals for monolete and trilete Pteridophyte spores. Taxa are sorted into arboreal pollen taxa, non-arboreal pollen taxa, terrestrial Pteridophytes and obligate aquatics and plotted against age (cal yrs BP). Pollen sums are as follows for selected taxa: Terrestrial Pollen (ΣTP), i.e. Arboreal Pollen minus *Pinus* (AP) plus Non-Arboreal Pollen (NAP); Terrestrial Pollen and Terrestrial Pteridophyte Spores (ΣTP + SPS); Terrestrial Pollen and Aquatic Pollen (including *Sphagnum*) (ΣTP + ΣAP); Terrestrial Pollen and Indeterminable Pollen (ΣTP + ΣIP). The first axis from the DCA analysis of the pollen spectra is plotted with the assigned palaeobiomes developed through the systematic biome analysis (see section 5.1.10.1). The GRIP ice core $\delta^{18}O$ data for the Lateglacial and early Holocene (Dansgaard et al., 1993; Johnsen et al., 1992) are plotted for correlation. LPAZs are indicated.

Figure 16 96

Lochan An Druim: Pollen influx data are displayed for a selection of taxa and plotted against age (cal yrs BP). LPAZs, and lithological units are indicated.

Figure 17 104

Lochan An Druim: Data indicating the presence of macrofossil evidence are plotted against age (cal yrs BP). LPAZs and lithological units are indicated.

Figure 18 106

The first axis of the DCA analysis of the pollen spectra (Eigenvalue 0.83) is plotted with the assigned palaeobiomes developed through the systematic biome analyses and correlated with the curve for the % woody taxa at Lochan An Druim. Both curves are plotted against age (cal yrs BP). LPAZs are indicated.

Figure 19 110

Lochan An Druim: Reconstructed bioclimate variables (indicating the unacceptable standard error values at 95% confidence) based on the 'direct analogue approach' and plotted against an age scale (ka cal BP). A) Chord distance for closest 10, B) MTCO, C) AET/PET, and D) GDD5.

Figure 20 111

A 'map' of the full set of modern analogue locations found in the direct analogue method of palaeoclimate reconstructions for Lochan An Druim (identified by the square symbol).

Figure 21 132

Age-depth model for Nikkupierjav'ri using linear segments, with sediment accumulation rates for each gradient section.

Figure 22 135

Nikkupierjav'ri: Relative abundance pollen data for the most common taxa, rare taxa mentioned in the text, and totals for monolete and trilete Pteridophyte spores. Taxa are sorted into arboreal pollen taxa, non-arboreal pollen taxa, terrestrial Pteridophytes and obligate aquatics and plotted against age (cal yrs BP). Pollen sums are as follows for selected taxa: Terrestrial Pollen (ΣTP), i.e. Arboreal Pollen minus *Pinus* (AP) plus Non-Arboreal Pollen (NAP); Terrestrial Pollen and Terrestrial Pteridophyte Spores (ΣTP + SPS); Terrestrial Pollen and Aquatic Pollen (including *Sphagnum*) (ΣTP + ΣAP); Terrestrial Pollen and Indeterminable Pollen (ΣTP + ΣIP). The first axis from the DCA analysis of the pollen spectra is plotted with the assigned palaeobiomes developed through the systematic biome analysis (see section 6.1.10.1). The GRIP ice core $\delta^{18}O$ data for the Lateglacial and early Holocene (Dansgaard et al., 1993; Johnsen et al., 1992) are plotted for correlation. LPAZs are indicated.

Figure 23 138

Nikkupierjav'ri: Pollen influx data are displayed for a selection of taxa and plotted against age (cal yrs BP). LPAZs and lithological units are indicated.

Figure 24 147

Nikkupierjav'ri: Data indicating the presence of macrofossil evidence are plotted against age (cal yrs BP). LPAZs and lithological units are indicated.

Figure 25 148

The first axis of the DCA analysis of the pollen spectra (Eigenvalue 0.38) is plotted with the assigned palaeobiomes developed through the systematic biome analyses and correlated with the curve for the % woody taxa at Nikkupierjav'ri. Both curves are plotted against age (cal yrs BP). LPAZs are indicated.

List of Tables

Table 1 42

Met Office weather data 1971-2000; monthly averages and annual totals for Stornoway (15 m AMSL) (http://www.metoffice.com, 20 October 2004).

Table 2 68

Assignment of the pollen taxa in this study to plant functional types (PFTs).

Table 3 69

Assignment of plant functional types (PFTs) found in this study, to the appropriate biomes.

Table 4 74

Description of the Lateglacial and early Holocene sediments from Lochan An Druim following Troels-Smith (1955) as proposed by Aaby and Berglund (1986). Four categories of physical qualities are described as follows: nigror (nig.) - the degree of darkness; stratificatio (strf.) - the degree of stratification; elasticitas (elas.) - the degree of elasticity; and siccitas (sicc.) - the degree of dryness.

Table 5 76

Terrestrial macrofossil and bulk sediment sample information, and results of AMS radiocarbon dating calibrated using CALIB 4.4.1(Stuiver and Reimer, 1993) with INTCAL98.14c calibration data set (Stuiver et al., 1998a), information provided after Lowe and Walker (2000).

Table 6 77

Number of shards of cryptotephra per drop (tephra float from 5cm^3 wet sediment in 0.5cm^3 distilled water).

Table 7 79

The major oxide concentrations of individual glass shards in sample S13. All oxides are shown as weight percent, and total iron is expressed as FeO.

Table 8 79

The major oxide concentrations of individual glass shards in sample S21. All oxides are shown as weight percent, and total iron is expressed as FeO.

Table 9 80

The major oxide concentrations of individual glass shards in sample S30. All oxides are shown as weight percent, and total iron is expressed as FeO.

Table 10 87

Summary of cryptotephra samples found at Lochan An Druim and the correlated tephra horizons and absolute dates.

Table 11 108

Table summarising the characteristic taxa for the eleven LPAZs identified at Lochan An Druim, and correlated with the event stratigraphy of the Lateglacial following Björck et al. (1998), and the biozones of Mangerud et al. (1974) together with the palaeobiomes assigned through systematic biome analyses.

Table 12 114

This table summarises the key features resulting from the correlation of the two palynological studies at Lochan An Druim, Birks (1984) and this study, on the basis of matching the common biozones.

Table 13 125

Description of the Lateglacial and early Holocene sediments from Nikkupierjav'ri following Troels-Smith (1955) as proposed by Aaby and Berglund (1986). Four categories of physical qualities are described as follows: nigror (nig.) - the degree of darkness; stratificatio (strf.) - the degree of stratification; elasticitas (elas.) - the degree of elasticity; and siccitas (sicc.) - the degree of dryness.

Table 14 129

Macrofossil sample information and results of AMS radiocarbon dating calibrated using CALIB 4.4.1 (Stuiver and Reimer, 1993); information provided after Lowe and Walker (2000).

Table 15 145

Table summarising the characteristic taxa for the nine LPAZs identified at Nikkupierajav'ri, and correlated with the event stratigraphy of the Lateglacial following Björck et al (1998), and the biozones of Mangerud et al (1974).

Table 16

Table to compare the onset dates (cal yrs BP) of Lateglacial and early Holocene climatic oscillations in the GRIP event stratigraphy and in selected terrestrial and ocean records on a southeast to northwest gradient in the northeast Atlantic region (GRIP ice-core years (Björck et al., 1998); Core 56/10/36 NE Atlantic (Austin and Kroon, 2001; Kroon et al., 1997); Core MD952011 and core HM79-6/4 (Birks and Koc, 2002); Rogaland area (Birks et al., 1994; Paus, 1988; Paus, 1989b; Paus, 1990); Kråkenes (Birks et al., 2000a); Lerstadvatn (Kristiansen et al., 1988); Andøya (Birks et al., 1994);and the North Timman Ridge (European Arctic Russia) (Paus et al., 2003)). The dates in italics indicate that the chronlologies at these points are not independent and therefore cannot be use to evaluate leads or lags in response time.

List of Plates

Plate 1 48

Arctic-alpine tundra at 80m asl above Nikkupierjav'ri: *Empetrum* heath with *Betula pubescens* subsp. *tortuosa*, *Betula nana*, *Salix herbacea* and *Juniperus communis* (courtesy Dr JRM Allen).

Plate 2 50

2km north west of Nikkupierjav'ri in April 2002 looking north west over the inlet of Straumen with the snow clearly picking out a section of the Outer Porsanger marginal moraine where it crosses and almost encloses the inlet.

Plate 3 55

Coring Lochan An Druim March 1999 (taken looking due west) (Courtesy Alex Huntley).

Plate 4 55

Coring in Finnmark April 2001.

List of Appendices

Appendix I

A new early Holocene cryptotephra from northwest Scotland

Patricia H Ranner, Judy R M Allen and Brian Huntley

Appendix II

Data tables for analyses at Lochan An Druim and Nikkupierjav'ri

Appendix III

Lochan An Druim: Relative abundance pollen data for all the taxa, and totals for monolete and trilete Pteridophyte spores. Taxa are sorted into arboreal pollen taxa, non-arboreal pollen taxa, terrestrial Pteridophytes and obligate aquatics and plotted against age (cal yrs BP). Pollen sums are as follows for selected taxa: Terrestrial Pollen (ΣTP), i.e. Arboreal Pollen minus *Pinus* (AP) plus Non-Arboreal Pollen (NAP); Terrestrial Pollen and Terrestrial Pteridophyte Spores (ΣTP + SPS); Terrestrial Pollen and Aquatic Pollen (including *Sphagnum*) (ΣTP + ΣAP); Terrestrial Pollen and Indeterminable Pollen (ΣTP + ΣIP).

Appendix IV

Nikupierajav'ri: Relative abundance pollen data for all the taxa, and totals for monolete and trilete Pteridophyte spores. Taxa are sorted into arboreal pollen taxa, non-arboreal pollen taxa, terrestrial Pteridophytes and obligate aquatics and plotted against age (cal yrs BP). Pollen sums are as follows for selected taxa: Terrestrial Pollen (ΣTP), i.e. Arboreal Pollen minus *Pinus* (AP) plus Non-Arboreal Pollen (NAP); Terrestrial Pollen and Terrestrial Pteridophyte Spores (ΣTP + SPS); Terrestrial Pollen and Aquatic Pollen (including *Sphagnum*) (ΣTP + ΣAP); Terrestrial Pollen and Indeterminable Pollen (ΣTP + ΣIP).

Abstract

Palynological studies from two lacustrine sites, Lochan An Druim in northern Scotland and Nikkupierjav'ri in northern Finnmark, have demonstrated quantitative changes in the vegetation of the northwest European continental margin, following deglaciation (*ca* 16.0 - 7.5 ka BP), and these changes have been correlated with the short term fluctuations and rapid changes in climate as recorded in the GRIP ice-core record. It has been shown that the palaeovegetation profiles from these sites, near to the potential extremities of northward penetration of warm ocean surface water during this time have recorded some of these events differentially, indicating a northward lag in response to Holocene warming that is not temporally consistent, and this has been attributed to the relative proximity of the North Atlantic Polar Front. In addition, evidence is presented for a previously unrecorded early Holocene Icelandic cryptotephra from Lochan An Druim, together with evidence in support of a 'Younger Borrobol' cryptotephra from Lateglacial sediments of Allerød age at the same location.

Chapter 1

Introduction

1.1 Introduction

1.2 Aims

1.3 A Guide to the Thesis

1.1 Introduction

One of the current foci of Quaternary research is the study of the rates and magnitudes of past rapid climate changes. Information about the systems involved, and their leads and lags, are pertinent to a better understanding of the potential mechanisms and impacts of impending anthropogenic climate changes. Key information can be obtained from palaeoecological studies of periods marked by series of such changes, and targeted in regions potentially sensitive to such changes. In particular, palaeoclimate studies that focus on the transition from the last glacial period, the Weichselian, to the present interglacial period, the Holocene, have become a central theme in this research, because this particular period has been shown to have encompassed rapid climatic shifts of interstadial / stadial amplitude (e.g. Dansgaard et al., 1993; Johnsen et al., 1992).

Across the terrestrial, oceanic and ice realms, this period provides many archives of natural climate proxies that reflect the temporal and spatial nature of these changes, and which can be used for developing models of climate change, thus furthering our understanding of the complex dynamics of the natural and anthropogenic drivers of such changes. Climate models require syntheses of palaeodata derived from these various sources and correlated across the realms. These correlations require a high-resolution climate proxy that is sensitive to change, supported by a dating framework that is robust enough to enable time-stratigraphic correlation, and thus capable of delivering reliable, quantified time-series of climatic information. According to Walker (2001) biological evidence is the single most reliable source of such information spanning this period. In this study high temporal resolution pollen data have been used to develop a terrestrial climate signal from the Lateglacial and early Holocene period. This is underpinned by the most robust dating framework available, in order to provide time-stratigraphic correlation with ice-core and marine records.

Two palynological records have come from study sites that were chosen at extreme locations along the northwest European continental margin, which lies adjacent to the northeast Atlantic, and the Norwegian, Greenland and Barents Seas. Both coastal and inland areas of this margin have a maritime climate, influenced by changes in the circulation and temperature of the North Atlantic Ocean (Koç et al., 1993; Ruddiman and McIntyre, 1981). The limits of this seaboard lie close to the northeasternmost and southwesternmost extent of the influences of the warm North Atlantic surface currents during the last deglaciation, and were, therefore, potentially very sensitive to the climatic fluctuations that have been recorded in that area at that time (Johnsen et al., 1992; Lehman and Keigwin, 1992; Taylor et al., 1993).

Independent chronologies to support the palynological profiles have been developed from AMS radiocarbon dating of terrestrial and marine macrofossils, and from the positive identification of two known cryptotephra horizons from Lateglacial stratigraphies. As a result of the tephrochronological analyses a previously unrecorded early Holocene Icelandic cryptotephra has been identified and dated, and in addition, evidence is presented in support of a 'Younger Borrobol' cryptotephra' from Lateglacial sediments of Allerød age (see Appendix I).

The palaeoenvironments at each study site have been inferred from the vegetational histories developed through qualitative and quantitative analysis of the pollen data, and these have been discussed in relation to other studies in these areas. The development of individual chronologies has enabled time-stratigraphic correlation between the two palynological sequences and with the marine and ice realms. The GRIP oxygen isotope signal ($\delta^{18}O$) (Dansgaard et al., 1993; Johnsen et al., 1992), recommended by the INTIMATE group as a type profile for this period (Björck et al., 1998; Walker et al., 1999), has provided some key links. The Lateglacial marine record of sea surface temperatures (SSTs) in the northeast Atlantic, estimated from changes in the composition of planktonic foraminiferal assemblages (Kroon et al., 1997) has provided a useful correlation in the south of the study area, and the diatom records from the eastern Norwegian sea (Birks and Koç, 2002; Koç et al., 1993) have been correlated during the Younger Dryas and early Holocene in the north of the study area.

Finally, a synthesis of the palaeoenvironment along this northwest European continental margin has been developed and discussed by comparing the nature and timing of vegetational development at the two sites. There is a similarity in the flora of the two areas but notable differences in levels of development and the timing of major changes. These have been discussed in the light of the profound influence on regional climate by fluctuations in the North Atlantic Ocean circulation at that time.

1.2 Aims

The principal objective of this study is to test the following two hypotheses:

1. That, following deglaciation, northwest European vegetation exhibited quantitative changes, related to short-term fluctuations and rapid changes in climate as recorded in the GRIP ice core record; and
2. That palaeovegetation profiles from sites near the potential extremities of northward penetration of the warm ocean surface water will record these events differentially.

In order to undertake this test, the following aims have been addressed:

- to describe the Lateglacial palaeoenvironmental history at Lochan An Druim in northern Scotland;
- to describe the Lateglacial palaeoenvironmental history at Nikkupierjav'ri in northern Finnmark;
- to investigate the potential for cryptotephras in the tephrochronology of the two study areas.

1.3 A Guide to the Thesis

Chapter 1 introduces the thesis in its immediate context and briefly justifies the selected time period, the regional choice of study sites and the chosen climate proxy. The broad aims of the study are set out, and finally a guide to the thesis is provided.

Chapter 2 of this thesis sets out a broad background to the study. The concept of natural climate variability, and the topical issue of 'climate change', are introduced. The complex ocean-atmosphere interactions in the North Atlantic provide a backdrop to this study, and a variety of dynamic systems is described that serve to influence the climate, and hence the vegetation, of the study areas. A useful study requires testable hypotheses, using a suitable proxy and the development of a robust and independent chronology. The choice of pollen as a climate proxy and the use of radiocarbon and tephrochronological techniques to develop a chronology are outlined. The palynological study is described in general terms and the methods of data analysis such as palaeoclimate reconstructions and correlation are introduced.

Chapter 3 presents the two study sites: Lochan An Druim in northern Scotland and Nikkupierjav'ri in northern Finnmark. Locations are detailed with descriptions of the geology, vegetation and climate, and local deglaciation and relative sea-level histories are discussed. Previous work in the two areas in relation to palynological and tephrochronological studies is documented.

Chapter 4 describes the fieldwork undertaken and the methods used in the laboratory analyses, and subsequent data analyses.

Chapters 5 and 6 present the results for Lochan An Druim and Nikkupierjav'ri respectively, with a discussion of the Lateglacial and early Holocene palaeoenvironment at each site in relation to other such studies in those areas.

The discussion in Chapter 7 provides a palaeoenvironmental synthesis for climate changes on the northwest European continental margin during the Lateglacial and early Holocene, in the context of the two hypotheses that have been tested.

Chapter 2

Background to the Study

2.1 Introduction

2.1.1 The Natural Variability of Climate

2.1.2 Quaternary Climate

2.2 The Background to the Present Study

2.2.1 North Atlantic Deep Water

2.2.2 The Migrating North Atlantic Polar Front

2.2.3 The Gulf Stream

2.2.4 Deglaciation and Relative Sea-level History

2.3 Developing Palaeoenvironmental Histories

2.3.1 Pollen as a Climate Proxy

2.3.1.1 Pollen Analysis

2.3.2 Developing Chronologies

2.3.2.1 Greenland Ice-core Chronology

2.3.2.2 Radiocarbon Dating

2.3.2.3 Tephrochronology

2.3.3 Other Palaeoenvironmental Evidence

2.3.4 Making Correlations

2.3.4.1 Palynological Profiles

2.3.4.2 The Greenland Ice-core Records

2.3.4.3 The Marine Sedimentary Record

2.3.4.3.1 The Lateglacial and Early Holocene Marine Sedimentary Record in the North Atlantic

2.3.4.4 Reconstructing Palaeoenvironments

2.1 Introduction

Popular interest in the functioning of the Earth's climate system has developed from sound scientific evidence that climate is changing; air temperatures have increased substantially in the last 100 years (e.g. Mann et al., 1998). Recognising the problem of potential global climate change, the World Meteorological Organisation and the United Nations Environment Programme established the Intergovernmental Panel on Climate Change (IPCC) in 1988. The role of the IPCC is to assess, on a comprehensive, objective, open and transparent basis, the scientific, technical and socio-economic information relevant to understanding the of risk of human-induced climate change, its potential impacts, and options for adaptation and mitigation (Houghton et al., 2001). However, palaeoclimatic data document a sensitive climate system subject to large, and perhaps unpredictable, abrupt changes, and these data suggest that neither the sensitivity nor the variability of the climate are fully captured in some climate change projections. Athropogenic influences on this system cannot as yet be qualified nor quantified until separated from the effects of natural variability, which needs to be defined and understood. Hindcasting, by means of palaeoclimatic studies, is therefore an imperative if we are to gain a better understanding of this background of natural variability, which is essential if we wish to detect and predict the climatic consequences of human activity.

2.1.1 The Natural Variability of Climate

Climate has an intrinsic natural variability. The Earth's internal system is complex, made up of components, including the hydrosphere, atmosphere, cryosphere and biosphere, which can influence regional and global climate each with its own response time and thermodynamic properties. These components have non-linear relationships, which are further complicated by their interacting with other complex systems such as the carbon-cycle. Climate can also be affected by external forcing mechanisms, principally the operation of the astronomical variables, and the influence of feedbacks (the amplification or modulation of one process by another). e.g. changes in snow albedo (a measure of the reflectivity of snow), affect the snow-temperature feedback, whereby the initial melting of a snow covered area causes a decrease in albedo and hence more sunlight is absorbed, thus raising the temperature and amplifying the snow melt. The converse of this is also true with the formation of snow promoting a cooling cycle.

The search for the causal mechanisms that initiate such changes began with Croll in 1875 proposing his 'Astronomical Theory', which was subsequently developed by Milankovitch in 1930 who suggested a process of climate control by insolation, due to

changes in the geometry of the Earth's orbit. Today, climatic variability is studied theoretically through the development of general circulation models which in their most complex form are 'coupled atmosphere-ocean general circulation models'. For example, according to Alley (2003), this type of model has been able to link the abrupt climate changes of the Lateglacial period to changing North Atlantic freshwater fluxes.

2.1.2 Quaternary Climate

The Quaternary (*ca* the last 2.6 million years) appears to be a period of major environmental changes as compared to any other time during the Cenozoic era of the last 65 million years. It is characterised by periodic glacier activity with the development of major continental ice sheets, and the expansion of mountain glaciers. This glacial condition has been interrupted periodically by warm interglacials, and in the mid- and high-latitudes, temperatures have sometimes been higher that those of the present day. The glacial - interglacial cycles have been further sub-divided into stadial and interstadial episodes of shorter duration and less extreme temperature shifts. Climatic oscillations therefore, are not in themselves unusual, since there may have been as many as 50 cold / temperate cycles during the Quaternary (Patience and Kroon, 1991; Ruddiman et al., 1989).

There are two types of natural and abrupt climate change that have been identified during the last glacial (60 - 10 ka), and these are known as the Dansgaard - Oeschger temperature oscillations, (D/O events) (Dansgaard et al., 1993), and the Heinrich ice-rafting events (e.g. Bond and Lotti, 1995; Heinrich, 1988). D/O events have a proposed cyclicity of *ca* 1,500 years (Alley et al., 2001) and they are centred on the North Atlantic, but can affect other regions that have an atmospheric response to changes in that area. They typically start with an abrupt warming of Greenland by 5 -10°C over a few decades or less, and are then followed by a gradual cooling lasting no more than 500-2000 years, and often ending in an abrupt return to stadial conditions (Ganopolski and Rahmstorf, 2001). Heinrich ice-rafting events are associated with major ice sheet breakouts in the North Atlantic (Sarnthein et al., 2002), and they have a variable millennial cyclicity, occuring in the stadial phase of some D/O cycles (Ganopolski and Rahmstorf, 2001). The most recent of these events 'Heinrich 1' is recorded as reaching its maximum extent at *ca* 14 ^{14}C kyr BP (*ca* 16.7 ka BP) just predating period of this study (Bond et al., 1993; McCabe et al., 1998). In addition, the Younger Dryas has sometimes been dubbed 'Heinrich 0' (e.g., Andrews, 2000; Clark et al., 2002).

The late Quaternary climate is now known to have been highly unstable and prone to major, rapid changes, that occurred within periods of a few decades or less. The history of these millennial to decadal scale climate changes is documented in the

fluctuations in $\delta^{18}O$ record in the Greenland ice sheet (Dansgaard et al., 1993; Grootes et al., 1993; North Greenland Ice Core Project members, 2004).

2.2 The Background to the Present Study

The complex ocean-atmosphere interactions in the North Atlantic are manifest in a variety of dynamic (and non-linear) systems that serve to influence the continental-margin climate in the region, and hence the development of different vegetational communities. Principally, the North Atlantic serves as a major contributor to deep-water formation in the world ocean. This North Atlantic Deep Water flux is part of a wider convection system known as the Global Thermohaline Circulation (GTC) that connects the world's ocean basins. The sensitivity of this 'conveyor' has important implications for global heat transfer, and its function has a direct effect on the position of the North Atlantic Polar Front and hence on the degree of northward penetration of the warm waters from the Gulf Stream. For example, data from marine sediment cores suggest that the changes in temperature and salinity caused by the meltwater pulses associated with Heinrich events can shut down or drastically reduce the formation of North Atlantic Deep Water (Broecker, 1992; Elliot et al., 2002; Sarnthein et al., 1994) and hence alter the path of the GTC in the North Atlantic.

These interdependent systems ultimately influence the phases of glaciation and deglaciation in the region, and hence impact on the relative sea-level history of this continental margin.

2.2.1 North Atlantic Deep Water

Within the North Atlantic basin at the present time, warm surface waters with a relatively high salinity (developed in the warmer conditions of the lower latitudes where evaporation is greater) move northward to around latitude 60°N, where the combinations of salinity and colder temperatures cause an increase in the density of the waters and they sink to form a cold salt-rich deep-water mass, North Atlantic Deep Water (NADW). This cold saline current is then returned to the southern oceans, via the global conveyor system. As a consequence of this sinking action, 'ventilation' of these higher latitude oceanic waters takes place, providing the driving force for the global conveyor and releasing heat to the overlying air masses that tend to move eastward towards northern Europe.

In the North Atlantic the impact of NADW formation on the climate is considerable, due to the release of heat to the atmosphere. The current release of heat energy has been calculated as equivalent to approximately 25 per cent of the solar heat reaching the surface of the Atlantic Ocean in the region north of 35°N (Broecker and Denton, 1990).

It follows that any variation in NADW production would significantly affect spatial patterns of heat release, and could therefore be responsible for generating regional climate changes. Past changes in the production and circulation of NADW have been inferred from $\delta^{13}C$ records in benthic foraminifera (a proxy for deep-water ventilation). Using these data, Sarnthein (1994) and Elliot (2002) have suggested that the changes in temperature and salinity caused by major meltwater pulses (e.g. those associated with Henirich Events, and anomalous meltwater events related to the draining of large glacial lakes) can shut down or drastically reduce the formation of NADW, and hence alter the path and/or intensity of the North Atlantic Thermohaline Circulation (NATC), thus reducing heat transfer to the northern hemisphere. Additional evidence in the form of the atmospheric ^{14}C record during the Lateglacial / early Holocene, shows sharp increases simultaneous with cold oscillations (Björck et al., 1996). These have usually been explained as the effect of reduced oceanic CO_2 ventilation following freshwater forcing of the NATC, thus suggesting that stagnation in the NATC is the cause of both climate change and increasing atmospheric ^{14}C (van Geel et al., 2003). An alternative hypothesis suggests that these fluctuations in ^{14}C are caused by changes in solar activity and therefore are not in the first instance the effect of climate change but reflect the triggering factor i.e. changes in solar activity (van Geel et al., 2003).

2.2.2 The Migrating North Atlantic Polar Front

The North Atlantic Polar Front (NAPF) is a prominent hydrographic/oceanographic boundary which separates the warm water of high salinity flowing northwards, from the cold low salinity water flowing from the Arctic (Lowe and Walker, 1997, p 236). It is a mobile boundary the position of which is dictated by the complex interaction of the extension of sea-ice and the extent of northward penetration of warm surface waters associated with the NATC. The position of this boundary has a significant effect on climate, since weather systems tend to be entrained along its southern flank.

The resulting climatic history of the North Atlantic during the last glacial - interglacial transition has been demonstrated primarily through the Ruddiman and McIntyre model of movements of the NAPF. Marine records of planktonic foraminiferal assemblages, and carbonate productivity by coccoliths and foraminifera, are used to infer the sequence of events of the movement of the front during this transition (Ruddiman and McIntyre, 1981). At the last glacial maximum the southerly limit of the NAPF lay close to Lisbon on its eastern flank (see Figure 1 position 1). Following initial warming, the front moved north to a position at the latitude of northern Portugal (see Figure 1 position 2). During the rapid climatic amelioration of the Lateglacial Interstadial the eastern flank of the NAPF shifted northward such that the front eventually lay north of Iceland (see Figure 1 position 3). However, a southward migration of this eastern flank

then followed, during the cooling of the Younger Dryas stadial, with the front returning to a position just north of its southerly limit (see Figure 1 position 4). The further climatic amelioration during the Holocene instigated a subsequent shift north with the front assuming its northern, interglacial position, which is characteristic of current ocean circulation patterns (see Figure 1 the dashed line indicating the approximate limit of the pack ice at the present day).

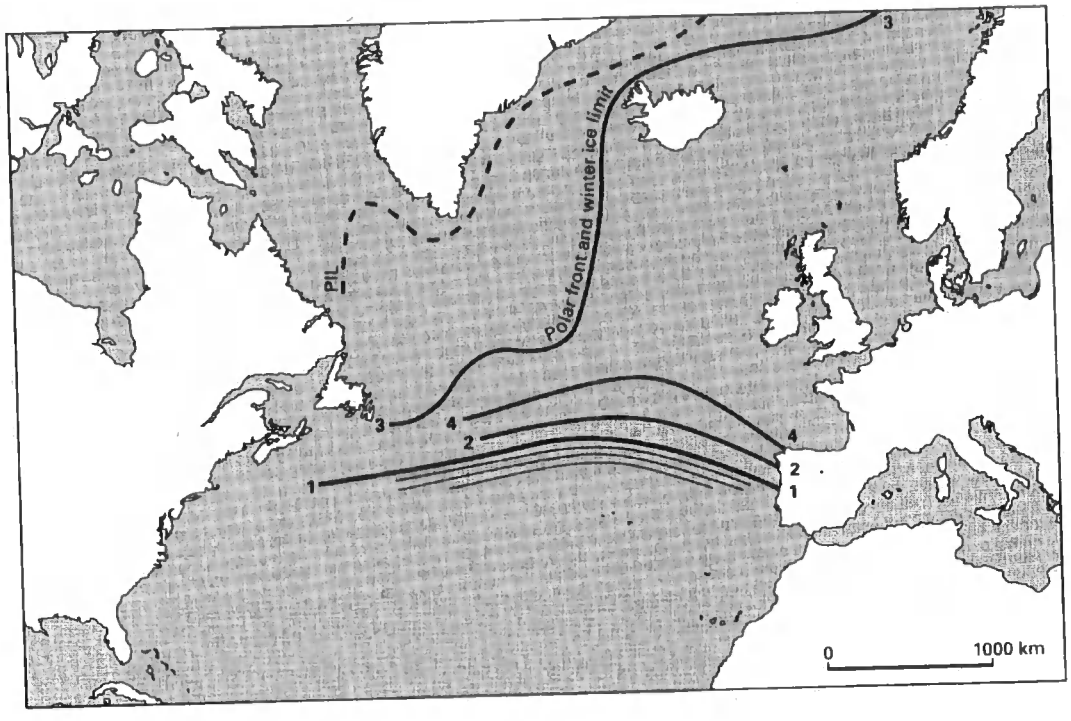

Figure 1

A chart of the North Atlantic showing the position of the NAPF and the limits of winter sea ice during, and immediately prior to the last glacial - interglacial transition (based on Ruddiman and McIntyre (1981) from Lowe and Walker (1997, p351): 1) *ca* 20 -19 ka BP; 2) 19-15.5 ka BP; 3) 15.5-13 ka BP; 4) 13-11.5 ka BP. Thin lines represent the pronounced thermal gradient to the south of the Polar Front; the dashed line marked PIL shows the approximate southern limit of the pack ice at the present day.

The data suggest a greater arc of north-south movement of the eastern flank compared to the western flank, and these movements are associated with the complex and abrupt climate changes indicated in some terrestrial records from the northwest continental margin (e.g. Alm, 1993; Birks, 1984)). The rate and magnitude of these oceanic changes have been reconstructed by Ruddiman et al. (1977) and suggest rates of atmospheric cooling or warming of 1-5°C ka^{-1}, with sea-surface temperature changes of 7-11°C, over distances ranging from 200-1,600 m yr^{-1}. These estimates of very rapid movements of the NAPF have been confirmed by Bard et al. (1987), who suggested that the first northward retreat (see Figure 1 position 3), between latitudes 35°N and

55°N (approx. 2,000 km) occurred at a rate of > 2 km yr^{-1}, and inferred even more rapid southerly movements of > 5 km yr^{-1} during the Younger Dryas event.

2.2.3 The Gulf Stream

Regional climate is intimately linked to ocean circulation, as is evident in the nature of the current mild maritime climate of Western Europe which contrasts with the more severe climate of comparable latitudes in North America. This amelioration of the climate can be attributed to a north-eastwards transfer of heat to Western Europe via the Gulf Stream. This warm current originates off the North American coast and flows northeast becoming the North Atlantic Current at about 40°N and 50°W. This then divides, such that the north-easterly flow passes between Scotland and Iceland, becoming the Norwegian Current (see Figure 2).

A major climatic influence therefore, in this eastern sector of the North Atlantic, would have been shifts in the path of the Norwegian Current (Lowe et al., 1994), which is able to flow round the British Isles and into the Norwegian sea when the NAPF lies towards its northern limit. However, with a southward migration of the NAPF, warm waters would not reach the northwest European continental margin. Research by Koç et al. (1993) into diatom assemblages from North Atlantic sediment cores, has shown that these organisms formed unique groups which reflect the significant changes in the climate boundary conditions during the transition from Lateglacial to early Holocene in that region. The study indicates that during deglaciation, in spite of increasing solar radiation, the Greenland, Norwegian and Barents seas were still extensively covered by sea-ice. However, a sea-ice-free corridor extending northward had opened along the Norwegian coast by *ca* 16.0 ka BP. This suggests a significant incursion by the warm Norwegian Coastal Current, and it is proposed that this rise in sea surface temperatures promoted the comparatively early deglaciation of the northwest European continental margin. The position and timing of this Lateglacial ice-free passage, and of the development of the following Holocene oceanic circulation, have been further constrained by analyses of additional diatom records from the Vøring Plateau (see Figure 2) which is located in a sensitive position with respect to these changes (Birks and Koc, 2002).

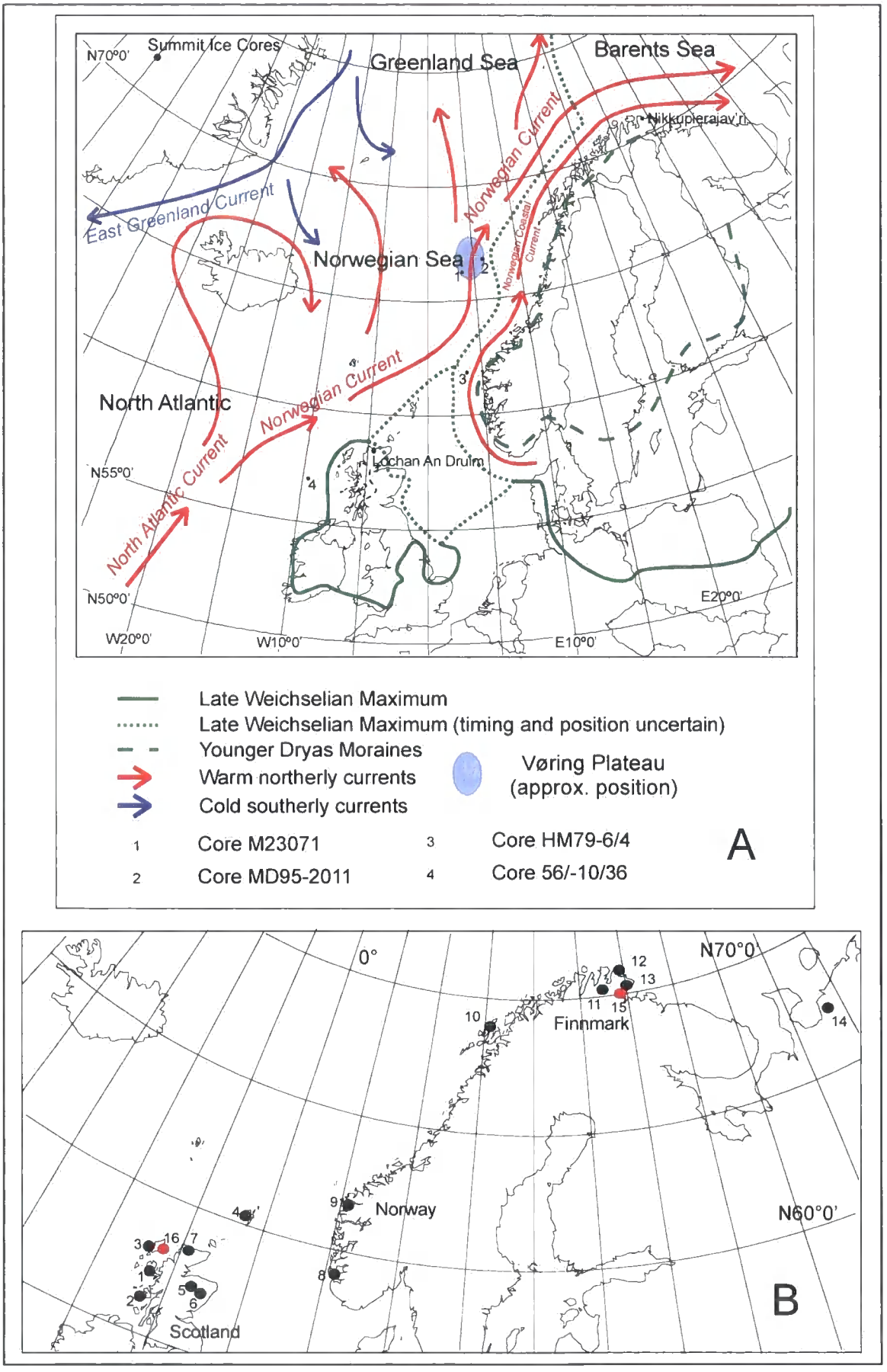
N70°0'
Summit Ice Cores
Greenland Sea
Barents Sea
Nikkuperajav'ri
East Greenland Current
Norwegian Sea
Norwegian Current
Norwegian Coastal Current
North Atlantic
Norwegian Current
North Atlantic Current
Lochan An Druim
N55°0'
N50°0'
W20°0'
W10°0'
E10°0'
E20°0'
Late Weichselian Maximum
Late Weichselian Maximum (timing and position uncertain)
Younger Dryas Moraines
Warm northerly currents
Cold southerly currents
Vøring Plateau
(approx. position)
1 Core M23071
2 Core MD95-2011
3 Core HM79-6/4
4 Core 56/-10/36
A
0°
N70°0'
Finnmark
Norway
N60°0'
Scotland
B

2.2.4 Deglaciation and Relative Sea-level History

Environmental Processes of the Ice-Age: Land, Oceans, Glaciers (EPILOG) is a multi-national collaborative programme which is facilitating development of a comprehensive reconstruction of the state of the Earth during the Last Glacial Maximum (LGM), and the transitions into and out of that period (Clark and Mix, 2002). This revisits the CLIMAP study of the LGM Earth (Denton and Hughes, 1981). The LGM is defined by the EPILOG project as an interval centred on 21,000 years ago (Clark and Mix, 2002). At this time three broad centres of glaciation affected the northwest continental margin: the British and Irish Ice Sheet (BIIS) centred on Scotland (Bowen et al., 2002); the Scandinavian Ice Sheet (SIS) with a centre of mass located over southern Norway (Kleman et al., 1997); and the Barents Ice Sheet (BIS) (Landvik et al., 1998).

The BIIS was a long-lived feature probably evolving as a mobile and sensitive ice sheet throughout the Weichselian (*ca* 116-11 ka BP), advancing to its LGM position at *ca* 22 ka BP. At this time the BIIS and SIS were not coalescent, and it is suggested that northeast Scotland would have been ice-free (Bowen et al., 2002). This most recent modelling of the LGM, places the northwestern extent of the BIIS well beyond the study site at Lochan An Druim. There were however, some ice free areas at this time, in the form of nunataks, which persisted in areas peripheral to the main centres of accumulation (Ballantyne et al., 1998). Extensive deglaciation of the BIIS followed the LGM, starting at *ca* 17.4 ± 1.3 ka BP; sub-glacial imprints and ice marginal patterns record massive deglaciation from the continental shelf towards terrestrial centres of ice dispersion (Bowen et al., 2002). The maximum extent of the Younger Dryas re-advance, after the initial deglaciation in Scotland, has been reconstructed by Hubbard (1999) from previously mapped limits and trimline studies. The northern extension of this re-advance lies well south of the study site at Lochan An Druim.

The major fluctuations of the SIS throughout the Weichselian have followed the precession cycles of the Earth's orbit of *ca* 23 ka (Mangerud et al., 1996). The evolution of ice-sheet configuration and flow pattern in Fennoscandia through the last glacial cycle has been modelled by Kleman et al. (1997), showing the build up of the main ice sheet starting *ca* 70 ka BP. The advance and retreat history of this ice-sheet prior to its maximum extent is not known, although reconstructions have been assembled. Glaciological inversion models suggest that Finland, and most of Sweden and Norway, were glaciated prior to 25 ka BP (Kleman et al., 1997), however reliable radiocarbon dates from Finnish mammoths suggest a large ice-free area in southeast Fennoscandia during the Middle Weichselian Substage (Marine Oxygen Isotope Stages 4 and 3 (see section 2.3.3.3)) (Ukkonen et al., 1999).

The major fluctuations of the BIS throughout the Weichselian have followed the *ca* 41ka obliquity cycles that are associated with the tilt of the Earth's rotation axis. This has a more significant effect on summer insolation at this latitude than further south in connection with the SIS. The Late Weichselian advance peaked at *ca* 22 ka BP, and in the western Barents Sea the maximum advance was probably of short duration (Mangerud et al., 1996). The LGM in the southern Barents Sea represents the confluence zone between the two dynamically independent ice sheets, the BIS and the SIS. The LGM in the southwestern Barents Sea occurred in two phases with the most recent advance after 19 ka BP (Laberg and Vorren, 1995; Vorren and Laberg, 1996; Vorren et al., 1988). Ice sheet extent and behaviour have been modelled by Landvik et al. (1998) and these models support ice sheet extension to the edge of the continental shelf at the LGM with deglaciation starting ca 15 ^{14}C ka BP; by 12 ^{14}C ka BP most of the central Barents Sea was ice free. In northern Norway, glaciological studies on the continental margin indicate that the Finnmark coast was deglaciated by *ca* 17.5 ka BP (Andersen, 1979; Sollid et al., 1973; Vorren and Plassen, 2002).

During this last deglaciation two distinct phases of rapid climate warming occurred in the North Atlantic region at *ca* 14.7 and *ca* 11.5 ka BP: the transition from Oldest Dryas stadial to Lateglacial Interstadial (GS-2 to GI-1e) and Younger Dryas stadial to Preboreal (GS-1 to Preboreal) respectively (Renssen and Isarin, 2001a; Renssen and Isarin, 2001b; Vandenberghe et al., 2001) (see section 2.3.2 and Figure 3 for guide to nomenclature). These rapid temperature increases are well represented in the biotic and abiotic proxy-records. There is also a signal of rapid change in global meltwater discharge recorded in the Tahati and Barbados corals at the same times (Bard et al., 1996; Fairbanks, 1989). More locally, the deglacial sea-level history from a site in northwest Scotland registers the older meltwater pulse as a temporary slowing down of the relative sea level fall and constrains the timing and magnitude of this event (Shennan, 1999).

Changes in relative sea level (RSL) have varied the position of the coastline of the northwest continental margin considerably during the Quaternary. However, this can only be inferred for the postglacial period, due to the erosion of former shorelines. During deglaciation relative sea-levels were dominated by glacio-eustatic fluctuations that had a global impact (Fairbanks, 1989), and were combined with localised isostatic adjustments. Together the effects of these two mechanisms are most apparent in areas adjacent to the ice margins, where raised shorelines terminating inland in glacial outwash are characteristic. Such areas have been identified in Scotland (Sutherland, 1984) and northern Scandinavia (Sollid et al., 1973).

In northwest Scotland, changes in RSL following deglaciation have been inferred from biostratigraphic and lithostratigrapic records in raised tidal marshes and isolation basins (see the end of this section); the two nearest sites to Lochan An Druim being Dubh Lochan (Shennan et al., 2000) and Wick River (Dawson and Smith, 1997). The main features of change show a regression from the marine limit, which lay between 36.5m and 40m OD at Kentra/Arisaig, at 15.9 ka yrs BP (range 15.6 -16.3 ka BP) (Shennan et al., 2000), and suggest rapid sea-level fall (*ca* 9mm ^{14}C yr^{-1}) until the early Holocene when levels remained stationary for a period before rising to a mid-Holocene maximum (Shennan et al., 1995).

By contrast with Scotland, the marine limits along the coast of Finnmark have been mapped using altitudinal measurements of coastal landforms (Sollid et al., 1973). This model provides an outline chronology for deglaciation based on the distribution of glacial and fluvioglacial deposits, coupled with a regional map depicting the elevation of the local marine limits. This is a relative chronology in which shorelines of different elevation (and hence age) provide local age estimates that are used to correlate local moraine sequences. The marine limit rises in a southerly direction from *ca* 50m OD on the outermost north coast, to elevations >100m OD at the heads of the fjords. The marine limit also becomes younger in a southerly direction, reflecting later deglaciation and greater ice load (hence increased rebound). The height difference between these limits and the Younger Dryas shoreline decreases, reflecting the progressively shorter time interval between deglaciation and the Younger Dryas (Anthony Long, pers. com.). A reconstructed RSL curve for Nikel-Kirkenes on the Norwegian-Russian border indicates a postglacial isostatic response to glacial unloading (Corner et al., 1999) and hence sustained regression.

Isolation basins are natural rock depressions that may, at various times in their history, be connected to, or isolated from, the sea by changes in RSL (Long et al., 1999). There are three common stratigraphical units within basins that have been isolated from the sea by a fall in the RSL: a basal clastic unit of marine origin; a brackish transitional unit formed as isolation occurs; and an upper freshwater gyttja deposited after isolation (Long et al., 1999). The transitional unit varies depending on the size of the basin, which can have an effect on water mixing, and the rate of the isolation process. Laminated sediment is commonly deposited as lakes become isolated from the sea and may reflect reduced bioturbation resulting from anoxic bottom conditions and/or from enhanced seasonal variability in oxygen content (Snyder et al., 1997). The pyritization of iron takes place under reducing conditions near the lake bottom and separate dark laminae will be formed in iron-rich lakes (Saarnisto, 1986).

2.3 Developing Palaeoenvironmental Histories

This section outlines the choice of climate proxy and broadly discusses the methods used in developing palaeoenvironmental histories and the potential value of correlations.

2.3.1 Pollen as a Climate Proxy

Palaeoclimates can be inferred from geomorphic features recording glacial activity and past sea-levels, or from sediments where fossil flora and fauna are recorded as a proxy for climate. The Quaternary palaeovegetation record of pollen is multivariate in nature, as well as multiscale with respect to both temporal and spatial dimensions, and therefore has the potential to provide a wealth of palaeoenvironmental information (Huntley, 2001). Pollen palaeodata can be compared with data from modern analogue assemblages and calibrated in terms of those environmental variables that are of particular interest (e.g., see section 2.3.3.4). However, these palaeoenvironmental reconstructions are reliant upon the uniformitarian assumption that the 'present is the key to the past' (first proposed by James Hutton in 1788 (Birks and Birks, 1980)), and must be supported by *inter alia* the assumption that species distributions are today in dynamic equilibrium with the contemporary environment, as were the fossil taxa with the changing palaeoenvironment (after, Huntley, 2001). Therefore, a principal disadvantage of using pollen as a climate proxy is the potential limitation imposed by the occurrence of 'no-analogue' assemblages in the fossil record as identified extensively by Huntley (1990a), and discussed in terms of indications that certain cold-stage plant communities have no analogues in the modern flora (see, e.g. (West, 2000)).

2.3.1.1 Pollen Analysis

Pollen is an aeolian deposit and can therefore become incorporated into the stratigraphic record, thus reflecting the vegetation at the time of deposition. The climatic signal therein can be distinguished from the other variables affecting pollen accumulation by aggregation of data at the regional scale, and interpretation at the appropriate temporal scale. Lacustrine pollen records have the potential to provide a continuous and undisturbed record with high temporal resolution, providing data with sedimentation rates of one order of magnitude higher resolution than marine records (Zolitschka and Negendank, 1999).

It has become traditional to present pollen data in a relative form. The continuation of such practice enables effective comparisons between historic records and provides a visual image of the vegetation changes that might have taken place throughout a

profile. However, pollen production and dispersal vary widely between different taxa, and since this representation of data is relative to the total pollen assemblage, results can be misleading, as the pollen type is only very rarely in a 1:1 relationship with the abundance of that taxon in the local vegetation. The theoretical 'Fagerlind Effect' predicts that within a system of three or more taxa the pollen percentage of any one depends not only on its own abundance but on that of the other taxa involved (Prentice and Webb III, 1986). Despite being counter to the intuitive nature of the 'Fagerlind Effect', the use of pollen percentages does provide robust first approximations for palynological studies (Prentice and Webb III, 1986), provided caution is applied to the interpretation of pollen types at very high and very low values. A more objective way of presenting results is by means of pollen influx data, whereby meaningful comparisons can be made, since the influx values for each taxon are independent. Pollen influx is an estimate of the annual rate of deposition of pollen grains in the accumulating sediment, developed from pollen concentration values and a robust age-depth model. The influx of a particular pollen taxon to a sediment is closely related to the distance of that taxon from the site; Hicks (2001) has developed threshold influx values for *Betula* and *Pinus* with reference to *Salix* and *Alnus*, from long-term annual influx data collected between 1982 and 1999 in northern Fennoscandia and these can be used to evaluate the proximity of the relevant tree lines. Thus changes in influx rates imply changes in taxon abundances that cannot necessarily be inferred from relative pollen representation.

The particular depositional environment at a study site directly influences pollen recruitment to the sediment. Differing erosional and hydrological processes acting on the surrounding topography and the catchment characteristics of airborne particles (generated by prevailing weather patterns interacting with topography), serve to dictate the allochthonous (transported) contribution; and the nature of any biological activity governs the autochthonous (non-transported) contribution. These differences are particularly important when considering marine and non-marine sites. Lacustrine environments tend to develop higher sedimentation rates due to more efficient trapping of sediment, compared to the more dynamic marine environments where sediment is more likely to be sorted and smaller particles can be removed in suspension, with the movement of the tides. The pollen record from marine sites has the potential to contain evidence of taxa on a much larger spatial scale, due to inwash and transport from many different freshwater outlets, and a much more vigorous mixing dynamic; some selection of the more resillient pollen grains would be expected.

Furthermore, influx values in lacustrine environments can be influenced as a result of local depositional and hydrological processes such that results from different parts of the same lake are not always comparable (Hyvarinen, 1976).

2.3.2 Developing Chronologies

The Lateglacial and early Holocene period poses unique problems for stratigraphic sub-division and correlation (Walker, 2001), since historically the mixed use of biostratigraphy, chronosratigraphy and lithostratigraphy has been applied. In addition, during this latter part of the Quaternary, climatic shifts occurring at the hemispherical scale and over time intervals of centuries and even decades (e.g. Hughen et al., 1996) have resulted in a stratigraphic record of such fine resolution that conventional geological procedures (e.g. Whittaker et al., 1991) have been difficult to apply.

2.3.2.1 Greenland Ice-core Chronology

The INTIMATE group has therefore proposed that the oxygen isotope signal ($\delta^{18}O$) from the appropriate section of the GRIP Greenland ice core should provide a type profile for this period (Björck et al., 1998; Walker et al., 1999), where the isotopic trace can be regarded as a proxy for mean local annual temperature (Jouzel et al., 1997), thus establishing a standard time-scale against which independently constructed schemes can be compared. However, the GRIP chronology (ss08c) (Von Grafenstein et al., 1999) is one of three such schemes between which there are important differences in the estimated ages of events, which need to be acknowledged when correlations are proposed between different realms (Lowe and Hoek, 2001). This proposed Event Stratigraphy defines a series of stadials and interstadials (further divided into sub-stadial or sub-interstadial episodes) based on marked oxygen isotope variations which identify a series of events, with dates derived from the independent GRIP (ss08c) chronology based on ice-core years (see Figure 3). It is proposed as a standard for comparing the synchroneity (or asynchroneity) of these events in the North Atlantic region, where the ice core records provide the highest available temporal resolution from which to derive chronologies.

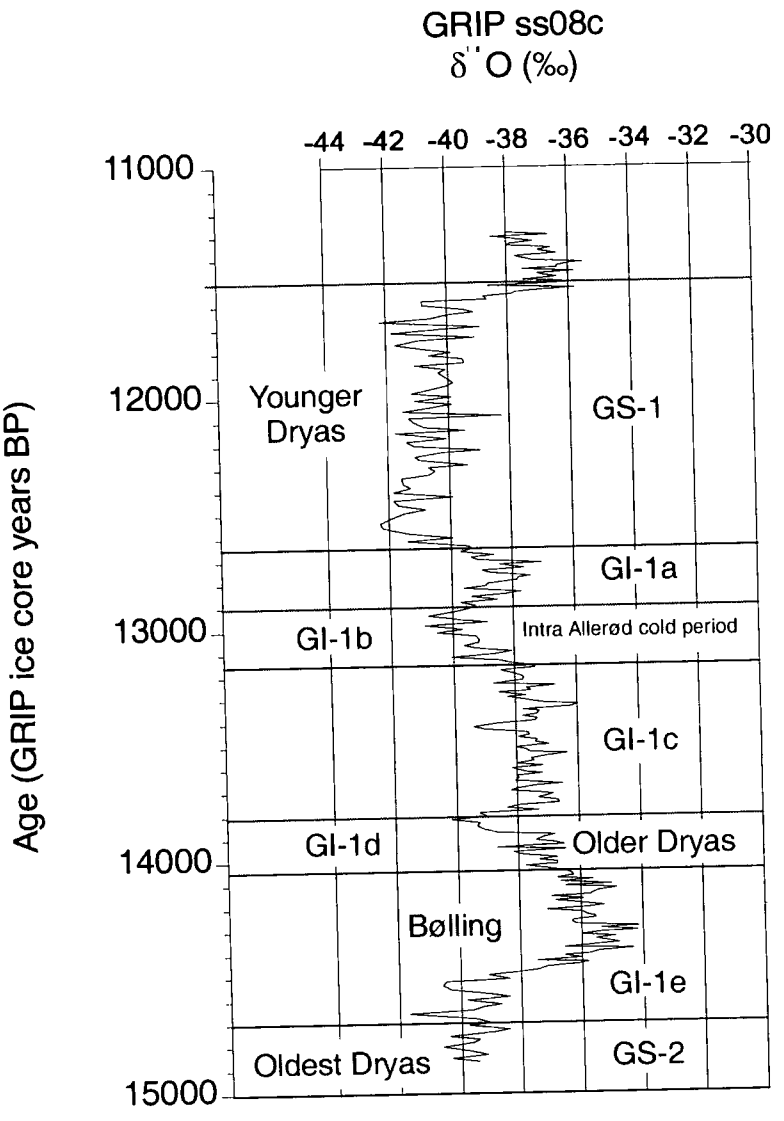

Figure 3

The solid line shows the $\delta^{18}O$ curve as measured in the GRIP Greenland ice core with the chronology of the Lateglacial following (Björck et al., 1998) and the chronozones of Mangerud et al.(1974) (GI = Greenland Interstadial; GS = Greenland stadial).

2.3.2.2 Radiocarbon Dating

Working with Lateglacial palaeodata is confounded by the problems with radiocarbon dating during this interval, but despite this the radiocarbon age time frame has been used extensively during the past 50 years in many disciplines.

Radiocarbon can be used to date organic materials up to 40 ka, and has proved to be an extremely useful dating technique for studying late Quaternary climate changes. The ubiquitous distribution of ^{14}C has enabled the technique to be used to date samples of, *inter alia,* peat, wood, 'old' sea-water, marine and lacustrine sediments and atmospheric CO_2 trapped in glacier ice. Conventional radiocarbon dating has been based on the detection and counting of β emissions i.e. decay products from ^{14}C atoms

over time. Results are compared with a modern reference standard such that the activity of the sample is interpreted as an age estimate. More recently the method has been improved by the use of accelerator mass spectrometry (AMS), used to measure directly the relative abundance of ^{14}C, ^{13}C and ^{12}C atoms in a sample. This technique can measure very much smaller samples and has thus improved the spectrum of potential sources for dating. However, several sources of possible error have been clearly identified in association with radiometric dating.

Fundamental to the principles of radiocarbon dating is the assumption that atmospheric ^{14}C levels have remained constant; however, temporal variations in atmospheric ^{14}C production, and hence atmospheric concentration, have occurred. 'plateaux' of constant age have been demonstrated during the Lateglacial; where AMS dates from lake sediments in Switzerland, record these events at around 12.7, 10 and 9.5 ^{14}C ka BP. It is suggested that these reflect episodes of decreasing atmospheric ^{14}C concentration (Ammann and Lotter, 1989), possibly linked to the rapid release of fossil carbon dioxide from the oceans during NADW formation (Sarnthein et al., 1994). It follows then, that instabilities in the North Atlantic Thermohaline Circulation (NATC) could be implicated as a possible influence on the periodic variation in the intensity of atmospheric ^{14}C.

Contamination by old or young carbon can influence the reliability of radiocarbon dating by creating an 'apparent age'. For example, contamination resulting in anomalously low levels of ^{14}C can arise when organic materials to be dated take up carbon from water containing bicarbonate derived from old inert sources (i.e. ^{14}C-free), such as areas of calcareous rocks, particularly in deglaciated terrain. This results in a lowered ^{14}C: ^{12}C ratio and will, when ^{14}C dated, give an older 'apparent age'.

Similarly, fossils obtained from marine sequences can be subject to what is known as the 'marine reservoir effect' causing an apparent radiocarbon age that is older than the true age. This is due to the slow mixing of ocean waters such that any upwelling of ^{14}C depleted waters, which occurs near some coasts, becomes incorporated in the fossil type and compromises the ^{14}C: ^{12}C ratio. Correction factors have been derived from measurements of ^{14}C activity in contemporary marine organisms from the part of the ocean from which the fossil material was obtained (Lowe and Hoek, 2001). The modern (pre-industrial) mean reservoir correction is about 400 years, but there are local variations of several hundred years or more (Reimer and Reimer, 2001). To accommodate these local effects, the difference 'Delta R' in reservoir age of the local region of interest and the model should be determined. A global Delta R database is available (see Reimer and Reimer, 2001).

There are a number of potential error sources that are recognised as influencing the AMS radiocarbon dates of bulk sediment samples, particularly from the Lateglacial period (e.g. Wohlfarth, 1996; Wohlfarth et al., 1993). Lacustrine sediments are composed of a heterogenous mixture of clastic particles and organic debris derived from a variety of sources and concentrated by differing erosional processes; if differentiated, these components would generate a range of ages. Thus, published ^{14}C dates from a vast majority of bulk sediment samples are almost certainly derived from averages of a range of activity values, and therefore ^{14}C dates based on organic detrital limnic sediments, obtained from Lateglacial sequences, are often characterised by an 'ageing effect' due to the dilution of the ^{14}C: ^{12}C ratio in organic residues (Lowe and Walker, 2000). Terrestrial plant macrofossils are now generally accepted as the routine material for the dating of Lateglacial sequences providing the most reliable AMS ^{14}C ages. However, Turney et al. (2000) and M J C Walker (pers. comm.) have approached these dates more critically, and provide data that suggest systematic age differences between dated series from different types of macrofossil. Turney et al. (2000) and Lowe (2000) suggest that the most reliable chronology for this time period might be obtained from the 'humic' sediment component that is not contaminated by older carbon residues.

Radiocarbon dates generally require calibrating against a chronology of calendar years, in order to standardise data and facilitate comparisons, particularly for high-resolution studies interested in rates of change and absolute timescales (Pilcher, 1991). Problems with calibrating radiocarbon dates from the Lateglacial and early Holocene using INTCAL98 are documented in Lowe and Hoek (2001). They emphasise the fact that the first section of the calibration curve, which is based on dendrochronological data, is in close agreement with both the GISP2 and GRIP chronology as far back as mid-GS-1 (close to the Vedde Ash), but thereafter, calibration is based on the Cariaco Basin (marine) dates that are in agreement only with the GISP2 reconstruction (GRIP ss09 reconstruction diverges by up to 200 years younger than the GISP2 reconstruction in this section). They conclude that the extent of the age uncertainties varies markedly throughout the Lateglacial. In only a few limited sectors of the calibration curve (i.e. the steep sections where the error ranges are small) do plots of radiocarbon ages give a limited range of possible calendar ages. In many areas, the radiocarbon age intersects with the calibration curve at more than one point generating two or more probability ranges. The best representation of the full uncertainties in calibrated dates is achieved by citing the full 2σ range of the calibrated radiocarbon date.

An alternative approach involves the 'wiggle-matching' of radiocarbon data sets to radiocarbon calibration curves. Gulliksen et al. (1998) used this technique with the

INTCAL98 data set for dating the GS1/Holocene boundary in Norway, and Davies et al. (2004) have tried both the Cariaco Basin dataset (Hughen et al., 2000), and the Lake Suigetsu dataset (Kitagawa and van der Plicht, 2000), to constrain the age of the Borrobol Tephra in Sweden, achieving the best fit with that from the Cariaco Basin. However, this method requires a large number of radiocarbon dates for confident matching to the calibration curves (Lowe and Walker, 2000).

To summarise, despite these uncertainties, the radiocarbon method is the most frequently used in developing chronologies for marine and terrestrial sequences. The robustness of this dating method depends on: the number of dates available for each sequence; quality assurance methods that underlie sample selection and treatment prior to radiocarbon measurement; the nature of the samples dated (e.g. bulk sediment, organic carbon content, selected fossils); and eventually the analytical precision achieved by the dating laboratory (Lowe and Hoek, 2001). In addition, the dating of fossils obtained from lacustrine sites can be affected by the local presence of old carbon, and those from marine sequences are subject to the marine reservoir effect. At present, this 'contamination' with old carbon is one of the major limitations of correlations between marine and terrestrial records. The uncertainties associated with age estimates based on marine fossils can be well in excess of the analytical precision of the ^{14}C dates themselves (Lowe and Hoek, 2001). Thus, the radiocarbon calibration curve for the Lateglacial is far from precise with uncertainties varying markedly throughout the time span, and problems that are compounded by temporal variations in atmospheric ^{14}C producing 'plateau-effects' (Lowe and Hoek, 2001).

2.3.2.3 Tephrochronology

Tephra, a rhyolitic or basaltic volcanic product, is a collective term for all airborne pyroclasts. Tephra layers constitute unique marker horizons in the stratigraphic record that are essentially isochronous. Tephra layers of Icelandic origin have been identified in sediments of Lateglacial and Holocene age in marine sediments from *inter alia* the North Atlantic ocean, Norwegian sea, and from terrestrial sequences in Scandinavia, the British Isles and Ireland (Haflidason et al., 2000). They have proved to be an outstanding tool for chronostratigraphical correlation and dating of Quaternary sedimentary sequences. Several tephras have been found in northwest European sequences spanning the Lateglacial and early Holocene, the three best known being the 'Vedde Ash' (mid-Younger Dryas), the 'Borrobol Tephra' (early Lateglacial interstadial) and the 'Saksunarvatn Tephra' (early Holocene).

The Vedde Ash was first identified at Ålesund in western Norway (Mangerud et al., 1984), and more recently in Lateglacial sequences in Scotland (Lowe et al., 1999; Lowe and Turney, 1997). It has been precisely dated most recently by AMS analyses

of terrestrial plant material and lake sediment at Kråkenes in western Norway to 10310 ± 50 ^{14}C yrs BP (Birks et al., 1996), which converts to a median estimate of 12125 ± 263 cal yrs BP (using CALIB 4.4.1(Stuiver and Reimer, 1993) with calibration data set: intcal98.14c (Stuiver et al., 1998a)). This date encompasses the range 11980 ± 80 ice core years assigned to the Vedde Ash found in the GRIP ice-core at Summit Greenland (Grönvold et al., 1995).

The Borrobol Tephra was first discovered at the lacustrine site of Borrobol in Scotland. The date 12260 ^{14}C yrs BP or 14400 cal yrs BP suggested for this tephra was based on AMS measurements of bulk sediment (Lowe et al., 1999; Turney et al., 1997). There are a number of potential error sources that are recognised as influencing the AMS radiocarbon dates of bulk sediment samples, particularly from the Lateglacial period (e.g. Wohlfarth, 1996; Wohlfarth et al., 1993) (see section 2.3.2.1), and therefore these early dates obtained for the Borrobol Tephra in Scotland are not generally considered robust.

Subsequent to the discovery of the Borrobol Tephra in Scotland, a cryptotephra of identical geochemical compostition has been reported in a marine record on the Icelandic plateau, with a considerably older age estimate of 13400 ^{14}C yrs BP, based on AMS measurements of foraminifera (Eiriksson et al., 2000). More recently, the Borrobol Tephra has been identified in lacustrine sediments in southern Sweden where a series of AMS radiocarbon measurements of terrestrial plant macrofossils has been used to attempt to constrain its age. Calendar age estimates for this event have been derived from a visual wiggle match of the ^{14}C age series to the Cariaco Basin data-set, giving an age of *ca.* 13900 Cariaco varve yrs BP, and also a method based on Bayesian probability analysis using the Cariaco Basin and Lake Suigetsu records as calibration data-sets giving ages of 13800-14450 and 13667-14331 cal yrs BP (95% confidence), respectively (Davies et al., 2004). Thus far, the wide range amongst these dates casts doubt on the coeval nature of the occurrences of the Borrobol Tephra in northern Europe.

The Saksunarvatn Tephra has been precisely dated by AMS analysis of terrestrial plant material and lake sediment at Kråkenes to 8930 - 9060 ^{14}C yr BP (Birks et al., 1996). It was first identified on the Faroe Islands (Mangerud et al., 1986), and is awaiting confirmation of identification at the Borrobol site in Scotland (Turney 1998 In: Lowe et al., 1999). Both the Vedde and Saksunarvatn tephras have been correlated with GISP2 (Zielinski et al., 1996) and GRIP ice cores (Grönvold et al., 1995), and the marine record (e.g. Eiriksson et al., 2000).

2.3.3 Other Palaeoenvironmental Evidence

The interpretation of the pollen stratigraphy can be supported by macrofossil evidence gleaned from the pollen washings, which contain the >180μm fraction from the sub-sample. Evidence of specific plant remains and the identification of seeds can help to confirm the presence of particular taxa. However, other types of macrofossil can be valuable in interpreting particular palaeoenvironmental conditions. In this study, the presence of various algae, Cladocera, Ostracoda, Bryozoa, Dinoflagellate cysts and even the formation of iron pyrites, together with evidence for the ubiquitous chironomid and other insects, have helped to form a general picture of the changing lake environment through the Lateglacial and early Holocene.

Algae are simple (eucaryotic) plants that are generally abundant in most aquatic or wet environments, and they are the dominant plants in the sea. In freshwater most species are microscopic unicellular or colonial organisms, but some do form visible plant bodies, and a variety of types of algae help to characterise the pollen washings. Of the unicellular taxa: the ubiquitous *Pediastrum* is non-flagellated and non-motile and is never fixed to a substratum; diatoms (Bacillariophyta) are non-flagellated and usually attached to a substratum; and dinoflagellates (Dinophyta), which are represented by only a few freshwater species, are solitary and motile (Fitter and Manuel, 1994, p 42-63). Some dinoflagellates are known to develop a benthic cyst stage, in response to adverse environmental conditions, or following sexual reproduction (Brasier, 1980, p 21-29), and it is this stage that can be preserved in sediments. In the marine realm dinoflagellates are represented by many more species, and their cysts are preserved such that their stratigraphies can be used to reconstruct palaeoclimates (Boessenkool et al., 2001; Shennan et al., 1996). Remains of the multicellular Thallophyta, which have usually at some stage in their life cycle been attached to a substrate (Dickinson, 1963, p 10-11), are also preserved in marine sediments.

The charophytes (Charophyta) are macroscopic green plants with a higher level of organisation than the unicellular algae and are well anchored to the substratum (Fitter and Manuel, 1994, p 42-63). Charophytes thrive in stable environmental conditions, e.g clear water and marl-rich lakes; their production of oospores (gametangia) are triggered by lengthening photoperiod. They can also be successful in habitats that experience extreme changes, e.g. ephemeral water bodies, with the plants developing from buried oospores. They are often successful colonisers since the oospore is a highly resistant cell that can remain dormant in unfavourable conditions, with some fast maturing species that hold an advantage over the slower growing macrophytes in these habitats and often become the dominant group in both the shallow and deep water niches. However, they are at a competitive disadvantage in more productive habitats

where they are out-competed by more robust macrophytes early in the succession (Moore, 1986).

Cladocera can be a dominant component of the zooplankton or microcrustacean fauna of standing waters, where they occur in open water and in the littoral zone (Duigan and Birks, 2000). In a northern climate during most of the open-water season only parthenogenetic females are found (reproducing by asexual reproduction) (Sarmaja-Korjonen, 2003). A stressful event such as the onset of winter triggers gamogenetic (sexual) reproduction; in Cladocera this always leads to the production of diapause or resting eggs (ephippia). These provide a mechanism for re-establishing populations eliminated by such recurring or aperiodic environmental stresses, where the principal climatic stimuli are temperature and the length of the photoperiod (Frey, 1982). Another small crustacean group, Ostracoda, are of biostratigraphic utility because both species and assemblages display rapid migration and successions in response to environmental and climatic change, and the Quaternary record contains evidence of both speciation and extinction (Griffiths, 2001). Ostracods are able dispersers, employing a wide range of methods. Some species can produce dessication resistant eggs or have diapausing life-history stages; they may be transported by other organisms, e.g. birds and amphibians, or in moving water and lastly, as aerial plankton. Some parthenogenetic taxa are able to establish new populations from single individuals. Such dispersal strategies allow them both rapidly to invade newly created or ephemeral habitats and to be able to 'track' their environmental and climatic optima. Palaeoecological records from European deep lakes suggest very early colonisation after deglaciation; candonids and limnocytherines have been found from the very start of site sedimentary records (Griffiths, 2001). Two different ostracoda faunas have been identified that discriminate between the Lateglacial and the Holocene, the *candida* - Fauna and the *cordata* - Fauna respectively (Griffiths, 2001). The *candida* - Fauna is essentially cold, oligotrophic and benthic, suited to shallow, newly formed water bodies necessarily low in accumulated nutrients and high in dissolved oxygen. By comparison, the *cordata* - Fauna includes more eurythermal, free-swimming and phytophylic forms, suited to waters with a higher nutritional status.

Bryozoa are colonial sessile "moss animals" usually fixed to a substratum and generally found in clean fresh water where they produce statoblasts (asexually), which are overwintering bodies that can be preserved in the fossil record (Fitter and Manuel, 1994, p 173).

Pyrite is one of the major diagenetic minerals in anoxic sediments, and is an indication of stagnating bottom conditions (Alm, 1993). An oxygen deficit in the bottom water

layers suggests a limited fauna and consequently little bioturbation, potentially resulting in laminated sediments.

Chironomidae (non-biting midges) is a diverse group of true-flies (Diptera) with an aquatic larval stage, which are often the dominant faunal element in muddy sediments (Fitter and Manuel, 1994, p 278-279). Their heavily chitinised head capsules are well preserved in lacustrine sediments. Many species are stenothermic (unable to tolerate wide variations in temperature) and therefore the group has considerable potential as a proxy indicator of palaeoclimate change (e.g. most recently Rosenberg et al., 2004).

Foraminifera are single-celled organisms, many species of which possess hard calcareous shells, often distinctively coiled, which are preserved as fossils in sediment profiles. Most are marine and benthic although a few genera are planktonic and some have adapted to freshwater. Due to their abundance and diversity, foraminifera have become an invaluable tool in Quaternary palaeoceanography and palaeoclimate reconstructions (Lowe and Walker, 1997, p 215).

2.3.4 Making Correlations

A crucial issue in late Quaternary palaeoenvironmental research is determining the timing and synchroneity or asynchroneity of the abrupt climatic events inferred from the oceanic, terrestrial and ice realms, and the resulting regional climatic effects. Therefore, the most appropriate correlations for securely dated high resolution palynological studies, involve direct comparisons between different pollen profiles at local and regional scales, as well as comparisons with other proxy data, primarily the Greenland ice core record and the marine sedimentary record.

2.3.4.1 Palynological profiles

Pollen analyses present a large amount of information on the covariance of different pollen types through time, such that the ordering of samples with depth and age enables the presentation of the palynological data within a stratigraphical sequence i.e. biostratigraphical assemblage zones. The identification of such zones indicates changes in a sequence, enabling interpretation of the data as a temporal record of changes in vegetation, and by inference, past environments at a local and regional scale. In order to avoid subjectivity in this exercise, objective computer-based zonation programmes have been developed (see Birks, 1986). Initial classification into local pollen assemblage zones, combined with a robust age-depth chronology, provides a means of correlation between individual pollen profiles.

2.3.4.2 The Greenland Ice-core Records

The Greenland ice sheet provides the most favourable conditions in the Northern Hemisphere for obtaining a high-resolution time-series of climate related parameters (Johnsen et al., 1992). The oxygen isotope record for GRIP and GISP2 ice cores have been studied and compared with previous deep Greenland ice cores, and the observed isotopic fluctuations have been evaluated for climatic significance (see Dansgaard et al., 1993; Grootes et al., 1993; Johnsen et al., 1992). This has provided a high-resolution record of climatic changes, not only in the vicinity of the Greenland ice sheet but also related to other areas of the northern hemisphere e.g. the tropical Atlantic region (Hughen et al., 1996; Taylor et al., 1997). Studies have shown that abrupt climate changes (i.e. century scale), of at least regional extent, characterise the last deglaciation period, and suggest the potential for rapid reorganisation of the climate systems in the North Atlantic region (Dansgaard et al., 1993). Most recently, the North Greenland Ice Core Project (NGRIP) has published an undisturbed climate record extending to 123 ka BP (North Greenland Ice Core Project members, 2004). The data have been published as a 50 year mean and compared to the annual mean data published for the GRIP record show a broadly similar pattern, although they do not provide sufficiently high resolution for comparisons with the palynological records from this study.

2.3.4.3 The Marine Sedimentary Record

Marine cores can provide long and continuous records as the floors of the deep ocean basins accumulate sediment formed from terrigenous material (from erosion of land masses) and biogenic material (accumulations of calcareous and siliceous skeletal remains of micro-organisms e.g. diatoms and Foraminifera), and they are relatively undisturbed over time. However, on account of very low sediment accumulation rates, i.e. *ca* 1-20 cm / 1000 yrs (Zolitschka and Negendank, 1999), marine records tend to show a poor resolution, particularly by comparison with the ice core records.

Within the ocean sediment sequence in the mid- and high-latitudes, the delivery of terrigenous detritus, i.e. periods of enhanced ice rafted debris (IRD), can be broadly correlated with glacial episodes (Ruddiman et al., 1989). A widespread feature of the North Atlantic Ocean record has been the identification of distinctive layers formed during the last glaciation, high in IRD and low in foraminifera (Bond et al., 1992; Heinrich, 1988). These cycles of IRD deposition form the distinctive Heinrich Layers, originating from massive discharges of icebergs from the eastern margins of the Laurentide ice-sheet (Bond et al., 1992). These discharges were accompanied by decreases in sea surface temperatures (SSTs) and salinity (Chapman et al., 2000).

The most recent and reliable of these deposits, denoted H1, has been AMS dated at 14.3 ka ^{14}C BP from DSDP site 609 (Bond et al., 1992) and 14.2 ka ^{14}C BP from core SU90-03 (Chapman et al., 2000). Similar ice rafting events in the northeast Atlantic have been associated with iceberg discharge from the Fennoscandian ice sheet and the Norwegian Sea and it is suggested that the Norwegian Sea IRD event 1 corresponds closely enough with the H1 event in the North Atlantic to infer a link between the behaviour of both ice sheets (Baumann et al., 1995).

Fine ocean sediments dominated by biogenic material tend to be characteristic of warmer periods, and these fossil remains can provide a record of ocean circulation and ocean temperature, and hence imply past atmospheric temperatures (Lowe and Walker, 1997, p 148). Environmental changes in the oceans are best reflected in the chemical and isotopic content of marine fossil organisms (such as diatoms, foraminifera, ostracods, radiolaria and coccolithophores) that are influenced by circulation, nutrient supply, salinity and water temperature. Analysis of the stable isotope ratios of both oxygen (^{18}O:^{16}O, i.e. $\delta^{18}O$) and carbon (^{13}C:^{12}C i.e. $\delta^{13}C$) have provided valuable data on oceanographic changes.

The $\delta^{18}O$ of carbonate in marine organisms depends on both temperature and the isotopic composition of seawater at the time of secretion of their tests. This signal varies locally with temperature and to a lesser degree salinity, and globally with variations in ice volume (Bradley, 1999, p 199). Oxygen isotope traces through deep-ocean cores can therefore be interpreted as a record of global palaeoglaciation, providing evidence of warm and cool episodes and hence glacial to interglacial transitions; a proxy record of Milankovitch or orbital scale climate change (Patience and Kroon, 1991). Thus, changes in the isotopic composition of benthic Foraminifera, (which tend to come from environments of more stable temperature and salinity, resulting in more constant traces) have been used as an index of global land-ice volume, and records have been developed into a standard oxygen isotope chronology. This isotopic signal is geographically consistent, so that inflections in the profiles represent time-parallel events and therefore constitute an age equivalent marker horizon. This has enabled these globally correlated divisions to be used to form the basis for a scheme of oxygen isotope stages. The first standard chronology - the SPECMAP timescale - was developed by Imbrie et al. (1984), and further developed at a higher resolution by Martinson et al. (1987). According to this scale the last glacial to interglacial transition occurred at Marine Oxygen Isotope Stage boundary 2/1.

2.3.4.3.1 The Lateglacial and Early Holocene Marine Sedimentary Record in the North Atlantic

In the North Atlantic efforts to improve the temporal resolution of marine records have focused on sites of high sediment accumulation rate provided by the North Atlantic drifts and continental slope sequences of the North Atlantic margins. Locations of the records discussed are in Figure 2. From the area of the Barra Fan northwest Scotland, high-resolution (century / decadal) marine records of SSTs have been estimated from changes in the composition of planktonic foraminiferal assemblages, and SSSs estimated from the oxygen isotope composition of two of these species (Kroon et al., 1997). These records have shown a series of rapid oscillations during the Lateglacial period that are very similar to those observed in the $\delta^{18}O$ records from the Greenland ice-cores, and attest to the inherent instability of the deglacial climate system during this interval (Austin and Kroon, 2001). They have been compared with other Atlantic Ocean records to evaluate the timing of deep-sea ventilation with changes in surface water characteristics. Results indicate that the northward transport of heat and salt was highest during the Bølling. They also suggest that NADW formation strengthened during the Bølling-Allerød period, when it was at least as strong as it has been through the Holocene, although it was reduced during the Younger Dryas period (Austin and Kroon, 2001). This coupling between surface and deep-water changes would suggest that the NATC is a potential driver for the climate changes that might be recorded coincidentally in the terrestrial record. This has been demonstrated by analysis of high-resolution diatom records from the eastern Norwegian Sea, to show patterns of SSTs from the Younger Dryas through the Holocene, and linking periods of terrestrial glacial advance with cool oscillations in SST reconstructions (Birks and Koç, 2002; Koç et al., 1993).

The problem of variability in marine reservoir age in the region has been assessed by Austin and Kroon (1996), Haflidason et al. (2000) and Eiriksson et al. (2004). Following the determination of a modern surface ocean reservoir correction of 405±40 yrs (Stuiver et al., 1998a; Stuiver et al., 1998b), Austin and kroon (1996) used Icelandic tephra from core 57/-09/46 to quantify the marine ^{14}C reservoir ages during the Younger Dryas period. From the age depth curve the marine radiocarbon age of the peak in shards of Vedde Ash was estimated to be 11 ka BP, as compared to a date of *ca* 10.3 ka BP estimated from terrestrial macrofossils (Birks et al., 1996), thus providing evidence to support a significant increase in the marine reservoir age correction at this time, to *ca* 700 years. Haflidason et al. (2000) have since investigated the ^{14}C ages of paired terrestrial and marine deposits using tephrochronology to demonstrate that marine reservoir corrections during the Younger Dryas in the north Atlantic and eastern

Norwegian sea could be as much as *ca* 800 years increasing to *ca* 1100 years in the western Nordic seas. They suggest that in the early Holocene reservoir age reduced to *ca* 700 years but was systematically higher in the western Nordic seas. In addition, Eiriksson et al. (2004) have researched marine reservoir age variability in the Iceland Sea during a period spanning AD 1717 to 12 ka BP; thirteen different tephra layers were utilised in the development of tephrochronological age models for the five marine cores studied. The deviations between reservoir corrected radiocarbon dates of molluscs or foraminifera and the tephrochronological age models show variations from tens to hundreds of years. The authors suggest that this highlights the need for independent control on ^{14}C dating of marine sediment cores, and particularly those obtained from oceanographic boundary regions such as that separating the Atlantic and Arctic water mases. This temporal variability in North Atlantic marine reservoir ages significantly alters the reliability of radiocarbon calibrations into calendar years Kroon (1997).

Age-depth models are only meaningful and useful when calculated using calibrated radiocarbon dates (Bartlein et al., 1995), since age-depth models calculated on uncalibrated radiocarbon dates make the implicit, and implausible, assumption that variations in the sedimentation rate cancel out the wiggles in the calibration curve (Telford et al., 2004). The marine reservoir corrections suggested by Austin and Kroon (1996) and Haflidason et al. (2000) were derived from uncalibrated age-depth models, which thus adds to the lack of definition for these corrections, and this is highlighted by Eiriksson et al. (2004) who demonstrate even more complexities in the nature of this variability using calibrated models. They postulate that the intervals with increased and variable marine reservoir age reflect incursions of Arctic water masses, and thus suggest a link between the southward movement of the NAPF and increased variability and hence unreliability of radiocarbon dates derived from those periods.

In the light of these uncertainties regarding protocols for both marine reservoir correction and radiocarbon calibration, three marine records of SSTs from the region have been selected for comparison with this palynological study: core 56/-10/36 (Austin and Kroon, 2001; Kroon et al., 1997); core HM79-6/4 (Birks and Koc, 2002; Koç et al., 1993); and MD95-2011 (Birks and Koc, 2002). These records contained the appropriate temporal period of this study, i.e spanning the Lateglacial and early Holocene in the south and the Younger Dryas / Holocene transition in the north, and in addition they have been developed from calibrated age models that take account of the variable marine reservoir correction for this period. The details of these records are discussed below.

Core 56/-10/36 (56° 43'N, 09° 19'W) is situated on the continental margin (Barra Fan) off northwest Scotland (see Figure 2). It provides a record of century scale deglacial surface circulation changes. The age-depth model is derived from four foraminiferal AMS ^{14}C dates outside the Younger Dryas period and so corrected for a modern marine reservoir effect of 400 years, plus three dated tephra horizons, and these are transferred into calendar years using the U/Th calibration curve of Bard et al. (1993) [recalibration of the corrected radiocarbon ages using CALIB 4.4.1(Stuiver and Reimer, 1993) with INTCAL98.14c calibration data set (Stuiver et al., 1998a) as per this study, gives the midpoint of the 2 sigma range for all the dates between –400 and +550 years.] The reconstructed SSTs and SSSs show a series of rapid oscillations that are broadly similar to the GRIP and GISP2 records during the last deglacial period, however some differences in the chronologies are highlighted. For example, the SST record appears to lead the GRIP ice core chronology by over 200 years during the Bolling/Allerod period, but this phase difference is not apparent in comparisons with the GISP2 record. It is suggested that the mismatches could be due to changes in sedimentation rates, bioturbation influencing the radiocarbon dates and unknown variations in the marine reservoir effect. For the accepted model, these problems were overcome by wigglematching the SST record to the GISP2 record, however it is recognised that this approach prevents further consideration of relative timing of events between different realms. This version of the age-depth model is supported by relative abundance records for *Neogloboquadrina pachyderma* in other nearby cores (V23-81(Broecker et al., 1988) and EN 120GGC1 (Keigwin et al., 1991)), and further supported by very similar relative abundance records from the marine core Troll 8903 taken in the Norwegian Channel (Haflidason et al., 1995), and thus it is suggested that the derived palaeotemperature records are representative of the North Atlantic as a whole.

Fossil diatoms assemblages have been used to reconstruct SSTs between 13 ka BP and 2.7 ka BP from analysis of core MD 95-2011 taken from the eastern Voring Plateaux (66° 58.18' N, 07° 8.35' E) (Birks and Koc, 2002). The age-depth model is derived from six AMS ^{14}C dates from monospecific foraminifera samples. None of these samples were within the Younger Dryas period and all ^{14}C dates were corrected for a marine reservoir age of 400 years (after (Haflidason et al., 2000)). Radiocarbon dates were calibrated using the INTCAL93 data set and method A in CALIB v3.0.3c (Stuiver and Reimer, 1993) in order to achieve consistency and comparability with previous calibrations on the same core. However, trial calibrations based on the INTCAL98 data set and CALIB v4.2 (Stuiver et al., 1998a) showed that the results were very similar in this age range. The lower part of the core was constrained by correlating the level interpreted in the SST reconstructions as the onset of the Holocene, with the

date of 11.5 ka BP for the Younger Dryas / Holocene boundary, from the terrestrial record at Kråkenes (Gulliksen et al., 1998) which is about 4 degrees south of this site. This removes any possibility of determining any relative terrestrial – ocean leads or lags in this onset of the Holocene. Within this study, new SST reconstructions were made for core HM79-6/4 and M23071 (for location see Figure 2) (Koç et al., 1992), using corrected and calibrated ^{14}C dates in order to achieve comparability between the cores, and also using an enlarged modern data set for HM79-6/4.

These marine records have not been directly correlated with the records from Lochan An Druim and Nikkupierjav'ri since the age-depth models in both cases precluded any assessment of leads or lags between the oceanic and terrestrial realm, but useful links between the studies are discussed.

2.3.4.4 Reconstructing Palaeoenvironments

Marine records can provide evidence of climate related variables such as past global ice volume and changes in ocean circulation, but only terrestrial records can reveal features of past atmospheric general circulation, i.e. patterns of seasonal temperature extremes, drought, growing-season temperature sums, and continental precipitation distribution (Huntley, 1993).

Palynological studies using surface samples have shown that the composition and amount of pollen rain broadly reflect geographical vegetation patterns, thus suggesting that fossil pollen can be useful in the subjective inference of palaeoclimatic conditions. There are, though, problems associated with resolving the magnitude and duration of any changes (Davis and Webb III, 1975; Huntley and Birks, 1983). The broad-scale relationships between modern pollen rain and modern climatic conditions have been shown to be robust (Huntley, 1990a; Huntley and Prentice, 1993) and therefore they can be used in a direct analogue approach, to calibrate the fossil pollen record. This enables quantitative palaeoclimate reconstructions to be produced by conversion of the fossil pollen record into specific palaeoclimate estimates using transfer functions (in this case: the mathematical derivations of the relationship between modern pollen rain and modern climatic conditions). However, many past communities have no modern analogue as a result of the individualism of response of taxa, and the development of novel climate regimes as a result of independent variation through time of major climate variables (Huntley, 1990a; Huntley, 1990b). Periods characterised by rapid climate change are therefore less likely to have representative modern analogues (e.g. Huntley, 1990a; Overpeck et al., 1985).

Attempts to overcome the 'no-analogue' problem, have involved the computation of 'climate response surfaces' by re-mapping abundance patterns from geographic space

into 'climate space' (Bartlein et al., 1986). Within a study area, e.g. the northern hemisphere or Europe, the pollen distribution from modern pollen samples is considered in terms of 'climate space' as defined by a three-dimensional array of the key bioclimate variables. These indicative driving variables for different functional types of plant are considered to be: the mean temperature of the coldest month (MTCO); the annual accumulated temperature over 5°C, referred to as the number of growing degree days over 5°C (GDD5); and a drought index, developed from the ratio of actual to potential evapotranspiration (AET/PET) (Prentice et al., 1992). The relationship is then described for each individual pollen taxon, so that the no-analogue spectra can be interpolated in the climatic space. This technique has been used to infer past climates using palynological data from eastern North America (Prentice et al., 1991), Scotland (Huntley, 1994) and southern Italy (Allen et al., 2000).

This response surface method of palaeoclimate reconstruction has been refined by using pre-determined biome constraints. Biomes are vegetational categories defined by their dominant plant functional types, and have been used to represent vegetation at a regional scale (Prentice et al., 1992). A systematic method for pollen-based palaeobiome reconstruction using surface sample data for validation, has been developed by Prentice et al. (1996). In addition, this model has been adapted to the biomes of southern Europe and used successfully to present another proxy for systematic comparison (Allen et al., 2000). This method has the advantage that the biomes emerge through the interaction of constituent plants (Prentice et al., 1996) and could therefore develop some representative for non-analogous situations.

Chapter 3

The Study Sites

3.1 Introduction

3.2 Lochan An Druim

3.2.1 Location

3.2.2 Geology and Vegetation

3.2.3 Climate

3.2.4 Deglaciation and Relative Sea-level History Summary

3.2.5 Tephrochronology

3.2.6 Previous Palynological Studies

3.3 Nikkupierjav'ri

3.3.1 Location

3.3.2 Geology and Vegetation

3.3.3 Climate

3.3.4 Deglaciation

3.3.5 Isolation Basins

3.3.6 Relative Sea-level

3.3.7 Tephrochronology

3.3.8 Previous Palynological Studies

3.1 Introduction

Coastal, lacustrine study sites were chosen according to several criteria; principal amongst these were their topographical location and size, and their accessibility with coring equipment. The lakes needed to have formed in glaciated terrain beyond the influences of the Younger Dryas readvance, therefore providing a record of the Lateglacial period. They also needed to be of sufficient surface area to recruit at least a landscape pollen signal (Jacobsen and Bradshaw, 1981). It was important that they contain adequate water depth, typically >2m, to minimise disturbance of the basal waters by wind or changes in thermal stratification. They should also ideally be a closed system, or at least have a minimal throughput, to increase the potential for a lengthy sedimentary sequence with continuous accumulation.

The site in northwest Scotland was selected following an extensive field campaign in 1999. Close scrutiny of the mapped topography of the area, indicated that potential sites might be found along the coast beween Tongue (NC 595570) on the north coast and Inverewe (NG 858819) on the west coast. Many potential sites were probed for depth of sediment and cores were taken from two sites, Lochan An Druim on the coast of Loch Eriboll in northwest Scotland and Inverewe further southwest. Visual inspection of the core from Inverewe did not indicate an adequate Lateglacial record, whereas a previous palynological study by Birks (1984) at Lochan An Druim indicated that there would be a Lateglacial record, and this work was supported by extensive macrofossil analysis that could be used to compliment a new study. The previous core had been recovered from the dense *Phragmites australis* fen on the west side of the lochan, and it was felt that a new core from the open water in the middle of the basin should yield a greater depth of sediment and thus provide the potential for a record of sufficiently high resolution that it could be compared with the GRIP ice core record.

The site in northern Finnmark, was chosen from twelve different sites that were cored close to the coast throughout the region, during a field campaign in 2001. Visual inspection of all the cores suggested that the sequence from Nikkupierjav'ri would be the only one to have a substantial Lateglacial record. This was subsequently confirmed with a basal AMS ^{14}C date (from marine algae) of 14 090 ±269 BP.

The study sites at Lochan An Druim in northern Scotland and Nikkupierjav'ri in northern Finnmark, Norway, are described in terms of their location, geology and vegetation, and the prevailing climate. Information is given about deglaciation and relative sea-level change in the regions, and a summary is provided of previous palynological and tephrochronological work at the sites and in the regions, that are pertinent to this study.

3.2 Lochan An Druim

3.3.1 Location

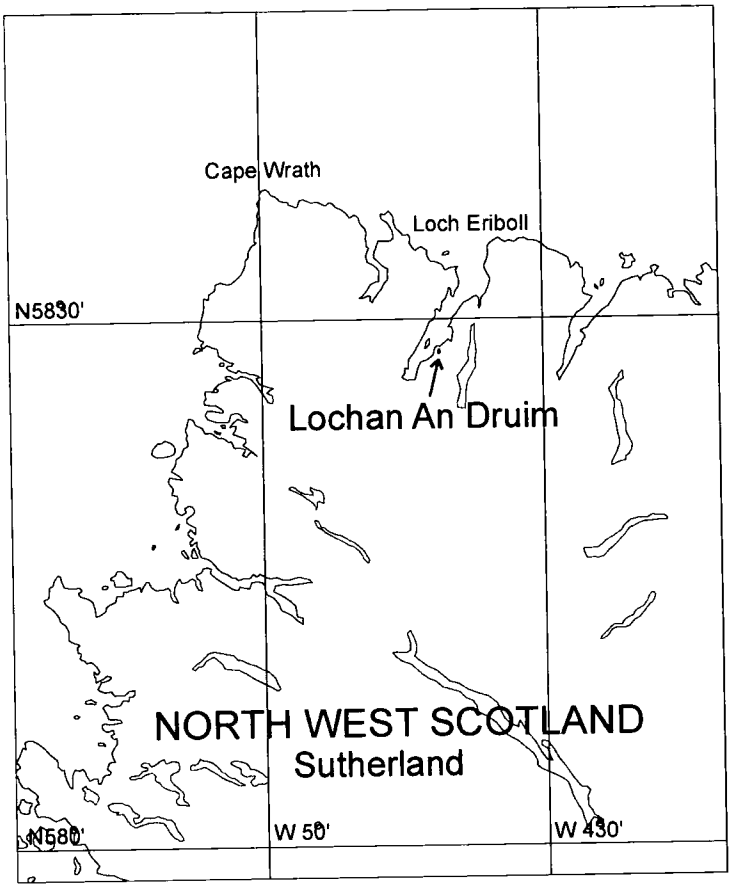

Figure 4

Location of Lochan An Druim beside Loch Eriboll in northwest Scotland.

An Druim is a small ridge orientated north /south between the sea loch, Loch Eriboll, and the A838 road (see Figures 4 and 6). A shallow valley is formed between the ridge and the road, which contains a small lochan (GR NC 435568 58° 28'30"N, 04° 40'18"W; altitude 25m asl). This site was given the name 'Lochan An Druim' in the previous study of the Late-Quaternary pollen and plant macrofossil stratigraphy at this location (Birks, 1984). It is a designated Geological Conservation Review site (GCR No. 1528) located within the Eriboll Site of Special Scientific Interest (1,770 ha), which is designated for the protection of its geological and biological specimens. The citation for Lochan An Druim includes the importance of its pollen and macrofossil stratigraphy, as evidence for Lateglacial and Holocene environmental conditions at low altitudes in northern Scotland.

Geologically, the site falls within the Moine Thrust Zone (see 3.1.2), with a bedrock of Durness Limestone. The basin is approximately 300m long, and 200m wide at its

widest point, giving a basin size of ~6 ha. However, at the time of sampling the basin was becoming infilled and there was only ~0.5 ha of open water surrounded by a dense fen of *Phragmites australis* (common reed).

3.2.2 Geology and Vegetation

In terms of global vegetation, northern Scotland lies just beyond the northerly limit of the Temperate zone and into the southern Boreal zone (Meusel and Jäger, 1992). The geology of the region is characterised by the very ancient Precambrian Lewisian Gneiss, which is exposed in westernmost areas of the Northwest Highlands. Inland it is overlain by a sequence of much younger rocks, with Torridonian Sandstone followed by a sequence of Cambro-Ordovician rocks that includes the Durness Limestone (consisting mostly of dolomite). All these rocks are separated from the rest of the Scottish Highlands by the Moine Thrust dislocation that runs up to twenty miles inland along the western seaboard of the Scottish Highlands, from Loch Eriboll and Whiten Head in the north, to the Sound of Sleat (Roberts, 2003 p. 21-27).

The Durness Limestone supports an Atlantic vegetation comprising a rich calcicolous flora of *Dryas octopetala-Carex flacca* heath on the outcrops, with the deeper soils between outcrops supporting aspecies-rich *Agrostis-Festuca* grassland. The grasslands around Lochan An Druim have been improved for grazing, and these grade through *Juncus effusus* dominated communities, to a dense *Phragmites australis* dominated reed swamp in the shallow waters around the circumference of the lochan (Birks, 1984). This dense *P.australis* fen extends into the lake leaving only 0.5 ha of open water that supports a dense aquatic flora, including *Potomogeton natans* and *Nymphaea alba* (J P Huntley, Pers. Comm. 2000). The lochan has two small inflowing streams, both draining higher ground that rises to Meall Bad Mhuidhe at 289m asl, *ca* 1km southeast of the site. The single outflow breaches the rock lip at the northwest margin of the basin, to flow the 700m north to Loch Eriboll. Fluctuations in the water level are driven by seasonal changes in the ground water table and the hydrogeology suggests it is either a sinkhole in the limestone or a spring fed depression; there is no evidence of brackish influence (J P Huntley, Pers. Comm. 2000).

3.2.3 Climate

Although rainfall data are available from Durness, the closest meteorological record of the diverse aspects of the regional weather at a coastal location in northwest Scotland is that for Stornaway (58° 11' 5" N 6° 22' W, 15m AMSL) see Table 1(for location see Figure 2).

Table 1

Met Office weather data 1971-2000; monthly averages and annual totals for Stornoway (15 m AMSL) (http://www.metoffice.com, 20 October 2004).

Month	Daily Max Temp (°C)	Daily Min Temp (°C)	Monthly Sunshine (hrs)	Monthly Rainfall (mm)	Rainfall >= 1mm (days)
January	7.0	2.0	31.9	141.1	20.3
February	7.0	1.9	62.7	104.5	16.0
March	8.0	2.6	98.9	112.7	19.7
April	9.5	3.7	141.6	70.7	14.5
May	12.1	6.0	196.5	57.3	11.6
June	13.9	8.2	162.3	63.8	12.7
July	15.8	10.3	129.6	72.5	14.1
August	15.9	10.3	132.1	81.7	13.7
September	14.0	8.6	109.5	113.4	17.0
October	11.7	6.4	82.5	134.5	20.3
November	8.9	3.7	43.2	143.8	20.6
December	7.6	2.7	26.0	135.8	20.9
Year	11.0	5.6	1216.8	1231.7	201.4

Over the last 30 years daily maximum temperatures average an August maximum of 15.9°C with the daily minimum dropping to a minimum of 1.9°C in February. May has the highest number of hours of sunshine and the wettest months are November, December and January. The data set reflects a typical Oceanic/Atlantic climate with cool moist conditions, limited temperature fluctuations, and mild winters, which are due to the close proximity of the Gulf Stream.

3.2.4 Deglaciation and Relative Sea-level History Summary

The BIIS (British and Irish Ice Sheet) models for the LGM show the north-western extent of the ice sheet well beyond the study site, and suggest extensive deglaciation beginning *ca* 17.4 ± 1.3 ka BP (Bowen et al., 2002). The subsequent Younger Dryas re-advance centred on Rannoch Moor, and, as reconstructed by Hubbard (1999), reached a northern margin well south of the study site. The main features of changing relative sea-levels in northwest Scotland show a regression from a marine limit between 36.5m OD and 40m OD, dated to 15.9 ka BP (range 15.6-16.3 ka BP) (Shennan et al., 2000) (nearest sites to Lochan An Druim, are Dubh Lochan (Shennan et al., 2000) and Wick River (Dawson and Smith, 1997)). A rapid sea-level fall (*ca* 9mm ^{14}C yr^{-1}) is suggested (Shennan et al., 1995), temporarily slowed by global meltwater discharge *ca* 14.0 ka BP (Shennan, 1999), until the early Holocene, when levels remained stationary before rising to a mid-Holocene maximum (Shennan et al., 1995).

3.2.5 Tephrochronology

Three well documented Icelandic tephra layers from Termination 1 have been recorded in sedimentary sequences in Scotland: the rhyolitic Borrobol Tephra (Turney et al., 1997); the rhyolitic component of the Vedde Ash (Lowe and Turney, 1997), the visible basaltic component of the Vedde Ash (Davies et al., 2001) and the non-visible basaltic component of the Vedde Ash (Mackie et al., 2002); and on the Faeroe Islands, the basaltic Saksunarvatn Tephra (Mangerud et al., 1986; Wastegård et al., 2001). Scotland is distal from the sources of Icelandic ash plumes and so there is limited evidence for visible tephra layers in this area (Davies et al., 2001). However, pioneering work in Scotland on density separation techniques to extract invisible or cryptotephra layers, has been very successful in extending the known limits of such marker horizons (Turney et al., 1997), and indicates a potential for the discovery of hitherto undocumented cryptotephras.

3.2.6 Previous Palynological Studies

The highlands and islands of northwest Scotland lie in the high-latitude North Atlantic Ocean (40°W – 65°N) adjacent to that sector of the ocean which experienced some of the most dramatic Lateglacial and early Holocene climatic shifts (Ruddiman and McIntyre, 1981). Pollen-stratigraphic data have been assembled from Scottish island and mainland sites to develop a regional pattern and chronology of environmental change through this transition (see Figure 2 for locations).

The first extensive investigation of the Lateglacial and early Holocene vegetational history of northwest Scotland was undertaken by Professor Winnifred Pennington, who

published pollen diagrams on a north-south transect of western Scotland (Pennington, 1977a). Interpretation of these pollen stratigraphies, correlated by uncalibrated ^{14}C dating, suggested the climatically conditioned chronozones of the Late-Weichselian as defined by Mangerud et al. (1974), could be recognised, with clear evidence of the Bølling / Allerød Interstadial (GI-1) divided by a very minor regression of vegetation during the Older Dryas (GI-1d) (Pennington, 1977b). This work was later extended to the far northwest of Scotland where the same climatic sequence was inferred at Lochan An Druim (Birks, 1984). Similarly, at Morrone in the eastern highlands of Scotland, where quantitative climate reconstructions from the Lateglacial record identifies a marked cooling consistent with the Older Dryas (GI-1d) event (Huntley, 1994), and at Abernethy Forest where the lowest local pollen assemblage zone has been correlated with this event. However, these records are supported by uncalibrated bulk sediment radiocarbon dates.

Skye has long provided a venue for palaeoecological research. The first pollen analytical work here was carried out on blanket peats by Erdtman (1923), and the first complete profiles published by Vasari and Vasari (1968) and (Birks, 1973). A collaborative research programme has since undertaken pollen-stratigraphic investigations at fourteen sites as part of a major revision of the Lateglacial record from the island (Walker et al., 1988), however these studies are only supported by uncalibrated ^{14}C dates dring the Holocene period. Most recently, work on four new sites (Walker and Lowe, 1990) suggests that these latest records are broadly similar to the Lateglacial sequences described from the mainland (e.g. Pennington, 1977a), and on the Isle of Mull (Lowe and Walker, 1986; Walker and Lowe, 1990). Again, these records are supported by uncalibrated bulk sediment radiocarbon dates.

The Lateglacial and Holocene vegetation of the Western Isles has been reconstructed by Fossitt (1996) from two lacustrine records. However, the resolution of the Lateglacial and early Holocene section is low since the record is confined to only about 10 cm in one profile and 30 cm in the other. In her review of the regional develoment, which included all the published Lateglacial records for the western Isles, Fossitt concludes that all the records show a similar successional sequence, but chronological control and stratigraphical resolution are poor, such that the timing of major vegetaion changes on the islands cannot be identified. Indications of the onset of the first major extenstion of plant cover were before *ca* 15 ka BP in the southeast of the islansds and after *ca* 14.5 ka BP in the northwest. The Younger Dryas (Lateglacial stadial) appears as an interruption of vegetational development characterised by an expansion of *Empetrum nigrum* that peaks during this period.

Similarly, (Whittington et al., 2003) and (Birnie, 2000) have published the only two Lateglacial records for Shetland, Clettnadal and Aith respectively (see Figure 2). However, neither study provides any conclusive evidence for terrestrial vegetational development or changes that could support the Lateglacial interstadial climatic episodes that have been identified on the mainland. Clettnadal registers the opening of the Holocene consistent with the date of the event in the GRIP record, *ca* 11.5 ka BP ice-core yrs BP whilst a lithological boundary marks this transition at Aith where there is no chronology.

3.3 Nikkupierjav'ri

3.3.1 Location

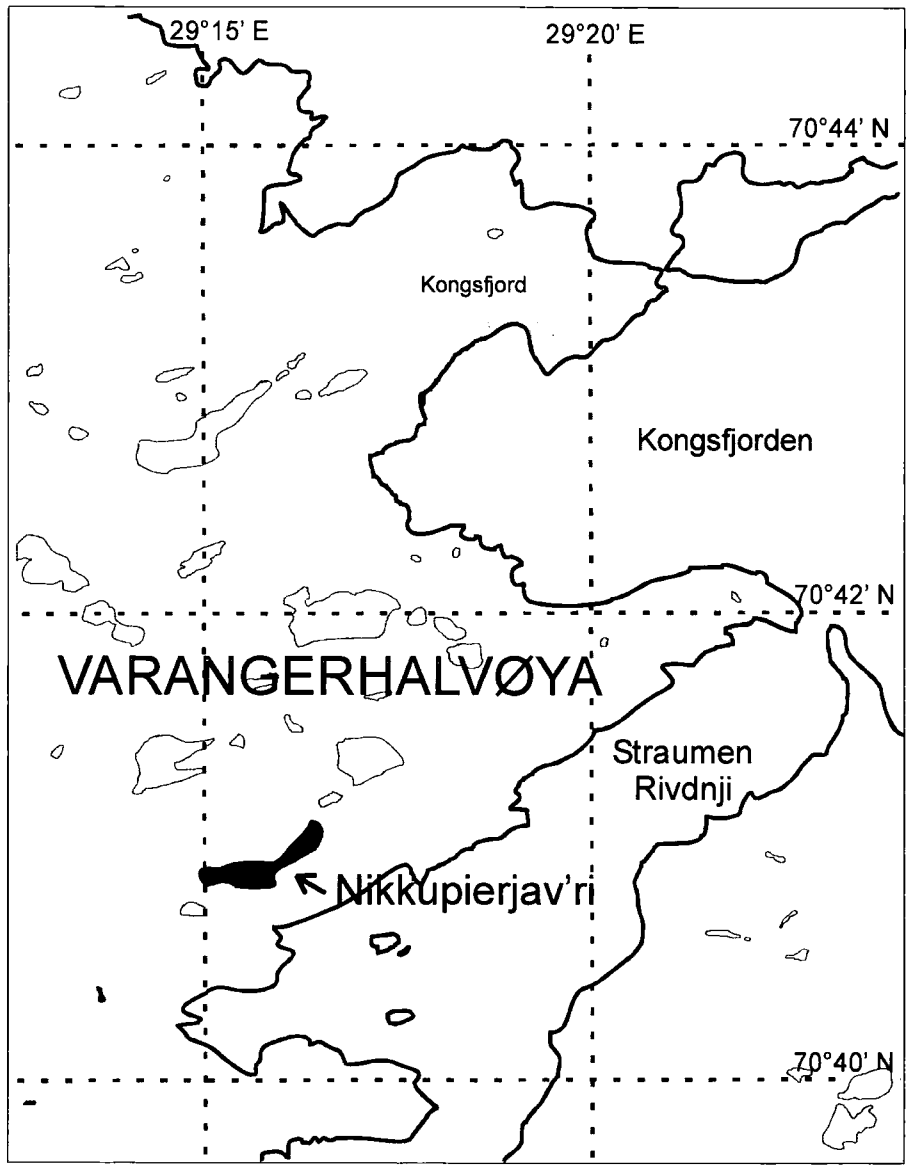

Figure 5

Location of Nikkupierjav'ri on Varangerhalvøya, northern Finnmark, Norway.

Nikkupierjav'ri is an isolation basin (Norwegian GR 35W 0583727; UTM7843549; 70° 40'48"N, 29°15'15"E; altitude 44m asl) lying below the marine limit (*ca.* 54.4m asl) (Sollid et al., 1973) (see Figure 5).

The lake is approximately 1000m long, by 250m wide at its widest point, giving a basin size of ~20ha. There are two sources of inflow: the higher ground to the northeast drains via two smaller vatnets (lakes) into a stream flowing in at the northern end of the

lake; and the higher ground to the west drains via a stream flowing in at the lake's westernmost point. There is one outflow stream, flowing south for 350m into Straumen Rivdnji (see Figures 5 and 6).

3.3.2 Geology and Vegetation

In terms of global vegetation, northern Finnmark lies just beyond the northerly limit of the Boreal zone and into the southern Arctic zone (Meusel and Jäger, 1992). The geology of the region is principally a sedimentary acidic sandstone bedrock of Precambrian-Eocambrian origin (Berglund et al., 1996, p154). In August 2000 the vegetation was recorded at two locations within 1.5 km north of this site: (a) 35W 0583503 UTM7845165; 70° 41.71' N, 29° 15.81' E; 80m asl; and (b) 35W 0583408 UTM7844309; 70° 41.25' N, 29° 15.60' E; 107m asl. The field notes associated with these sites record an Arctic dwarf-heath tundra; taxa recorded include: *Betula pubescens* subsp. *tortuosa*, *Betula nana*, *Empetrum nigrum*, *Rubus chamaemorus*, *Salix herbacea*, *Salix* spp., *Juniperus communis*, *Vaccinium* spp., *Loiseleuria procumbens*, *Phyllodoce caerula*, *Dryas octopetala*, *Campanula* sp., *Bartsia* sp., *Cirsium helenoides*, *Solidago virgaurea*, *Equisetum* sp., *Selaginella* sp., *Eriophorum* spp., *Carex* spp. and mosses (See Plate 1).

Plate 1

Arctic-alpine tundra at 80m asl above Nikkupierjav'ri: *Empetrum* heath with *Betula pubescens* subsp. *tortuosa*, *Betula nana*, *Salix herbacea* and *Juniperus communis* (courtesy Dr JRM Allen).

3.3.3 Climate

The location of Varangerhalvøya in the low lying (0 - 500m altitude) coastal area of the extreme northwestern margin of the Eurasian continent dictates its oceanic climate with a low amplitude of the mean monthly temperatures, despite the Arctic latitude. In addition, the present ameliorating effect of the proximity of the Norwegian Current maintains a temperate climate. The oceanic character of the climate in this area is reflected in the climate data for the period 1931-1960. These give annual precipitation of 400-600mm, January mean temperatures 4°C to 0°C, and July mean temperatures 8°C to 12°C (Berglund et al., 1996, p 156-159). Vadsø provides the nearest meteorological record of the regional weather at coastal locations in eastern northern Finnmark recorded over the last thirty years (for location see Figure 2). The warmest month is July, with an average of 19.2 days with maximum temperature 10°C or higher and 0.9 days with maximum temperature 20°C or higher. Precipitation is generally lower during the summer months with an average 14.3 days with 0.1 mm precipitation or less, however the more extreme precipitation events also occur during the summer months, with an average 1.5 days with 10 mm precipitation or more. Most significantly, there are no records of days with a snow fall of 5 cm or more (weather data for 1971-2000 from the Meteorologisk Institutt http://met.no/english/climate, 20.10.04).

3.3.4 Deglaciation and Relative Sea Level History Summary

In northern Finnmark conspicuous end moraines mark the outer limits of the different recessional stages of the northern limits of the Scandinavian Ice Sheet (SIS). To date, there is no absolute chronology for the timing of deglaciation; however, a baseline (relative) chronology for deglaciation is provided by Sollid et al. (1973). Their model is based on the distribution of glacial and fluvioglacial deposits coupled with a regional map depicting the elevation of the local late Weichselian marine limit. Based on the elevation of these shorelines, three main sub-stages in the retreat of the SIS are identified: Phase 1, the Outer Porsanger and Korsnes substage; Phase 2, the Repparfjord substage; and Phase 3, the main (Tromsø-Lyngen) or Younger Dryas substage. Beyond the Outer Porsanger substage moraine is the less well defined Risvik substage, representing the oldest of the retreat phases in the ice sheet.

Nikkupierjav'ri lies well beyond the Tromsø-Lyngen marginal moraine, reliably dated to the Younger Dryas (11-10 ^{14}C ka BP (Andersen, 1979)) and just inside the Outer Porsanger marginal moraine which crosses the Varanger peninsula and has been dated by correlation with corresponding raised shorelines to *ca.* 14 ^{14}C ka BP (Marthinussen 1974 in: Seppä, 1996) (see Plate 2).

The northern Fennoscandian seaboard lies close to the confluence zone between the dynamically independent Barents Sea and Fennoscandian ice sheets. The Lateglacial history of the interactions between these two ice sheets in the southern Barents Sea region has been evaluated by Vorren and Laberg (1996). Two Lateglacial maxima are indicated - the first before 22 ka BP and the younger after 19 ka BP. They identify a major deglaciation phase initiated during a warm spell between 16 and 15 ka BP, but retarded between 13.7 and 13 ka BP. A close interrelation between summer air temperatures and the expansion and contraction of these ice sheets suggests that most of the ice sheet decay was due to climatic warming. The subsequent halts and re-advances due to climatic deteriorations were caused by influxes of icebergs into the Norwegian Sea, thus cooling surface water and promoting sea ice preservation through the summer.

Plate 2

2km northeast of Nikkupierjav'ri in April 2002 looking northeast over the inlet of Straumen Rivdnji with the snow clearly picking out a section of the Outer Porsanger marginal moraine where it crosses and almost encloses the inlet.

3.3.5 Isolation Basin Characteristics

The sediment core from Nikkupierjav'ri contains the three common stratigraphical units found in basins isolated from the sea by a fall in relative sea level, i.e. the basal clastic unit of marine origin, the brackish transitional unit formed as isolation occurs, and the upper freshwater gyttja deposited after isolation. Theoretically, there are four biostratigraphical isolation contacts that can be defined using diatom analysis Kjemperud (1986). However, it is only the sedimentological isolation contact, recording the change from a predominantly allochthonous (transported) sediment of marine origin to an autochthonous (not transported) freshwater organic deposit, that can be identified in this study.

3.3.6 Tephrochronology

There is no tephrochronological research in this area available to date.

3.3.7 Previous Palynological studies

The Varanger peninsula has long been a focus for Lateglacial and early Holocene palynological studies, due to the fact that it was already ice-free during this period despite its extreme northerly position on the northwest European continental margin. Qualitative interpretations of pollen diagrams from this area have been carried out (Hyvarinen, 1975; Hyvarinen, 1976; Prentice, 1981; Prentice, 1982; Seppä, 1996).

However, only the record at Østervatnet (Prentice, 1981) extends beyond GS-1 (Younger Dryas), where the inferred vegetational history characterises the major Lateglacial climatic oscillations including GI-1d (Older Dryas). The record at Lake Ifjord is supported by a series of calibrated ^{14}C dates from bulk sediment samples (Seppä, 1996) and has been used in quantitative climate reconstructions of the GS-1 (Younger Dryas) to early Holocene transition (Seppä et al., 2002).

Further south along the Norwegian coast palynological studies at three lakes on the island of Andøya in the Vesterålen islands have yielded long late Weischselian sequences: Endletvatn *ca* 18 ^{14}C ka BP (Vorren, 1978); Nedre Æråsvatn *ca* 20 ^{14}C ka BP (Vorren et al., 1988); and Øvre Æråsvatn *ca* 22 ^{14}C ka BP (Alm, 1993). These records provide evidence of a unique early deglaciation in the Scandinavian peninsular (Birks et al., 1994). Here also, the chronology is not detailed but bulk sediment radiocarbon dates again conform to the biozones of Mangerud et al. (1974). For the Lateglacial and early Holocene period, only Nedre Æråsvatn provides a complete record since the other two sequences are incomplete due to low sedimentation rates and several hiatuses (Birks et al., 1994). Analyses of the plant macrofossils at this site has improved the resolution such that the oscillations of GI-1 (Lateglacial Interstadial), including GI-1d (Older Dryas) are differentiated (Alm and Birks, 1991).

In the Sunnmøre area, a more recent multi-proxy study (including pollen) has led to the reconstruction of the palaeoclimate at Kråkenes, with special emphasis on the development of the Lateglacial and early Holocene aquatic ecosystem of the Lake (Birks et al., 2000a). The chronology is developed for one core only, with AMS radiocarbon measurements made on terrestrial plant material, except for the early Holocene where the humic fraction of bulk sediment samples was used. The Holocene dates were calibrated using the Hohenheim dendrochronology and for the Lateglacial by approximation from the Lake Suigetsu chronology (Gulliksen et al., 1998). This age depth model is supported by the fact that the dates attributed to the two tephra layers identified at the site, the Saksunavatn Ash and the Vedde Ash, closely match the GRIP ice-core ages for these tephras (Birks et al., 2000a). There appears to be no differentiation of GI-1d (Older Dryas) at this site.

In the Rogaland area of southwest Norway a suite of four Lateglacial lacustrine sites have been studied by Aage Paus, covering the Lateglacial and early Holocene at Utsira (Paus, 1990), and the Lateglacial at Sandvikvatn (Paus, 1988), Liastemmen (Paus, 1989b) and Eigebakken (Paus, 1989a), and further north in the area of Sunnmøre, a site at Lerstadvatn (Kristiansen et al., 1988). None of these sites have a detailed chronology although there are a few radiocarbon dates that conform to the biozones of Mangerud et al. (1974) (Birks et al., 1994).

The Late Weichselian and Holocene vegetation and environmental history of the northern Timan Ridge, European Arctic Russia, is documented from the LGM up to the present (Paus et al., 2003). The chronology for the site is calibrated according to Stuiver et al. (1998a) and developed from sixteen calibrated AMS dates (usually on terrestrial macrofossils) with seven conventional radiometric dates on bulk sediments and peat, and two TL-dates. Thus providing the most robust correlation of some of the key events during the lateglacial and early Holocene for comparison with this study. (see Figure 2 for locations).

Chapter 4

Methods and Data Analyses

4.1 Fieldwork

4.2 Laboratory Analyses

4.2.1 Lithostratigraphy

4.2.2 Sub-sampling Methods

4.2.3 Analytical Methods

4.2.3.1 Estimate of the Organic Content of the Sub-samples

4.2.3.2 Preparation of Sub-samples for Radiocarbon Dating

4.2.3.3 Pollen Preparation Techniques and Identification

4.2.3.4 Cryptotephra Preparation Techniques and Identification

4.3 Data Analyses

4.3.1 Subjective - Qualitative Inferences

4.3.2 Systematic - Quantitative Analyses

4.3.3 Land - Sea - Ice Correlations

4.1 Fieldwork

The cores were taken using Wright-modified square-rod piston corers (Livingstone) of 5cm and 7.5cm diameter (Wright, 1979).

Lochan An Druim (~ 0.5 ha. surface area) was cored in March 1999, from a floating platform (2.2 x 2.8m) secured by cross ropes in the open water (see Plate 3). The raft surface was taken as datum, and all depth measurements hereafter are given as metres below this datum.

A set of overlapping cores were taken 30cm apart, using the 5cm diameter corer, from the open water in the middle of the lochan, where the sediment water interface was 2.5m below datum (see Figure 6). These cores yielded 9.5m of sediments, with ~1.6m of Lateglacial sediments, and bottomed on sand. The two cores taken were differentiated LAD1 and LAD2, where LAD2 was used for most of the analyses, with LAD1 used only when additional material was needed. The core used by Birks (1984) was recovered from the dense *Phragmites australis* fen on the west side of the lochan.

Plate 3

Coring Lochan An Druim March 1999, taken looking due west (Courtesy Alex Huntley).

Plate 4

Coring in Finnmark April 2001.

Nikkupierjav'ri (~ 20 ha. surface area) was cored in April 2001, from a small wooden platform over a hole (20 cm diameter) drilled in the frozen lake surface (see Plate 4). The platform surface was taken as datum, and all depth measurements hereafter are given as metres below this datum.

The topography of the surrounding land was assessed to estimate the deepest part of the lake, which was likely to hold the maximum amount of accumulated sediment. To find a suitable position for coring, several locations were investigated by drilling through the ice and measuring the depth with a weighted line. Water depth was a limiting factor, since the time and effort required to recover a core was sensibly restricted to ~15m of coring equipment. Several locations were tried before optimum conditions were found, i.e. the deepest possible location in an area where sediment accumulation would be greatest.

A set of overlapping cores taken ~30cm apart, was recovered from the middle of the narrowest part of the lake (see Figure 6), where the sediment water interface was 6m below datum. These cores were taken with the 7.5cm corer and yielded ~3.5m of sediments with ~2.5m of Lateglacial sediments, and bottomed on sand and stone.

At both sites the cores were extruded in the field, and the more fragile sections rolled into plastic gutters to help maintain their structure. Field-notes were taken to record the sequence of core sections, and outline lithologies were drawn. The core sections were then wrapped in plastic film and aluminium foil to help retain moisture and for protection from the air, which can cause oxidation of the minerals. The cores were labelled at this stage, and the top of each section clearly marked. The cores were subsequently stored at 4°C at Durham University; at this temperature there is no freezing action which would damage fine sediment structures, but it is sufficiently cold to minimise fungal or algal growth which are damaging to the organic content of the core.

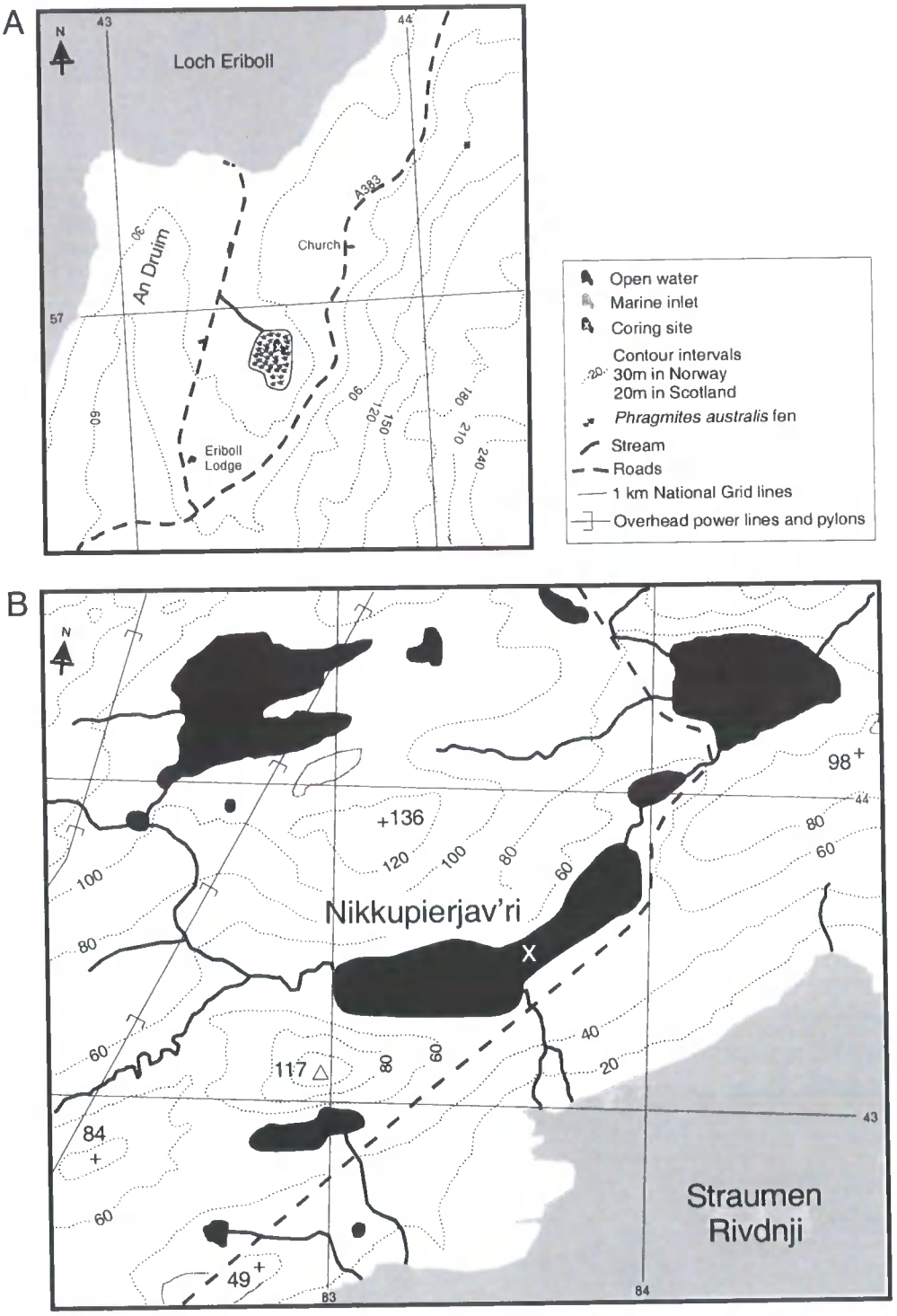

Figure 6

Details of core locations: (A) Lochan An Druim (based on the Ordnance Survey Landranger 9 1:50000 scale); and (B) Nikkupierjav'ri (based on Topografisk Hovedkartserie – M711 1:50000 scale).

4.2 Laboratory Analysis

The laboratory techniques used for the palynological and geochemical studies are described in the following sections.

4.2.1 Lithostratigraphy

The cores were split longitudinally using a cheese wire, to expose uncontaminated sediments suitable for obtaining a photographic record, and then sub-sampling. At this stage, the overall stratigraphy of both the cores suggested that the basal sediments, from the bedrock to just beyond the sharp transition from minerogenic sediments to gyttja, represented the Lateglacial and early Holocene (~1.6m at Lochan An Druim; ~2.5m at Nikkupierjav'ri). The stratigraphies have been described for these Lateglacial and early Holocene sections, following a modification of the Troels-Smith system (Troels-Smith, 1955) as proposed by Aaby and Berglund (1986) (see Tables 4 and 12) and have been generated graphically using TILIAGRAPH (Grimm, 1997) (see Figures 8 and 22).

4.2.2 Sub-sampling Methods

All the core surfaces were scraped clean (by removing the outer *ca.* 2.5mm) prior to any sub-sampling. Adjacent sub-samples for pollen and percentage loss on ignition analysis were taken using a calibrated 0.5cm^3 circular brass sampler. These were initially removed every 2 cm, with areas of particular interest, later resolved down to 1cm intervals. Sub-samples for pollen analysis were stored under glycerol, in glass vials, until they could be analysed; the loss on ignition sub-samples were transferred to weighed porcelain crucibles and analysed directly. A ruler and spatula were used to measure and remove contiguous blocks (5cm x 1cm x 1cm) for tephra analysis, and also to remove smaller regular segments for sieving for macrofossils, potentially suitable for radiocarbon dating.

4.2.3 Analytical Methods

The methods are described for estimating the organic content of the sediment sub-samples, and for extracting and preparing suitable samples for radiocarbon dating. The techniques used in the preparation and identification of pollen and cryptotephra are outlined.

4.2.3.1 Estimation of the Organic Content of the Sub-samples

The estimate of organic content for each sub-sample by calculating the percentage loss on ignition (dry weight) can be used to infer past biological productivity and provide information to help select potential levels for sampling for macrofossils and can provide a potential for core correlation. In addition this calculation conversely provides information about the erosion of sediment from the surrounding landscape as represented by the degree of mineral inwash into the basin.

Sediment sub-samples of 0.5cm^3 were dried in porcelain crucibles of known weight, in a fan oven at 105°C for ~12 hours, and allowed to cool in a desiccator before being re-weighed to get a dry weight. Samples were then transferred to a muffle furnace and left overnight at 550°C, and then allowed to cool in a desiccator before re-weighing to get an ignited weight (Dean Jr, 1974). The percentage loss on ignition (LOI) (dry weight) was then determined as follows:

%LOI of sample (dry weight) = [(dry weight - ignited weight) / dry weight] x 100

Data are displayed within the pollen diagrams (see Figures 15 and 23, 8 and 22) and a table of data is provided in Appendix II.

4.2.3.2 Preparation of Sub-samples for Radiocarbon Dating

The sub-samples for radiocarbon dating (~5cm^3) were taken from strategic points, chosen according to the sediment composition, pollen assemblage zones, the location of cryptotephra horizons and the % LOI (dry weight) results (which gave an indication of the potential amount of carbon). Sub-samples were washed over a 250μm wire mesh (the fine fraction was saved, labelled and stored), which collected any coarse material that might be suitable for radiocarbon dating. This was subsequently examined using a low power binocular microscope, Leica WILD MC3 with variable magnification up to x60. Macrofossil remains of terrestrial higher plants, and where appropriate macro-algae, i.e. seaweeds, were extracted and identified as far as possible, and then cleaned of silt and other contaminants. The presence of other organisms was noted. Samples were air dried overnight at 50°C, and an estimate of total carbon was made, according to the type of material (http://www.radiocarbon.pl/samptypes.htm, 17.08.05) and the weight of the dry sample. The material was then wrapped in aluminium foil and samples were submitted for AMS ^{14}C analysis at: the Ångström Laboratory, Uppsala University, Sweden; the NERC Radiocarbon Laboratory, SUERC East Kilbride, Scotland; or the Poznan Radiocarbon Laboratory, ul. Rubiez 46, PL-61-612 Poznan, Poland.

Terrestrial plant macrofossils were sought to date the tephra horizon S13 (see 5.1.3) at Lochan An Druim but there was insufficient material found in the gyttja at this level and a different strategy had to be adopted. A bulk sediment sample was used, however, as there is a known problem with contamination from old carbon from the carbonate bedrock at this site (Birks, 1984), a further bulk sediment sample coincident with the closest possible plant macrofossil sample was also dated, in order to estimate a correction for the contamination. Results are presented in Tables 5 and 13.

4.2.3.3 Pollen Preparation Techniques and Identification

At the beginning of the analysis, sub-samples of 0.5cm^3 (organic) or 1cm^3 (mineral, i.e. LOI (dry weight) < 10%) were used; however, sub-sample size for the mineral sections was later increased to 4 or 5cm^3 depending on the availability of material, in order to increase the pollen count.

Pollen was extracted from the sediment sub-samples, and prepared for counts by standard methods (Fægri and Iversen, 1964; Huntley and Allen, 1989; Moore et al., 1991). Where necessary, any residues or supernatants were transferred and washed using distilled water, and unless otherwise stated, centrifugation was carried out for 5 minutes at 3000 rpm. The following treatments were carried out in sequence.

Absolute pollen counts were facilitated by the addition of a calibrated suspension of *Eucalyptus ficifolia* grains. These were prepared from a dried sample of *E. ficifolia* collected by Dr Paul Adam in New South Wales, Australia in 1998. The stamens were separated from the flowers and soaked in 10% sodium hydroxide for 1 hour prior to sieving through a 180μm nylon mesh. The suspension of pollen was then washed in distilled water and acetolysed as per the method described below. The cleaned pollen was suspended in 10% glycerol and calibrated using a haemocytometer slide. Three batches were used: 48 000 [SD ± 2.6] grains cm^{-3}; 33 000 [SD ± 2.0] grains cm^{-3}; and 30 000 [SD ± 2.0] grains cm^{-3}. 1cm^3 of a calibrated suspension was added to each sub-sample prior to preparation.

Sub-samples were disaggregated in 10% sodium hydroxide (NaOH), heated in a boiling water bath for 2-5 minutes and then sieved through a 10μm nylon monofilament mesh to remove the bulk of the clay size particles, which were discarded. Sieving was then repeated using a 180μm nylon monofilament mesh (i.e. the pollen fraction 10-180μm). The coarse fraction was collected for later examination of contents and identification where possible.

Following disaggregation and sieving, excess cold 10% hydrochloric acid (HCl) was added to the pollen fraction to test for and remove any carbonates (as indicated by effervescence due to the production of carbon dioxide (CO_2)), and then heavy liquid

separation was used to remove the heavy mineral fraction. Residues were suspended in a saturated zinc chloride solution ($ZnCl_2$; relative density > 1.9 g cm^3), and centrifuged for 15 minutes at 3000rpm.

Acetolysis was then carried out in order to remove cellulose (by acid hydrolysis). Pollen samples were dehydrated by washing twice with glacial acetic (CH_3COOH) acid and then suspended in ~10cm^3 of a fresh mixture of acetic anhydride ($(CH_3CO)_2O$) and concentrated sulphuric acid (H_2SO_4)(9:1), and heated in a boiling water bath for 2 minutes. After washing with glacial acetic acid (CH_3COOH), samples were re-hydrated prior to staining.

Pollen grains were stained with dilute aqueous safranin, and then dehydrated using tertiary butyl alcohol (C_4H_9OH), before being suspended in silicone oil (viscosity 2000cs). A sample of the residue was then placed on a glass slide with further dilution with silicone oil as necessary, and protected with a square cover slip which was secured at the four corners with nail varnish. The combination of viscous oil and the slightly elastic mounting for the cover slip allows, where necessary, the pollen grains to be rolled when under the microscope objective lens, in order to aid identification.

Pollen grains, and spores of Pteridophytes and *Sphagnum* were counted using a compound light microscope, either Leitz Dialux or Leitz Labourlux K, with regular examination at a magnification of x400, and an oil immersion objective x1000 used for more detailed inspection, anisole (C_7H_8O) being used as the immersion medium. Traverses were counted at 1mm intervals across the slide and counts included any grain that entered the field of view. The target count of 300-500 terrestrial pollen grains was not always achievable, especially in the more mineral sediments, so thresholds were chosen according to specific conditions as outlined in sections 5.1.4 and 6.1.4. These data are presented in both proportional and absolute terms using traditional pollen diagrams generated in TILIAGRAPH (Grimm, 1997) (see Figures 15, 16, 23 and 24). The pollen diagrams include both a % LOI (dry weight) curve and a curve for the total concentration of terrestrial pollen, where an indication of the frequency of sampling is expressed as bars on these curves. The terrestrial pollen sum for each sub-sample is indicated on the percentage pollen diagrams. Indeterminable grains have been classified into four groups according to Birks (1973): deteriorated (degraded+corroded), obscured, crumpled and broken. However, for presentation purposes these numbers have been combined, together with the number of grains that could not be identified, and used to give one figure for all indeterminable grains.

Relative proportions of each taxon, and the indeterminable pollen, are plotted with respect to the given pollen sum as indicated below. In order to examine the regional vegetational history the terrestrial pollen sum excludes obligate aquatic plants and taxa

that represent the local lowland mire vegetation (Janssen, 1976-7; Prentice, 1988). *Pinus* has also been excluded from the terrestrial pollen sum. There is no Lateglacial or early Holocene macrofossil evidence for *Pinus* at Lochan An Druim (Birks, 1984), or in more southerly areas of Scotland in either the Morrone Birkwoods (Huntley, 1994) or Abernethy forest (Birks and Mathewes, 1978), nor is *Pinus* represented as far south as Llanilid in South Wales (Walker et al., 2003). According to Huntley and Birks (1983) the earliest colonisation of *Pinus* dates to *ca* 8.8 ka BP (8.0 ^{14}C ka BP). Similarly, for Nikkupierajav'ri, there is no Lateglacial or early Holocene macrofossil evidence for *Pinus* in northern Finnmark at this time, and according to Huntley and Birks (1983) the earliest colonisation of *Pinus* here dates to *ca* 7.8 ka BP (7.0 ^{14}C ka BP). Jensen and Vorren (2002) have found evidence of *Pinus* macrofossils and suggest that the first *Pinus* individuals may have become established *ca* 9.7 to 9.6 ka BP in central Troms (approximately 600 km south west of Nikkupirerajav'ri. Therefore it is proposed that the presence of *Pinus* pollen at either of the study sites would not indicate a local or even regional presence for this taxon (see 5.1.4 and 6.1.4). Therefore, pollen sums are specified as follows for selected taxa: Terrestrial Pollen (ΣTP), i.e. Arboreal Pollen minus *Pinus* (AP) plus Non-Arboreal Pollen (NAP); Terrestrial Pollen and Terrestrial Pteridophyte Spores (ΣTP + ΣPS); Terrestrial Pollen and Aquatic Pollen (including *Sphagnum*) (ΣTP + ΣAP); Terrestrial Pollen and Indeterminable Pollen (ΣTP + ΣIP). In addition, proportional curves for *Pinus* have been developed individually for each site by including the *Pinus* count in the ΣTP, i.e. AP plus *Pinus*, plus NAP.

Absolute pollen counts have been calculated with reference to the *Eucalyptus ficifolia* counts, (i.e. a known quantity of exotic grains were added to a specific volume of wet sediment) giving pollen concentration values [Pollen Sample] as follows:

[Pollen Sample] grains cm^{-3} =

Pollen Counted x [Eucalyptus Spike] x Volume Eucalyptus Spike / Eucalyptus Grains Counted x Volume of Sample

Data tables are given in Appendix II.

Identification of pollen grains and spores of Pteridophytes and *Sphagnum* was carried out to the lowest possible taxonomic category following the set of conventions for naming the morphological categories proposed by Birks (1973) and used by Moore et al. (1991). Pollen identification was based principally on Moore et al. (1991) and the substantial photographic collection by Reille (1992), as well as the reference collection held at the University of Durham. Pollen nomenclature follows that recommended by Berglund and Ralska-Jasiewiczowa (1986) and plant nomenclature follows that used in the *Flora Europaea* (Tutin et al., 1964-1993).

The coarse fraction (>180μm) from all the sub-samples was examined using a low power binocular microscope (Leica WILD MC3) with variable magnification up to x60, and the presence of plant remains and other organisms was recorded with the pollen macrofossil data.

4.2.3.4 Cryptotephra Preparation Techniques and Identification

The Lateglacial sections of the cores were sub-sampled contiguously using 'vertical' 5 x 1cm^3 sub-samples, which were then analysed for the presence of cryptotephra shards. Where cryptotephra was present, the 5cm section was re-sampled using 'horizontal' 5 x 1cm^3 sub-samples (see Figure 7), in order to enumerate the peak counts and hence resolve more closely the level of maximum deposition and the spread of shards about that point.

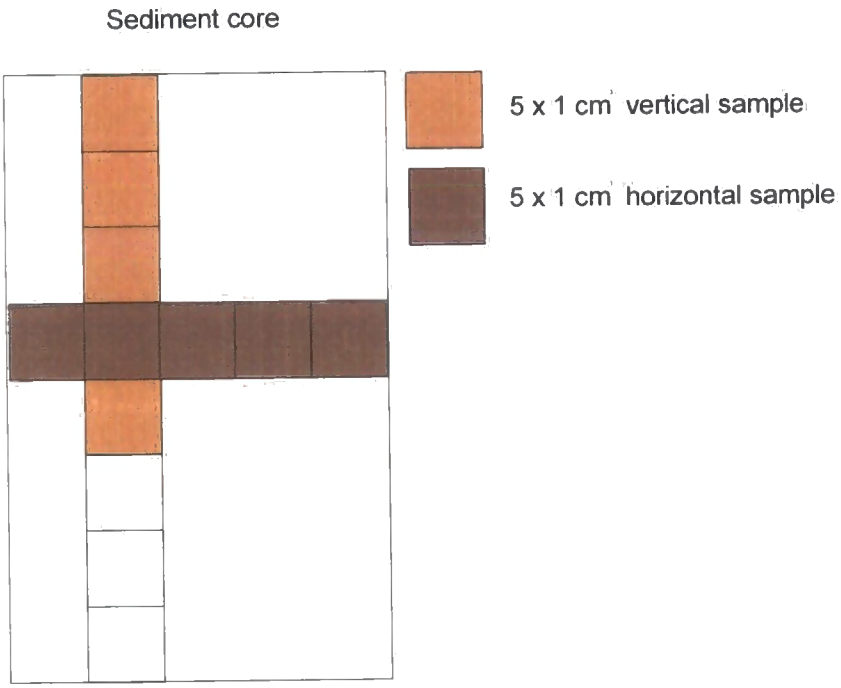

Figure 7

Illustration of the sampling pattern used to remove sub-samples for cryptotephra analysis.

There was insufficient material remaining in the core LAD2 to take the necessary horizontal sub-samples for the vertical sub-sample between 10.92m and 10.96m. It was therefore necessary to use the parallel core LAD1. The cores were matched by eye using the closest lithological boundaries and an organic band. The correlation of the two cores was subsequently confirmed by the AMS dates: LAD1 10.94m at 8590±50 cal yrs BP; and LAD2 10.95m at 8689±50 cal yrs BP.

Sub-samples were prepared for cryptotephra analysis using the density separation technique outlined by Turney (1998), which is particularly suitable for concentrating

cryptotephra particles from mineral-rich lacustrine sediments. Where necessary, any residues or supernatants were transferred and washed using distilled water, and unless otherwise stated, centrifugation was carried out for 10min at 2500 rpm. Standard methods, which included the following series of treatments, were carried out in sequence.

Acid digestion of the sediment sub-samples was carried out by refluxing in hot concentrated nitric acid (HNO_3) for 90 minutes at ~180°C, which removes the organic and calcareous material (Daniell et al., 2000). The residue was then heated in 0.3M sodium hydroxide (NaOH) for *ca* 3 hours at 80-90°C, to remove as much of the biogenic silica as possible (this leaves the more robust forms of silica, amorphous and minerogenic) (Rose et al., 1996). It was then sieved through a 10μm nylon monofilament mesh to remove fine silt and clay particles. Heavy liquid separation, using sodium polytungstate ($Na_6(H_2W_{12}O_{40}).H_2O$) as a flotation medium, was then used to remove the heavier material and hence concentrate any cryptotephra particles present. A relative density value of 2.5 g cm^{-3} was chosen as the optimum density for recovering the rhyolitic cryptotephras that might be encountered at these study sites (Turney et al., 1997). Residues were suspended in the solution and centrifuged for 20 minutes at 2500rpm. Following this treatment some samples were found still to be contaminated with large quantities of diatoms; these were mostly removed by a further density separation at a relative density of 2.0 g cm^{-3}.

For the first set of samples (5cm^3 'vertical'), the residues were slowly pipetted onto warm microscope slides, allowing the water to evaporate, before being mounted in Canada Balsam. Cryptotephra shards were then identified by optical examination using a polarizing light microscope Leica DM/LM. Slides were initially examined with crossed polars and a 1λ compensator inserted, at a magnification of x100, in order to identify isotropic grains. These were then examined critically at a magnification of x400 using the Becke Line Method (Strobier and Morse, 1994), in which plane-polarised light is used to determine the sign of relief of the isotropic grains. Using this method, when the distance between the sample and the objective is increased, the Becke Line appears in the material of higher refractive index (n); i.e. where $n_{cryptotephra} < n_{canada\ balsam\ (1.54)}$ the relief is negative. Cryptotephra shards were subsequently positively identified on the basis of their morphology and relief (*cf* (Dugmore et al., 1995; Mangerud et al., 1984), and the presence of shards per sample was recorded.

For the second set of samples (5cm^3 'horizontal'), the residues needed to be retained for subsequent geochemical analyses, so they were each made up to 0.5cm^3 with distilled water, and a single drop was mounted and examined, and then returned to the tube. Tephra shards were positively identified on the basis of their morphology, and the

total number of shards per drop (i.e. the residue from a $5cm^3$ sample of wet sediment suspended $0.5cm^3$ of distilled water) was recorded. Results are presented in Table 6 and Figure 9.

The residues from the samples with peak shard counts were dried on duplicate frosted glass slides, where specific areas had been marked out and labelled for each sample. The grains in each discrete area were then incorporated into an epoxy resin by mixing with a fine wooden stick and left overnight to cure. The dried resin films were ground to a uniform 75μm, and then polished using first 6μm and then 1μm-diamond paste, and where necessary slides were cleaned in an ultrasonic bath. Both slides were carbon coated prior to geochemical analysis, and the ends of the slides and the sample areas on each slide were connected with aquadite to improve electrical transmission (A J Newton Pers. Comm.).

Quantitative geochemical analysis of the micro-tephra shards was undertaken on a CAMECA SX100 Electron Probe Microanalyser, at the Tephrochronology Analytical Unit, Department of Geology and Geophysics, University of Edinburgh, UK. Nine major elements were measured, using a standard WDS (wavelength dispersive spectrometry) technique with an accelerating voltage of 20keV, a beam current of 4nA, and with a raster beam size: scan:5.0μm. Calibration was carried out using standards of known composition (pure metals, synthetic oxides, and simple silica compounds), and at regular intervals throughout the analytical sessions an andradite (Ca_3 Fe_2 Si_3 O_{12}) sample of known composition was analysed to control for any variation in the machine operating conditions. Sequential acquisition of elemental data with the WDS technique enables monitoring of sodium mobilisation. A rejection threshold for shard data, of 95%, was applied because totals in the range 95-97% are consistently reproducible from tephra found at British sites. Lower totals are probably a reflection of partial alteration of the volcanic glass which increases with increasing vesicularity, reducing glass thickness and increasing surface area to volume ratios (Dugmore et al., 1995). The results are presented in Tables 7, 8 and 9.

4.3 Data Analyses

Independent chronologies have been developed for both stratigraphies, with age-depth models (cal yrs BP, m(BD)) using various combinations of (a) ages for the tops of the cores (-49 yrs for Lochan An Druim, and -51yrs for Nikkupierjav,ri), (b) the accepted AMS radiocarbon dates, (c) literature dates associated with the known tephra horizons and (d) published palynological dates. The sediment stratigraphy was then used as a guide to major changes in sedimentation rate so that linear segments or polynomial

curves could be extrapolated to these boundaries in order to complete the model. Hence, the sample ages have been determined by interpolation.

Pollen diagrams have been drawn using TILIAGRAPH (Grimm, 1997). and CorelDRAW™. Taxa have been grouped into arboreal pollen taxa and non-arboreal pollen taxa, terrestrial Pteridophytes, and aquatics (including *Sphagnum*), and plotted against a continuous age scale interpolated from the age-depth model (a depth scale is also presented for reference). Exaggeration x10 has been used to better illustrate the less abundant taxa. Data for all taxa are presented in Appendices III and IV, but summary diagrams with selected taxa have been used to best illustrate the trends that are discussed throughout the text (see Figures 15 and 23). An individual proportional curve for *Pinus* has been plotted with respect to an (AP+NAP) sum that includes *Pinus*, since this pollen curve can provide information relating to its remoteness from the site.

Pollen influx diagrams (grains cm^{-2} yr^{-1}) for selected taxa have been developed in combination with the age-depth models, with estimates obtained by multiplying the observed pollen concentration (grains cm^{-3}) by sediment deposition time (cm yr^{-1}) (see Figures 16 and 24).

The coarse fraction of the pollen sub-samples contains material that is representative of the local flora and fauna and presence/absence data have been tabulated and used to help interpret the pollen record. However, these data do not contribute to the numerical and systematic data analyses, which are aimed at interpreting the regional signal (see Figures 17 and 25).

Analysis of these palynological data has involved the use of several different methods in order to infer the character of the palaeovegetation and palaeoenvironment at the two locations. Initially, subjective qualitative techniques were used and these were subsequently developed further by applying systematic quantitative analysis.

4.3.1 Descriptions of the Pollen Zones

The pollen stratigraphical sequences have been sub-divided into a series of local pollen assemblage zones (LPAZs), on the basis of variations in the relative curves for the principal taxa (typically, *Betula*, Ericales, Gramineae etc.), and guided by a constrained incremental sum of squares (CONISS) analysis using data for all terrestrial taxa, and carried out within the TILIA program (Grimm, 1987). These LPAZs are used as a framework in which to discuss the palaeovegetation and inferred palaeoenvironment at each study site (see Figures 15 and 23).

4.3.2 Systematic - Quantitative Analysis

The regional palaeovegetation and palaeoenvironment represented at both study sites have been quantitatively re-constructed enabling inference of the prevailing climatic factors.

A systematic method for pollen-based palaeobiome reconstruction, initially developed by Prentice et al. (1996) has been applied to the proportional pollen data from all the arboreal and non-arboreal pollen taxa. This provides a basis for quantitative inference of the regional palaeo-macroclimate since each palaeobiome has a modern analogue that is associated with a particular range of climatic conditions (Prentice et al., 1992). This method uses two key rule-sets. The first allocates each pollen taxon to one or more of a set of plant functional types (PFTs) which have been defined according to the stature, leaf form, phenology and climatic adaptations of the plant species contributing to the pollen taxon (Prentice et al., 1992). The second rule-set determines those PFTs that contribute to the affinity score for each of a set of inferred biomes. It is based upon the relationships between the patterns of occurrence of pollen of each PFT in surface samples and the biomes from which those samples are derived (Allen et al., 2000). This assignment of PFTs to biomes has been modified by Tarasov et al. (1998) to improve the distinction between the non-arboreal warm and cool steppes. This was done by broadening the scope of criteria for selecting PFTs by assigning a wider range of herbaceous and arboreal taxa across the set, then-modifying the rule sets used to assign PFTs and biomes. An additional step was then added to the biomization process to use evidence from the tree taxa represented in the pollen spectrum to determine the eventual PFT assignments of herbaceous and shrub taxa that may ambiguously represent either cool or warm steppe. The rule sets that apply to this study and which are used in this method are presented in Tables 2 and 3.

The data for *Pinus* have not been included in this analysis. The argument for *Pinus* not being established in the vegetation at either site is discussed in section 4.2.3.3, and since the data used to develop the palaeobiomes uses proportional data, it was felt that the inclusion of *Pinus* could influence the final biome determinations, particularly at Nikkupierjav'ri where the Lateglacial pollen counts were especially low.

Table 2

Assignment of the pollen taxa in this study to plant functional types (PFTs).

PFT code	PFT	Pollen taxa
cgs	cool herb/shrub	*Oxyria*-type (mountain sorrel), Polygonaceae undiff. (dock and knotweed family), *Rumex* (dock).
wgs	warm herb/shrub	*Armeria* (thrift), Cruciferae (Brassicaceae) (cress family), Crassulaceae (stonecrop family), *Hypericum* (St John's wort).
sf	steppe forb/shrub	Caryophyllaceae (pink family), Compositae (Asteraceae) (daisy family), Compositae subfam. Tubuliflorae (Asteroideae) (aster sub-family), Compositae subfam. Liguliflorae (Cichorioideae) (chicory sub-family) *Chamaenerion* (rosebay willowherb), *Filipendula* (meadowsweet), *Galium*-type (bedstraw), *Geum* (avens), *Plantago* undiff. (plantain), *Potentilla* (cinquefoil), Ranunculaceae (buttercup family), Rosaceae undiff. (rose family), *Thalictrum* (meadow rue), Umbelliferae (Apiaceae) (carrot family), *Urtica* (nettle).
sf/df	steppe/desert forb/shrub	*Artemisia* (wormwood), Chenopodiaceae (goosefoot and orache family).
g	grass	Gramineae (Poaceae)(grass family).
h	Heath	Ericales (heath family), *Calluna* (ling).
s	sedge	Cyperaceae (sedge family).
aa	arctic-alpine dwarf shrub/herb	*Betula nana*-type (dwarf birch), *Dryas octopetala* (mountain avens),Saxifragaceae (saxifrage family), *Saxifraga* cf. *S. stellaris* (starry saxifrage), Salix (willow).
ab	arctic/boreal herb	*Rubus chamaemorus* (cloudberry).
bs	boreal summergreen tree	*Betula* (birch).
ec	eurythermic coniferous tree/shrub	*Juniperus*-type (juniper), *Pinus* subgen. *Diploxylon* (yellow pine).
bts	boreal/temperate summergreen shrub	Cornaceae (dogwood family), *Sorbus* (mountain ash).
bs/ts	boreal/temperate summergreen tree/shrub	*Alnus* (alder), *Populus* (poplar), *Salix* (willow).
ts	temperate summergreen tree/shrub/liane	*Quercus robur*-type (oak).
ts_1	cool-temperate summergreen tree/shrub	*Corylus* (hazel),*Tilia* (lime), *Ulmus* (elm).
ts_2	warm-temperate summergreen tree/shrub/liane.	Cannabaceae (hemp family).

Table 3

Assignment of plant functional types (PFTs) found in this study, to the appropriate biomes

Biome	PFTs
cold mixed forest	(h), bs, ec, bs/ts, (ts_1), ab
temperate deciduous forest	(h), bs, ec, bts, bs/ts, ts, ts_1
cold deciduous forest	(h), bs, ec, (ab)
warm steppe	wgs, sf, sf/df, g
cool steppe	cgs, sf, sf/df, g
shrub tundra / dwarf-shrub tundra / prostrate shrub tundra / cushion-forb–lichen–moss tundra	g, h, s, aa, ab

Note 1) - PFTs in parentheses are restricted to part of the biome.

The results of biomization of the pollen spectra for Lochan An Druim are presented in Figure 19 and for Nikkupierjav'ri in Figure 27. The assigned biomes are shown plotted along a stratigraphic plot of sample scores on the first axis of the detrended correspondence analysis (DCA) of the proportional pollen data, which was carried out within the TILIA program (Grimm, 1987).

The influence of climate on terrestrial plants has been shown to be expressed through at least three distinct controlling variables: tolerence of low temperature extremes; requirements for accumulated warmth during the growing season; and tolerence of moisture deficiency (Huntley, 2001). The case has been made for using these three bioclimatic variables together to determine species' overall range (e.g. Huntley et al., 1995; Sykes et al., 1996). These indicative climate variables are expressed as: the mean temperature of the coldest month (MTCO °C); the annual temperature sum above 5°C (GDD5 degree days); and the estimated ratio of actual to potential evapotranspiration (AET/PET).

Biomization implicitly infers a broad range of indicative climate variables, since each biome is developed from several different PFTs. For example, the presence of the 'temperate deciduous forest' biome implies that the MTCO lies above -15°C, the GDD5 is above 1200° days, and the AET/PET is high, generally above 0.8, although temperate summergreen trees can occur as long as AET/PET is above 0.65. This approach, however, does not directly utilise the large amount of quantitative information provided by the palynological data (Allen et al., 2000). In order to improve the quantitative estimates of palaeoclimates made by biomization, the method of

pollen-climate response surfaces, developed by Bartlein et al. (1986) and Huntley (1993) has been applied to the palynological data.

These palaeoclimate reconstructions, following Huntley (1993), use pollen-climate response surfaces fitted to pollen data for 7816 surface samples, which provide direct analogues from across the temperate and boreal latitudes of the northern hemisphere. These are fitted in a three-dimensional climate space derived from an extensive modern climate database (Leemans and Cramer, 1991), with axes of the indicative climate variables MTCO, GDD5 and AET/PET. All the major taxa and some of the minor taxa that have climate indicative value[1] are utilised, and actual values are calculated using the algorithms of the Prentice et al. (1992) BIOME model. Potential analogue pollen spectra are then interpolated at intervals of 1°C for MTCO, 100 degree days for GDD5 and 0.025 for AET/PET. This process serves to smooth the data, thereby removing some of the 'noise' and it also eliminates any problems associated with replication in the sample set (i.e. a cluster of samples in the same area providing a majority of the ten closest samples identified in the subsequent analysis using fossil pollen). Each fossil pollen spectrum was compared with the response surface in order to identify the "closest" 10 interpolated analogues, but subject to the constraint that they represented the same biome as had been reconstructed for the fossil pollen spectrum. This "closeness" distance is measured in terms of chord distance that expresses the degree of analogy (i.e. dissimilarity). Reconstructed bioclimate values were then calculated as the distance-weighted mean of the values for these 10 closest analogues. The mean chord distance indicates the overall reliability of the reconstructed value, and the standard error provides an indication of the likely precision.

The results of the palaeoclimate reconstructions for Lochan An Druim and Nikkupierjav'ri are discussed in section 5.2.4.2.

4.3.3 Land - Sea - Ice Correlations

The GRIP event stratigraphy scheme provides a standard profile for the entire North Atlantic region (Renssen and Isarin, 2001a). This sequence of climatic events, as recognised in the GRIP ice-core record and recommended by INTIMATE (Björck et al., 1998; Walker et al., 1999) as the standard for comparison, has been used throughout this study. It provides a framework for the interpretation of the individual study sites and a means of teleconnection between the study sites. The GRIP $\delta^{18}O$ record (Dansgaard

[1] *Abies*, *Alnus*, *Betula*, *Carpinus betulus*, *Castanea*, *Cedrus*, *Corylus*, *Ephedra*, *Fagus*, *Juniperus*-type, *Larix*, *Olea*, *Ostrya*-type, *Phillyrea*, *Picea*, *Pinus* subgen. Diploxylon, *Pinus* subgen. Haploxylon, *Pistacia*, *Quercus robur*-type, *Quercus ilex*-type, *Salix*, *Tilia*. *Ulmus*, *Artemisia*, Chenopodiaceae, Cyperaceae, Ericales (Ericaceae plus *Empetrum*) and Gramineae

et al., 1993; Johnsen et al., 1992) has been plotted alongside the appropriate summary diagrams for Lochan An Druim and Nikkupierjav'ri with their own independent timescales (calibrated ^{14}C years BP for the pollen records, with GRIP ice-core years (Johnsen et al., 1997)) (see Figures 15 and 23). Marine data indicating deglacial surface circulation changes in the northeastern Atlantic recorded off northwest Scotland (Kroon et al., 1997) are also provided for correlation (see Figure 28). Marine data from the eastern North Atlantic documenting rapid changes in ocean circulation and SSTs (Birks and Koç, 2002; Koç et al., 1993) are also discussed.

Chapter 5

The Lateglacial and early Holocene Palaeovegetation and Palaeoenvironment at Lochan An Druim in northwest Scotland

5.1 Results

5.1.1 Sediment Stratigraphy

5.1.2 Radiocarbon Chronology

5.1.3 Tephrochronology

5.1.4 The Age-Depth Model

5.1.5 Correlation with Greenland Ice Record

5.1.6 Pollen Analyses

5.1.7 Pollen Influx

5.1.8 Descriptions of the Pollen Zones

5.1.9 Macrofossil Analyses

5.1.10 Systematic - Quantitative Analyses

5.1.10.1 Palaeobiome Reconstructions

5.1.10.2 Palaeoclimate Reconstructions

5.2 The Palaeoenvironment at Lochan An Druim

5.1 Results

5.1.1 Sediment Stratigraphy

A description of the sediments for the Lateglacial and early Holocene section of the core from Lochan An Druim is presented in Table 4. The lithological boundaries are identified, principally according to the proportion of organic material.

Sedimentation commences at 12.18m(BD), which provides evidence for deglacial activity and hence gives a projected date for deglaciation beyond 15.0 ka BP. The lowermost 1.6m of sediments from the core LAD2, contain the 'tripartite' lithological sequence typical of Lateglacial successions in Britain (e.g. Lowe and Walker, 1986; Walker et al., 1988; Walker and Lowe, 1990): minerogenic-organic-minerogenic, underlying the uniformly organic sediments of the Holocene. This sequence commences with a minerogenic basal unit of glacial sand and clay (Lith1), with a well defined lithostratigraphic boundary at 12.00m, at the onset of some organic accumulation. This is overlain by 0.35m of organic rich silts and clays (Lith2), divided by a fine organic band (6mm) at 11.782m. These are in turn overlain by a predominantly minerogenic unit, 0.47m of silts and clays (Lith3), with two organic bands between 11.30 and 11.33m. There is a well defined boundary at 11.18m, above which lie the organic rich gyttja sediments (Lith4), which extend to the lake bed.

Table 4

Description of the Lateglacial and early Holocene sediments from Lochan An Druim following Troels-Smith (1955) as proposed by Aaby and Berglund (1986). Four categories of physical qualities are described as follows: nigror (nig.) - the degree of darkness; stratificatio (strf.) - the degree of stratification; elasticitas (elas.) - the degree of elasticity; and siccitas (sicc.) - the degree of dryness.

Lithological Section	Depth m(BD)	Physical Properties				Texture	Munsell Colour			Characterisation following Troels-Smith (1955)				Description
		nig.	strf.	elas.	sicc.									
Lith.4	10.50 - 10.67	3	0	2	2	firm / rubbery	7.5YR	2/0	black	Ld^1 3	Ag 1		Dg+	silt with fine organic detritus / darkens with exposure to air
	10.67 - 11.18	3	0	2	2	firm / rubbery	10YR	2/1	black	Ld^1 3	Ag 1		Dg+	silt with fine organic detritus / darkens with exposure to air
Lith.3	11.18 - 11.31	1	0	1	2	firm / rubbery	2.5Y	4/2	dark grayish brown	As 2	Ld^1 1	Ag 1	Dg+	clay / silt with few fine organic detritus
	11.31 - 11.325	4	0	0	0	loose / coarse	5Y	2.5/1	black	Dg 3	Ld^1 1			organic band
	11.325 - 11.65	1	0	1	2	firm / rubbery	5Y	4/1	dark gray	As 2	Ld^1 1	Ag 1	Dg+	clay / silt with few fine organic detritus
Lith.2	11.65 - 11.782	2	0	2	2	firm / rubbery	2.5Y	3/2	very dark grayish brown	Ld^1 2	Ag 1	As 1	Dg+	clay / silt with fine organic detritus
	11.782 - 11.788	4	0	0	4	loose / coarse	5Y	2.5/2	black	Dg 3	Ld^1 1			organic band
	11.788 - 12.00	2	0	1	2	firm	5Y	4/2	olive gray	Ld^1 2	Ag 1	As 1	Dg+	silt and clay with fine organic detritus
Lith.1	12.00 - 12.15	1	0	0	1	firm	5Y	5/1	gray	Ag 3	Gmin 1		Dg+	clay
	12.15 - 12.18	0	0	0	1	firm	5Y	5/2	olive gray	Gmin 4			Ag+	sand

The %LOI (dry weight) curve (see section 5.1.6 below) supports these broad divisions with very low values in the minerogenic units Lith1 (mean 1.08 [SE ±0.11]) and Lith3 (mean 4.77 [SE ±0.18]) excluding the organic band about 11.32m), and higher values in the more organic units Lith2 (mean 13.04 [SE ±1.56]) and Lith4 (mean 39.86 [SE ±1.54]).

5.1.2 Radiocarbon Chronology

The sample information and the results of AMS radiocarbon dating of terrestrial macrofossils and bulk sediment samples are shown in Table 5. The results are corrected for isotopic fractionation by normalising to -25‰ relative to PDB standard using measured $\delta^{13}C$ values. These AMS radiocarbon dates have been calibrated using CALIB REV4.4.1, using the calibration data set INTCAL98, based on dendrochronologically dated tree rings, uranium-thorium dated corals and varve-counted marine sediment (Stuiver et al., 1998a).

The results for the plant macrofossil samples RC1, RC2, RC3, RC4 and RC8(2), present a chronological sequence with depth (Samples RC5 and RC6 are from the study site Nikkupierjav'ri). However, it was considered that the results for RC3 at 11.65m and RC4 at 11.28m were indistinguishable, since their ranges overlapped, so these have been averaged to give one date of 12,335 cal yrs BP at 11.435m. Results for RC8(1), RC8(2) and RC7 are discussed in section 5.1.3.

Table 5

Terrestrial macrofossil and bulk sediment sample information, and results of AMS radiocarbon dating using CALIB 4.4.1(Stuiver and Reimer, 1993) with INTCAL98.14c calibration data set (Stuiver et al., 1998a), information provided after Lowe and Walker (2000).

Sample	Laboratory Number	Depth m(BD)	Material	Sample Dry Weight (mg)	Estimated Carbon Content (%)	^{14}C Ka BP	δ^{13}C‰ PDB	Calibrated range Ka BP (2σ)	Relative Area Under Probability Distribution	Mid-point of the 2σcalibrated range BP (to nearest 10yrs)
RC1	Ua-21239	12.00	mixed Spermatophyta leaves	10.3	40	12 625 ±100	-27.8	14 265 – 15 620	1.00	14 940 ± 678
RC2	Ua-21240	11.77	mixed Spermatophyta leaves and stems	9.6	40	11 095 ±75	-30.9	12 872 – 13 218	0.914	13 040 ±173
RC3	Ua-21241	11.65	mixed Spermatophyta leaves and stems	12.1	40	10 465 ±75	-29.0	12 070 – 12 837	0.968	12 450 ±384
RC4	Ua-21242	11.28	mixed Spermatophyta leaves and stems	8.5	40	10 345 ±100	-28.4	11 746 – 12 681	0.955	12 220 ±468
RC8(1) (LAD2)	POZ-6527	10.95	organic gyttja (bulk)	915.4	35	10 010 ±50	no information	11 254 – 11 694	0.961	11 470 ± 220
RC8(2) (LAD2)	POZ-6526	10.95	mixed Spermatophyta leaves and stems	2.3	40	8 680 ±50	no information	9 538 – 9 781	0.955	9 660 ±122
RC7 (LAD1)	POZ-6525	10.94	organic gyttja (bulk) [-offset 1330 ^{14}C years]	412.3	38	9 920 ±50 [8 590 ±50]	no information	11 197 – 11 364 [9 488 – 9 633]	0.736 0.870	11 280 ±84 [9 560 ±73]

5.1.3 Tephrochronology

Analyses of the first run of tephra extractions (5cm^3 'vertical') identified four horizons containing cryptotephra (size range 10-100μm): (1) 10.87 – 10.96 (S13); (2) 11.12 – 11.16; (3) 11.32 – 11.36 (S21); and (4) 11.82 – 11.96. Subsequently, analyses of the second run of extractions (5cm^3 'horizontal') provided a quantitative estimate of the peak counts (see Table 6, peak counts in bold), and the spread of shards about that point for each horizon (see Figure 8)

Table 6

Number of shards of cryptotephra per drop (tephra float from 5cm^3 wet sediment in 0.5cm^3 distilled water).

Horizon	Depth m(BD)	Sample	no. shards
1	10.87		5
	10.88		11
	10.89		9
	10.90		61
	10.91		30
	10.92		128
	10.93		290
	10.94	S13	**600+**
	10.95		10
	10.96		55
2	11.12		1
	11.13		0
	11.14		2
	11.15		1
	11.16		4
3	11.32	S21	**21**
	11.33		3
	11.34		1
	11.35		0
	11.36		0
4	11.82		0
	11.83		0
	11.84		0
	11.85		0
	11.86	S30	**9**
	11.87		1
	11.88		0
	11.89		2
	11.90		1
	11.91		3
	11.92		0
	11.93		0
	11.94		0
	11.95		0
	11.96		0

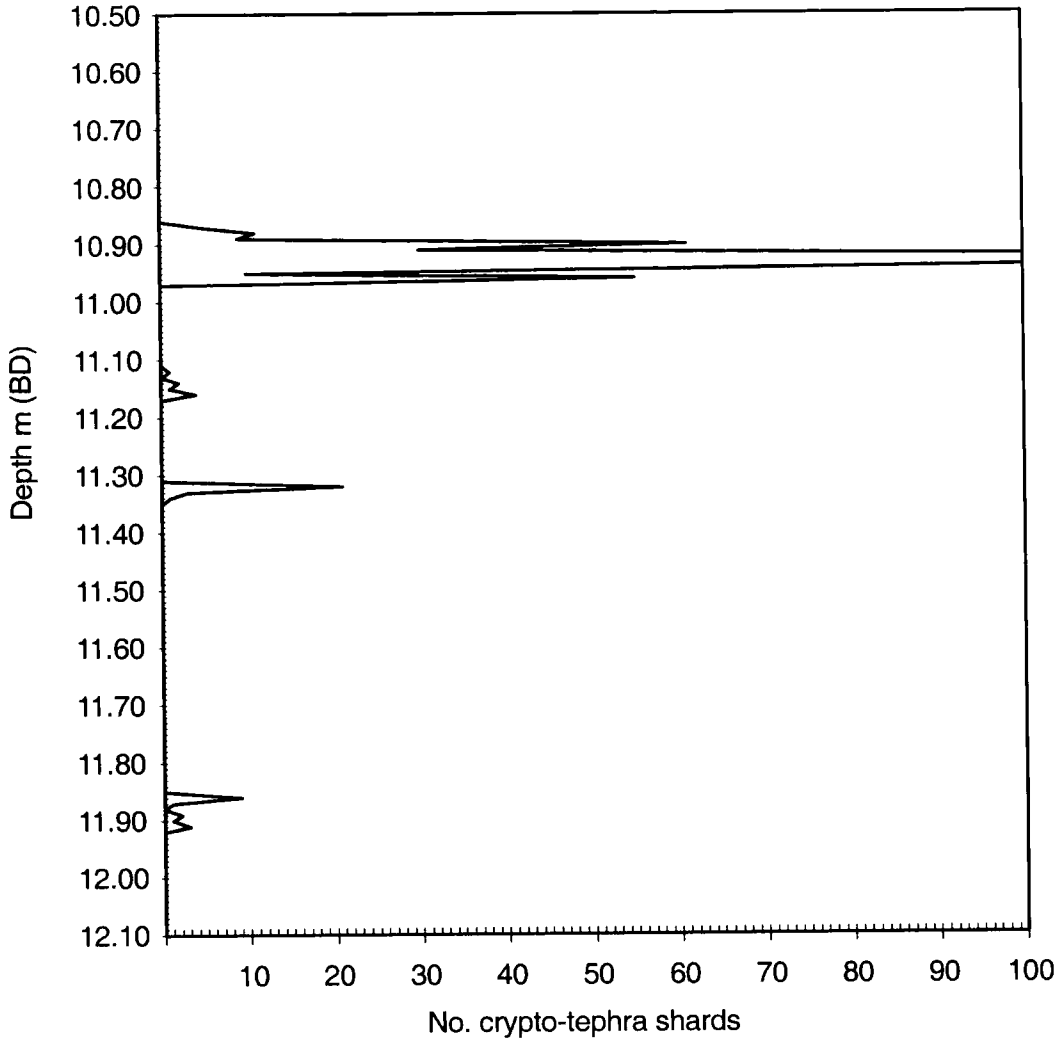

Figure 8

Graph of the number of shards of cryptotephra per drop (tephra float from 5cm^3 wet sediment in 0.5cm^3 distilled water).

The peak count in horizon 1 (sample S13) at 10.94m, was very clear but not well defined, with the bulk of the spread above suggesting some bioturbation for ~7cms. The individual counts in horizon 2 were consistently low, and it was considered that there was insufficient material for further analysis on this occasion. The peak counts in horizons 3 (sample S21) and 4 (sample S30), at 11.32m and 11.86m respectively, were both abrupt with only a small spread of shards 1 – 2 cm below. This would indicate more stable conditions than in horizon 1, with movement due only to migration of the shards caused by to gravitational sorting.

The levels with peak counts of cryptotephra (S13, S21 and S30) were re-sampled for quantitative geochemical analyses. The results are shown in Tables 7, 8 and 9.

Table 7

The major oxide concentrations of individual glass shards in sample S13. All oxides are shown as weight percent, and total iron is expressed as FeO.

No.	SiO_2	TiO_2	Al_2O_3	FeO	MnO	MgO	CaO	Na_2O	K_2O	Total
1	72.28	0.18	11.91	2.85	0.06	0.07	0.36	5.34	4.52	97.57
2	70.67	0.16	12.25	3.03	0.07	0.07	0.35	5.65	4.18	96.43
3	70.80	0.15	12.33	2.75	0.08	0.08	0.38	5.39	4.41	96.36
4	71.19	0.16	12.11	2.70	0.13	0.06	0.35	5.34	4.29	96.32
5	70.58	0.09	13.09	2.42	0.15	0.08	0.29	5.35	4.19	96.24
6	71.43	0.13	11.87	2.84	0.08	0.06	0.35	5.07	4.27	96.09
7	70.65	0.17	11.90	2.90	0.07	0.07	0.38	5.36	4.45	95.96
8	70.80	0.17	11.72	2.96	0.08	0.04	0.38	5.37	4.44	95.95
9	71.05	0.16	11.83	2.88	0.10	0.05	0.37	5.09	4.33	95.85
10	70.94	0.16	11.62	2.77	0.12	0.08	0.41	5.46	4.26	95.82
11	70.71	0.12	12.02	2.59	0.12	0.04	0.40	4.84	4.43	95.27
12	70.81	0.17	11.79	2.96	0.00	0.06	0.40	4.88	4.16	95.22
13	70.16	0.17	12.02	2.56	0.07	0.04	0.35	5.17	4.48	95.00
mean	70.92	0.15	12.03	2.79	0.09	0.06	0.37	5.25	4.34	96.01
1SD	0.51	0.02	0.37	0.18	0.04	0.01	0.03	0.23	0.12	0.65

Table 8

The major oxide concentrations of individual glass shards in sample S21. All oxides are shown as weight percent, and total iron is expressed as FeO.

No.	SiO_2	TiO_2	Al_2O_3	FeO	MnO	MgO	CaO	Na_2O	K_2O	Total
1	70.97	0.27	13.48	3.83	0.23	0.23	1.34	4.66	3.47	98.47
2	69.99	0.23	12.99	3.72	0.16	0.18	1.36	5.11	3.53	97.28
3	69.77	0.28	13.21	3.47	0.18	0.24	1.30	5.22	3.55	97.22
4	69.37	0.32	13.29	3.80	0.12	0.19	1.29	5.34	3.31	97.03
5	69.70	0.21	13.06	3.87	0.14	0.21	1.27	4.89	3.40	96.75
6	68.34	0.20	13.26	3.92	0.19	0.21	1.31	4.96	3.45	95.85
7	68.69	0.29	12.81	3.70	0.06	0.21	1.32	5.15	3.42	95.65
8	68.36	0.27	13.12	3.88	0.23	0.20	1.33	4.98	3.28	95.64
9	68.59	0.23	12.93	3.57	0.06	0.22	1.23	5.34	3.37	95.54
10	68.43	0.23	13.00	3.69	0.13	0.23	1.29	5.03	3.37	95.38
11	69.75	0.28	12.95	3.87	0.10	0.23	1.30	3.34	3.16	94.97
mean	69.27	0.26	13.10	3.76	0.14	0.21	1.30	4.91	3.39	96.34
1SD	0.85	0.04	0.20	0.14	0.06	0.02	0.04	0.56	0.11	1.07

Table 9

The major oxide concentrations of individual glass shards in sample S30. All oxides are shown as weight percent, and total iron is expressed as FeO.

No.	SiO2	TiO2	Al2O3	FeO	MnO	MgO	CaO	Na2O	K2O	Total
1	74.59	0.10	12.76	1.37	0.00	0.08	0.73	4.05	3.66	97.34
2	72.93	0.11	12.97	1.20	0.02	0.06	0.82	4.57	3.38	96.06
3	73.45	0.11	12.32	1.49	0.10	0.07	0.75	4.00	3.68	95.97
4	72.88	0.13	12.44	1.51	0.02	0.08	0.76	4.08	3.95	95.85
5	73.95	0.09	12.34	1.37	0.00	0.07	0.74	3.63	3.47	95.66
6	73.30	0.09	12.23	1.40	0.03	0.10	0.77	3.98	3.58	95.47
7	72.52	0.12	12.38	1.48	0.05	0.10	0.76	4.00	3.96	95.38
8	73.08	0.09	11.88	1.51	0.06	0.07	0.75	4.04	3.89	95.37
9	72.65	0.11	12.38	1.51	0.02	0.04	0.77	3.95	3.90	95.34
10	72.74	0.12	12.28	1.40	0.05	0.07	0.72	4.02	3.80	95.20
11	72.56	0.09	12.18	1.53	0.07	0.09	0.73	4.14	3.80	95.20
12	72.65	0.09	12.42	1.46	0.03	0.07	0.75	3.97	3.67	95.10
mean	73.11	0.10	12.38	1.44	0.04	0.08	0.76	4.04	3.73	95.66
1SD	0.63	0.02	0.27	0.09	0.03	0.02	0.03	0.21	0.19	0.61

The three cryptotephra horizons can be clearly characterised and differentiated by their major element geochemistry as illustrated by examples of two bi-plots in Figure 9.

Using a model based on Le Maitre (1989), a plot of potassium against silica discriminates the three cryptotephra horizons but also illustrates their common silicic/rhyolitic character, see Figure 11. All three fall into the high K area, which would indicate that they all have Icelandic sources (http://www.geo.ed.ac.uk 19.08.05).

a)

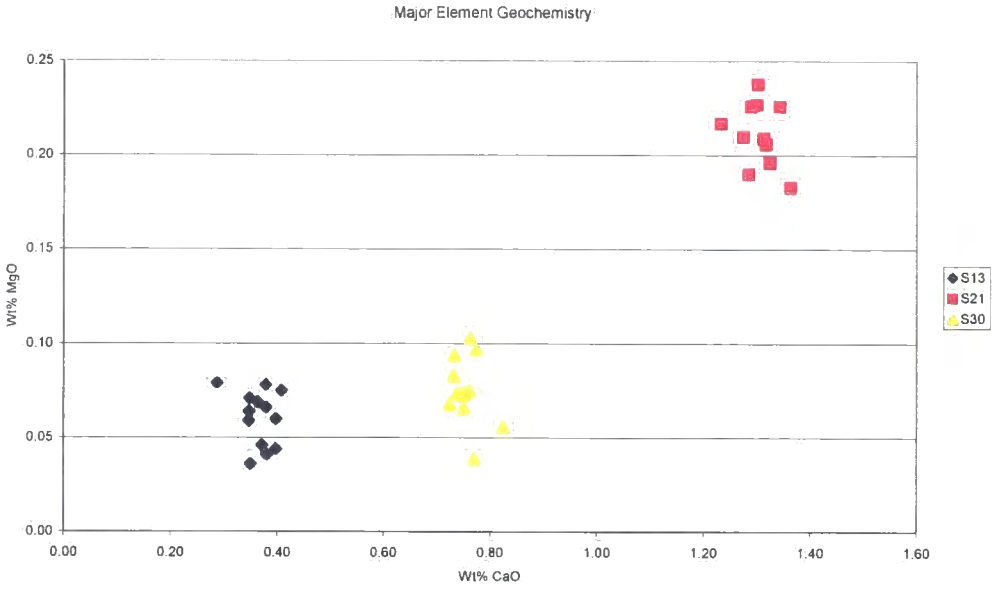

b)

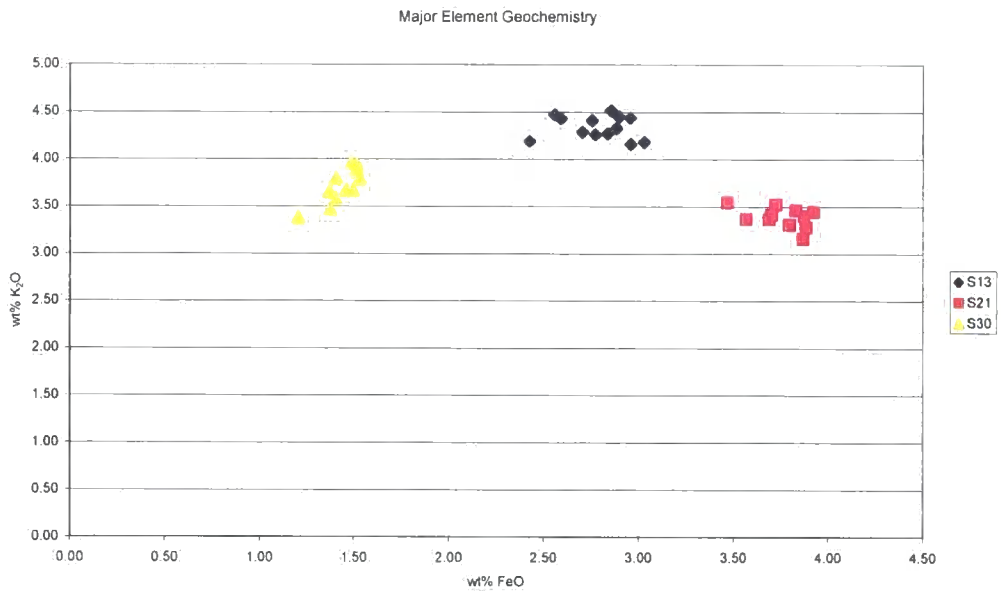

Figure 9

Two examples of major element bi-plots for the cryptotephra horizons S13, S21 and S30, showing the relationship between: a) magnesium and calcium ratios; and b) potassium and total iron ratios.

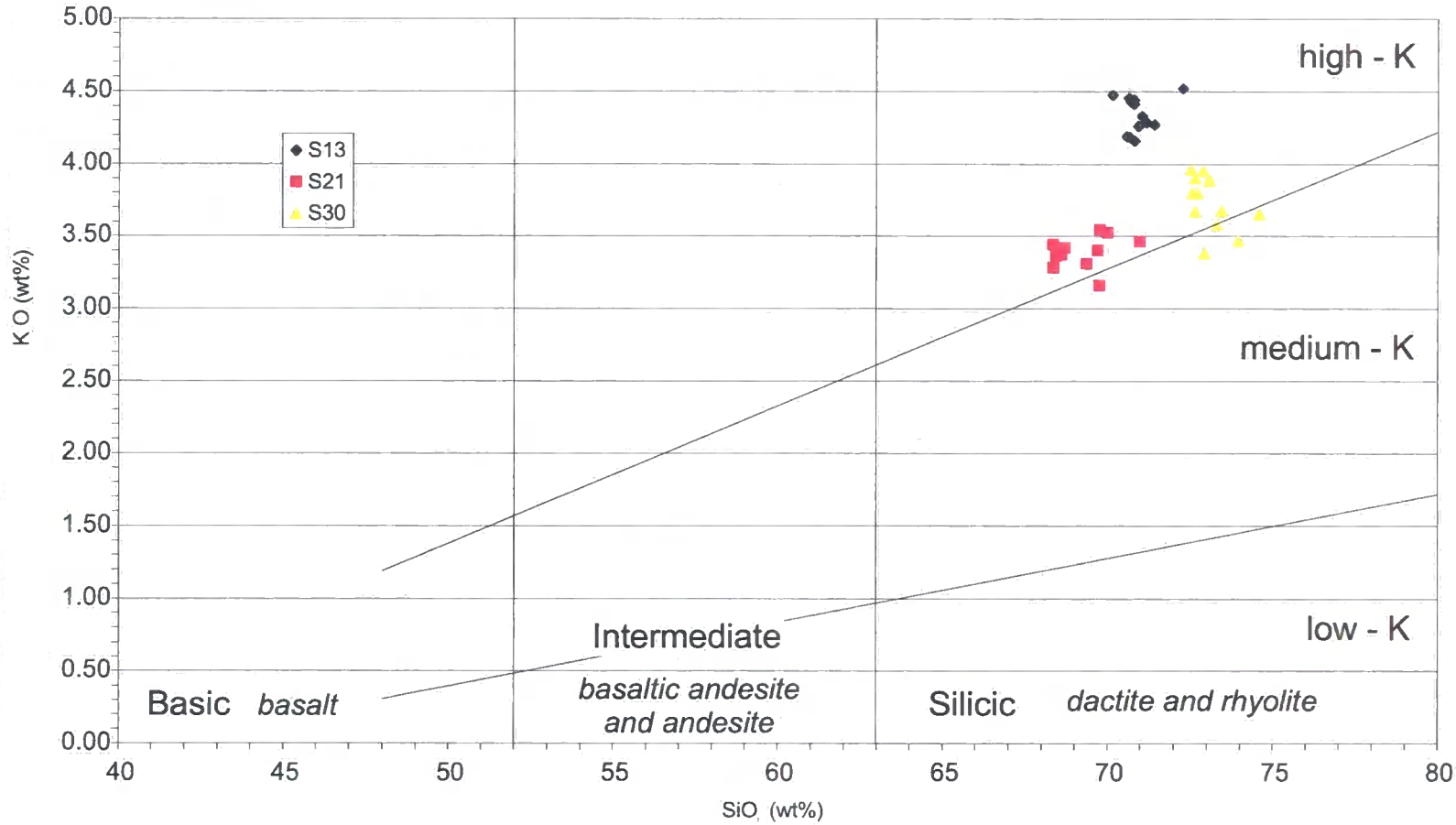

Figure 10

A model based on Le Maitre (1989) using a plot of potassium against silica to characterise the cryptotephra horizons S13, S21 and S30.

The horizon S30 lies in Lith2, sediments of early interstadial age, and above the oldest AMS date of 12625 ^{14}C yrs BP (14940 cal yrs BP). The Borrobol Tephra, dated in Scotland at 12260 ^{14}C yrs BP (14400 cal yrs BP) (Turney et al., 1997) and of Hekla origin (Haflidason et al., 2000), is well documented in Scotland by Turney (1997), and provides an obvious choice for comparison. The horizon S21 lies in Lith3, the stadial sediments; the Vedde Ash of Katla origin (Haflidason et al., 2000) is also well documented in Scotland (e.g. Davies et al., 2001; Lowe and Turney, 1997; Turney, 1998; Wastegård et al., 2000a). It has also been detected in the GRIP Greenland Ice core and has been assigned an age of 11980 ±80 GRIP ice-core years BP (Grönvold et al., 1995). This is also an obvious choice for comparison.

The ternary diagram in Figure 11 shows the ratio of calcium, iron and potassium. It illustrates the similarities between the chemical signature of the S21 horizon and the Vedde Ash (Björck and Wastegård, 1999; Turney et al., 1997; Wastegård et al., 1998; Wastegård et al., 2000b) and of the S30 horizon and the Borrobol Tephra (Turney et al., 1997). This supports the correlations: S21 with the Vedde Ash, and S30 with the Borrobol Tephra. (Data from http://www.geo.ed.ac.uk/tephraexe/ 19.08.05).

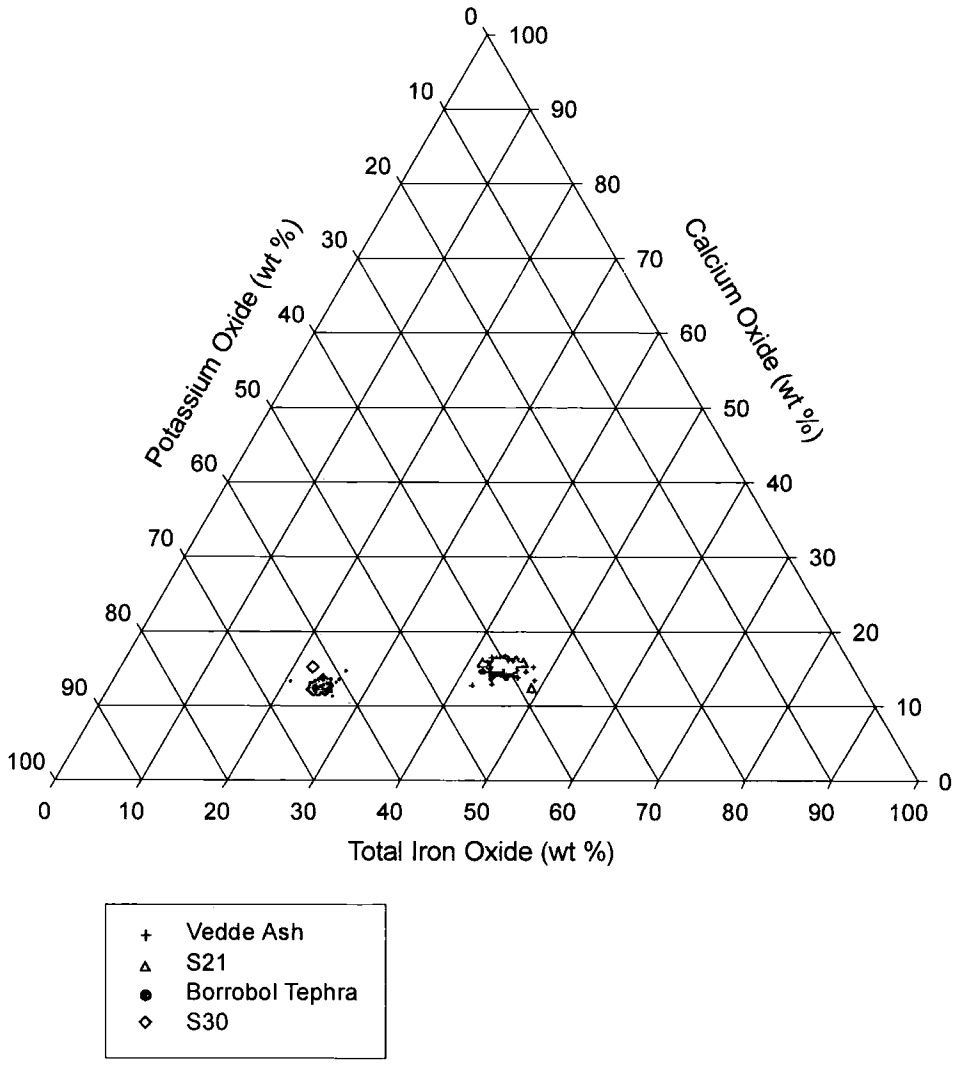

Figure 11

A ternary diagram of the ratio of calcium oxide (wt %), potassium oxide (wt %) and total iron oxide (wt %), to compare the S21 and S30 horizons with the Vedde Ash and Borrobol Tephras. The fields are defined by data from Tephrabase (http://www.geo.ed.ac.uk/tephraexe/ 19.08.05).

The horizon S13 lies in Lith4, the early Holocene deposits, and this is confirmed by the proximal AMS date of 8590 ^{14}C yrs BP or 9560 cal yrs BP. However, there is a dirth of comparable known tephras around this time (Haflidason et al., 2000; Wastegård, 2002). The three closest are: Lairg B dated *ca.* 6000 ^{14}C yrs BP, with Torfajökull as a suggested source (Dugmore et al., 1995); SSn dated *ca.* 6-7000 ^{14}C yrs BP, with Snæfellsjökull as a suggested source (Boygle, 1999); and Hovsdalur dated *ca.* 10500 yrs BP, with Snæfellsjökull as a suggested source (Wastegård, 2002).

Data from Tephrabase (http://www.geo.ed.ac.uk/tephraexe/ 19.08.05) for known early Holocene Icelandic tephras with high potassium have been plotted in the ternary diagram in Figure 12. These are: Lairg B (Dugmore et al., 1995); Snn (Boygle, 1999);

and Hovsdalur (Wastegård, 2002), and are plotted together with the data from horizon S13. This illustrates both the compactness of the geochemical analyses for horizon S13 and also its geochemical isolation from the three other known Holocene tephras (although it is similar to three outlying samples from the Lairg B data, which has a much larger chemical footprint).

However, care must be exercised when identifying an apparently novel tephra. It is not necessarily the case that a unique geochemical signature is indicative of a previously undiscovered tephra. Pollard et al (2003) have studied variations in the chemical durability of tephra in the post-depositional environment, where cryptotephra shards, which have a high surface to volume ratio, might be expected to undergo some chemical alteration by leaching, particularly in an aqueous and possibly acid environment. They applied established models of vitreous durability to the published chemical analysis of a large number of Icelandic tephras, in order to predict their relative durabilities under equivalent conditions. They conclude that tephras should be expected to show predictable differential chemical stability in the post-depositional environment. Their preliminary results show that some tephras are likely to be less stable than others in any given depositional environment, and they rank the Borrobol Tephra and Vedde Ash (rhyolitic) as essentially stable.

In the case of the cryptotephra in horizon S13, which shows a compact and characteristic geochemical signature, it has been dated and this date is sufficiently isolated from the other known tephras, to suggest that it is a new addition to the suite of early Holocene tephras. It is therefore proposed that this is the first documented find of this particular tephra that will hereafter be referred to as the 'An Druim Tephra' (see (Ranner et al., 2005) in Appendix I).

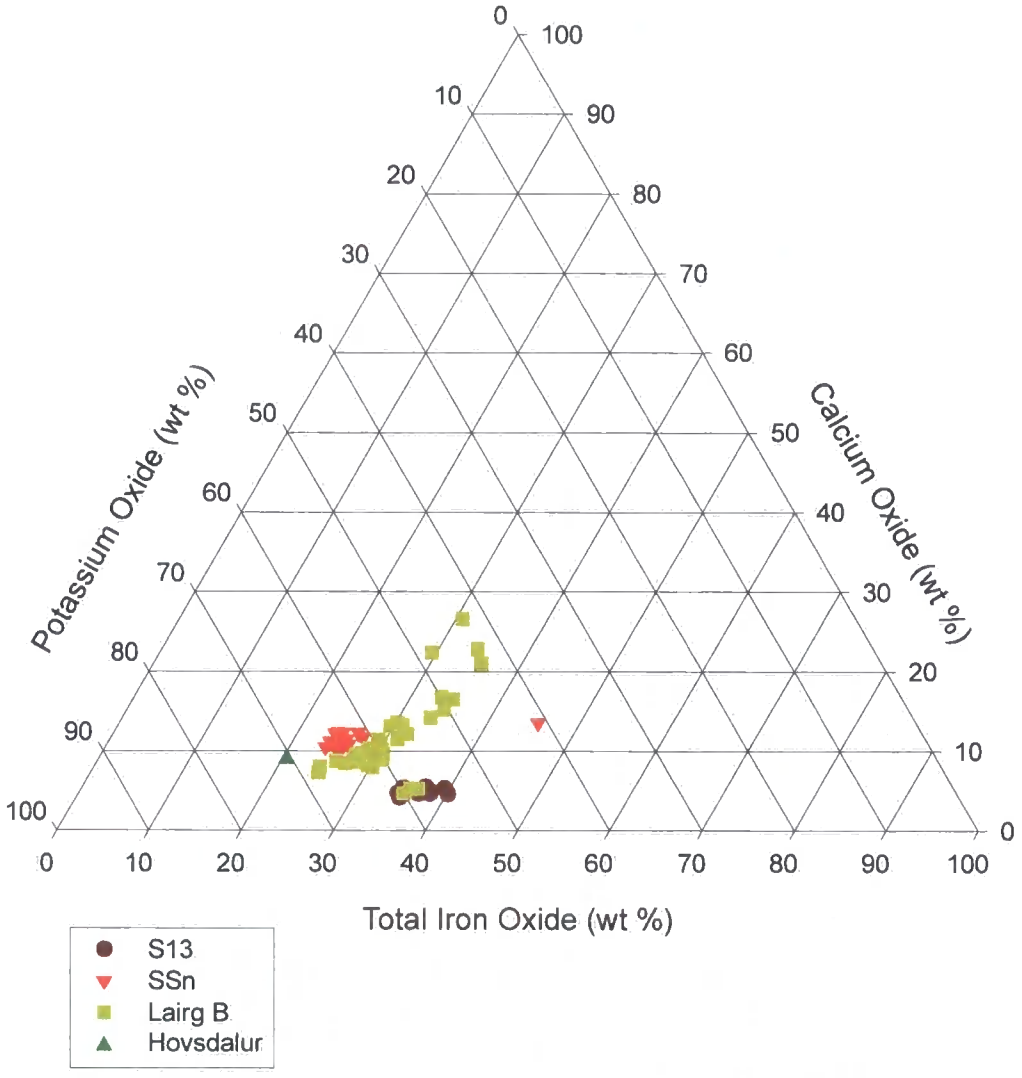

Figure 12

A ternary diagram of potassium oxide (wt %), calcium oxide (wt %) and total iron oxide (wt %), comparing data for the three known early Holocene silicic Icelandic tephras with high potassium (Lairg B (Dugmore et al., 1995), Snn (Boygle, 1999) and Hovsdalur (Wastegård, 2002)) with the data for the cryptotephra from horizon S13.

The Total Alkali ($Na_2O + K_2O$) vs. Silica (TAS) plot in Figure 13 shows the geochemical evolutionary trends of three of the most active Icelandic volcanic systems (modelled by Haflidason et al. (2000), after Jakobsson (1979) and Oskarsson et al. (1985). It also illustrates the proximity in character of the three cryptotephra horizons S13, S21 and S30. The Borrobol Tephra is known to be of Hekla origin and the Vedde Ash of Katla origin (Haflidason et al., 2000); it is likely therefore that with such a characteristically high potassium component that the An Druim Tephra was sourced from the Torfajökull area.

Table 10 provides a summary of the cryptotephra horizons found in this study at Lochan An Druim, together with their correlated tephra horizons and the assigned dates. This tephrochronology has been combined with the radiocarbon chronology at this site and used to develop an independent age-depth model for this sequence. (see section 5.1.4)

Table 10

Summary of cryptotephra samples found at Lochan An Druim and the correlated tephra horizons and absolute dates

Sample	Depth m(BD)	Cryptotephra	Age ^{14}C yrs BP	Age cal yrs BP		Reference
S13	10.94	An Druim	8 590 ±50	9 560 ±73		(Ranner, 2005)
S21	11.32	Vedde	10 310 ±50		11 980 ±80 GRIP ice-core yrs BP	(Birks et al., 1996) (Grönvold et al., 1995)
S30	11.86	Borrobol	12 260			(Lowe et al., 1999; Turney et al., 1997)
			13 400			(Eiriksson et al., 2000)
					ca 13 900 Cariaco Varve yrs	(Davies et al., 2004)
				13 800 – 14 450		
				13 667 – 14 331		

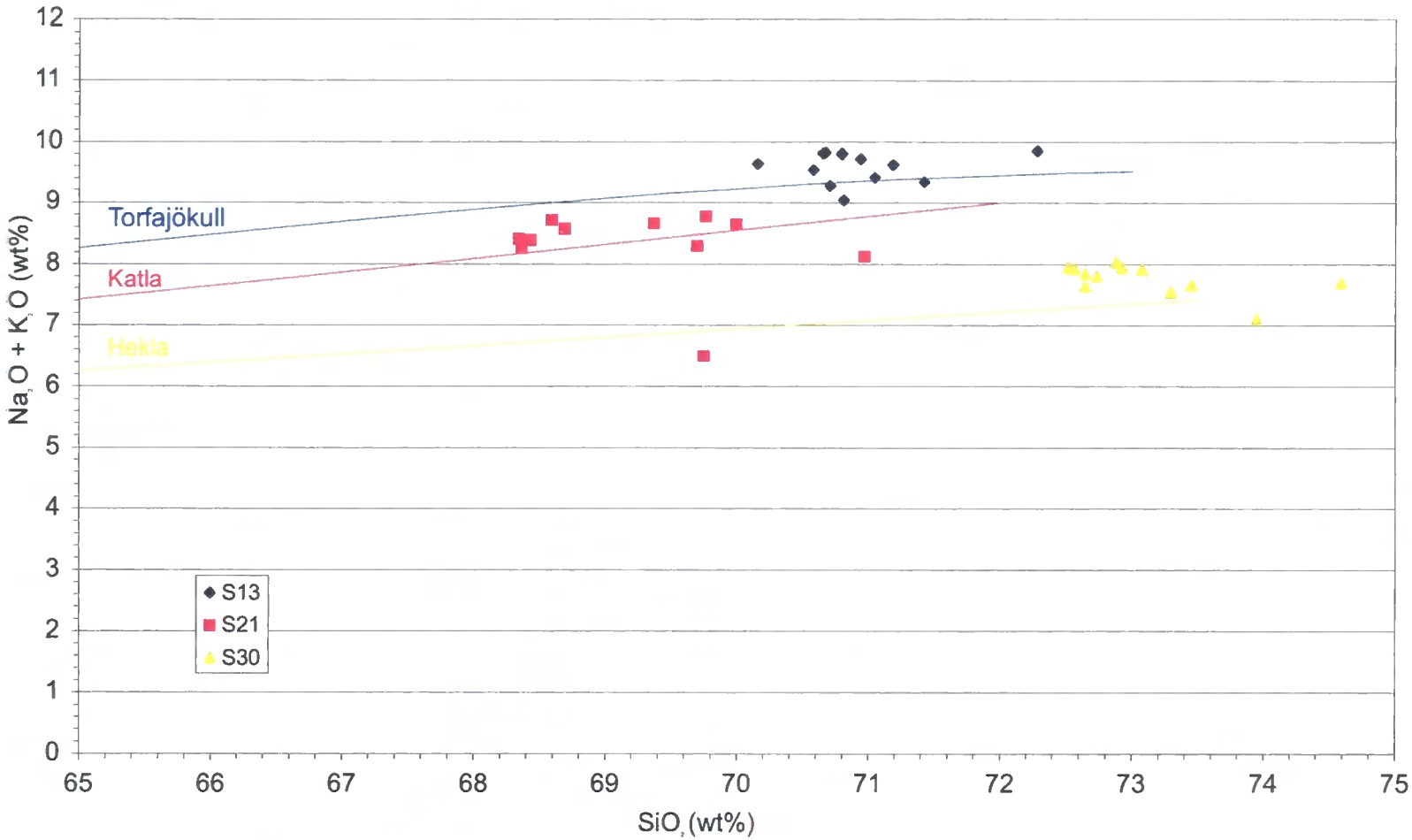

Figure 13

A TAS plot showing the geochemical evolutionary trends of three of the most active Icelandic volcanic systems (modelled by Haflidason et al. (2000), after Jakobsson (1979) and Oskarsson et al. (1985), and the proximity in character of the three tephra horizons S13, S21 and S30.

5.1.4 The Age-Depth Model

The age-depth relationship for the Lateglacial section of this sequence has been constructed using a polynomial model fitted to the accepted and calibrated radiocarbon dates (within the 2 sigma age range), and the literature date assigned to the Vedde Ash (see Figure 14). Although a Borrobol like tephra was identified, the widespread nature of the dates assigned to this layer casts doubt on its coeval nature in northern Europe, and it was therefore not included in this model. However, the model indicates a date of *ca* 13.6 ka yrs BP for this cryptotephra, which does fall within the younger age range for this tephra calculated from the Lake Suigetsu calibration data-set (see section 2.3.2.1). For a more in depth discussion about this cryptotephra see Ranner et al. (2005) in Appendix I.

A third order polynomial provided a good fit to these Lateglacial data points ($R^2 = 0.99$). However, extrapolating this curve back to the top of the core produced a negative date, since it did not provide an inflexion that would connect with the top of the sequence i.e. -49 years cal BP.

Since the Lateglacial was the area of most interest in this study, and the polynomial model provided an acceptable fit for the period, it was accepted. However, it was decided to make a tentative attempt to model the early Holocene section separately. In order to constrain this lower section within the temporal scope of the study, and enable a realistic back projection to the present day, three other points were chosen and linked by linear segments. These were: a point extrapolated from the polynomial where the pollen profile indicates a short climatic reversal; the palynological date for the expansion of *Alnus* which appears at the top of the core section; and a point of inflexion which was extrapolated to a point in Lith4 at 10.67m (BD) where there was a slight colour change in the sediment. These choices are discussed below.

The Lateglacial polynomial model was extrapolated to 10.84m, a level at which there was an uncharacteristically low total pollen concentration for the Holocene, i.e. only 24% of the samples at 2cm above and below that point The extrapolated date of 8088 cal yrs BP at this level, falls within the proposed scope of the 8.2 ka event (i.e. 8.4 ka - 8 ka) as recorded, *inter alia,* in the GISP2 core from central Greenland (Alley et al., 1997). It is noted however, that this reversal does not register in the %LOI (dry weight) curve. At the time of this study the Holocene sediments were not of paramount interest and analysis was carried out at 2cm intervals, so that this proposed reversal could in future be better constrained by higher resolution analysis about that depth.

The palynological date for the expansion of *Alnus*, was used to fix a date for the expansion of Alnus at Lochan An Druim which is indicated at 10.56m (BD) in the profile. The potential woodland zones identified by McVean and Ratcliffe (1962) in their

assessment of the plant communities of the Scottish Highlands, place Lochan An Druim and the Isle of Skye in the same coastal zone 'Predominant Birch Forest'. Three palynological records from the Isle of Skye record the expansion of *Alnus* in the early Holocene, ranging from *ca.* 6500 - 6300 ^{14}C yrs BP (Birks and Williams, 1983). The average 6400 ^{14}C yrs BP, converts to a median estimate of 7320 ± 166 cal yrs BP (using CALIB 4.4.1 (Stuiver and Reimer, 1993) with calibration data set: intcal98.14c (Stuiver et al., 1998a)). In addition, the record at Loch a Phuinnd in the Western Isles, indicates a date between 7422 and 5527 cal years BP (Fossitt, 1996). These dates agree with the *Alnus* fossil pollen isopoll maps of Huntley and Birks (1983), where Lochan An Druim (with a value at 10.56m of 1.28% *Alnus*) lies close to the 2% isopoll at 6500^{14}C yrs BP.

It was felt that a back projection to the present day was justified since a visual inspection of the complete core suggested that the Holocene sediments were of a uniform gyttja with no obvious lithological changes. Therefore, the first linear segment connected the top of the core (2.5m (BD), -49 yrs BP) with the Alnus rise (10.56m (BD), 7320 cal. yrs BP)

An inflection was then needed to link this first segment to the climatic reversal extrapolated from the polynomial model. A slight change in colour of the sediment in Lith4 provided such a point and so the first segment was extrapolated to this boundary (10.67m (BD), 7420 cal. yrs BP). The second linear segment then connected (10.67m (BD), 7420 cal. yrs BP) to the point extrapolated from the polynomial for the 8.2 event (10.84m (BD), 8088 cal. yrs BP). These two linear segments are combined with the third order polynomial to give the completed age-depth model down to 12m (BD) at *ca* 15.0 ka BP. However, in view of the uncertainties discussed above in connection with the Holocene section of the model, the age-depth relationship for this period is not considered to be robust and a lens has been placed over this section in all the figures for Lochan An Druim to indicate the unreliability in the model at this time.

The age-depth model has been divided into smaller sections (1-9) of similar gradient in order to estimate sediment accumulation rates, which are indicated on the diagram (see Figure 14).

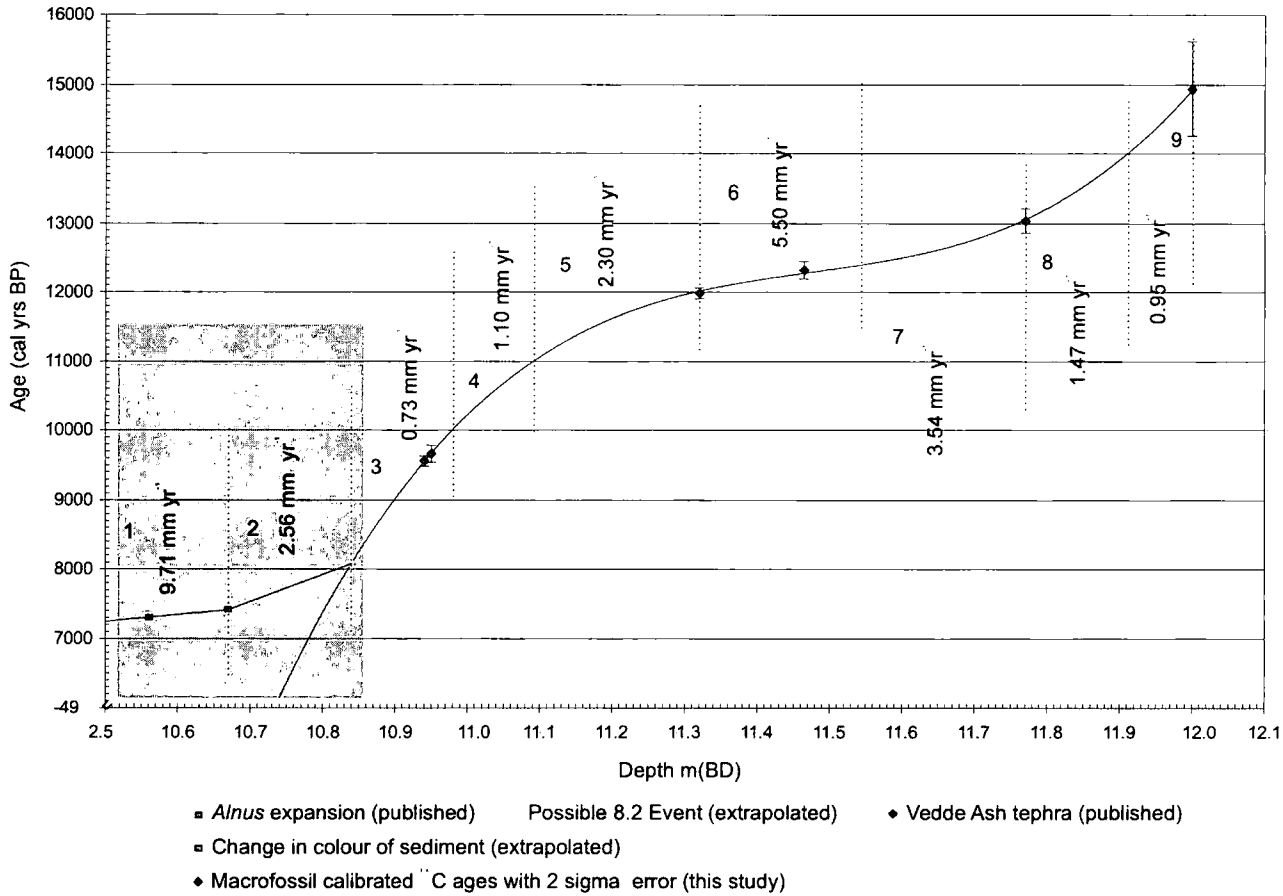

Figure 14

Age-depth model for Lochan An Druim using a third order polynomial (y = 12778.69x3 - 439890.75x2 + 5049058.30x - 19311069.03, R2 = 0.9997507938) for the lower sections (10.84 - 12.07 m) and two linear segments for the uppermost section (10.56 - 10.84 m), with mean sediment accumulation rates for each gradient section.

5.1.5 Correlation with the Greenland Ice Record

The proportional pollen data, pollen influx data and the macrofossil data have been plotted with respect to the age-depth model developed in section 5.1.4. This provides a calendar years age scale that has been correlated directly with the ice core years scale in the GRIP ice core $\delta^{18}O$ data for the Lateglacial and early Holocene (Dansgaard et al., 1993; Johnsen et al., 1992), thus providing a direct correlation with the event stratigraphy recommended by Björck et al. (1998) for this period (see section 2.3.2.1). This correlation is shown in subsequent palaeoclimate records from this site.

5.1.6 Pollen Analyses

The aim was to sub-sample at decadal to centennial resolution. Pollen counts have been accepted (AP+NAP counts >200 grains) for 61 sub-samples at intervals of 4 cm throughout the early Holocene and 1-2 cm in the Lateglacial. The mean count for AP+NAP was 514 grains [SE±33]. Calendar ages have been assigned to each sub-sample, interpolated from the age-depth model (see section 5.1.4) and the resulting mean temporal interval between the sub-samples is 256 [SE±44] years for the Holocene and 80 [SE±8] years for the Lateglacial. A total of 51 arboreal and non-arboreal taxa have been identified, 9 obligate aquatic taxa including *Sphagnum*, and various spore taxa.

Relative abundance pollen data are displayed for the most common taxa, rare taxa mentioned in the text, and totals for monolete and trilete Pteridophyte spores (see Figure 15). Taxa are sorted into arboreal pollen taxa, non-arboreal pollen taxa, terrestrial Pteridophytes and obligate aquatics and plotted against age (cal yrs BP). There is an overall summary for the main terrestrial groups of woody taxa (i.e. trees plus shrubs but not including Ericales), Ericales and herbaceous taxa. % LOI (dry weight) and the percentage of pollen not specifically identified (indeterminate pollen) is displayed. The total number of AP+NAP grains counted is plotted, with depth bars to indicate the frequency of sampling. Below 12m four samples yielded pollen information but there were insufficient grains to justify analysis and so these taxa have been marked as present where appropriate. The results of the CONISS analysis carried out on the proportional data of all AP+NAP is displayed as a dendrogram, and the resultant divisions used to guide the divisions representing the local pollen assemblage zones (LPAZs). These same divisions have been added to the diagrams in Figures 16 and 17. Figure 16 shows pollen influx data for taxa mentioned in the text, and the total pollen influx for arboreal and non-arboreal taxa (see section 5.1.7), and Figure 17 shows macrofossils information from the pollen washings as presence data (see section 5.1.9).

Figure 15

Lochan An Druim: Relative abundance data are displayed for the most significant taxa with totals (undifferentiated) for the monolete and trilete Pteridophyte spores; taxa have been grouped into arboreal taxa and non-arboreal taxa, terrestrial Pteridophytes and obligate aquatics and plotted against age (cal yrs BP). Pollen sums are specified as follows for selected taxa: Terrestrial Pollen (ΣTP), i.e. Arboreal Pollen minus Pinus (AP) plus Non-Arboreal Pollen (NAP); Terrestrial Pollen and Terrestrial Pteridophyte Spores (ΣTP + ΣPS); Terrestrial Pollen and Aquatic Pollen (including Sphagnum) (ΣTP + ΣAP); Terrestrial Pollen and Indeterminable Pollen (ΣTP + ΣIP). The first axis from the DCA analysis of the pollen spectra is plotted with the assigned palaeobiomes developed through the systematic biome analysis (see section 5.1.10.1). The GRIP ice core $\delta^{18}O$ data for the Lateglacial and early Holocene (Dansgaard et al., 1993; Johnsen et al., 1992) are plotted for correlation. LPAZs are indicated.

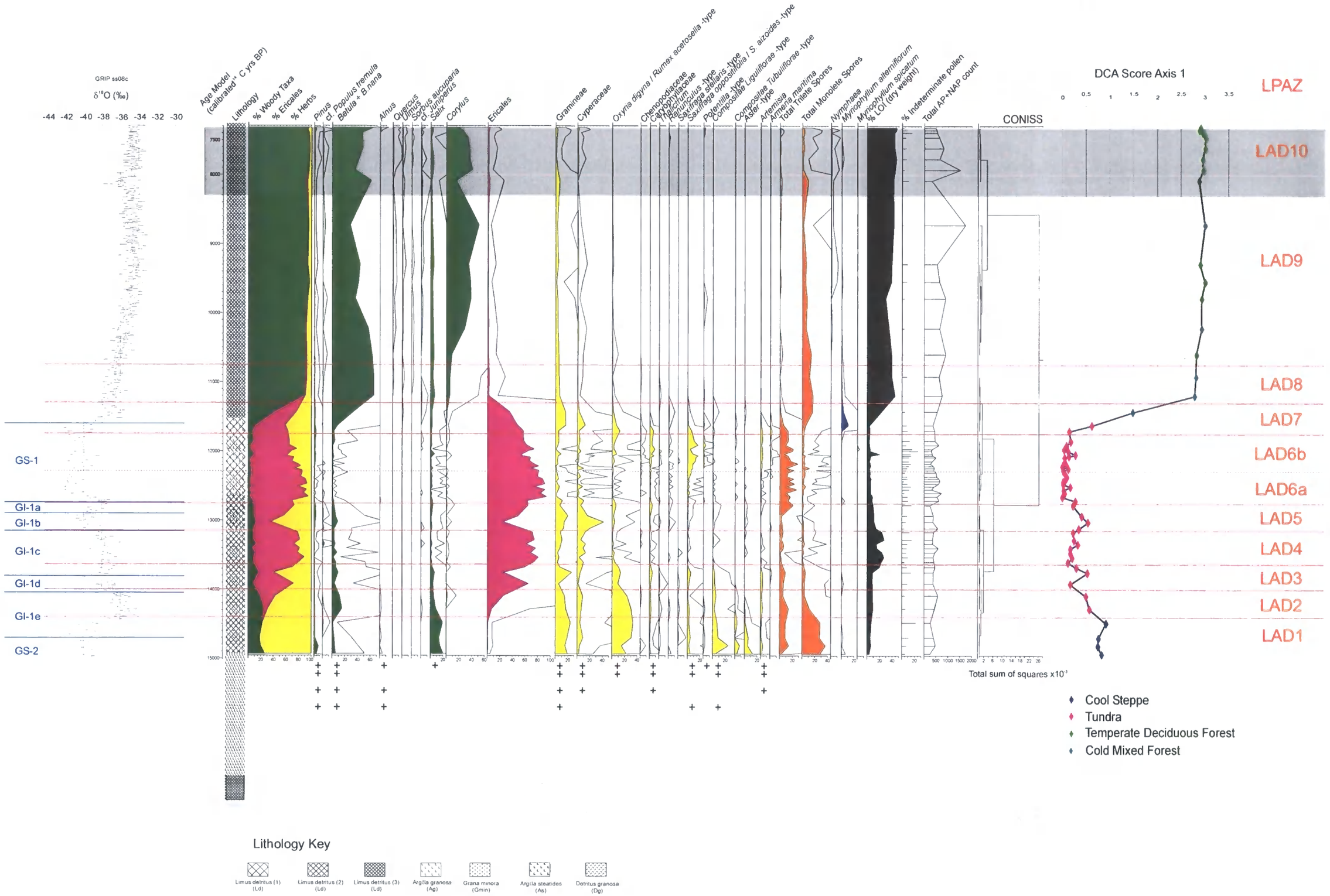
GRIP ss08c
δ18O (‰)
-44 -42 -40 -38 -36 -34 -32 -30
GS-1
GI-1a
GI-1b
GI-1c
GI-1d
GI-1e
GS-2
Age Model (calibrated 14C yrs BP)
Lithology
% Woody Taxa
% Ericales
% Herbs
Pinus
cf. Populus tremula
Betula + B.nana
Alnus
Quercus
Ulmus
Corylus avellana
cf. Juniperus
Salix
Ericales
Gramineae
Cyperaceae
Oxyria digyna / Rumex acetosella -type
Chenopodiaceae
Caryophyllaceae
Thalictrum
Ranunculus -type
Saxifraga stellaris -type
Saxifraga oppositifolia / S. aizoides -type
Potentilla -type
Compositae Liguliflorae -type
Compositae Tubuliflorae -type
Aster -type
Artemisia
Armeria maritima
Total Triete Spores
Total Monolete Spores
Nymphaea
Myriophyllum alterniflorum
Myriophyllum spicatum
% LOI (dry weight)
% Indeterminate pollen
Total AP+NAP count
CONISS
DCA Score Axis 1
0 0.5 1 1.5 2 2.5 3 3.5
LPAZ
LAD10
LAD9
LAD8
LAD7
LAD6b
LAD6a
LAD5
LAD4
LAD3
LAD2
LAD1
Total sum of squares x10-3
Cool Steppe
Tundra
Temperate Deciduous Forest
Cold Mixed Forest
Lithology Key
Limus detritus (1) (Ld)
Limus detritus (2) (Ld)
Limus detritus (3) (Ld)
Argilla granosa (Ag)
Grana minora (Gmin)
Argilla steatides (As)
Detritus granosa (Dg)

5.1.7 Pollen Influx

The influx of AP+NAP (see Figure 16) increases upwards through the lithological sequence, suggesting a very general amelioration in climate following deglaciation. This is evidenced by: insufficient pollen to assess Lith1; Lith2, mean 299 [SE ±56] grains cm^{-2} yr^{-1}; Lith3, mean 892 [SE ±141] grains cm^{-2} yr^{-1}; and Lith4 mean 4333 [SE ±903] grains cm^{-2} yr^{-1}. However, there were fluctuations in influx within the different units. In Lith2 there are two isolated spikes: a small peak of 182 grains cm^{-2} yr^{-1}, at 14089 cal yrs BP (11.92m); and a more significant peak of 851 at 13464 cal. yrs BP (11.84m). Lith3 is more complex, the lower section exhibiting small fluctuations peaking at 2717 grains cm^{-2} yr^{-1} at 12365 cal yrs BP (11.52m), before declining in the upper section to a low of 165 grains cm^{-2} yr^{-1} at 11706 cal yrs BP (11.22m), then followed by a rapid increase into Lith4. This initial steep rise in influx at the beginning of Lith4, peaked at 4835 grains cm^{-2} yr^{-1}, at 11198 cal yrs BP, following which lower levels of between 1120 and 2563 grains cm^{-2} yr^{-1} were sustained for *ca* 2800 years. There was then a significant rapid increase up to 12434 grains cm^{-2} yr^{-1} at 7393 cal yrs BP (10.64m).

Lith3 has the highest rate of matrix sedimentation (mean 0.048 m yr^{-1} [SE ±0.003], compared to a mean 0.021 m yr^{-1} [SE ±0.003] for the rest of the core section), with a higher silt/clay proportion, suggesting a larger allochthonous contribution that could also contain pollen that was originally deposited outside the basin. This might provide an explanation for the high influx rates. Similar explanations are offered by Birks (1984) for the Lateglacial sediments at Lochan An Druim, Pennington (1973) relating to the Lateglacial sediments of Blea Tarn in northern England, and by Hyvarinen (1976) relating to the Lateglacial sediments of Domsvatnet in Fennoscandia. Walker (1990) discusses pollen preservation data for *Empetrum* through the Lateglacial and demonstrates a significant increase in damaged grains at the transition from the Lateglacial Interstadial to the Younger Dryas Stadial. This evidence for abrasion by mineral material during inwash from catchment soils suggests that increases in *Empetrum* and possibly also Ericales at this stage could be as a result of secondary rather than primary deposition. The percentage of unidentifiable pollen grains in this lithological section (see Figures 18 and 19) is generally higher than the rest of the Lateglacial section, and thus supports this inference of secondary deposition.

The influx during Lith3 is composed almost entirely of NAP with a minimal amount of *Betula*, a proportion of which could be *B. nana*, although this species has not been positively differentiated in this study nor in Birks (1984). However, there was no macrofossil evidence either during this period (Birks, 1984), thus, the combination of very low pollen influx combined with the absence of macrofossils would indicate a local

absence of *Betula* at this time (see section 5.2 for a discussion of *Betula* influx, and the assignment of *B. nana* in the Lateglacial.)

The presence of *Pinus* pollen through the Lateglacial and early Holocene at this site can be shown not to be a significant component of the local pollen rain. Generally, influx figures of over 500 grains cm^{-2} yr^{-1} can be used to indicate the presence of *Pinus* (Hyvarinen, 1975), but the record at Lochan An Druim is very low with values of 0-32 grains cm^2 yr^{-1} in LPAZ LAD1-10 and only up to 353 grains cm^2 yr^{-1} in LPAZ LAD11 (see Figure 16). Therefore, this analysis supports the suggestion (see section 4.2.3.3) that *Pinus* was not growing in the region at this time, and that the low levels of *Pinus* pollen throughout this period must reflect long distance transport.

Figure 16

Lochan An Druim: Pollen influx data are displayed for a selection of taxa and plotted against age (cal yrs BP). LPAZs, and lithological units are indicated.

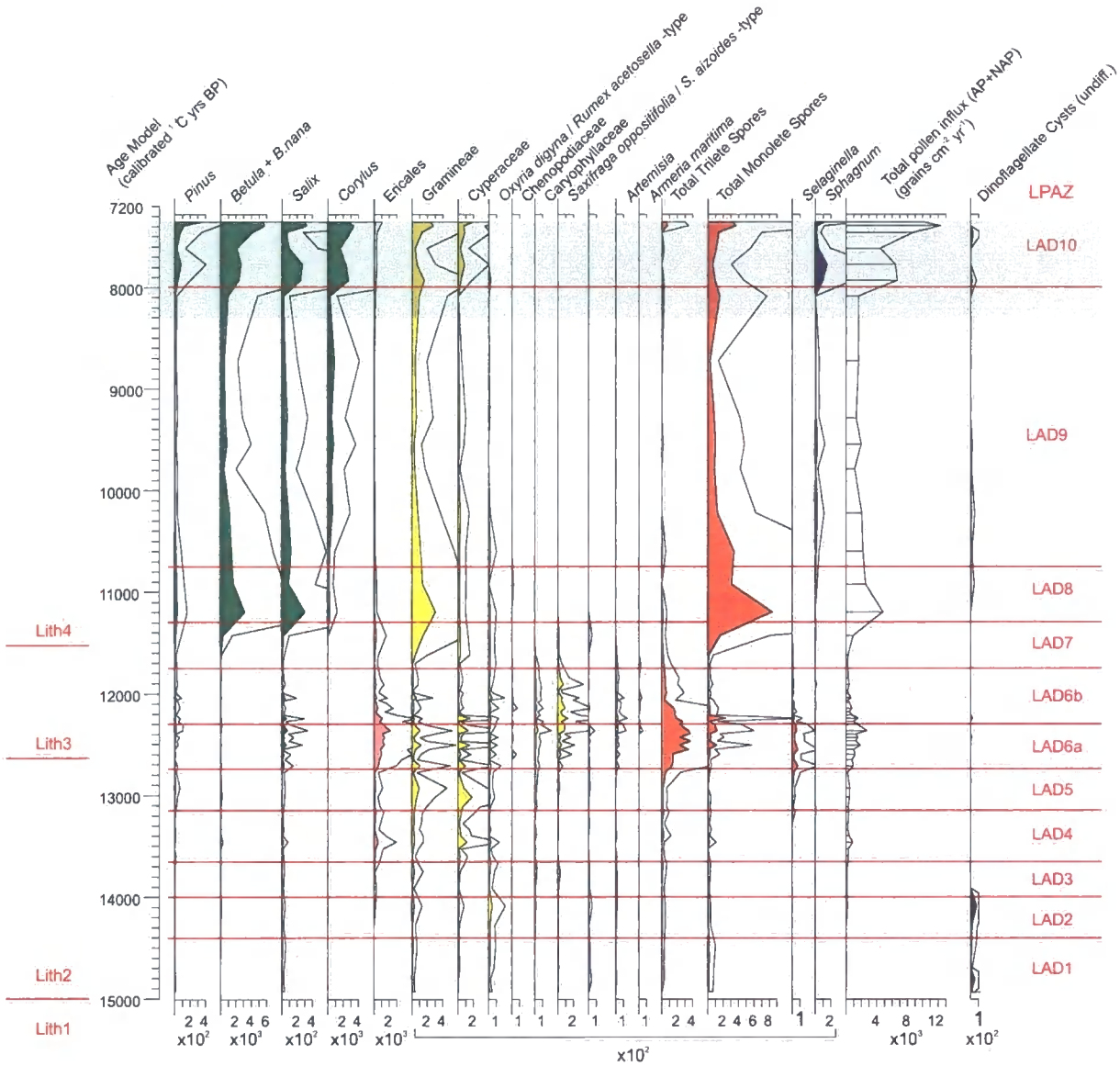
Age Model (calibrated ¹⁴C yrs BP)
Pinus
Betula + B.nana
Salix
Corylus
Ericales
Gramineae
Cyperaceae
Oxyria digyna / Rumex acetosella -type
Chenopodiaceae
Caryophyllaceae
Saxifraga oppositifolia / S. aizoides -type
Artemisia
Armeria maritima
Total Trilete Spores
Total Monolete Spores
Selaginella
Sphagnum
Total pollen influx (AP+NAP) (grains cm⁻² yr⁻¹)
Dinoflagellate Cysts (undiff.)
LPAZ
LAD10
LAD9
LAD8
LAD7
LAD6b
LAD6a
LAD5
LAD4
LAD3
LAD2
LAD1
Lith4
Lith3
Lith2
Lith1
7200
8000
9000
10000
11000
12000
13000
14000
15000
x10²
x10³

5.1.8 Descriptions of the Pollen Zones

Ten local pollen assemblage zones (LPAZs) and two sub-zones have been identified from the relative pollen data (see Figure 19), supported by the dendrogram divisions, and correlated with the event stratigraphy of the Lateglacial, following Björck et al. (1998). The biozones of Mangerud et al. (1974) have also been correlated. The LPAZs are numbered from the bottom up the sequence and are described from the oldest to the youngest. This information is summarised in Table 11 in section 5.1.10.1.

LAD1

15000(+) - 14400 cal yrs BP
Greenland Stadial 2: GS-2a
Late Pleniglacial
Sample Resolution *ca* 150 years

Polypodiaceae -type – *Oxyria digyna / Rumex acetosella* - type – Gramineae – S*alix*

A predominantly herbaceous flora dominated by *Oxyria digyna / Rumex acetosella - type* (*ca.* 30%) and Gramineae (*ca.* 20%) with Cyperaceae and Compositae, and some *Saxifraga oppositifolia / S. aizoides* -type, Carophyllaceae and *Artemisia.* The woody taxa are comprised mostly of *Salix* (*ca.* 20%) with generally less than 5% of *Betula.* Although the percentage of *Salix* pollen is relatively high here, the influx is very low suggesting that *Salix* was not abundant in the vegetation. Pteridophytes are relatively abundant (*ca.* 40%) and are dominated by Polypodiaceae -type. The mean organic content is 5.2 [SE ±0.7]% (dry weight) and the mean influx of terrestrial pollen is very low at 41 [SE ±5] grains cm^{-2} yr^{-1}.

LAD2

14400 - 14000 cal yrs BP (400 yrs)
Greenland Interstadial 1: GI-1e (Bølling)
Sample Resolution *ca* 200 years

Ericales – *Oxyria digyna / Rumex acetosella -type* – Gramineae

The dominant patterns in this zone are the proportional declines in the herbaceous and the woody taxa, which are replaced by Ericales, which increases from <1% in the previous zone to around 25%. However, within the declining woody taxa the proportional representations change, with *Betula* dominating over *Salix.* The herbaceous flora is still dominated by *Oxyria digyna / Rumex acetosella* -type (*ca.* 30%) and Gramineae (*ca.* 15%) with Cyperaceae and Compositae, and some *Saxifraga oppositifolia / S. aizoides -type*, Carophyllaceae and *Artemisia.* Pteridophytes

decline to <10% towards the boundary with LAD3. The mean organic content has increased to 8.8 [SE ±0.2]% and the mean influx of terrestrial pollen increased to 117 [SE ±64] grains cm^{-2} yr^{-1}.

LAD3

14000 - 13650 cal yrs BP (350 yrs)
Greenland Interstadial 1: GI-1, including G1-1d (Older Dryas)
Sample Resolution *ca* 117 years

Ericales – *Oxyria digyna* / *Rumex acetosella -type* – Gramineae

Ericales continue to expand through this zone to *ca* 60%, however there is a significant reversal between 13900 and 13700 cal yrs BP with a corresponding relative increase in the woody taxa, herbaceous taxa and Pteridophytes. The relative proportions of the representative herbs remain constant. The mean organic content has increased to 11.8 [SE ±3.6]% and the mean influx of terrestrial pollen increased slightly 146 [SE ±42] grains cm^{-2} yr^{-1}.

LAD4

13650 - 13150 cal yrs BP (500 yrs)
Greenland Interstadial 1: GI -1, encompassing G1-1c (Allerød)
Sample Resolution *ca* 71 years

Ericales

Ericales remain dominant throughout this zone with a sustained relative abundance that fluctuates between 60 and 80%. The herb flora consists mainly of Cyperaceae (<15%) and Gramineae (<10%) and is much reduced, as is the Pteridophyte flora, although *Selaginella* appears and starts to increase. The mean organic content has increased to 21.7 [SE ±1.9]% and the mean influx of terrestrial pollen increased to 374 [SE ±83] grains cm^{-2} yr^{-1}.

LAD5

13150 - 12670 cal yrs BP (480 yrs)
Greenland Interstadial 1: GI-1, (GI-1b (Intra-Allerød cold period) and GI-1a)
Sample Resolution *ca* 96 years
Ericales – Cyperaceae

The proportional representation of the main groups of woody taxa, Ericales and herbaceous taxa in this zone is very similar to that in LPAZ - LAD3, repeating a similar reversal in dominance of Ericales. However, the representation of the main

components of the herbaceous flora has changed, with up to 40% Cyperaceae with *ca* 20% Gramineae and <10% *Oxyria digyna* / *Rumex acetosella* -type, at this time. Generally the relative proportion of Pteridophytes begins to increase towards LPAZ - LAD6, driven principally by *Lycopodium* spp. but with some *Selaginella*. The mean organic content has decreased significantly to 10.5 [SE ±1.1]% and the mean influx of terrestrial pollen increases further to 459 [SE ±127] grains cm^{-2} yr^{-1}.

LAD6a

12670 - 12300 cal yrs BP (370 yrs)
Greenland Stadial 1: GS -1
Younger Dryas
Sample Resolution *ca* 41 years

Ericales – *Lycopodium* spp. – *Selaginella*

This zone is dominated by Ericales *ca* 90% with generally <3% *Salix* and between 10 and 25% Pteridophytes, principally *Lycopodium* spp. and *Selaginella*, with woody taxa generally <5%. The herbaceous flora is represented by very low proportions of Gramineae and Cyperaceae with - *Saxifraga oppositifolia* / *S. aizoides* -*type* and *Artemisia*, although the diversity of herbaceous taxa is beginning to increase. The mean organic content continues to decrease to 5.6 [SE ±0.4]% but the mean influx of terrestrial pollen increases substantially to 1443 [SE ±188] grains cm^{-2} yr^{-1}.

LAD6b

12300 - 11750 cal yrs BP (550 yrs)
Greenland Stadial 1: GS-1
Younger Dryas
Sample Resolution *ca* 46 years

Ericales – *Lycopodium* spp. – *Saxifraga oppositifolia* / *S. aizoides* -type

Ericales are still dominant in this zone but begin to decline to *ca* 55% towards PAZ - LAD8, the Pteridophytes *Lycopodium* spp. and *Selaginella* decline also, but the herbs - principally *Saxifraga oppositifolia* / *S. aizoides* -type, *Artemisia* and the Caryophyllaceae, begin to increase. The herbaceous flora becomes much more diverse with the expansion of, *inter alia*, the Chenopodiaceae, *Potentilla* and *Armeria maritima*. The mean organic content decreases slightly to 4.5 [SE ±0.3]%, except for an isolated spike about 12000 cal yrs BP (11.31-11.325 m), adjacent to the organic band. However, the mean influx of terrestrial pollen decreases significantly to 568 [SE ±113] grains cm^{-2} yr^{-1}. The organic band does not coincide with any marked increase in influx of terrestrial pollen and investigations of the coarse fraction of the sub-samples at this

level indicate the presence of miscellaneous mosses and *Sphagnum* with Spermatophyta leaf fragments. This would suggest that it was principally a moss band, which is typical of Younger Dryas sediments from such successions in northern Britain (Walker et al., 1993).

LAD7

11750 - 11300 cal yrs BP (450 yrs)
GS-1 to Preboreal
Sample Resolution *ca* 150 years

Ericales – *Betula*

This zone encompasses the clear change in lithology from minerogenic to organic sediments. There is a much reduced representation of Ericales (from *ca* 60% to *ca* 35%) and a dramatic increase in *Betula* (from *ca* 3% to *ca* 33%) with small short-lived expansions of up to 20% each of Gramineae, Cyperaceae, *Oxyria digyna* / *Rumex acetosella* -type, and *Myriophyllum alterniflorum*. Caryophyllaceae, *Saxifraga oppositifolia* / *S. aizoides* -type, *Artemisia* and *Armeria maritima* phase out completely. *Corylus* appears in this zone representing <1%, and there is some *Salix ca* 5%. The balance of the Pteridophytes also changes as the *Lycopodium* spp. phase out, to be replaced by a variety of Filicales taxa. The mean organic content increases significantly to 10.1 [SE ±6.1]%, but the mean influx of terrestrial pollen remains similar to the previous zone at 445 [SE ±241] grains cm^{-2} yr^{-1}.

LAD8

11300 - 10750 cal yrs BP (550 yrs)
Preboreal
Sample Resolution *ca* 275 years

Betula

Woody taxa are dominant at *ca* 90% throughout. This is a very stable zone with *Betula* dominating at *ca* 60%, with *Salix* increasing slightly but remaining below 10%. *Corylus* achieves *ca* 5% at about 10923 cal yrs BP. This accords broadly with the 5% isopoll of Huntley and Birks (1983) at *ca* 9500 ^{14}C yrs BP or 10855 cal yrs BP (CALIB REV4.4.1 (Stuiver et al., 1998a)). The monolete Pteridophyte taxa remain *ca* 15%, and *Sphagnum* occurs at <1%.

This zone marks the beginning of qualitative changes in the representation of arboreal taxa with the introduction of very small proportions of *Quercus*, *Ulmus* and *Sorbus aucuparia* that are maintained throughout the rest of this section of the core. The

herbaceous flora is now essentially Gramineae at *ca* 5% with *ca* 15% monolete Pteridophyte taxa.

The mean organic content continues to increase to 41.4 [SE ±2.5]%, as does the mean influx of terrestrial pollen which rises dramatically to 3661 [SE ±1129] grains cm^{-2} yr^{-1}.

LAD9

10750 - 8000 cal yrs BP (2750 yrs)
Sample Resolution *ca* 400 years

Betula – Corylus

The woody taxa remain *ca* 90%, but throughout this zone there is an apparent juxtapositioning between the proportions of *Corylus* and *Betula*, with a constant representation of Salix *ca* 5% throughout, with Gramineae (<6%) and the monolete Pteridophyte taxa generally <10%. *Corylus* appears to expand *ca* 10200 cal yrs BP to *ca* 35%; this accords broadly with the expansion of *Corylus* in Britain. This was documented by Huntley (1983) at *ca* 9000 ^{14}C yrs BP or 10088 cal yrs BP (CALIB REV4.4.1 (Stuiver et al., 1998a), (Stuiver et al., 1998a)), where local values of >60% were reached. The herbaceous flora is still primarily Gramineae, but <10% with generally <10% monolete Pteridophyte taxa and *ca* 1% *Sphagnum*.

The mean organic content decreases to 37.4 [SE ±1.7]%, and the mean influx falls significantly to 1685 [SE ±148] grains cm^{-2} yr^{-1}.

LAD10

8000 (-) cal yrs BP
Sample Resolution *ca* 93 years

Betula – Corylus

The boundary into this zone marks a subtle but significant change in the relative proportions of pollen. Woody taxa are still dominant at *ca* 95%, represented principally by *Betula* and *Corylus* with *ca* 4% *Salix* and slightly increased representation of *Quercus* and *Ulmus*, and the first occurrence of *Alnus* 7350 cal yrs BP. The herb flora is still principally Gramineae, but <3%, with <3% monolete Pteridophyte taxa and <1% *Sphagnum*. The mean organic content is slightly increased to 44.4 [SE ±0.6]%, but the mean influx increases to 8088 [SE ±1179] grains cm^{-2} yr^{-1}, significantly higher than that in PAZ - LAD10.

5.1.9 Macrofossil Analyses

The macrofossils found in the pollen washings were recorded only as presence / absence data (see Figure 17) and as such can only serve to help interpret the pollen data. The results for the aquatic invertebrates, Algae and Charophyta, are described within respect to the INTIMATE event stratigraphy (see section 5.1.5 and correlated LPAZs in Figure 15), as these divisions are broader than the LPAZs and provide a more general framework that is better suited to the distribution of these particular organisms.

Miscellaneous insect parts and Chironomid head capsules were present throughout, although in varying numbers. *Pediastrum* was present throughout and diatoms were only absent during two of the warmer periods, GI-1e (Bølling) and GI-1a (Allerød). Cladocera remains were present throughout; however, Cladoceran ephippia were only found in the Lateglacial sediments, coinciding with the warmer periods of GI-1e (Bølling), GI-1c (Allerød), GI-1a (Allerød) and the GS1 (Younger Dryas) / Preboreal transition. During harsh climatic conditions the open-water season can be reduced, and it is possible that in very severe climatic conditions gamogenetic reproduction takes place during most of the open-water season (Frey, 1982). Since the general climate of the Lateglacial would fall into the severe category, the occurrence of patches of presence of Cladoceran ephippia could be indicative of periods of relatively milder climatic conditions facilitating summer open-water. Ostracods were found principally in the basal glacial clays with one record in GI-1b (Intra-Allerød cold period).

Charophyte oogonia were only found in the Lateglacial sediments and particularly in the basal glacial clays. Charophytes thrive in stable environments and the production of gametangia is essentially a reaction to ameliorating conditions, and an increased photoperiod (Moore, 1986). This presence of Charophyte oogonia could therefore be associated with reduced ice cover at this time, and/or low bioproduction in the lochan due to the cool conditions. Both factors would contribute to an increase in photoperiod. Bryozoan statoblasts also appear to coincide with the cooler periods of the Lateglacial, indicating a similar response

A single *Selaginella* megaspore was found in GI-1a (Allerød) and corresponds directly with the peak in *Selaginella* microspores. In addition, leptosporangia which are produced by the Filicales (higher ferns), were found throughout the Preboreal and Holocene gyttjas, but also in the very early organic clays/silts of GI-1e (Bølling); these occurrences correspond to the two periods where there were substantial proportions of monolete Pteridophyte spores. Both these records would confirm a local presence of these taxa and suggest moister conditions that correspond well with the GI-1e (Bølling) and Holocene warmings.

The various seeds, leaf fragments and moss fragments (not specifically identified) were found throughout the Lateglacial sediments, with some isolated records through the Holocene. *Polytrichum* sp. and *Sphagnum* sp. were present in GS-1, *Polytrichum* principally in LPAZ - LAD6a and *Sphagnum* principally in LPAZ – LAD6b. These coincide with the presence of *Juncus* spp. seeds throughout GS-1 and regular records of Ericales seeds and two records of Caryophyllaceae seeds. *Juncus* spp. seeds were found throughout GS-1, but *Juncus* pollen is very delicate and hence poorly preserved and difficult to extract (Fægri and Iversen, 1964, p 79) and no grains were identified throughout. Leaf fragments from woody plant species were found throughout the LPAZs, but not in the basal clays and sands. Specific identification was only possible for Lateglacial specimens, where preservation was sufficiently good to enable identification of *Salix herbacea*, *Betula nana* and *Dryas octopetala* fragments. *Betula* fruits (tree *Betula*) were only found in the very early Holocene sediments and again at the very top of the core section in LPAZ - LAD10.

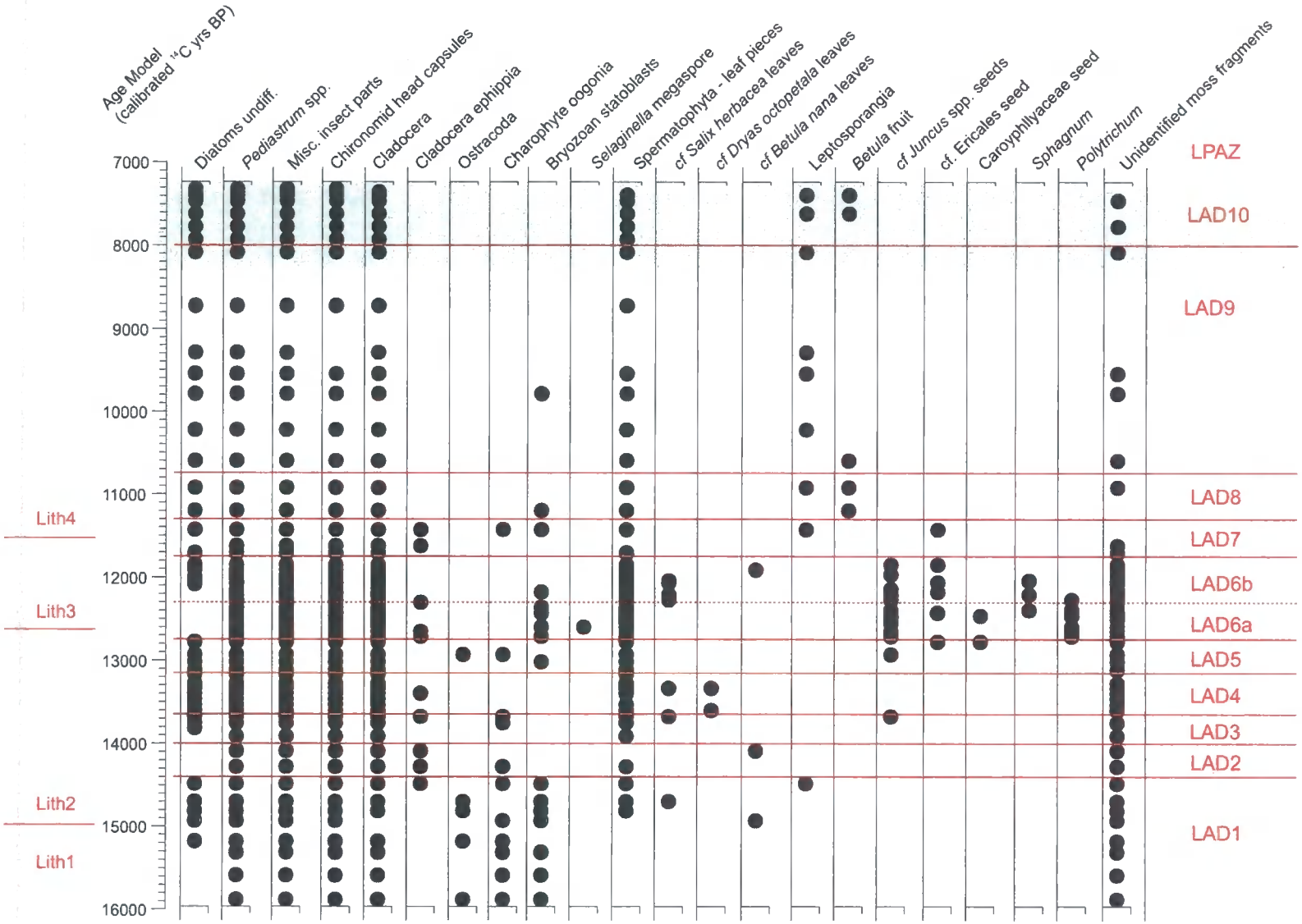
Age Model (calibrated ^{14}C yrs BP)
Diatoms undiff.
Pediastrum spp.
Misc. insect parts
Chironomid head capsules
Cladocera
Cladocera ephippia
Ostracoda
Charophyte oogonia
Bryozoan statoblasts
Selaginella megaspore
Spermatophyta - leaf pieces
cf Salix herbacea leaves
cf Dryas octopetala leaves
cf Betula nana leaves
Leptosporangia
Betula fruit
cf Juncus spp. seeds
cf. Ericales seed
Caroyphillyaceae seed
Sphagnum
Polytrichum
Unidentified moss fragments
LPAZ
7000
8000
9000
10000
11000
12000
13000
14000
15000
16000
LAD10
LAD9
LAD8
LAD7
LAD6b
LAD6a
LAD5
LAD4
LAD3
LAD2
LAD1
Lith4
Lith3
Lith2
Lith1

5.1.10 Systematic - Quantitative Analyses

5.1.10.1 Palaeobiome Reconstructions

Four biomes were identified, based on the pollen data, as a result of the systematic palaeobiome reconstructions: tundra; cool steppe; cold mixed forest; and temperate deciduous forest. This assignment of biomes is plotted stratigraphically in relation to the pollen sample scores on the first axis of the detrended correspondence analysis (DCA) of the palynological data (see Figure 18). This first axis of the DCA analysis (Eigenvalue 0.83) represents the primary pattern of variation amongst the pollen data, matching in many features with a curve of the % woody taxa in the pollen data, and thus describes the changes between those spectra dominated by the pollen of woody taxa representing forested conditions, and those spectra dominated by the pollen of herbaceous taxa representing cool steppe and tundra conditions.

Cool steppe prevailed in the Late Pleniglacial, changing to tundra throughout the Lateglacial Interstadial, before developing into cold mixed forest at the beginning of the Holocene, and thereafter, through the early Holocene, fluctuating between cold mixed forest and temperate deciduous forest. The sequence of biomes through this period reflects the changes in the prevailing vegetation that can be used to infer more specific climate detail.

Cool steppe is defined here principally by the presence of *Oxyria digyna* / *Rumex acetosella* -type, with various steppe forbs, (e.g. Compositae, Caryophyllaceae, Umbelliferae, *Potentilla*, *Ranunculus*, Rosaceae and *Thalictrum*), *Artemisia* and Chenopodiaceae, steppe/desert forbs and Gramineae. This biome is associated with regions with summer temperatures cooler than 22°C and enough precipitation to meet 28-65% of demand (Prentice et al., 1992).

Tundra is represented here principally by Ericales with Gramineae and Cyperaceae, and with the Arctic Alpines, *Salix* and *Saxifraga* spp. It is found in humid regions where precipitation meets >65% of demand, but GDD5 is insufficient for tree growth, i.e. <350. This biome is today analogous with the Arctic tundra (Prentice et al., 1992).

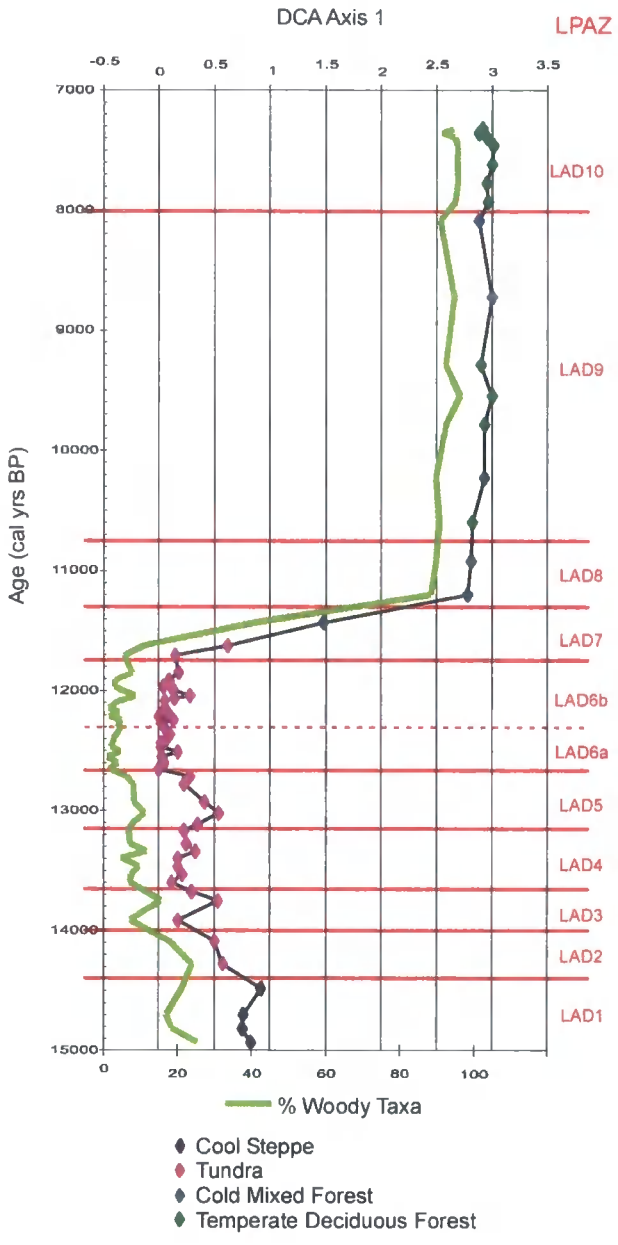

Figure 18

The first axis of the DCA analysis of the pollen spectra (Eigenvalue 0.83) is plotted with the assigned palaeobiomes developed through the systematic biome analyses and matching many of the features of the curve for the % woody taxa at Lochan An Druim. Both curves are plotted against age (cal yrs BP). LPAZs are indicated.

Cold mixed forest is defined by the dominance of cool temperate conifers and boreal summergreen trees. *Abies* and *Taxus* are the two cool temperate conifers and both these taxa were confined to central Europe at this time (Huntley, 1990b). *Betula* is the only boreal summergreen tree represented here, since again, an alternative that could have been *Larix* was only growing in central Europe at this time (Huntley, 1990b). These taxa occur in humid maritime climates with mild winters (-2 to 5°C), and summers too cool (GDD5 <1200) for temperate summergreen trees. This biome is found today occupying relatively small areas on the extreme maritime fringes of northwest Europe (Prentice et al., 1992). At first glance the biome 'cold deciduous forest' might seem more appropriate. Although both biomes are defined with a eurythermic conifer component represented only by *Juniperus* at this site, it is the occurrence of *Corylus*, a cool-temperate summergreen, in the 'cold mixed forest' biome that differentiates them here. In a maritime climate it is the prevailing summer

temperatures that define the two biomes, both cool summers, but in contrast, cold deciduous forests have a GDD5 <900 (Prentice et al., 1992). *Corylus* must therefore be an indicator of less-cool summers. Prentice et al. (1992) alludes to a lack of differentiation between predominantly coniferous or predominantly deciduous forests in his temperate deciduous biome definition and suggests that the missing factor may be the seasonality of drought stress rather than the annual total as used.

Temperate deciduous forest is defined here by the dominance of boreal and cool-temperate summergreen trees and shrubs, principally *Betula* and *Corylus,* but also with *Quercus*, *Alnus*, *Salix*, *Sorbus aucuparia* and some Ericales and *Juniperus*. It is found in areas with cool winters (-2 to 5°C) and enough precipitation to meet 65% of demand, and where GDD5 >1200.

The fluctuating 'temperate deciduous forest' and 'cold mixed forest' biomes throughout the early Holocene can be accounted for by the varying proportions of the temperate summergreen tree *Quercus* (values range from 0.2 to 1.4%). *Sorbus aucuparia*, a boreal/temperate summergreen shrub, also fluctuates here but never represents >0.5% of any pollen spectrum, as compared to *Quercus*. These fluctuations suggest a response to the length of the growing season, where perhaps the high summer insolation (June-July) of the early Holocene (Laskar et al., 2004) could be holding GDD5 values close to the threshold between the requirement of <1200 for cold mixed forest and > 1200 for temperate deciduous forest.

Table 11

Table summarising the characteristic taxa for the eleven LPAZs identified at Lochan An Druim, and correlated with the event stratigraphy of the Lateglacial following Björck et al. (1998), and the biozones of Mangerud et al. (1974) together with the palaeobiomes assigned through systematic biome analyses.

LPAZ	Characteristic Taxa	Biome	Date (cal yrs BP)	Event Stratigraphy	Biozones
LAD10	*Betula* – *Corylus*	Cold Mixed Forest becoming Temperate Deciduous Forest	8000 (-)		Holocene
LAD9	*Betula* – *Corylus*	Cold Mixed Forest with an episode of Temperate Deciduous Forest	10750 - 8000		Early Holocene
LAD8	Ericales – *Betula*	Cold Mixed Forest	11300 - 10750	PB	Preboreal
LAD7	Ericales – *Betula*	Tundra turning to Cold Mixed Forest	11750 - 11300	GS1 / PB	Younger Dryas / Preboreal
LAD6b	Ericales – *Lycopodium* spp. – *Saxifraga oppositifolia* / *S. aizoides* -type	Tundra	12300 - 11750	GS1	Younger Dryas
LAD6a	Ericales – *Lycopodium* spp. – *Selaginella*	Tundra	12670 - 12300	GS1	Younger Dryas
LAD5	Ericales – Cyperaceae	Tundra	13150 - 12670	GI-1b/1a	incl. Intra-Allerød cold period
LAD4	Ericales	Tundra	13650 - 13150	GI-1c	Allerød
LAD3	Ericales – *Oxyria digyna* / *Rumex acetosella* -type –- Gramineae	Tundra	14000 - 13650	GI-1d	Older Dryas
LAD2	Ericales – *Oxyria digyna* / *Rumex acetosella* -type – Gramineae	Tundra	14400 - 14000	GI-1e	Bølling
LAD1	Polypodiaceae -type – *Oxyria digyna* / *Rumex acetosella* -type – Gramineae – *Salix*	Cool Steppe	15000(+) - 14400	GS-2a	Late Pleniglacial

5.1.10.2 Palaeoclimate Reconstructions

The palaeoclimate reconstructions of the indicative climate variables MTCO, GDD5 and AET/PET using the climate surface response method of Huntley (1993) were unsuccessful. All the sets of data that was generated using three different methods of biome constraint produced a range of mean chord distances (i.e. for the closest ten interpolated analogues) that were >0.4 and hence outside the acceptable range. This would suggest that there were no suitable interpolated analogues for these fossil pollen spectra.

Further analysis was carried out using a direct analogue approach, which compared the same fossil pollen spectra directly with the original surface sample analogues. This produced a data set with a range of chord distances that were acceptable. However, on further investigation the range of SE values at 95% confidence were generally very high (see Figure 19), which suggested that sets of very disparate analogues were being found. The full set of analogue locations are mapped in Figure 20, which demonstrates an extensive longitudinal range of 173° in Alaska to 180° in eastern Siberia. The latitudinal range is much tighter at 82° to 36° but covers a very diverse selection of geographic areas from high Arctic to central and southern Asia, which actually embraces a greater range of climates.

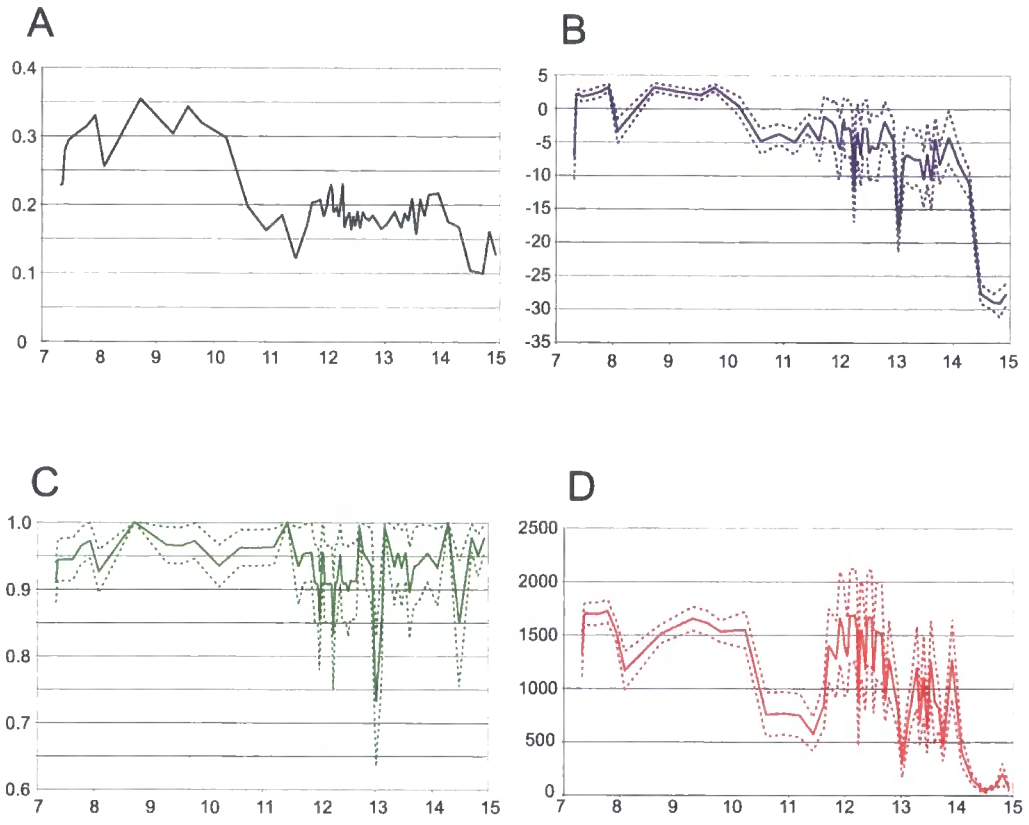

Figure 19

Lochan An Druim: Reconstructed bioclimate variables (indicating the unacceptable standard error values at 95% confidence) based on the 'direct analogue approach' and plotted against an age scale (ka cal BP). A) Chord distance for closest 10, B) MTCO, C) AET/PET, and D) GDD5.

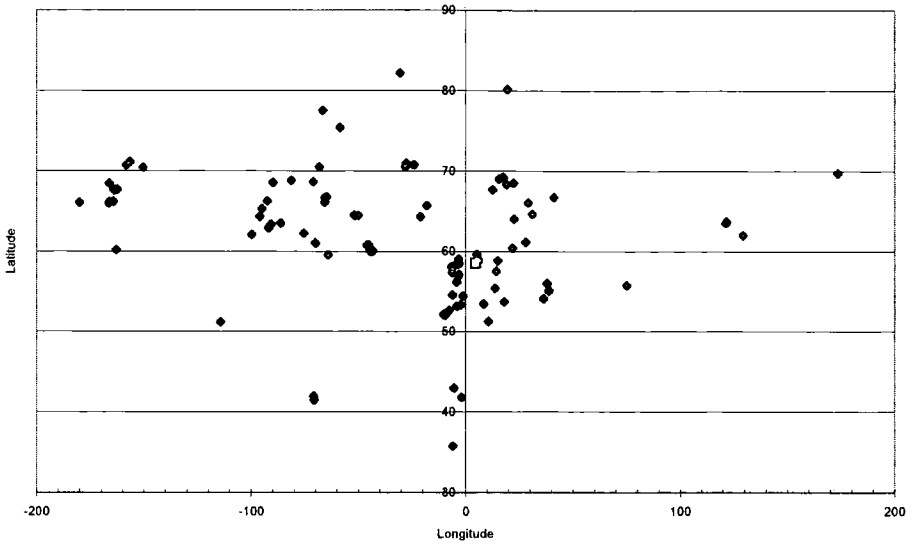

Figure 20

A 'map' of the full set of modern analogue locations found in the direct analogue method of palaeoclimate reconstructions for Lochan An Druim (identified by the square symbol)

The problems incurred in reconstructing these palaeoclimates raises the question of the possibility of non-analogue situations, i.e. that there are no present-day analogues in existence for these Lateglacial fossil pollen spectra. Quantitative no-analogue assemblages of fossil pollen occur extensively (Huntley, 1990a), and it is suggested that these assemblages might have developed as a consequence of environmental change that is so rapid that species with slower migration rates might have lagged behind their potential environmental thresholds. Alternatively, they might reflect combinations of environmental conditions for which no spatially extensive analogue exists today (Huntley, 2001). The dominant Lateglacial assemblages of cool steppe taxa and tundra taxa at Lochan An Druim appear to co-exist throughout the Lateglacial period, showing a quantitative response to the fluctuating climate with no apparent qualitative change in taxa until the early Holocene.This would suggest that migration is not the issue here, however, it could have been a factor following the rapid warming at *ca* 11.5 ka BP, where the rapidly expanding *Betula* initially out-competes the tundra and cool steppe taxa, but where the arrival of a more diverse selection of the boreal and cool temperate summergreen trees takes longer to effect (see Figure 18).

On investigation of the data sets for the modern analogues used in the reconstructions, there was a dirth of samples with such relatively high proportions of Ericales pollen. The Allerød interval in northern Scotland is characterised by a tree-less dwarf-shrub heath frequently dominated by *Empetrum* (presumably *nigrum*) (Birks, 1984; Fossitt, 1996) (Huntley, 1994) (Birks and Mathewes, 1978). Any further definition of associated pollen spectra that could be provided by specific identification of *Empetrum* pollen,

would inevitably be lost in any subsequent climate reconstruction analysis, since in processing the pollen data, Ericales is the only category for all the heath taxa. This would suggest that Ericales is inadequate as a summary group for Lateglacial reconstructions, and closer modern analogues could perhaps be found with more refined definition of this group. However, in order to find a suitable modern analogue for the conditions at this site during the Lateglacial and early Holocene, there would need to be a seaboard at a similar latitude but experiencing summer insolation in the order of between 3% and 8% higher than at the present-day, and winter insolation in the order of between -1% and -4% lower than at the present-day (Laskar et al., 2004). In addition, following the initial warming at GI-1e (Bølling), SSTs would have been much cooler than present-day (*ca* 8°C - 12°C) ranging between *ca* 0°C to below 12°C at the opening of the Holocene (Kroon et al., 1997). Furthermore, the climatic effects of the proximity of the receeding continental glaciers and of their periodic readvance, cannot at present be found in this type of geographical location. Taken together, these facts suggest that there is not likely to be any modern spatially extensive analogue for such a coastal maritime community.

It is clear that the use of such quantitative palaeoclimate reconstructions from areas such as Lochan An Druim, requires a much more extensive set of modern analogues than has hitherto been identified. Efforts to develop a more representative and more highly refined dataset may need to be focussed in very specific (and probably geographically smaller) areas. However, in reality, there are probably no modern analogues to be sampled that could compare with such unique Lateglacial pollen spectra.

5.2 The Palaeoenvironment at Lochan An Druim

The previous palynological study at Lochan An Druim (Birks, 1984) (study 'A') is correlated with this new study (study 'B'), in order to combine the different attributes of each, and hence improve the palaeoenvironmental interpretation of the Lateglacial and early Holocene period at this site. These improvements are manifest principally in a more robust and independent chronology and higher resolution analysis added in study 'B'.

The two stratigraphies have been correlated using the patterns of organic content of the sediment and the characteristic taxonomic features as defined by the LPAZs. The individual LPAZs are related to four key biozones common to both studies (see Table 12).

The chronology developed for study 'A' uses four ^{14}C bulk sediment dates; however, it is suggested that these dates are 600-800 years older than dates for comparable pollen stratigraphical horizons at Abernethy Forest (Birks and Mathewes, 1978). Following the correlation of the two sequences, and using the key biozones, the time - stratigraphic scale in study 'B' suggests that the calibrated ^{14}C dates for study 'A' are *ca* 900 years older, with the exception of the date marking the onset of organic accumulation which appears to correspond to within *ca* 100 years. This reduction in the effect of old carbon on the older age estimate could have been due to the ambient temperature of the lake being too low to facilitate the dissolving of the carbonate, or that the water was too alkaline.

Study 'A' was carried out at lower resolution than study 'B'. Birks (1984) sampled at 5 cm intervals, which according to the chronology of study 'A' gives intervals of *ca* 163 years (calendar years), and according to the chronology of study 'B' gives intervals of *ca* 218 years (calendar years). In study 'B' samples were taken every 1 or 2 cm giving intervals throughout the Lateglacial of 80 [SE±8] years.

Interpretation of Birks (1984) palynological study is supported by quantitative macrofossil analysis. This is an important additional technique for identifying the taxa that are locally present as opposed to those taxa represented by anemophilous pollen that has been transported over long-distances (e.g. *Pinus*). It also provides evidence for taxa that may not be well represented in the pollen spectra due to degradation of the pollen grains (e.g. *Juncus*), and particularly for those taxa that are entomophilous and which therefore produce less pollen (e.g. *Dryas octopetala*).

This study includes the addition of systematic analysis of the pollen spectra to define the regional biomes and thus infer a range of indicative climate variables, MTCO, GDD5 and AET/PET (see section 5.1.10.1).

Table 12

This table summarises the key features resulting from the correlation of the two palynological studies at Lochan An Druim, Birks (1984) and this study, on the basis of matching the common biozones.

Biozones	**Biozone 1**		**Biozone 2**		**Biozone 3**		**Biozone 4**			
LPAZ (Birks, 1984) (LAD = this study)	**AD-1**	**LAD3** **LAD2** **LAD1**	**AD - 2**	**LAD5** **LAD4**	**AD – 3**	**LAD6b** **LAD6a**	**AD - 4a**	**LAD7**	**AD - 4b**	**LAD8**
Sediment Accumulation (m)	0.09	0.15	0.19	0.175	0.34	0.45	0.10	0.075	0.15	0.095
Mean Influx of Terrestrial Pollen (AP+NAP) (grains cm^{-2} yr^{-1})	500-700	76 [SE± 18]	1500-2000	395 [SE± 65]	1800 (max.)	907 [SE± 137]	4000 (mean)	445 [SE± 241]	4000 - 7000 (mean)	3661 [SE± 1129]
% LOI (dry weight)	0.50 - 5.00	6.86 [SE± 0.70]	13 (mean)	17.21 [SE± 1.88]	4 (mean)	5.66 [SE± 0.70]	13 - 39	10.1 [SE± 6.1]	13 - 39	41.4 [SE± 2.5]
Biozone (Mangerud et al., 1974)	Older Dryas	Older Dryas Bølling Late Pleniglacial	Lateglacial Interstadial	Intra Allerød Cold Period Allerød	Younger Dryas	Younger Dryas Allerød	Younger Dryas to Flandrian (Holocene)		Preboreal	
Event Stratigraphy (Björck et al., 1998)		GI-1d GI-1e GS2a		GI-1b GI-1c		GS-1 GI-1a		GS1 / PB		PB

The organic content of the compared LPAZs broadly concurs. However, the figures for the mean influx of terrestrial pollen are consistently higher in study 'A' and this must be attributed essentially to the differing physical conditions at the different locations of the cores. In study 'A' the core was recovered from the dense *Phragmites australis* fen towards the perimeter of the lake, whereas the cores used in study 'B' were taken from the deepest part of the lake in open water. The overall accumulation of Lateglacial sediment in study 'A' was 0.86m compared to 0.94m in study 'B' (i.e. 0.08m less), as might be expected with sediment accumulation higher in the more central location due to inwash and settling, and since neither core is consistently different across the LPAZs, these variations must be attributed to localised spatial and temporal taphonomic effects. Although the values for the mean influx of terrestrial pollen are consistently higher in study 'A', both studies follow a similar pattern with values increasing up the sequence. Again, this difference is likely to be due to the taphonomic dynamics of the lake, combined with an increased trapping effect due to the macrophyte growth around the perimeter of the water.

The palaeoenvironment of each of the four biozones is discussed below, together with a brief comment concerning the boundary into a fifth zone which represents the opening of the main Holocene period.

Biozone 1

In study 'A' the highest pollen percentages reported for this biozone are for *Salix* Gramineae and Cyperaceae with comparitively high percentages of *Rumex* spp. and *Oxyria digyna*, with *Empetrum nigrum* and Ericales (undifferentiated) increasing through the zone. Macrofossil evidence indicates the presence of *Dryas octopetala*. Although the percentages of *Salix* pollen are high its influx is very low, suggesting that it was not abundant in the vegetation (Birks, 1984).

In study 'B' a similar pattern of relatively dominant taxa occurs through LADs 1, 2, and 3 but with analyses at a higher resolution it has been possible to differentiate three distinct LPAZs. The earliest, the Late Pleniglacial stage (LAD1), is dominated by *Oxyria digyna* / *Rumex acetosella* -type and Gramineae with some *Salix* (again influx values suggest that it was not abundant in the vegetation), and abundant Pteridophytes dominated by Polypodiaceae -type. *Oxyria digyna* as specifically identified in study 'A', is a pioneer species of recently deglaciated terrain (Polunin and Walters, 1985, p 167) and Polypodiaceae are characteristic of rocky habitats (Tutin et al., 1964-1993), which would indicate a newly deglaciated landscape with unstable gravels and rocks with little yet in the way of soil development, and supporting a sparse vegetation.

The climatic amelioration of the Bølling (GI-1e, LAD2) registers with evidence for vegetational development, a decline in the herbaceous taxa and a proportional increase in Ericales. Whilst some *Empetrum* pollen was identified, the overall nature of most of the grains, which were distorted, reduced confidence in accurate identification and it was decided to present only one count for total Ericales. Birks (1984) identified significant proportions of *Empetrum nigrum* pollen (increasing to *ca* 30%) in this biozone, and *E. nigrum* macrofossils in the upper biozone 2. Taken together, this evidence supports the suggestion that *E. nigrum* was an important constituent of the Ericales taxon in this zone. The proportional representations of *Betula* and *Salix* within the woody component appear to change, with *Salix* declining and *Betula* increasing. However, the influx values for both are extremely low and since Birks (1984) has no record of either *Salix* or *Betula* macrofossils in this zone, it must be supposed that neither formed a significant part of the local vegetation and that the pollen present was probably transported from a distance. This apparent dominance of *E. nigrum,* which is characteristic of Arctic dwarf-heath tundra and indicative of nutritionally poor soils (Polunin and Walters, 1985), suggests a more extensive ground cover and indicates the beginning of the development of more stable soils following deglaciation. The presence of *D. octopetela* macrofossils found in Study 'A', would suggest perhaps a tundra mosaic with *D. octopetela* occupying the drier raised areas, and *E. nigrum* forming a more dense cover of the lower ground.

In LAD3 the continued expansion of Ericales (*cf Empetrum nigrum*) is interrupted by a reversal between 13.9 and 13.7 ka BP that has been correlated with GI-1d (Older Dryas) (see Figure 15). This reversal episode, which only lasted *ca* 200 years, registers as a quantitative change in the vegetation cover, with an expansion of the relative proportion of herbs, principally Gramineae with some *Saxifraga oppositifolia / S. aizoides* -type, and a corresponding contraction of Ericales (*cf E. nigrum*), but where the diversity of the representative taxa (i.e. the variety of other taxa in the pollen spectrum that remain constant but which fluctuate quantitatively) remains constant. This change suggests that the tundra patchwork might have opened out in response to the cooling event; a theory supported by the identification of *S. oppositifolia* seeds in this biozone in study 'A', since this species is characteristic of more open habitats.

The lochan itself appears to have been unproductive throughout this biozone. According to Birks (1984) the macrophyte vegetation was dominated by *Nitella* associated with some *Chara*, and Charophyte oogonia were found in study 'B'. This would suggest that this biozone corresponds with the early colonisation of the Lochan following deglaciation, where cold stable conditions prevailed. Dinoflagellate cysts (undiff.) were recorded throughout LAD1 and LAD2 with influx values of up to 50 cysts

cm^{-2} yr^{-1} in LAD1 and 70 cysts cm^{-2} yr^{-1} in LAD2, but they were not present in LAD3 when it is suggested that the climate deteriorated.

Biozone 2

The pollen influx and the organic content of the sediment in this biozone show a greater than threefold increase in both studies suggesting vegetational development in response to the ameliorating environmental conditions.

The most abundant pollen types in study 'A' are *Empetrum nigrum* with Cyperaceae and Gramineae and a considerably reduced representation of *Salix*. However, the macrofossil evidence for *Salix herbacea* suggests that this species was probably abundant throughout this zone. The pollen of *S. herbacea* is anemophilous but it is only produced in small amounts, and due to the stature of the plant, necessarily close to the ground; therefore dispersal is limited (Birks, 1984). This would suggest that generally *S. herbacea* might not be adequately represented in lacustrine palynological records. Again, there is a small proportion of *Betula* pollen supported by very low influx, and no macrofossil evidence for the presence of this taxon.

In both studies most of the herb taxa from biozone 1 persist but with reduced representation due to the dominance of Ericales (*cf Empetrum nigrum*). Birks (1984) records abundant *E. nigrum* macrofossils, which are virtually confined to this zone. Again there is macrofossil evidence for *Dryas octopetala*, recorded throughout this zone (AD2) in study 'A', and in the lower LPAZ in study 'B' (LAD4), although there is no pollen evidence for this species. *D. octopetala* is entomophilous and therefore produces relatively low amounts of pollen, which could account for this discrepancy. *Selaginella* spores appear in both records towards the younger boundary of this zone, from where they begin to increase. This lesser clubmoss is widely found today in damp, base-rich grasslands and flush communities. Coincidentally with the appearance of *Selaginella*, the Pteridophyte flora begins to expand, driven principally by the club moss *Huperzia selago*.

Study 'B' differentiates two LPAZs, LAD4 and LAD5, in this biozone. The former dominated by Ericales (*cf Empetrum nigrum*) and the latter registering another reversal with the juxtaproportions of Ericales (*cf E. nigrum*) and Cyperaceae, and which has been correlated with GI-1b (Intra-Allerød cold period) (see Figure 15). This increase in the proportional representation of Cyperaceae is reflected in an increased influx of pollen, and supported by macrofossil evidence from study 'A'. This second reversal episode also lasts for *ca* 200 years and similarly registers as a quantitative change in vegetation cover with the diversity of the representative taxa remaining constant.

The biomes throughout biozone 2 indicate a continuation of the 'tundra' landscape, with the same representative taxa but with fluctuating relative abundances. The tundra mosaic in this biozone would be similar to that discussed for biozone1 with additional evidence for the presence of *Salix herbacea*, which would probably have colonised the more open areas. This species is indicative of late snow patches. The particular taxa discussed here would indicate that moisture availability was increasing through this zone, suggesting a general warming trend as might have been expected during the Lateglacial interstadial.

According to Birks (1984), the environment of the lochan becomes more productive in this biozone, as indicated by abundant *Nitella* and *Chara* oospores (also recorded in study 'B') and the appearance of aquatic *Ranunculus* spp., recorded in the macrofossil evidence.

Biozone 3

Pollen influx continues to increase in this biozone but both studies record a reduction in the sedimentation rate. Pollen percentages are still dominated by Ericales, but Birks (1984) notes that the tetrads in this zone could not be identified to species because of their poor state of preservation. She suggests however, that the majority belong to *Empetrum nigrum*, although, there is no supporting macrofossil evidence for Ericales in this zone. This dominance by Ericales causes a reduction in the relative proportions of the representative taxa in both studies, but both records show a marked increase in pollen from *Saxifraga oppositifolia / S. aizoides* -type, *Artemisia*, Carypohyllaceae and *Huperzia Selago* (referred to as *Lycopodium selago* in study 'A') and the appearance of a hitherto unrecorded species, *Armeria maritima*.

Study 'B' differentiates two LPAZs, sub-zones LAD6a and LAD6b in this biozone. The former is still dominated by Ericales, but with an abundant Pteridophyte flora, principally *Lycopodium* spp. and *Selaginella* with a reduced herbaceous flora, but with *Saxifraga oppositifolia / S. aizoides* -type and *Artemisia* beginning to increase towards the end of the zone. This has been correlated with GI-1a (the end of the Allerød) and develops into LAD6b correlated with GS-1 (Younger Dryas) (see Figure 15). In this LPAZ, the Ericales begin to decline, with a corresponding increase in principally, *Saxifraga oppositifolia / S. aizoides* -type, *Artemisia* and Caryophyllaceae. At the same time the herbaceous flora becomes more diverse with the reappearance of *Potentilla* -type and the appearance of *Armeria maritima*, while *Selaginella* declines.

The marked lithological change in this zone to a more minerogenic sediment would indicate that the surrounding soils had become unstable, allowing increased mineral inwash. The significant increase in pollen influx and rise in deteriorated grains, would

suggest that pollen was being transported from the surrounding soils with the mineral erosion. Birks (1984) identifies increased macrofossils of *Polytrichum sexangulare* leaves and abundant *Salix herbacea* remains that suggest an increased extent of snow beds at this time.

The nature of the 'tundra' vegetation has changed again, with the contraction of the dwarf-shrub heaths of *Empetrum nigrum* and *Dryas octopetela,* and the development of a more open community of abundant *Saxifraga oppositifolia / S. aizoides* -type with *Artemisia*, Caryophyllaceae, and *Armeria maritima.* The appearance of *A. maritima* in this biozone is the first qualitative response of the vegetation to changing climate since the rapid expansion of Ericales (*cf E. nigrum*) towards the end of biozone 1. *A. maritima* has a widespread distribution in arctic and temperate regions and is therefore not of value in inferring past climate, but it is a successful species in open communities (West, 2000), and was therefore able to take advantage of the opening up of the landscape during the Younger Dryas cooling.

Birks (1984) records a virtual absence of any evidence from aquatic plants and animals, and describes the lochan as barren except for a few algae. In this study the presence of bryozoan statoblasts and cladoceran ephippia are recorded, particularly in the early part of this biozone, which correlates with the end of the Allerød. This suggests a response to the deteriorating conditions at the end of this warm period before moving into the more severe climate of GS-1 (Younger Dryas).

Biozone 4

In biozone 4, both studies record a rise in pollen influx values and a corresponding increase in organic content of the sediment together with a return to former, higher sedimentation rates.

This biozone is characterised by rising values for *Betula*, with its presence in the local flora supported by macrofossil evidence, together with a corresponding decline of Ericales. In addition, Study 'A' records a peak of 10% *Juniperus communis* and although *Juniperus* does peak here in study 'B', the proportions are lower at 1%. *J. communis* is notoriously difficult to identify, and as a result care was taken in study 'B' to check for significant amounts of pollen at this level, with a selection of samples being checked and recounted by Dr JRM Allen; however, no more grains were found. One explanation could be that *J. communis* would have developed as a low lying shrub at this time, possibly ssp. *nana*, pioneering the change from the severe conditions that prevailed during GS-1 (Younger Dryas), and it is possible that the characteristics of this anemophilous pollen were not sufficient to enable it become airborne before being trapped in any peripheral vegetation around the lochan. Birks (1984) records

macrofossil evidence for *Juncus*, suggesting that it was common, probably around the perimeter of the lochan. This lack of accord between the sites highlights the problems encountered in the proportional representation of pollen counts that are particularly low. The influx value for *J. communis* in study 'B' is 52 grains cm^{-2} yr^{-1}, unfortunately there is no comparable figure for study 'A', however, the two records have quite different AP+NAP influx rates in this biozone, with study 'A' showing a nine fold increase in influx over study 'B' during this time. The higher pollen influx value for Study 'A' in this particular biozone could be accounted for by increased inwash from the surrounding unstable soils left after the Younger Dryas stadial being trapped by the macrophyte growth around the perimeter of the lake (sediment accumulation here is higher in Study 'A'). Therefore, it is suggested here that the difference between the studies is as a result of this increased inwash, and the lower results for *J communis* in Study 'B' could therefore reflect the airboure component of the total pollen for this taxon at this time.

Both studies differentiated this biozone into two distinct LPAZs: AD-4a / LAD7 and AD-4b / LAD8. In AD-4a/LAD7 there is a marked decline in the taxa characteristic of biozone 3, particularly *Saxifraga oppositifolia* / S. *aizoides* –type, *Artemisia*, Caryophyllaceae, and *Armeria maritima*, corresponding to a brief increase in Cyperaceae, Gramineae and *Oxyria digyna* / *Rumex acetosella* -type. *Salix* pollen values remain low, and *S. herbacea* macrofossils cease to be represented. *Huperzia selago* (*Lycopodium selago*) declines with a corresponding rise in monolete Pteridophytes. During this time the vegetation changed from a species rich 'tundra' assemblage through a dwarf-shrub heath phase, dominated by *Juniperus communis* and *Empetrum nigrum* with abundant ferns, to 'cold mixed forest' principally of *Betula*. The quantitative changes in the herbaceous taxa precede the most significant qualitative change in this record i.e. the arrival of *Betula*, which very quickly came to dominate the surrounding landscape (macrofossil evidence suggests that there was little or no *Betula nana* represented).

This shift from 'tundra' to 'cold mixed forest' is characterised by ameliorating winter conditions, and typified by the arrival and expansion of *Betula*. A continuing maritime influence maintained the humidity, and whilst there was a change towards milder winters (-2 to 5°C), summers temperatures were too cool (GDD5<1200) for temperate summergreen trees at this site. These conditions are analogous today with relatively small areas on the extreme maritime fringes of northwest Europe.

Major changes took place in the lochan at the opening of this biozone, with *Chara* and *Nitella* proliferating. Subsequently other submerged aquatic plants arrived, notably *Myriophyllum alterniflorum* that registered a significant signal in both studies, and Birks (1984) records increases in both algae and aquatic animals.

The sudden change in both terrestrial and aquatic vegetation during this biozone reflects a rapid and substantial amelioration of climate over a period of *ca* 450 years, and corresponding with the start of the Holocene.

The LPAZ AD-4b/LAD8 is dominated by *Betula*, and as this birch forest developed *Juniperus communis* and monolete Pteridophytes remained common understorey plants, with Gramineae gradually declining. Very low pollen values for *Quercus*, *Ulmus*, *Populus tremula* and *Sorbus aucuparia* appear, the former two probably due to long distance transportation from the south (Huntley, 1990b). According to Birks (1984) there is macrofossil evidence for the persistence of some of the plants of open ground, namely, *Saxifraga* spp., Caryophyllaceae and *Dryas octopetala*, and several of these species still grow near to An Druim today, notably *D. octopetala*.

Biozone 4/Holocene boundary

The boundary of biozone 4 with established Holocene conditions marks a major change in the fossil pollen assemblage with the rapid expansion of *Corylus*, giving rise to relative pollen values equalling those of *Betula*. The local presence of *Corylus* is confirmed by macrofossil evidence in study 'A'. The relative dominance of these two woody taxa (*ca* 90%) suggests substantial woodland and the resident understorey appears to decline through this phase, probably as a result of the increased canopy.

The burst of aquatic plant productivity in the previous zone declines here, with the apparent disappearance of, *inter alia*, *Myriophyllum alterniflorum*. There is, however, both pollen and macrofossil evidence for the arrival of *Nympaea*. Birks (1984) suggests that the perimeter of the lake could have become shallow enough to allow for the growth of this taxon, which would have consequently shaded out the submerged aquatic plants. The absence of cladoceran ephippia in both studies suggests that the winter conditions were not sufficiently severe to initiate ephippial production.

This study documents the next LPAZ, LAD9, which covers a span of *ca* 2750 years during which the characteristic taxa from biozone 4 prevail. There appears to be continuous juxtaproportioning between *Betula* and *Corylus* throughout, reflecting early Holocene climate oscillations, and suggesting fluctuations about the threshold conditions that limit the growth of boreal taxa (i.e. *Betula*) and cool-temperate summergreen taxa (i.e. *Corylus*). This is predominantly a reflection of fluctuating summer temperatures, where cool-temperate summergreens require GDD5 >1200 (Prentice et al., 1992). These changes register in the biome assignments that oscillate between 'cold mixed forest' and 'temperate deciduous forest'. This is particularly apparent towards the upper boundary of this LPAZ, where it is suggested that the revertence episode at *ca* 8.1 ka BP registers the '8200 event' (Alley et al., 1997). This

is a widespread cooling event recorded in many early Holocene records (Duplessy et al., 2001; Johnsen et al., 2001; Paus et al., 2003; Snowball et al., 2002; von Grafenstein et al., 1998) (see also section 5.1.4).

The boundary between LAD9 and LAD10 marks an important qualitative change in taxa, as the relative proportion of *Quercus* pollen begins to rise and the woody taxa begin to diversify. This new community is reflected in a consistent biome change from 'cold mixed forest' to 'temperate deciduous forest'.

The pollen profile in Study 'A' has been compared and correlated according to the chronozones of Mangerud et al. (1974) with other Lateglacial sites in northern Scotland (see Birks (1984)); both the Lateglacial and Younger Dryas chronozones are defined throughout the region. However, there appears to be no evidence for the Bølling chronozone; at all the sites the lowest pre interstadial zones are correlated with the Older Dryas, and similarly at Abernethy Forest (Birks and Mathewes, 1978). Only at At Morrone (Huntley, 1994), where the record is longer, is there evidence for the interruption of the Lateglacial interstadial with the Older Dryas reversal at *ca* 11.5 ^{14}C ka yrs BP (13.5 cal yrs BP), compared to 13.75 ka yrs BP at Lochan An Druim (Study 'B'). Allerød vegetation across the region appears to be a treeless dwarf-shrub heath frequently dominated by *Empetrum*. There is no evidence in any other records of the Intra Allerød Cold Period that is so clearly defined by a decline in the proportional representation of this taxon in the record at Lochan An Druim *ca* 13 ka yrs BP (Study 'B').

Study 'B' thus provides a high resolution terrestrial record for the Lateglacial in the north of Scotland, revealing both of the Lateglacial interstadial reversals indicated in the GRIP record, and providing an independent chronology for these events. This unique record serves to justify the original decision to re-sample an existing site.

Chapter 6

The Lateglacial and early Holocene Palaeovegetation and Palaeoenvironment at Nikkupierjav'ri in Northern Finnmark

6.1 Results

6.1.1 Sediment Stratigraphy

6.1.2 Radiocarbon Chronology

6.1.3 Tephrochronology

6.1.4 The Age-Depth Model

6.1.5 Correlations with Greenland Ice Record

6.1.6 Pollen Analysis

6.1.7 Pollen Influx

6.1.8 Descriptions of the Pollen Zones

6.1.9 Macrofossil Analyses

6.1.10 Systematic - Quantitative Analyses

6.1.10.1 Palaeobiome Reconstructions

6.1.10.2 Palaeoclimate Reconstructions

6.2 The Palaeoenvironment at Nikkupierjav'ri

6.1 Results

6.1.1 Sediment Stratigraphy

A description of the sediments for the Lateglacial and early Holocene section of the core from Nikkupierjav'ri is presented in Table 13. The lithological boundaries are identified, principally according to the proportion of organic material.

These sediments show a marine-transitional-freshwater facies succession, indicating a single isolation event. Sedimentation commences at 9.60m BD. The lowermost 2.5m of sediments contain the lithological sequence typical of Lateglacial and early Holocene successions in an isolation basin, with minerogenic postglacial marine sediments underlying the uniformly organic sediments of the Holocene. This sequence comprises five broad lithological units. The basal unit of glacial sand (Lith1), has a well defined lithostratigraphic boundary at 9.45m with the onset of some organic acccumulation. This is overlain by 1.6m of marine sediments (Lith2) indicating that the basin was below sea level at deglaciation. These sediments are divided into three sub-sections. The lowermost sub-section (Lith2a) consists of 0.74m of clayey silt with abundant marine algae that tends to form organic bands towards the base of the unit, but mixes upward with the mineral to form a homogenous black sediment (that oxidises to pink). The mid 0.185m sub-section (Lith2b) forms a band of grey homogenous silty clay with only a few organics. Above this lies the upper sub-section (Lith2c) of 0.675m of coarser sediment, sandy silt with a few stones (<1cm) and layered organic bands of varying width up to 0.5cm. Overlying these marine sediments is 2cm of paper-thin laminae indicating the isolation contact (the marine to freshwater diatom transition occurs about this level).

Table 13

Description of the Lateglacial and early Holocene sediments from Nikkupierjav'ri, following Troels-Smith (1955) as proposed by Aaby and Berglund (1986). Four categories of physical qualities are described as follows: nigror (nig.) - the degree of darkness; stratificatio (strf.) - the degree of stratification; elasticitas (elas.) - the degree of elasticity; and siccitas (sicc.) - the degree of dryness.

Lithological Sedtion	Depth m(BD)	Physical Properetie				Texture	Munsell Colour			Characterisation following Troels-Smith (1955)				Description
		nig.	strf.	elas.	sicc									
Lith5	6.89 – 7.30	2	0	3	3	firm	5Y	4/2	brown	$Ld^3$3	Dg1			gyttja with few organic macros
Lith4	7.30 – 7.62	2	0	3	3	firm	5Y	4/3	yellow/brown	$Ld^3$2	Ag2			silty gyttja / colour gets paler with depth / abrupt lower boundary
Lith3	7.62 – 7.85	0	0	0	1	firm	7.5YR	5/2	blue-grey	As4				clay
Lith2c	7.85 – 7.87	3	4	1	2	firm				As2	Gmin1	Ld^1+	Ag+	paper thin laminae isolation contact
	7.87 – 7.915	2	1	2	3	soft	5Y	4/1		Gmin2	$Ld^1$1	Ag1	Gmaj+	sandy silt (with stones <1cm) / layered organics (marine algae) / lens of coarse grains
	7.915 – 7.92	4	0	0	3	loose				$Ld^1$4				organic band (marine algae)
	7.92 – 8.525	2	1	2	3	soft	5Y	4/1		Gmin2	$Ld^1$1	Ag1	Gmaj+	sandy silt (with stones <1cm)) / layered organics (marine algae)
Lith2b	8.525 – 8.71	1	0	0	1	soft			grey	Ag3	As1			homogenous silty clay
Lith2a	8.71 – 9.25	4	1	1	2	soft			black	Ag3	As1	Ld^1+	Gmaj+	silty clay with coarse gravel and marine algae/ oxidises to pink / darker with depth
	9.25– 9.325	4	0	1	2	firm			black	Ag3	As1			homogenous black silty clay / oxidises to pink / abrupt lower boundary
	9.325 – 9.40	3	3	1	2	soft				$Ld^1$2	As1	Ag1		clayey silt / organic bands (marine algae)
	9.40 – 9.45	3	4	1	2	soft				As2	Ag2			clayey silt / mineral laminations
Lith1	9.45 – 9.615	3	0	1	2	loose/ coarse				Gmin3	Ag1			silty sand

This laminated section would have been formed during the transition between the marine and lacustrine phases, when the basin no longer received a regular supply of marine water across the threshold. During this phase marine bottom water in the basin would have become anoxic, or subject to enhanced seasonal variability in oxygen content, causing the cessation of bioturbation. Laminated facies in most basins are thought to have formed during a meromictic (salinity stratified) phase that would have developed and persisted for some time after isolation and thus the isolation contact should be placed at the bottom of the laminated section corresponding to mean high tide level (Corner et al., 1999). Earlier interpretations of this phase have indicated that the laminated unit represents a brackish phase occurring immediately before isolation, and therefore places the isolation contact at the top of the unit (Kaland et al., 1984). Limited diatom analysis in this study indicated brackish diatoms at 2cm below the unit (J Lloyd Pers. Comm.), thus supporting the former interpretation.

Above the laminated section lies a 0.230m band of blue-grey clay (Lith3) with an abrupt upper boundary overlain by 0.320m of silty gyttja (Lith4), which suggests the beginning of organic non-marine sedimentation in the lake. Overlying this is the beginning of organic rich gyttja sediments (Lith5) that extend to the lake-bed.

The %LOI (dry weight) curve (see section 6.1.6 below) supports these broad divisions with the lowest values in the minerogenic marine units, Lith2a, 2b and 2c, these increase upwards from a mean of 1.76 [SE ±0.06] in Lith2a to a mean of 3.24 [SE ±1.7] in Lith2c. There is a slight increase in Lith3 (mean 5.87 [SE ±0.72]), and a more significant increase into the organic sediments of Lith4 (mean 17.02 [SE ±0.77].

.

6.1.2 Radiocarbon Chronology

Sample information and results of AMS radiocarbon dating are shown in Table 14. The results are corrected for isotopic fractionation by normalising to -25‰ relative to PDB standard using measured $\delta^{13}C$ values.

The AMS radiocarbon dates have been calibrated using CALIB REV4.4.1, using the calibration data set INTCAL98, based on dendrochronologically dated tree rings, uranium-thorium dated corals and varve-counted marine sediment (Stuiver et al., 1998a).

For comparison, the marine samples have also been calibrated using the MARINE98 dataset (Stuiver et al., 1998a), which incorporates a time-dependent global ocean reservoir correction of 400 years. In addition, the on-line marine reservoir correction database (http://www.calib.org/marine) has been used to select an appropriate correction factor for the Barents Sea area of: Delta R = 109.0 ± 70 (Reimer and Reimer, 2001). These corrections for the marine reservoir age inevitably give younger age estimates. Preliminary diatom assessment at 7.89m (2cm above sample RC5) indicated a brackish assemblage (Pers. Comm. J Lloyd), and in the environment of an isolation basin the degree of marine influence cannot be estimated without concurrent proxy studies, e.g. diatom assemblages. However, $\delta^{13}C$ values can give some indication of the carbon sources incorporated into the material dated, since $\delta^{13}C$ values tend to be high in samples containing predominantly marine/brackish diatoms and low in samples containing predominantly freshwater diatoms (Corner et al., 1999). The $\delta^{13}C$ values in this study show some variation with a decreasing trend upward through the sediments and a clear distinction between the brackish and freshwater sediments (-2.7 ‰ PDB). This would suggest that the source of the organic material changes upwards through the succession. However, the relatively high $\delta^{13}C$ in this study is not necessarily indicative of marine carbon content. Isolation basin studies in the Nikel-Kirkenes area in northwestern Russia (120 km southwest of Nikkupierjav'ri), and at Polyarny (250 km southwest of Nikkupierjav'ri), have demonstrated that the $\delta^{13}C$ values in marine and terrestrial organic material overlap. The values obtained from the study at Nikkupierjav'ri, i.e. -23.6 to -28.7, lie within this overlap. In addition, Corner et al. (2001) have compared dates from closely spaced samples of gyttja containing different proportions of marine/brackish diatoms, and achieved reasonably close agreement without any reservoir age adjustment. Furthermore, they developed inverted age relationships when a reservoir age adjustment was used, based on the percentage content of marine/brackish diatoms.

The AMS radiocarbon age for sample RC5 in the brackish sediments in this study, 10085 ±70 years at 7.910m, becomes inverted with respect to the upper date from non-marine sediments of 9548 ±88, if a marine reservoir adjustment is made (see Table 14). In the light of the evidence presented above it was decided not to use a marine reservoir correction for any of the dates in this isolation basin.

The ^{14}C date for sample RC6 at 8.485m was inverted with respect to the next upper date for sample RC5, and results for RC6 gave an error of ±100 years as compared to an error of ±70 for RC5. Since the sub-sample for RC6 was taken from close to the top of a core section and could therefore have suffered some contamination, this date has been rejected.

Table 14

Macrofossil sample information and results of AMS radiocarbon dating using CALIB 4.4.1 (Stuiver and Reimer, 1993); information provided after Lowe and Walker (2000).

Sample	lab no.	Depth m(BD)	Material	Sample Dry Weight (mg)	Estimated Carbon Content (%)	^{14}C yrs BP	δ^{13}C‰ PDB	Calibration data set	Calibrated range BP (2σ)	Relative area under probability distribution	Mid-point of the 2σcalibrated range BP (to nearest 10yr)
PS5-2B	AA-49014	8.675	mixed marine algae	32	40	12 111± 78	-24.3	intcal98.14c (Stuiver et al., 1998a)	13 821 – 14 359	0.664	**14 090** ±269
								marine98.14c (Stuiver et al., 1998a) Delta R = 109 ±70	13 161 – 13 821	0.995	**13 490** ±330
RC6	Ua-21244	8.385	mixed marine algae	70	40	9 810 ±100	-24.6	Intcal98.14c (Stuiver et al., 1998a)	11 056 – 11 563	0.871	**11 300** ±254
								marine98.14c (Stuiver et al., 1998a) Delta R = 109 ±70	10 066 – 10 826	0.925	**10 440** ±380
RC5	Ua-21243	7.910	mixed marine algae	51.9	40	10085 ± 70	-26.0	intcal98.14c (Stuiver et al., 1998a)	11 259 – 11 782	0.776	**11 520** ±262
								marine98.14c (Stuiver et al., 1998a) Delta R = 109 ±70	10 329 - 11 288	0.999	**10 800** ±480
PS5-2A	AA-49013	7.555	mixed woody leaves and stems	10	40	9 548 ±88	-28.7	intcal98.14c (Stuiver et al., 1998a)	10 667 – 11 163	0.960	**10 910** ±248

6.1.3 Tephrochronology

Cryptotephra shards were found in only one vertical sub-sample of the core (7.35m to 7.39m) and this horizon was rationalised to 7.36m. Unfortunately, although several shards were identified in the final sub-sample, no shards were found on the ground resin surface prepared for electron microprobe analyses. Therefore it was felt that there was likely to be insufficient material to warrant any further grinding and re-probing (A J Newton, Pers. Comm.).

The record of cryptotephra in this early Holocene deposit in northern Finnmark appears to lie well to the northeast of the known distributions of European early Holocene cryptotephras (Davies et al., 2002). Other traces of volcanic shards have been found (Pers. Comm. J R M Allen) but again, not in sufficient quantity to enable geochemical analysis. These discoveries suggest that Holocene cryptotephras might be more widespread than hitherto recorded. A more specific study in this area could therefore establish the potential for developing a tephrochronology for northern Finnmark, which would provide a key correlative tool for records spanning the length of the northwest continental margin.

6.1.4 Age-Depth Model

In order to obtain the best age-depth relationship for this sequence linear segments and polynomial models were fitted to the accepted and calibrated radiocarbon dates, and a date of -51 years for the top of the core. Visual inspection of the Holocene sediments suggested that sedimentation had been relatively uniform throughout this period, and therefore it would be acceptable to include a date for the top of the core. Three models were tried.

Firstly, a line of best fit was drawn to the calibrated radiocarbon data points ($R^2 = 0.98$), however, it was felt that this did not take sufficient account of the changes in lithology through the section.

Secondly, a third order polynomial provided a good fit to the 2 sigma age range of the calibrated radiocarbon data points ($R^2 = 1.00$); however, projecting this curve to the base of the core produced a deglaciation date of *ca* 22 ka BP, somewhat earlier than that suggested by Vorren (1978), Vorren (2002) and Andersen (1979).

Finally, a series of linear segments were fitted between the date for the top of the core (5.25m, -51 yrs BP) and the calibrated AMS radiocarbon date (7.555m BD, 10910 yrs BP) and this was extrapolated to the prominent lithological boundary (Lith4/Lith3) giving a date of 11267 yrs BP at 7.63m BD. This point was then joined to the calibrated AMS radiocarbon date (7.91m BD, 11520 yrs BP) close to the prominent Lith3/Lith2

boundary, giving the second linear segment. Finally, the third linear segment was developed between the calibrated AMS radiocarbon date at (7.91m BD, 11520 yrs BP) and the calibrated AMS radiocarbon date at (8.675m BD, 14090 yrs BP), and then extrapolated to the beginning of sediment accumulation at 9.615m, to give an estimated date for deglaciation of *ca* 17200 cal years BP. These three linear segments are combined in Figure 21 to give the completed age depth model.

These last two models gave the same date of 11520 cal yrs BP for the Lith3/Lith2 boundary, but different projected dates for deglaciation. In view of the closeness of these two models at the top of the sequence it was decided to use the linear segment model since it projected a more realistic date for deglaciation.

It is noted that extrapolation of the model both to the top and the bottom of the core reduces confidence in the projected sections of the model, and this is taken into account in further discussions.

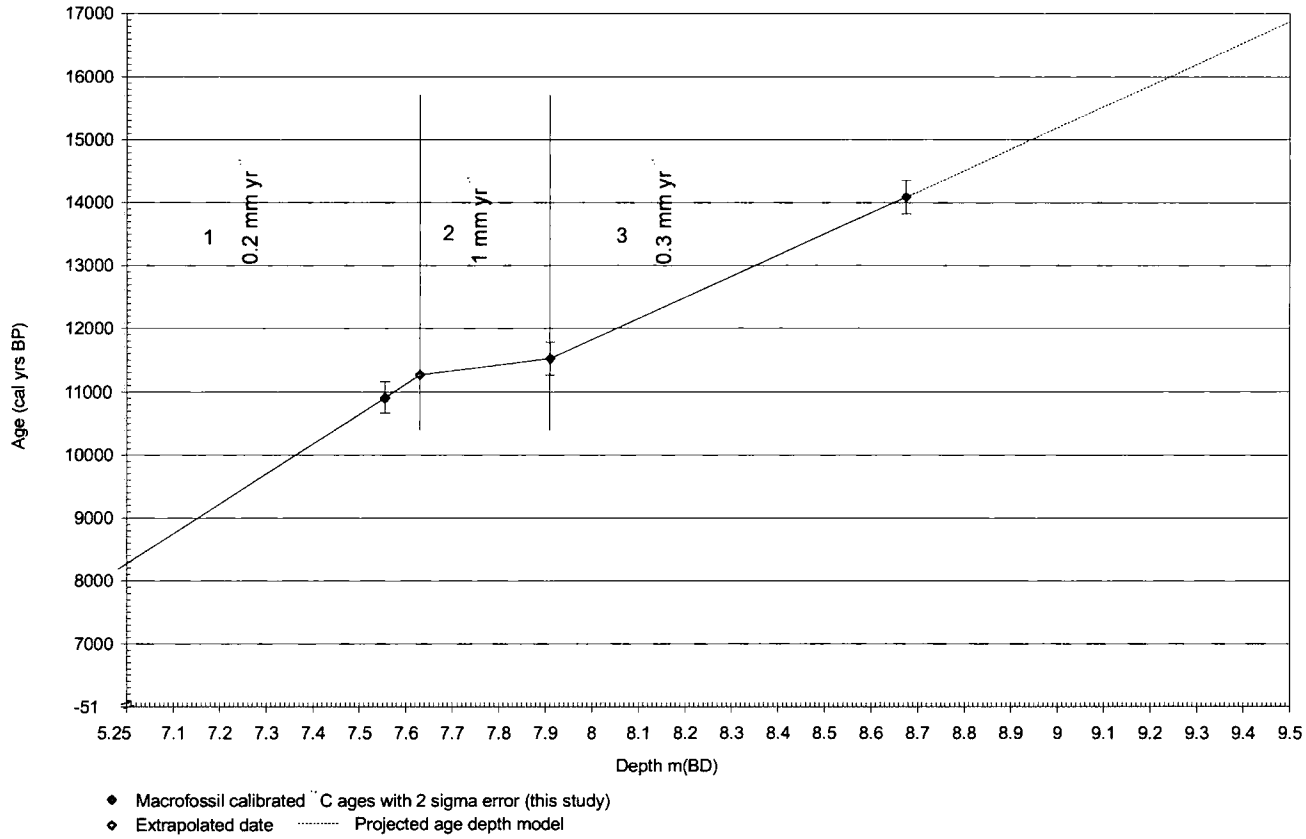

Figure 21

Age-depth model for Nikkupierjav'ri using linear segments, with sediment accumulation rates for each gradient section

6.1.5 Correlations with Greenland Ice Record

The proportional pollen data, pollen influx data and the macrofossil data have been plotted with respect to the age-depth model developed in section 6.1.4. This provides a calendar years age scale that has been correlated directly with the ice core years scale in the GRIP ice core $\delta^{18}O$ data for the Lateglacial and early Holocene (Dansgaard et al., 1993; Johnsen et al., 1992), thus providing a direct correlation with the event stratigraphy recommended by Björck et al. (1998) for this period (see section 2.3.2.1). This correlation is shown in subsequent palaeoclimate records from this site.

6.1.6 Pollen Analyses

The core was sub-sampled at decadal to centennial resolution, and the rationale for accepting sub-samples is explained. For the Holocene section of the study (7.31m to 7.86m) pollen counts have been accepted for all sub-samples where the AP+NAP counts were >200 grains sample^{-1}, with the exception of the sub-samples at 7.59m and 7.87m. These gave counts of 163 and 146 grains respectively, and were accepted on the basis of the relative percentage of *Eucalyptus filicifolia* grains counted with the sample (this gave an indication of the proportion of the whole sub-sample that was counted); these were 4.94 and 6.47 respectively, which compared well with the mean of 2.97 [SE±0.43] for the other accepted Holocene samples and suggested that these low counts would be an acceptable representation of the pollen spectra at those two levels. This rationalisation of sub-samples resulted in the selection of a total of 23 sub-samples at intervals of 2-4 cms, where the mean count for AP+NAP was 445 grains [SE±39].

Developing a rationale for the Lateglacial section was more difficult since all the AP+NAP counts were between only 4 and 157 grains, and therefore not statistically viable. This problem has also been encountered in other investigations of isolation basins on the Kola Peninsula in northern Russia; Snyder et al. (2000) record that the Lateglacial marine section of the core was deemed to have insufficient pollen for further investigation, and Yelovicheva et al. (1998) in Corner et al. (2001) record less than 50 grains per gram in the Lateglacial marine sediments. It was therefore decided that preliminary analysis of the data recovered at Nikkupierjav'ri for the Lateglacial would provide novel research, provided that interpretation of the data is presented within this constraint, and it is recognised that pollen data from these sediments are not suitable for confident palaeoclimate reconstructions. In order to make the best use of the data for this, a threshold of >20 grains was chosen as this would provide a full range of samples covering the entire span of the Lateglacial. Therefore, for this section of the study (7.88m to 9.45m) pollen counts have been accepted for all sub-samples where

the AP+NAP counts were >20 grains sample^{-1}, with the exception of the sub-samples at 8.29m and 8.31m. These gave counts of 13 and 11 grains respectively, and were accepted on the basis of the relative percentage of *Eucalyptus filicifolia* grains (as above); these were 3.31 and 3.91 respectively, which compared well with the mean of 2.97 [SE±0.43] for the accepted Holocene samples. This rationalisation of sub-samples resulted in the selection of a total of 53 sub-samples at intervals of 2-4 cms. There were, however, five sections where the intervals were greater, ranging from 5-11cms. The mean count for AP+NAP was 41 grains [SE±4].

Calendar ages have been assigned to each sub-sample, interpolated from the age-depth model and the resulting mean temporal interval between sub-samples is 88 [±18] years for the Holocene and 98 [±9] years for the Lateglacial. A total of 41 arboreal and non-arboreal taxa have been identified, with 5 obligate aquatic taxa including *Sphagnum*, and various spore taxa.

Relative abundance pollen data are displayed for the most common taxa, rare taxa mentioned in the text, and totals for monolete and trilete Pteridophyte spores (see Figure 22). Taxa are sorted into arboreal pollen taxa, non-arboreal pollen taxa, terrestrial Pteridophytes and obligate aquatics and plotted against age (cal yrs BP). There is an overall summary for the main terrestrial groups of woody taxa (i.e. trees plus shrubs but not including Ericales), Ericales and herbaceous taxa. % LOI (dry weight) and the percentage of pollen not specifically identified (indeterminate pollen) is displayed. The total number of AP+NAP grains counted is plotted, with depth bars to indicate the frequency of sampling. The results of the CONISS analysis carried out on the proportional data of all AP+NAP is displayed as a dendrogram, and the resultant divisions used to guide the divisions representing the local pollen assemblage zones (LPAZs). These same divisions have been added to the diagrams in Figures 23 and 24. Figure 23 shows pollen influx data for taxa mentioned in the text, and the total pollen influx for arboreal and non-arboreal taxa. Figure 24 shows macrofossils information from the pollen washings as presence data.

Figure 22

Nikkupierjav'ri: Relative abundance data are displayed for the most significant taxa with totals (undifferentiated) for the monolete and trilete Pteridophyte spores. Taxa have been grouped into arboreal and non-arboreal taxa, terrestrial Pteridophytes and obligate aquatics plus *Sphagnum*, and plotted against age (cal yrs BP). Pollen sums are specified as follows for selected taxa: Terrestrial Pollen (ΣTP), i.e. Arboreal Pollen minus Pinus (AP) plus Non-Arboreal Pollen (NAP); Terrestrial Pollen and Terrestrial Pteridophyte Spores (ΣTP + ΣPS); Terrestrial Pollen and Aquatic Pollen (including Sphagnum) (ΣTP + ΣAP); Terrestrial Pollen and Indeterminable Pollen (ΣTP + ΣIP). The first axis from the DCA analysis of the pollen spectra is plotted with the assigned palaeobiomes developed through the systematic biome analysis (see section 6.1.10.1). The GRIP ice core $\delta^{18}O$ data for the Lateglacial and early Holocene (Dansgaard et al., 1993; Johnsen et al., 1992) are plotted for correlation. LPAZs are indicated.

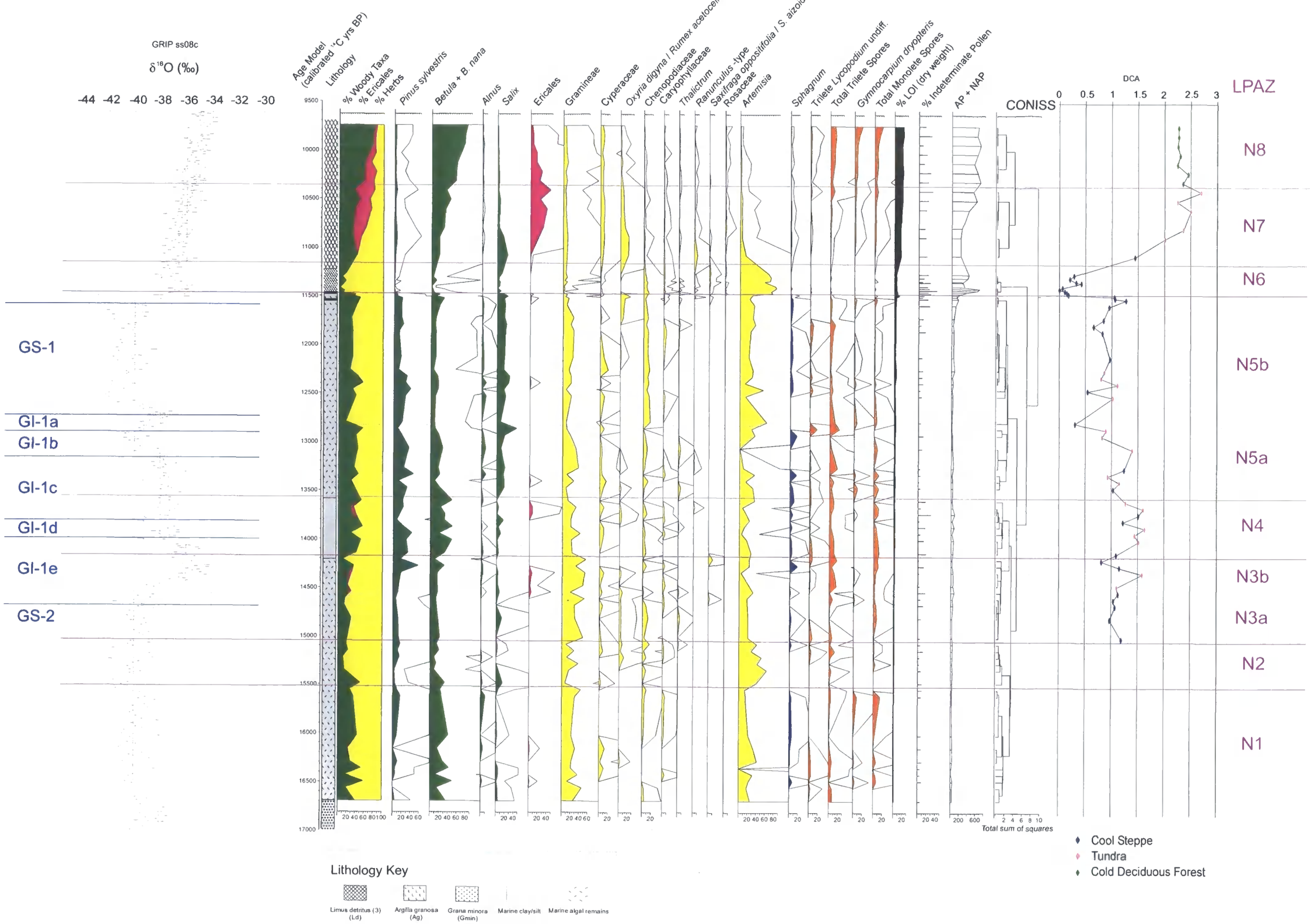
GRIP ss08c
δ18O (‰)
-44 -42 -40 -38 -36 -34 -32 -30
GS-1
GI-1a
GI-1b
GI-1c
GI-1d
GI-1e
GS-2
Age Model (calibrated 14C yrs BP)
Lithology
% Woody Taxa
% Ericales
% Herbs
Pinus sylvestris
Betula + B. nana
Alnus
Salix
Ericales
Gramineae
Cyperaceae
Oxyria digyna / Rumex acetocella -type
Chenopodiaceae
Caryophyllaceae
Thalictrum
Ranunculus -type
Saxifraga oppositifolia / S. aizoides -type
Rosaceae
Artemisia
Sphagnum
Trilete Lycopodium undiff.
Total Trilete Spores
Gymnocarpium dryopteris
Total Monolete Spores
% LOI (dry weight)
% Indeterminate Pollen
AP + NAP
CONISS
DCA
LPAZ
N8
N7
N6
N5b
N5a
N4
N3b
N3a
N2
N1
Total sum of squares
Cool Steppe
Tundra
Cold Deciduous Forest
Lithology Key
Limus detritus (3) (Ld)
Argilla granosa (Ag)
Grana minora (Gmin)
Marine clay/silt
Marine algal remains

6.1.7 Pollen Influx

The mean rate of pollen influx (AP+NAP) trends upwards through the lithological units with: 5 [SE±1] grains $cm^{-2}\,yr^{-1}$ in Lith2a; 11 [SE±2] grains $cm^{-2}\,yr^{-1}$ in Lith2b; 19 [SE±8] grains $cm^{-2}\,yr^{-1}$ in Lith2c; 339 [SE±87] grains $cm^{-2}\,yr^{-1}$ in Lith3; and 325 [SE±71] grains $cm^{-2}\,yr^{-1}$ in Lith4.

Pollen influx values are very low throughout the Lateglacial section of this sequence - *ca* 5 to 19 grains $cm^{-2}\,yr^{-1}$, as might be expected at such extreme northerly latitudes during deglaciation and especially in marine sediments where taphonomic effects exacerbated by even the weakest tidal flows can lead to a relative loss of grains. The sedimentation rate during this time is 0.3 mm yr^{-1} (see Figure 23), and consists of a silty clay with marine algal remains. The sediments in this section are generally faintly laminated, suggesting relatively stable conditions.

Lith3 is a complex unit where the isolation of the basin from marine influence coincides with the major environmental transition from GS-1 (Younger Dryas) to the Holocene. Here, there is an increase in sedimentation rate from 0.3 to 1.0 mm yr^{-1}. This could be accounted for by an increased retention of fine minerogenics, since the basin is no longer affected by tidal action. The input of this material might not have actually increased but rather has had the opportunity to settle out of suspension, whereas previously it would have been removed in suspension by tidal action. Coincident with this increase in sedimentation rate is an increase in pollen influx values. This rise is from 19 to 339 grains $cm^{-2}\,yr^{-1}$, and represents a 17.8 -fold increase as compared to the increase in sediment accumulation rate from 0.3 to 1.0 mm yr^{-1}, which is only a 3.3 – fold increase; i.e., pollen influx increased 5.4 times as much as sediment accumulation rate and cannot therefore be accounted for by the latter. This would indicate a substantial increase in the vegetation cover of the surrounding landscape at this time.

The pollen influx values of *ca* 325 grains $cm^{-2}\,yr^{-1}$ during the early Holocene (Lith4), can be compared with the rate for the same period at Domsvatnet (see Hyvarinen, 1976) a small lake situated near the eastern coast of the Varanger peninsular (70° 19'N, 31° 02'E; altitude *ca* 120m asl). Sediment deposition rates are slower at Nikkupierjav'ri: 0.2 mm yr^{-1}, compared to 0.37 mm yr^{-1} at Domsvatnet. The pollen influx rates at Domsvatnet of 500-2000 grains cm-2 yr^{-1} are higher than would be expected from early Holocene records from other tundra locations where values range from 100 - 600 grains cm^{-2} yr-1 (see Hyvarinen, 1976), and so, the influx value of *ca* 325 for Lith4 would appear to be more typical for such a site. The difference between the two records must be attributed to the nature of the surrounding vegetation suggesting higher productivity and or vegetation cover at the more southerly site with less severe tundra conditions.

The presence of *Pinus* pollen throughout the Lateglacial and early Holocene at this site can be shown not to be a significant component of the local pollen rain. Generally, influx figures of over 500 grains cm^{-2} yr^{-1} can be used to indicate the colonisation of *Pinus* (Hyvarinen, 1975), the record at Nikkupierjav'ri never exceeds 30 grains cm^{-2} yr^{-1}. Therefore, this analysis supports the suggestion (see section 4.2.3.3) that *Pinus* was not growing in the region at this time, and that the low levels of *Pinus* pollen throughout this period must reflect long distance transport.

Figure 23

Nikkupierjav'ri: Pollen influx data are displayed for a selection of taxa and plotted against age (cal yrs BP). LPAZs and lithological units are indicated.

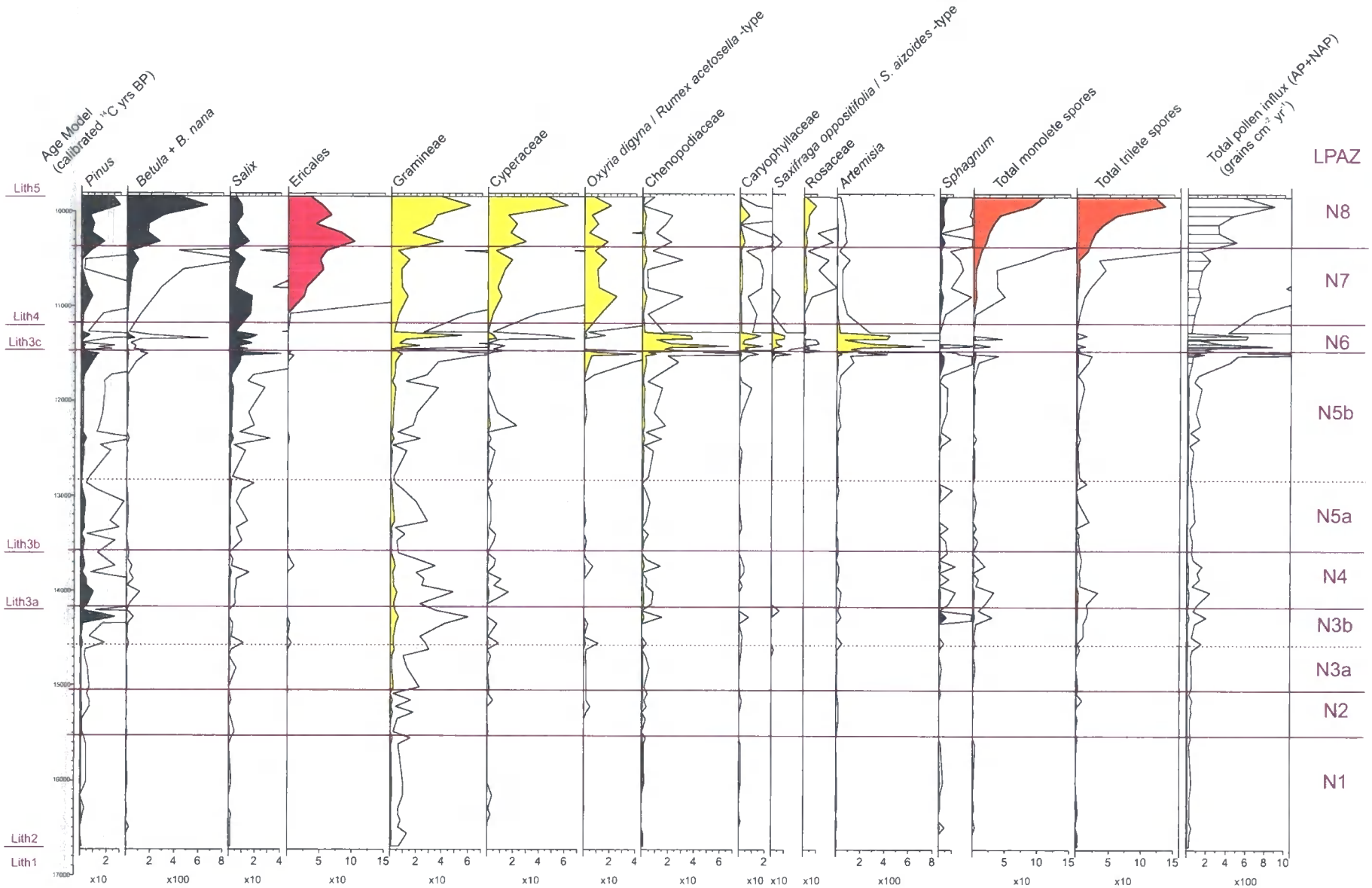
Age Model (calibrated ¹⁴C yrs BP)
Pinus
Betula + B. nana
Salix
Ericales
Gramineae
Cyperaceae
Oxyria digyna / Rumex acetosella -type
Chenopodiaceae
Caryophyllaceae
Saxifraga oppositifolia / S. aizoides -type
Rosaceae
Artemisia
Sphagnum
Total monolete spores
Total trilete spores
Total pollen influx (AP+NAP) (grains cm⁻² yr⁻¹)
LPAZ
Lith5
Lith4
Lith3c
Lith3b
Lith3a
Lith2
Lith1
N8
N7
N6
N5b
N5a
N4
N3b
N3a
N2
N1
10000
11000
12000
13000
14000
15000
16000
17000
x10
x100

6.1.8 Descriptions of the Pollen Zones

Eight local pollen assemblage zones (LPAZs) and two sub-zones have been identified from the relative pollen data (see Figure 21), supported by the CONISS dendrogram divisions, and correlated with the event stratigraphy of the Lateglacial following Björck et al. (1998). The biozones of Mangerud et al. (1974) have also been correlated. These LPAZs are described below from the oldest to the youngest, and they are also summarised in Table 15. It is noted that the zoning of the Lateglacial section of the core is very tentative, in view of the unacceptably low pollen counts for this period (see discussion in section 6.1.6).

Mean values for % LOI (dry weight) and AP+NAP pollen influx are not given for the separate zones since these values are very low throughout. In the Lateglacial sediments values for % LOI (dry weight) range from 1% to 12% and influx values from *ca* 3 to 160 grains $cm^{-2}\,yr^{-1}$. In the Holocene sediments, values for % LOI (dry weight) increase to *ca* 20%, and influx values to *ca* 900 grains $cm^{-2}\,yr^{-1}$.

The relative proportions of woody taxa are described but should be viewed in the context of very low pollen influx values. *Betula* is the most significant component of this group but throughout the Lateglacial and the start of the Holocene pollen counts remain below the threshold influx value of 500 grains $cm^{-2}\,yr^{-1}$ (Hicks, 2001) suggested as evidence for established *Betula* woodland. This would indicate that the tree line (the limit of expansion) for this taxon was not present to within at least 1 km of the sampling site until *ca* 10 ka BP. *Salix* influx values remain <4 grains $cm^{-2}\,yr^{-1}$ throughout the Lateglacial rising to a maximum of 39 grains $cm^{-2}\,yr^{-1}$ *ca* 11.5 ka BP, and *Alnus* only ever achieves a value of 1 grain $cm^{-2}\,yr^{-1}$ until *ca* 10 ka BP when it rises to only 3. It is suggested here, that such low pollen influx values are indicative of the presence of the prostrate species of these taxa, several of which grow in Finnmark today (Hultén, 1950), but also including *Alnus viridis* ssp. *fruticosa* which is found in north east Russia (B Huntley, Pers. Comm.). Small amounts of *cf Betula nana* pollen were identified throughout the Lateglacial sediments, and one *B. nana* fruit was identified *ca* 11.7 ka BP in LPAZ N6. Since the colonisation of tree *Betula* in this sequence would appear to be *ca* 10 ka BP (see LPAZ N9 below), and it is estimated to be between 10 and 9.5 ka BP at Domsvatnet on the eastern coast of the Varanger peninsular (Hyvarinen, 1976), the presence of this macrofossil confirms a local presence of *B. nana*. Thus, the inference is made that most/all of the Lateglacial *Betula* pollen is representing *B. nana*, with the possibility that any representation of tree *Betula* pollen suggests long distance transport of this taxon.

N1

16700(+) - 15520 cal yrs BP

Greenland Stadial 2: GS-2
Late Pleniglacial
Sample resolution *ca* 114 yrs

Gramineae – (*Betula nana)* – *Artemisia*

The pattern throughout this zone is of fluctuating proportions of herbaceous taxa (up to 84%) and woody taxa (up to 67%) with occasional Ericales, a mixed Pteridophyte flora including *Lycopodium* spp. and *Gymnocarpium dryopteris*, and some *Sphagnum*. The herbaceous flora is characterised by Gramineae and *Artemisia* with some Chenopodiaceae and Cyperaceae. The woody taxa are represented principally by *Betula*, with occasional *Salix* and *Alnus*. Following the discussion above it is suggested that *B. nana* was a local component of the tundra mosaic at this time. Of note in this zone, is a single grain of *Typha latifolia* at *ca* 16 ka BP. This thermophilous (thrives in warmer temperatures) species is found today only where mean July temperature is ≥ 13°C (Isarin and Bohncke, 1999).

N2

15520 - 15050 cal yrs BP (470 yrs)
Greenland Stadial 2: GS-2
Late Pleniglacial
Sample resolution *ca* 78 yrs

Artemisia – Gramineae – (*Betula nana)*

This is a herb dominated zone, principally *Artemisia* between 28% and 63% with some Gramineae between 9% and 38%. The taxa are more diverse than previously and there are small but increasing proportions of *Oxyria digyna* / *Rumex acetosella*-type, Chenopodiaceae and Caryophyllaceae. The woody taxa are again principally represented by *Betula nana* at generally <20%, with occasional *Salix* and *Alnus*. Pteridophytes maintain a low level, generally <15% and are principally *Lycopodium* spp. *Sphagnum* is absent for most of this zone, but reappears at the border with LPAZ-N3.

N3

15050 - 14175 cal yrs BP (875 yrs)
Greenland Stadial 2: GS-2 to Greenland Interstadial 1 - GI-1e
Late Pleniglacial to Bølling
Sample resolution *ca* 97 yrs

Gramineae — *Artemisia* — *(Betula nana)*

The CONISS analysis suggests that this zone is divided into two sub-zones 3a and 3b. The sub-zone 3b correlates with GI-1e (Bølling) and the sublte differences are described below. Again, this is a herb dominated zone, principally Gramineae (up to 55%) with 30-35% *Artemisia* throughout. The relatively low levels of *Oxyria digyna* / *Rumex acetosella*-type and Chenopodiaceae continue from the previous zone, but decline in N3b. The woody taxa are represented principally by *Betula* at <33%, again with some *Salix* throughout, and developing up to 4% *Alnus* and 6% Ericales in N3b. The Pteridophytes maintain a low level at generally <30% and are principally *Lycopodium* spp. *Sphagnum* is absent for most of the zone, but there is an isolated peak of *ca* 20% in N3b. Pollen influx values for *Betula* peak at 6 grains cm^{-2} yr^{-1} in N3b, indicating an increased density of *B. nana* shrub tundra on the landscape.

N4

14175 - 13575 cal yrs BP (600 yrs)
Greenland Interstadial 1: GI-1 (GI-1e - d)
Allerød
Sample resolution *ca* 75 years

(Betula nana) — Gramineae — *Artemisia*

The woody and herbaceous taxa in this zone are of similar proportions to each other. Gramineae represents up to 41% and *Artemisia* up to 35%, with some Cyperaceae, Chenopodiaceae and Caryophyllaceae, but a wider variety of herbs has developed with, *inter alia*, occasional *Galium* and *Chamaenerion angustifolium*-type. Amongst the woody taxa *Betula* has the highest representation of up to 49%, with some *Salix*, and there is a small spike of Ericales. The balance of Pteridophytes is similar to the previous zone. Pollen influx values for *Betula* rise to 11 grains cm^{-2} yr^{-1}, reinforcing the previous suggestion of an increased density of *B. nana* shrub tundra on the landscape.

N5a

13575 - 12830 cal yrs BP (745 yrs)
Greenland Interstadial 1 - GI-1 (GI-1c - a)
Allerød
Sample resolution *ca* 106 years

Salix — Gramineae — *Artemisia*

This zone is dominated by herbaceous taxa which expand up to 71%, principally Gramineae up to 37%, and *Artemisia* up to 35%, with some Chenopodiaceae. There is still a variety of other herbs such as *Thalictrum*, *Geum* and Umbelliferae present occasionally. The woody taxa are dominated here by *Salix*, up to 45%, with only *ca* 15% *Betula*, and occasional *Alnus*. The Pteridophytes are still <20% and predominantly *Lycopodium* spp. with occasional *Gymnocarpium dryopteris*. *Sphagnum* is also present occasionally. Pollen influx values for *Betula* and *Salix* do not rise above 2 grains cm^{-2} yr^{-1}, throughout this zone.

N5b

12830 - 11480 cal yrs BP (1350 yrs)
Greenland Stadial 1 - GS-1
Younger Dryas
Sample resolution *ca* 96 years

Artemisia

This zone is dominated by herbaceous taxa at *ca* 65%, with up to 62% *Artemisia*, and up to 24% Gramineae, with Chenopodiaceae expanding to a maximum of 14%, and with some Cyperaceae and Caryophyllaceae. The woody taxa at *ca* 34%, comprise *Betula* and *Salix* in similar proportions, and never more than 29% of each, with some *Alnus*. The Pteridophyte flora is slightly reduced, usually <10% and dominated by *Lycopodium* spp. with occasional *G. dryopteris*. *Sphagnum* is present throughout, up to 7%.

N6

11480 - 11180 cal yrs BP (300 yrs)
Greenland Stadial 1 - GS-1 / PB
Younger Dryas / Preboreal
Sample resolution *ca* 33 years

Artemisia

This zone is dominated by herbaceous taxa, at *ca* 91%, including up to 83% *Artemisia* where its pollen influx values peak at 439 grains cm^{-2} yr^{-1}. There is <10% Gramineae, with Chenopodiaceae, Caryophyllaceae and *Saxifraga* spp, but the overall diversity of taxa has increased. The woody taxa represent only 9% with *Betula* and *Salix*, and occasional *Alnus*. The Pteridophyte flora is reduced further to <1%. There is no record of Ericales and a very small amount of *Sphagnum*. Pollen influx values for *Betula* rise to 67 grains cm^{-2} yr^{-1} towards the top of the zone, which supports the suggestion of further expansion of the *B nana* shrub tundra. It is possible however, that some of this increase in influx could be accounted for by long-distance transport of tree Birch pollen, providing evidence for the expansion of *Betula* forest elsewhere. The position of the Younger Dryas moraines indicates that this would have come from either the southwest or the east. In the east, Paus et al. (2003) suggest the possibility of tree Birch in the pollen record of the northern Timan Ridge, European Arctic Russia, at *ca* 13.5 ka BP, but this is not supported by macrofossil evidence. In the southwest, however, the establishment of Birch woodland, in northern Norway, is constrained by pollen and macrofossil analyses in the Tromsø area (*ca* 400 km from Nikkupierjav'ri), to around *ca* 9.9 ka BP (Jensen et al., 2002). It is probable therefore that the increase in influx of *Betula* pollen at Nikkupierjav'ri is principally that of *B nana*.

N7

11180 - 10370 cal yrs BP (810 yrs)
PB
Preboreal
Sample resolution *ca* 135 years

Ericales — *Betula*

This zone is characterised by a very rapid rise in the proportion of Ericales pollen, from 0 to *ca* 45%, with woody taxa and herbaceous taxa sharing similar proportions i.e. *ca* 36% and *ca* 33% respectively. The change in herbaceous taxa is typified by declining proportions of *Artemisia*, to <5%, and Chenopodicaeae to <1%. *Oxyria digyna* / *Rumex acetosella*-type expands initially to a maximum of 19% and then begins to decline,

while other herbs such as Rosaceae and *Ranunculus* become established. The woody taxa are dominated by *Betula* that expands to 42%, with declining proportions of *Salix* and occasional *Alnus.* The Pteridophytes expand again, to 16% at the upper boundary; principally *Lycopodium* spp. *Sphagnum* is present throughout and *Equisetum* expands to >5%. Pollen influx values for *Betula* continue to rise slowly reaching 97 grains cm^{-2} yr^{-1} towards the top of the zone.

N8

10370 - 9750 cal yrs BP

Holocene

Sample resolution *ca* 103 years

Betula — Pteridophyta (*Lycopodium* spp. and *Gymnocarpium dryopteris*)

The proportional representation of the woody taxa, principally *Betula* with some *Salix* and occasional *Alnus*, expands in this zone from 57% to 81%, while the proportion of Ericales declines to 15%, and the herbaceous taxa to 15%. The herbaceous taxa comprise principally Gramineae and Cyperaceae in equal proportions with *Artemisia*, *Oxyria digyna* / *Rumex acetosella*-type, Caryophyllaceae and Chenopodiaceae declining to <1%. The Pteridophyte flora expands significantly to *ca* 30% driven by *Lycopodium* spp. and *Gymnocarpium dryopteris,* whilst *Sphagnum* remains at <1%. Pollen influx values for *Betula* continue to rise achieving 664 grains cm^{-2} yr^{-1}, indicating that tree Birch probably becomes established in the regional vegetation in this zone, i.e. *ca* 10 ka BP.

Table 15

Table summarising the characteristic taxa for the nine LPAZs identified at Nikkupierjav'ri, and correlated with the event stratigraphy of the Lateglacial following Björck et al (1998), and the biozones of Mangerud et al (1974).

LPAZ	Characteristic Taxa	Biome	Date (cal yrs BP)	Event Stratigraphy	Biozones
N8	*Betula* - Pteridophyta (*Lycopodium* spp. and *Gymnocarpium dryopteris*)	Cold Deciduous Forest	10370 - 9750		Holocene
N7	Ericales - *Betula*	Cool Steppe turning to Tundra and then to Cold Deciduous Forest	11180 - 10370	PB	Preboreal
N6	Artemisia	Cool Steppe	11480 - 11180	GS1 - PB	Preboreal
N5b	*Artemisia*	Cool Steppe with two Tundra episodes	12830 - 11480	GS1	Younger Dryas
N5a	*Salix* - Gramineae - *Artemisia*	Cool Steppe with two Tundra episodes	13575 - 12830	GI-1c-a	Allerød incl. Inter Allerød Cold period
N4	(*B. nana*) - Gramineae - *Artemisia*	Cool Steppe	14175 - 13575	GI-1e-d	Allerød
N3b	Gramineae - *Artemisia* - (*B. nana*)	Cool Steppe with a short Tundra episode	14575 - 14175	GI-1e	Bølling
N3a	Gramineae - *Artemisia* - (*B. nana*)	Cool Steppe with a short Tundra episode	15050 - 14575	GS2	Late Pleniglacial
N2	*Artemisia* - Gramineae - (*B. nana*)	unreliable	15520 - 15050	GS2	Late Pleniglacial
N1	Gramineae - (*B. nana*) - *Artemisia*	unreliable	16700(+) - 15520	GS2	Late Pleniglacial

6.1.9 Macrofossils

The macrofossils found in the pollen washings were recorded as presence/absence data (see Figure 24) and serve to help interpret the quantitative data.

The sediments in this core are clearly differentiated by the algal content into the marine sediments containing Foraminifera and marine algae, and the freshwater sediments with diatom spp. Diatom samples assessed from sediments about the marine contact grade from brackish species at 7.89m to freshwater species at 7.59m (J Lloyd, Pers. Com.). *Pediastrum*, a freshwater taxon, is present throughout the Lateglacial sediments, indicating some run off of freshwater into the basin during this period.

Miscellaneous insect parts, Chironomid head capsules and *Pediastum* spp. are present throughout the sequence. During the marine phase, these must have come with freshwater influx from streams draining freshwater lakes in the surrounding landscape. Macrofossils associated with freshwater are present only during Lith3 and Lith4, from the GS-1 (Younger Dryas) transition to the Preboreal and the beginning of the Holocene sediments, e.g. Cladocera remains don't appear until Lith3. Ostracods and the fossil remains of Charophytes (oogonia), appear in Lith4 suggesting their early colonisation, with the oogonia being produced in response to environmental stress such as seasonal freezing. This is also indicated by the presence of Cladoceran ephippia and Bryozoan statoblasts. Moss fragments (unidentified) were found during the Lateglacial and throughout the Holocene sediments, indicating some degree of freshwater run off from the land into the lake from the point of deglaciation, and indicating some brackish element from the beginning of deposition. *Polytrichum* and *Sphagnum* were identified in the upper levels of Lith4. Leaf fragments from woody plant species were found from the middle of Lith2 upwards, indicating the beginning of the development of the surrounding vegetation *ca* 14 ka BP. A few *Betula* macrofossils and miscellaneous seeds are present from the beginning of Lith3, and one Ericales seed coincided with the peak in these taxa in Lith4.

Two discrete horizons of pyrite globules were found, both associated with the more compact silt/clay sections of Lith2b and Lith3. The development of these structures indicates stagnating bottom conditions where the lack of oxygen would suggest a poor fauna and little bioturbation. This would have probably contributed towards the clearly laminated sediments at the lower boundary of Lith3.

Figure 24

Nikkupierjav'ri: Data indicating the presence of macrofossil evidence are plotted against age (cal yrs BP). LPAZs and lithological units are indicated.

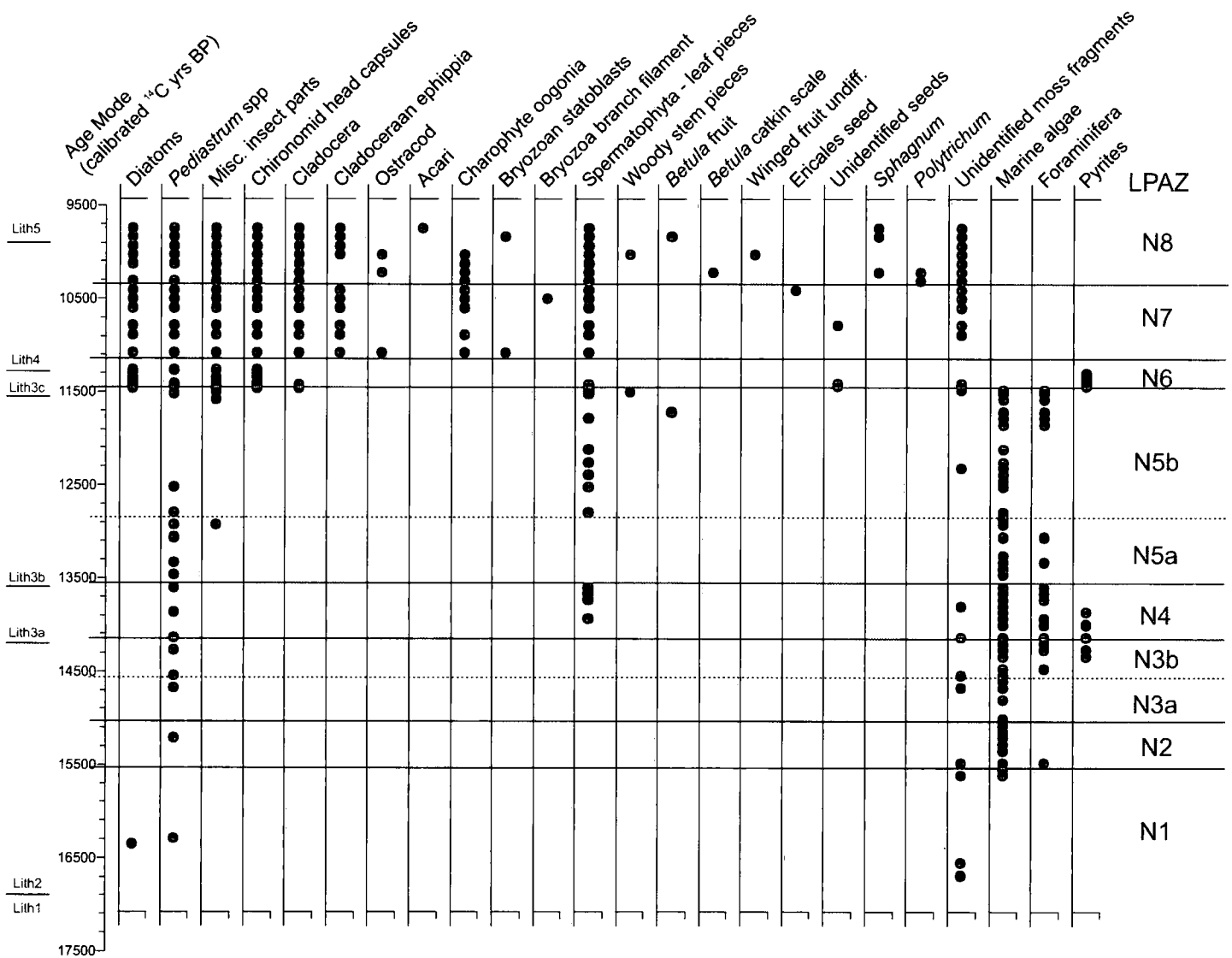
Age Mode (calibrated ^{14}C yrs BP)
Diatoms
Pediastrum spp
Misc. insect parts
Chironomid head capsules
Cladocera
Cladoceraan ephippia
Ostracod
Acari
Charophyte oogonia
Bryozoan statoblasts
Bryozoa branch filament
Spermatophyta - leaf pieces
Woody stem pieces
Betula fruit
Betula catkin scale
Winged fruit undiff.
Ericales seed
Unidentified seeds
Sphagnum
Polytrichum
Unidentified moss fragments
Marine algae
Foraminifera
Pyrites
LPAZ
9500
10500
11500
12500
13500
14500
15500
16500
17500
Lith5
Lith4
Lith3c
Lith3b
Lith3a
Lith2
Lith1
N8
N7
N6
N5b
N5a
N4
N3b
N3a
N2
N1

6.1.10 Systematic - Quantitative Analyses

6.1.10.1 Palaeobiome Reconstructions

Three biomes were identified, based on the pollen data, as a result of the systematic palaeobiome reconstructions: tundra; cool steppe; and cold deciduous forest. This assignment of biomes is plotted stratigraphically in relation to the pollen sample scores on the first axis of the detrended correspondence analysis (DCA) of the palynological data (see Figure 25).

This first axis of the DCA analysis (Eigenvalue 0.38) represents the primary pattern of

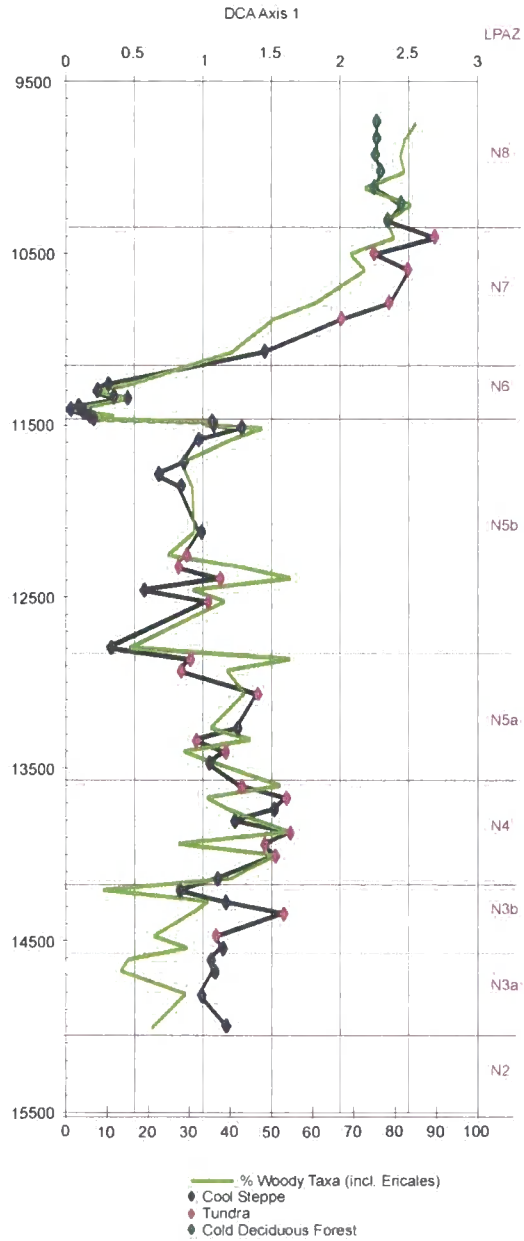

Figure 25

The first axis of the DCA analysis of the pollen spectra (Eigenvalue 0.38) is plotted with the assigned palaeobiomes developed through the systematic biome analyses and matching many of the features of the curve for the % woody taxa (incl. Ericales) at Nikkupierjav'ri. Both curves are plotted against age (cal yrs BP). LPAZs are indicated.

variation amongst the pollen data, matching in many features with a curve of the % woody taxa (incl. Ericales) in the pollen data, and thus describes the changes between those spectra dominated by the pollen of the woody taxa *cf B nana*, Ericales and *Salix*,

low-lying Arctic Alpine shrubs representative of tundra conditions and those spectra dominated by the pollen of herbaceous taxa, representative of cooler and drier steppe conditions.

Throughout the Lateglacial the dominent biomes fluctuated between tundra and cool steppe, only developing into cold deciduous forest in the early Holocene, at *ca* 10.4 ka BP. The sequence of biomes through this period reflects changes in the prevailing vegetation that can be used to infer more specific climate detail, although confidence in the interpretation of the switching biomes in the Lateglacial is low (as discussed in section 6.1.6).

Tundra is represented here principally by the Arctic Alpine taxa, *cf B. nana*, *Salix* and *Saxifraga* spp, with some Ericales (including *Empetrum*) and Cyperaceae. Tundra indicates a humid environment where precipitation meets >65% of demand, but GDD5 is insufficient for tree growth, i.e. <350 (Prentice et al., 1992).

Cool steppe (there were two samples that invoked the steppe test to differentiate between cool and warm steppe (after, Tarasov et al., 1998)) is defined here, principally by the presence of the steppe/desert forbs *Artemisia* and Chenopodiaceae with *Oxyria digyna* / *Rumex acetosella* -type and a variety of other steppe forbs, mainly Caryophyllaceae, *Ranunculus*, Rosaceae, *Thalictrum*, and Asteraceae, with some Gramineae. Cool steppe is predicted for the less humid regions with MTCO <5°C (Tarasov et al., 1998) and where precipitation meets <65% of demand, but GDD5 remains insufficient for tree growth.

Cold deciduous forests are dominated by boreal summergreen trees (Prentice et al., 1992) represented here by *Betula*. Ericales are also present although representation is very low, not more than 7% in the Holocene spectra, and according to Prentice et al. (1992) they only occur in restricted parts of the biome. This biome occurs in maritime climates where the GDD5 is <900, as required by cool temperate conifers, but where winters are too warm for boreal evergreen conifers (-2 to 5°C). This climate type is today represented by the 'sub-arctic' *Betula* woodlands of coastal Iceland, part of Scotland and coastal Scandinavia and Beringia (Prentice et al., 1992).

6.1.10.2 Palaeoclimate Reconstructions

In view of the unsuccessful palaeoclimate reconstructions using the climate surface response method of Huntley (1993), that were tried for the pollen data from Lochan An Druim (see discussion in section 5.1.10.2), it was decided not to pursue this analysis at Nikkupierjav'ri. As already discussed (see section 6.1.6), the pollen counts for the Lateglacial at this site were unacceptably low, and would not therefore stand up to robust statistical analysis. In addition, the training set used does not include any sub-

tidal arctic sample sites (B Huntley, Pers. Comm. 2006) and would therefore present a poor source of modern analogous environments. The inclusion of data collected from such sites would greatly enhance the model, and offer the potential for developing such reconstructions in the future.

6.2 The Palaeoenvironment at Nikkupierjav'ri

Throughout the Lateglacial period the basin at Nikkupierjav'ri was principally marine. There is, however, evidence of some freshwater influence with macrofossil analysis indicating the presence of mosses, spermatophyta leaf pieces and *Pediastrum*, suggesting some freshwater run off into the basin. Sedimentation rate appears constant throughout this period and so fluctuations in pollen influx values can be taken to reflect local or regional vegetation productivity. These values, though, are very low throughout (<25 grains cm^{-2} yr^{-1}) and therefore difficult to interpret in vegetational terms. Prentice (1981) also has estimated pollen influx rates of only 20-40 grains cm^{-2} yr^{-1} from Allerød sediments at three lacustrine sites on the Varanger Peninsular, which she suggests indicates very sparse vegetation and implies harsh tundra conditions at this time. Some general observations at Nikkupierjav'ri have however been made during this period. Pollen influx values do show a slight increase between *ca* 14.5 and 13.7 ka BP, which correlates closely with the period of initial warming, GI-1e (Bølling) in the GRIP record, but values decrease again for the next 2000 years from *ca* 13.6 to 11.6 ka BP. Lohne et al. (2004) have suggested that according to sea-level changes in western Norway, the Younger Dryas re-advance had already started in the late Allerød, with significant glacial loading of the lithosphere starting *ca* 13.3 ka BP. This suggestion of such an early cooling is supported by the sustained low levels of pollen influx following the initial warming of the Bølling at Nikkupierjav'ri. Whilst the pollen influx values are very low, the systematic palaeobiome reconstructions use pollen percentage data, and it would seem that the relative proportions of the few characteristic taxa that were identified can have some indicative value. The taxa of the tundra and cool steppe biomes prevail throughout the Lateglacial, where the fluctuations in palaeobiome assignments are principally characterised by the relative proportions of the steppe taxa *Artemisia* and Chenopodiaceae, with the principal Arctic Alpine taxon *B. nana*, and with some *Salix*. These fluctuations in dominant PFT indicate relatively high frequency quantitative shifts of the vegetation with respect to the changing climate boundary conditions, with the differences accounted for in terms of moisture availability; the tundra biome indicates more humid conditions, where precipitation meets >65% of demand (Prentice et al., 1992). The vegetation at this time probably formed a discrete mosaic, with the tundra communities occupying the lower more moist ground, and the steppe communities on the higher and drier ground. The

changes in dominance from tundra to cool steppe i.e. the expansion and contraction of the relevant mosaic patches, would therefore suggest short cooling events with reduced moisture availability, except during the GS-1 (Younger Dryas) event, where the constant cool steppe biome suggests a more stable period of drier and colder conditions.

The characteristic *Artemisia* signal for GS-1, recorded all around the northern and eastern margin of the Scandinavian Ice Sheet (Hyvarinen, 1975; Hyvarinen, 1976; Prentice, 1982; Seppä, 1996; Vorren, 1978) is not directly apparent in the data at Nikkupierjav'ri. However, the establishment of the cool steppe biome in LPAZ-N5b that correlates with GS-1 (Younger Dryas), would indicate a significant representation of steppe taxa at this time, of which *Artemisia* is the most dominant. An alternative interpretation might suggest that the chronology at this time is incorrect, and that the *Artemisia* peak in LPAZ-N6 should correlate with GS-1 (Younger Dryas). However, the record does indicate the beginning of a response to the Holocene warming at the very top of LPAZ-N5b where the influx values begin to rise *ca* 11.6 ka BP. This registers as very short lived increases in the proportions of *Betula*, Ericales, *Salix* and *Oxyria digyna* / *Rumex acetosella*-type, before a rapid change in pattern to the herbaceous dominated LPAZ-N6.

The transition from GS-1 (Younger Dryas) to Preboreal provides a complex record that is difficult to interpret. This transitional zone coincides with the period of isolation of the basin, identified by preliminary diatom analysis (J Lloyd, Pers. Comm.), where the prevailing influence changes from marine through brackish to freshwater. The isolation contact shows clearly in a section of finely laminated sediments and is dated to *ca* 11.5 ka BP. This period of isolation therefore coincides with the second major warming of the postglacial period, and also with the beginning of the rise in pollen influx values identified in the sequence. Thereafter, both sedimentation rate and pollen influx increase for a period of *ca* 250 years. The sediment here is a fine clay which would suggest that it originated from an unstable landscape (raw mineral soils following recent deglaciation) supporting sparse vegetation, as might have been expected during the previous GS-1 (Younger Dryas) period. The landscape was not glaciated during this time but would have experienced some severe conditions, and perhaps been subjected to freeze-thaw effects that would have loosened and degraded the soil, thus contributing fine minerogenics to the allochthonous input into the basin. The isolation of the basin subsequently allowed sedimentaion of these fine particles. It has been demonstrated that during this period pollen influx increased 5.4x as much as sediment accumulation rate, and therefore cannot be accounted for by the latter, but would indicate that the vegetation cover at that time was greatly increased. This increase in pollen influx is driven principally by *Artemisia* with some Chenopodiaceae, and is

coincident with a reduction in the representation of woody taxa, and stable cool steppe conditions. This signal in the pollen profile, correlates with the Preboreal Oscillation (PBO), a cooling event in the GRIP record, and also to a cooling event recorded in the terrestrial pollen record at Lake Ifjord *ca* 11.45 - 11.2 ka BP (Seppä et al., 2002). The record at Nikkupierjav'ri demonstrates very clear quantitative responses to the fluctuating climate at this time. Vegetation showed an initial and short-lived response to the ameliorationg climate with relative increases in the pollen of the woody taxa. However, with the PBO reversal, the herbaceous taxa associated with the cool steppe dominate the pollen spectrum again, but demonstrate a significant increase in influx. The climate is still very harsh but this expansion suggests a response to a reduction in environmental stress, but not sufficient to effect qualitative changes in taxa or even expansion of the woody taxa of the tundra.

The frequent occurrence of the PBO in proxy records from central Europe has been reviewed by Björck (1997) and dated in the terrestrial record at *ca* 11.3 - 11.15 ka BP. It indicates a widespread climatic cooling around the North Atlantic region. The ocean records of SSTs in the eastern Norwegian sea also indicate a cooling event following the early Holocene steep temperature rise, and this has been related to the PBO and dated to between 11.26 and 11.04 ka BP (Birks and Koc, 2002). Birks and Koç (2002) suggest that the warm North Atlantic Water in the very early Holocene promoted ice-sheet melting, leading to an increase in the glacial meltwater input. This freshening of the ocean caused a slowing down and a reduction in the NATC, and the consequent southerly displacement of the NAPF would have led to this renewed cooling of the North Atlantic region.

At Nikkupierjav'ri at this time there are no trees established in the vegetation, and therefore the signal in the pollen is necessarily an herbaceous one (and is probably confounded by its coincidence with the isolation event). There is a very slight indication of vegetational development in response to the initial Holocene warming (as discusssed above), before the cooling event is registered. It is suggested here that the very limited response to the initial Holocene warming and the pronounced response to the PBO event indicates that at this extreme northerly location the PBO became an extension of GS-1 (Younger Dryas), thus delaying the onset of vegetational development that could be associated with the Holocene warming. Koç et al. (1993) have mapped a seasonally ice free passage to 72°N along the Norwegian coast throughout GS-1 (Younger Dryas). Although Nikkupierjav'ri lies at 70° 40'N, it lies to the east of the northernmost point of the mainland at *ca* 71°N; this must have been a very sensitive location as regards fluctuations in this ice free passage. Evidence at this site

would suggest that sea ice persisted throughout this period, and that Nikkupierjav'ri lay close to the NAPF at this time.

Marine evidence from core M23071 from the western Vøring Plateau (see Figure 2), which lies off western Norway in the path of the Norwegian Current but outside the influence of the Norwegian Coastal Current (which maintains the ice free passage), indicates a gradual transition over 1500 years out of GS-1 (Younger Dryas) (Koç et al., 1993; Birks and Koc, 2002). This is a more gradual impact of the re-organisation of the water-masses in the early Holocene than was experienced in the ice-free passage along the Norwegian coast (Birks and Koc, 2002). This response time is more in line with the record at Nikkupierjav'ri, where it takes *ca* 1600 years to progress from the cool steppe flora of GS-1 (Younger Dryas) to the pioneering birch woodland of the Holocene. The terrestrial site at Kråkenes Lake in western Norway, which would have benefited from the warming of the Norwegian Coastal Current, records this GS-1/Preboreal transition at *ca* 11.5 - 11.1 ka BP, and shows no evidence in the temperature reconstructions of any reversion to colder conditions that could be referred to as the PBO (Birks et al., 2000b). Here, the vegetational development from the end of GS-1 (Younger Dryas) to the onset of the pioneer birch phase takes *ca* 700 years compared to the 1600 years at Nikkupierjav'ri. This lends support to the suggestion of the close proximity of the NAPF to the site at Nikkupierjav'ri throughout the GS-1/Preboreal transition.

The pattern of succession into the early Holocene that follows this transiton at Nikkupierjav'ri, begins with declining proportions of *Artemisia*, continues through a brief period dominated by *Salix* and *Oxyria digyna* / *Rumex acetosella*-type, on to the expansion of Ericales and *Betula*, and then to the development of the pioneering birch woodland. This pattern is typical of other records in the area at this time (Hyvarinen, 1975; Hyvarinen, 1976; Prentice, 1982; Seppä, 1996). However, comparing the calibrated chronologies at Lake Ifjord and Nikkupierjav'ri, there is some disagreement. The onset of the development of the pioneering birch woodland at *ca* 9.9 ka BP at Nikkupierjav'ri, is between 1000 and 1200 years later than that suggested at Lake Ifjord. The age depth model for Lake Ifjord was developed using the estimated age of 11.5 ka BP for the GS-1 (Younger Dryas) / Holocene boundary as the basal age for the core. This boundary was identified by a change from the *Artemisia* dominated spectra to the *Salix* and *Oxyria digyna* / *Rumex acetosella*-type dominated spectra, a characteristic feature of other pollen records in northern Fennoscandia. The estimated date was then obtained by correlating this change with the GS-1 / Preboreal transition in the Greenland ice cores, and with calibrated radiocarbon dates derived from wiggle-matching in western Norway, and with tree-ring chronologies from northern Europe (Seppä et al., 2002). This basal date was then used with three calibrated ^{14}C bulk

sediment dates from the early Holocene sediments, and extended to an assumed modern age for the top of the core. By contrast, at Nikkupierjav'ri this boundary lies between two AMS ^{14}C dates from macrofossils, the lower date derived from marine algae, and the upper date from terrestrial woody leaves and stems. This model is similarly extended to an assumed modern age for the top of the core. This latter model places the GS-1 / Preboreal boundary coincident with a rise in *Artemisia*, and thereafter suggests that the early Holocene vegetation developed more slowly than at Lake Ifjord, with the pioneering birch woodland not developing until *ca* 9.9 ka BP. The possible proximity of the NAPF to the study site at this time has already been discussed, and it is suggested that this apparent delay in vegetational development could be attributed to the persistent harsh conditions prevailing along the coast at this time. Lake Ifjord is not a coastal site and does lie much further south at 70° 26'N°. However, this discrepancy in dates is perhaps rather more than might be expected bearing in mind the proximity of the two sites, and could have been exacerbated by the unreliability of the bulk sediment dates, which are prone to contamination by old carbon (see the discussion in section 2.3.2.1).

Following the PBO the first major qualitative change in vegetation takes place. The dominant herbaceous taxa of the cool steppe and tundra that have waxed and waned over the previous deglacial period are succeeded initially by Ericales (still a taxon indicative of tundra) and subsequently by the colonisation of tree birch. Tree birch becomes established *ca* 9.9 ka BP, with these first birch woods characterised by abundant *Lycopodium* spp. and *Gymnocarpium dryopteris*, a feature commonly found associated with the early Holocene pioneer birch phase elsewhere in Fennoscandia (Hyvarinen, 1975; Hyvarinen, 1976; Prentice, 1982; Seppä, 1996).

Chapter 7

Synthesis

The southerly study site along the northeast Atlantic seaboard, Lochan An Druim, is broadly compared with the northerly study site at Nikkupierjav'ri. Their differences in vegetation type and vegetational development are discussed for the period following deglaciation and up to the onset of the development of pioneer birch woodland in the early Holocene. Independent chronologies have been developed for each profile that have been compared with the GRIP event stratigraphy scheme (Björck et al., 1998; Walker et al., 1999).

Deglaciation dates for the study sites have been suggested from estimated dates for the beginning of mineral accumulation. Sedimentation commenced at Lochan An Druim at 12.18m(BD), providing evidence for deglacial activity, and giving a projected date for deglaciation before 15.0 ka BP (the age-depth model was not developed beyond the lowest radiocarbon date). According to Bowen (2002) deglaciation is estimated to have begun *ca* 17.4 ± 1.3 ka BP, beginning from the continental shelf and retreating towards terrestrial centres of ice dispersion. At Lochan An Druim there are records of the presence of a few herbaceous taxa and of *cf Betula nana*, beyond *ca* 15.0 ka BP. The onset of organic accumulation is not apparent in the lithology until *ca* 15.0 ka BP, corresponding with the beginning of the initial warming phase GI-1e (Bølling) in the GRIP record. At Nikkupierjav'ri, mineral accumulation is estimated to have begun *ca* 17.2 ka BP which accords well with the suggestion that most of the western part of the Fennoscandian Ice Sheet and the Barents Sea Ice Sheet had receded from the outer continental shelf by *ca* 17.5 ka BP (Andersen, 1979; Vorren and Plassen, 2002). Evidence for the onset of organic accumulation is difficult to estimate from this site since it was a marine basin at that stage. However, there is evidence of a very low influx of pollen into the inlet (<7 grains cm^{-2} yr^{-1}), consisting of *Artemisia*, Gramineae and *cf B. nana*. Together with evidence of moss inwash, this would suggest that the surrounding landscape was ice free and supporting a sparse cover of low growing vegetation by *ca* 16.5 ka BP. Retreat of the ice sheets is estimated to have begun from the continental shelf at about the same time in both locations, and this study would suggest that the continental margin was free of ice in Fennoscandia by 16.5 ka BP.

Throughout GI-1 (Lateglacial Interstadial) at Nikkupierjav'ri, the pollen influx values remain generally well below 25 grains cm^{-2} yr^{-1}. This might be attributed to the fact that at this time the basin was a marine inlet and therefore not such an efficient environment for collecting pollen. However, the terrestrial record at Østervatnet (100 km south southeast and still on Varangerhalvøya) also indicates very low values of 20-

40 grains cm^{-2} yr^{-1} during this interstadial, rising to only 60-150 grains cm^{-2} yr^{-1} during GS-1 (Younger Dryas), and this is indicative of very harsh tundra-like conditions (Prentice, 1981). These figures can be compard with modern pollen influx rates in Arctic areas; in Greenland Fredskild (1985) demonstrates a decrease in values from Low Arctic to High Arctic, i.e. >70 grains cm^{-2} yr^{-1} to <10 grains cm^{-2} yr^{-1} respectively. By comparison, the pollen influx values at Lochan An Druim during GI-1 (Lateglacial Interstadial) are somewhat higher, with a mean of 357±62 grains cm^{-2} yr^{-1}, still suggesting tundra-like vegetation but with more ground cover. Nevertheless, due to the very low level of pollen recovered (or deposited) at Nikkupierjav'ri, it is difficult to correlate this site with Lochan An Druim in terms of vegetational characteristics. There are, however, some observations to be made.

The GI-1 (Lateglacial Interstadial) period is characterised at both sites by the taxa of the cool steppe and tundra biomes. At Lochan An Druim cool steppe is characterised by *Oxyria digyna /Rumex acetosella*-type, but at Nikkupierjav'ri *Artemisia* prevails as the dominant taxon. In the tundra biome at Lochan An Druim, Ericales (*cf Empetrum nigrum*) is very dominant and is accompanied throughout by the Arctic Alpines *Salix* and *Saxifraga oppositifolia / S. aizoides* -type. At Nikkupierjav'ri, by comparison, the predominent taxa are *Salix* and *cf Betula nana* with only very occasional *Saxifraga oppositifolia / S. aizoides*-type or Ericales (*cf E. nigrum*). Tundra prevails for most of the GI-1 (Lateglacial Interstadial) at Lochan An Druim compared to Nikkupierjav'ri where the conditions appear to be more unstable with generally more cool steppe. GS-1 (Younger Dryas) is stable in both profiles but characterised by cool steppe in the north and tundra in the south; both represent treeless floras, but with warmer and moister conditions in the south.

During a relatively warm period such as GI-1 (Lateglacial Interstadial) when the NAPF tends to migrate north (see Figure 1), the site at Nikkupierjav'ri would be much closer to the front than the site at Lochan An Druim, and therefore more susceptible to minor fluctuations in its position. The cooler and drier periods of expansion of the steppe taxa may suggest brief southerly movements of the NAPF during this time.

At Lochan An Druim the first increase in pollen influx, of up to 55 grains cm^{-2} yr^{-1}, occurs *ca* 14.9 ka BP, with a further sustained increase correlating with the beginning of the warming phase GI-1e (Bølling) at *ca* 14.5 ka BP. There is a coincident and corresponding signal at Nikkupierjav'ri. Here pollen influx remains <7 grains cm^{-2} yr^{-1} until *ca* 14.5 ka BP, after which there is a sustained increase to *ca* 25 grains cm^{-2} yr^{-1}, which is also taken to indicate the beginning of this warming phase. Both sites were ice-free at this time, and the warming signal perhaps indicates an expansion of the existing flora in response to the ameliorating conditions, and therefore more expansive

colonisation of the relatively bare ground left after the retreat of the ice. Pollen influx rates at Nikkupierjav'ri fall again *ca* 13.5 ka BP, and it is suggested here that this could be an early response to GI-1b (Intra-Allerød cold period), since there is no further increase in pollen influx that would suggest vegetational development before the onset of the early Holocene. In contrast, this cold interval presents a significant signal in the taxa at Lochan An Druim *ca* 13.0 ka BP, with a reduction in Ericales (*cf Empetrum nigrum*) and an expansion of the steppe herbs; however, the Ericales (*cf E. nigrum*) appear to expand again for a time before the onset of GS-1 (Younger Dryas).

Following the southward movement of the NAPF during GI-1b (Intra-Allerød cold period), it may not have shifted northward again during GI-1a, as much as it had during GI-1c, and hence remained south of Nikkupierjav'ri. As a result neither GI-1a nor the subsequent GS-1 (Younger Dryas) is distinguishable in the pollen record from Nikkupierjav'ri and cannot be directly compared with that from Lochan An Druim.

An initial response to the warming of the Holocene registers as quantitative changes in vegetation at both sites. This is typified by an increase in the relative proportion of woody taxa and a reduction in the relative proportion of the herbaceous flora. This first signal occurs at *ca* 11.7 ka BP at Lochan An Druim and *ca* 100 years later at Nikkupierjav'ri. Thereafter, the first qualitative change in the vegetation at Lochan An Druim is the succession of the pioneering birch woodland, which begins at *ca* 11.4 ka BP. This most significant and indicative change of taxa in response to the Holocene warming is delayed by a substantial *ca* 1500 years at Nikkupierjav'ri, until *ca* 9.9 ka BP.

In summary - both sites show a coincident quantitative response to postglacial warming in terms of the pollen influx of pioneering taxa following deglaciation, although the signal is much more pronounced in the south. Thereafter, the vegetation at Lochan An Druim responds very sensitively to minor fluctuations in the climate through GI-1 (Lateglacial Interstadial), with quantitative shifts in the proportional representation between the dominant taxa, and showing an increasing trend in productivity. The record in the north from Nikkupierjav'ri is far less responsive and appears to be constrained by the colder intervals, i.e, GI-1b (Intra-Allerød cold period), GS-1 (Younger Dryas) and the PBO, which seem to persist with no evidence of any vegetational recovery between them. This has a cumulative effect, such that the timing of the initial development of the pioneering birch woodland takes place 1500 years later at Nikkupierjav'ri.

These two records have been placed in the wider context of the North Atlantic region by comparing the onset dates of key climatic events in both the terrestrial coastal records and the ocean records. Appropriate marine records for comparison have been chosen as discussed in section 2.3.4.3.1, and coastal terrestrial records as discussed

in sections 3.2.6 and 3.3.7. Only the early Holocene record at Nikkupierjav'ri had been used for this comparison owing to the uncertainties attached to the interpretation of results for the Lateglacial section, on account of the very low pollen counts for that period. Published and uncalibrated radiocarbon dates for some of these events have been calibrated using CALIB 4.4.1 (Stuiver and Reimer, 1993) with the INTCAL98.14c calibration data set (Stuiver et al., 1998a) for the purposes of this discussion. The limitations of such detailed comparisons must be viewed in the context of the problems of radiocarbon dating and the different calibration methods as discussed generally in section 2.3.2.2., and more specifically to the records that are compared here, in sections 3.2.6 and 3.3.7. These records and events are compared in Table 16.

The onset of the Lateglacial Interstadial (GI-1) begins about 14.4 ka BP at Lochan An Druim, laggging the 14.7 ka GRIP ice-core yrs BP. This warming event is delayed northeastward until *ca* 13.4 ka BP at Kråkenes and 13.8 ka BP at the North Timan Ridge. The 400 year difference between these sites is probably due to dating inaccuracies, but nonetheless there is an evident delay of *ca* 1000 years in the warming of the north of the region (the very early date of 15 ka BP at Andøya follows the early terrestrial deglaciation of the area).

The subsequent Lateglacial interstadial reversals are not well recorded in the area. Evidence for the Older Dryas (GI-1d) in two records in the Rogaland area show a response at *ca* 14.3 ka BP, which is about 400 years before Lochan An Druim where it registers to within 150 years of the 14.05 ka GRIP ice-core yrs BP. Similarly, the Intra Allerød Cold Period (GI-1b) reversal in the Rogaland and Sunnmøre areas leads the record at Lochan An Druim by about 300-400 years. The Lochan An Druim record is coincident with GRIP at 13.15 ka GRIP ice-core yrs BP.

The onset of the Younger Dryas (GS-1) appears to be a broadly coincident event throughout the terrestrial and marine records of the region, registering earliest in the northeast at 13 ka BP and slightly later in the southwest at 12.75 ka BP, just leading the GRIP record at 12.65 ka GRIP ice-core yrs.

Similarly, the Younger Dryas (GS-1)/Holocene transition in both terrestrial and marine records is broadly coincident, but also correlates with the GRIP record of 11.5 ka GRIP ice-core yrs BP (the record in the Sunnmøre area at Lerstadvatn appears rather old by comparison).

Table 16

Table to compare the onset dates (cal yrs BP) of Lateglacial and early Holocene climatic oscillations in the GRIP event stratigraphy and in selected terrestrial and ocean records on a southeast to northwest gradient in the northeast Atlantic region (GRIP ice-core years (Björck et al., 1998); Core 56/10/36 NE Atlantic (Austin and Kroon, 2001; Kroon et al., 1997); Core MD952011 and core HM79-6/4 (Birks and Koc, 2002);Rogaland area (Birks et al., 1994; Paus, 1988; Paus, 1989b; Paus, 1990); Kråkenes (Birks et al., 2000a); Lerstadvatn (Kristiansen et al., 1988); Andøya (Birks et al., 1994);and the North Timman Ridge (European Arctic Russia) (Paus et al., 2003)). The dates in italics indicate that the chronlologies at these points are not independent and therefore cannot be use to evaluate leads or lags in response time.

	Gradient	**SW ↔ NE**									
	Core 56/10/36 NE Atlantic	**Lochan An Druim**	**Core MD952011**	**Core HM79-6/4**	**Rogaland area**	**Sunnmøre area Kråkenes**	**Sunnmøre area Lerstadvatn**	**Andøya**	**Nikkupierjav'ri**	**North Timman Ridge**	**GRIP Ice core years BP**
Pre-Boreal Oscillation	*ca* 11.45	No evidence	*11.3-11*	Evident but date unclear	No evidence	No evidence	No evidence	Suggested but not dated	11.5	No evidence	11.3
Younger Dryas/Holocene transition	*ca* 11.55	11.5-11.3	*11.55*	11.3	*ca* 11.6	*ca* 11.53	*ca* 12	Not dated	11.6	11.8	11.5
Onset of Younger Dryas	*ca* 12.8	12.75	12.77	No record	*ca* 12.9	12.7-12.6	*ca* 12.9	12.9-12.7	No clear evidence	13	12.65
Reversal (IACP)	*ca 12.9*	13.15	No evidence	No record	*ca* 13.4	No evidence	*ca* 13.5	No evidence	Noclear evidence	No evidence	13.15
Reversal (Older Dryas)	*ca 14.1*	13.9	No record	No record	*ca* 14.3	No evidence	No evidence	No vidence	No clear evidence	No evidence	14.05
Onset of Lateglacial Interstadial	*ca 14.8*	*ca* 14.4	No record	No record	No evidence	*ca* 13.43	No evidence	*ca* 15.1	No clear evidence	*ca* 13.8	14.7

The GRIP record tends to lag the terrestrial and ocean records to varying degrees, in response to the periods of climatic deterioration as indicated by the cold reversals of the Older Dryas (GI-1d), the Intra Allerød Cold Period (GI-1b), the Younger Dryas (GS-1) and the Preboreal oscillation. By contrast, it leads the terrestrial record relatively significantly at the onset of the Lateglacial Interstadial and is coincident with it at the transition to the Holocene. This lag in vegetational development at the beginning of the Lateglacial Interstadial could be explained in terms of the time taken for the processes of migration and colonisation, following deglaciation, to take effect. By comparison, the response in vegetational development at the beginning of the Holocene, would show a signal earlier, with the expansion and development of existing taxa able to respond to the ameliorating conditions, and hence indicating a coincident response with the ice-core record. It might be expected that vegetation would respond quite rapidly to the stress of climatic deterioration, with retreat or extinction processes initiated rather more quickly than migration and colonisation. Hence the terrestrial record tends to lead, marginally, the GRIP record for these colder periods.

Comparison of the northeast Atlantic marine record and the timing of the climatic events at Lochan An Druim for the onset of the Younger Dryas (GS-1) and the Younger Dryas (GS-1) / Holocene transition, show coincident timing, and must indicate a close coupling of the marine record with the adjacent terrestrial record for these periods. Thus suggesting the potential for a rapid terrestrial response to changing SSTs.

In terms of the relative timing of these events along the northwest European continental margin there is a general pattern described here of a southwest to northeast lag in response to warming events, and the reverse in response to cooling events. It is suggested that these gradients result from the relative penetration of warm surface currents during times of climatic amelioraton and their withdrawl during climatic deterioration. If the link between SSTs and terrestrial vegetational changes is as close as suggested above, a more specific chronology for these events could be developed in the future, with further high-resolution analysis and robust calendar age chronologies for both marine and terrestrial records along this seaboard.

The Lateglacial is known to provide a record of frequent, and sometimes relatively high amplitude, climate changes. In view of the problems associated with low pollen production generally at this time (and especially at high latitudes), and particularly of recovery of a suitable record from an isolation basin environment, effort needs to be focused on sites that have not had a marine influence, and in addition, would benefit from a multi proxy approach. Holocene records generally can provide a fuller account of vegetational developmet and the Holocene marine record in the North Atlantic is more comprehensive, so that such coupling could perhaps be better assessed for this

period instead, although this would require very high resolution analyses in order to attempt to overcome the loss of amplituded during the more stable climatic conditions of this period.

****

The principal objectives of this study i.e., to test the two hypotheses related to quantitative changes in vegetation, as outlined in chapter1, have been met. This study has demonstrated quantitative, as well as the well-known qualitative, changes in the vegetation of the North Atlantic European continental margin following deglaciation. These changes have been shown to correspond with the short-term fluctuations and rapid changes in climate as recorded in the GRIP ice-core record. It has also been shown that palaeovegetation profiles from sites near to the potential extremities of northward penetration of warm ocean surface water during this time have recorded some of these events differentially, indicating an irregular northward lag in vegetational development, and this has been attributed to the relative proximity of the NAPF. In addition, the Lateglacial palaeoenvironmental histories at Lochan An Druim in northern Scotland, and Nikkupierjav'ri in northern Finnmark have been described. The investigation into the tephrochronology of the two study areas has provided evidence for a new early Holocene Icelandic cryptotephra from Lochan An Druim, together with evidence in support of a 'Younger Borrobol' cryptotephra from Lategalcial sediments of Allerød age at the same location.

Appendix I

A new early Holocene cryptotephra from northwest Scotland

Patricia H Ranner, Judy R M Allen and Brian Huntley

JOURNAL OF QUATERNARY SCIENCE (2005) **20**(3) 201–208

Published online in Wiley InterScience (www.interscience.wiley.com). DOI: 10.1002/jqs.910

A new early Holocene cryptotephra from northwest Scotland

PATRICIA H. RANNER, JUDY R. M. ALLEN* and BRIAN HUNTLEY
Institute of Ecosystem Science, School of Biological and Biomedical Sciences, University of Durham, South Road, Durham DH1 3LE, UK

Ranner, P. H., Allen, J. R. M. and Huntley, B. 2005. A new early Holocene cryptotephra from northwest Scotland. *J. Quaternary Sci.*, **Vol. 20** pp. 201–208. ISSN 0267-8179.

Received 18 October 2004; Revised 21 December 2004; Accepted 9 January 2005

ABSTRACT: Clarification of the temporal relationships amongst records of environmental change is dependent on accurate timescales. Event markers such as tephra layers are extremely important for constraining chronologies and providing tie points. In this report we present evidence of a previously unknown early Holocene Icelandic cryptotephra from a lake in northern Scotland—the 'An Druim Tephra'. The calibrated radiocarbon age of 9560 cal. yr BP for this new cryptotephra makes it an important addition to the suite of cryptotephras now recorded from the last glacial termination and early Holocene in northwest Europe. In addition we report evidence in support of a 'Younger Borrobol Tephra' from Lateglacial sediments of Allerød age. Copyright © 2005 John Wiley & Sons, Ltd.

KEYWORDS: An Druim Tephra; Younger Borrobol Tephra; cryptotephra; Iceland; Lateglacial; Torfajökull.

Introduction

Event horizons, such as tephra layers, are important synchronous markers that enable precise correlation between different records of past environmental changes. Such correlation is essential to clarify the temporal relationships between changes in different environmental components during times of rapid global environmental change such as the last glacial termination and early Holocene. In regions distal to volcanic sources, the identification of very thin or sparse layers of tephra shards, cryptotephra layers (Turney *et al.*, 2004), in sedimentary records from this interval is increasingly important. Although no discernible changes in vegetation are associated with most such layers (Hall, 2003), they are nonetheless of great importance in constraining the chronologies of sedimentary sequences. Such layers frequently are overlooked, however, especially in lake sediments that often have a high proportion of inorganic components; only through careful, targeted scrutiny of such sediments can these layers be detected.

Several cryptotephras previously have been found in northwest European sedimentary sequences spanning this interval, the three best documented being: the Borrobol Tephra (Turney *et al.*, 1997; Davies *et al.*, 2003, 2004); the Vedde Ash (Mangerud *et al.*, 1984; Birks *et al.*, 1996; Lowe and Turney, 1997; Wastegård *et al.*, 2000a, 2000b; Davies *et al.*, 2001); and the Saksunarvatn Tephra (Mangerud *et al.*, 1986; Grönvold *et al.*, 1995; Björck *et al.*, 2001). An increasing number of such layers is also reported from more recent Holocene sediments in northwest Europe, especially those from Ireland (Dwyer *et al.*, 1995; Hall and Pilcher, 2002; Hall, 2003), Scotland (Dugmore, 1989; Dugmore *et al.*, 1995) and Germany (van den Bogaard *et al.*, 2002; van den Bogaard and Schmincke, 2002). Most of the layers found in the British Isles are from Icelandic volcanoes, in particular Hekla, Katla, Snæfellsjökull, Grimsvötn/Kverkfjöll and Torfajökull. Here we report the identification of a new Icelandic cryptotephra layer from early Holocene sediments of a small lake, Lochan An Druim, in northwest Scotland, as well as new records of a 'Borrobol-like tephra' and of the Vedde Ash from the same location. The calibrated radiocarbon age of 9560 cal. yr BP for what we name as the An Druim cryptotephra makes it an important addition to the suite of cryptotephras now recorded from the last glacial termination and early Holocene in northwest Europe.

Study site and coring

Lochan An Druim (58° 28′ 30″ N, 4° 40′ 18″ W; UK NGR NC/435568; 25 m OD) is a small (ca. 0.5 ha) lowland lake to the east of Loch Eriboll, a sea loch on the north coast of Sutherland, Scotland, UK. (Fig. 1). The present open water surface of the lake is surrounded by a fen, dominated by the common reed, *Phragmites australis* (Cav.) Trin. ex Steudel, that occupies the majority of the area of the basin that extends to ca. 6 ha in total. The basin has two small inflowing streams and a single small outflow to the northwest. The sediment sequence from this site previously was studied by H. H. Birks in the 1970s (Birks, 1984) using a core taken within the *P. australis* fen on the western side

* Correspondence to: Judy R. M. Allen, Institute of Ecosystem Science, School of Biological and Biomedical Sciences, University of Durham, South Road, Durham DH1 3LE, UK. E-mail: j.r.m.allen@durham.ac.uk

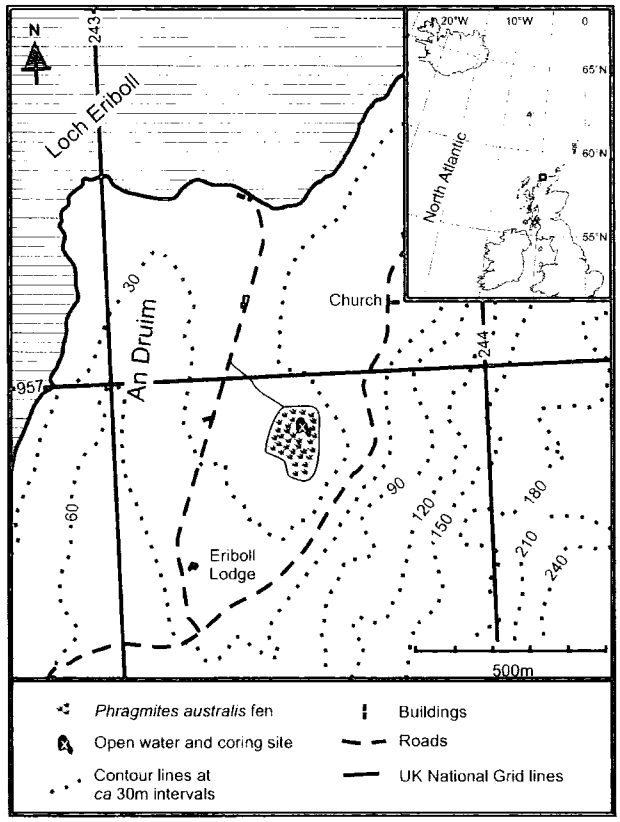

Figure 1 Location maps. Main map shows the location of Lochan An Druim on the eastern shore of Loch Eriboll, northwest Scotland; × marks the coring position. (Contour interval 30 m.) Inset indicates the position of the study area in northwest Scotland (black rectangle) and shows the proximity of Iceland to northern Scotland

of the lake. Her record of the pollen and macrofossil stratigraphy at this site provides unique evidence for low-altitude environmental conditions in northern Scotland during the Lateglacial and Holocene. The site has since been designated as a Geological Conservation Review site (GCR No. 1528: Gordon and Sutherland, 1993), located within the Eriboll SSSI (Site of Special Scientific Interest), its citation as such being based upon the importance of the palaeoenvironmental record preserved in its sediments. The site was re-cored in 1999 as part of a study investigating Lateglacial environmental changes along the northwest European continental margin at decadal to centennial resolution (Ranner, in prep.). In order to maximise recovery of Lateglacial sediments, overlapping cores were collected from the deepest part of the lake using a 5 cm diameter Wright-modified square rod piston corer (Wright, 1967) operated from a raft moored using cross ropes. After brief field logging, the 1-m core sections were wrapped in plastic film and aluminium foil; following transport to Durham they were stored at 4 °C until needed for analysis. The field datum point was 2.5 m above the sediment–water interface. A total core length of 9.50 m was collected; coarse sand and gravel encountered at this depth prevented further penetration. The basal 1.3 m of sediments recovered represents Lateglacial and early Holocene sedimentation and forms the subject of this paper.

Tephra analysis

Concurrently with high temporal resolution pollen analyses (Ranner, in prep.) the Lateglacial and early Holocene sediments were searched systematically for microscopic tephra shards. Contiguous samples (5 cm^3), each spanning a depth of 5 cm, were first examined. Where tephra shards were detected the relevant 5-cm section was re-sampled using contiguous samples (5 cm^3) each spanning a depth of 1 cm. In this way the depth of maximum shard abundance was in each case resolved to 1 cm. Geochemical analyses were performed on shards extracted from these depths of maximum abundance.

Samples were prepared as follows: organic and calcareous components were broken down by acid digestion in HNO_3 (Daniell *et al.*, 2000; Chambers *et al.*, 2004); biogenic silica was removed by NaOH treatment (Rose *et al.*, 1996); fine particles were removed by 10 μm sieving; and rhyolitic tephras were extracted by density separation using sodium polytungstate ($Na_6(H_2W_{12}O_{40})\cdot H_2O$) solution with a density of 2.5 g cm^{-3} (Turney, 1998a). Where necessary remaining diatoms were removed using a second density separation at 2.0 g cm^{-3}.

Residues from the initial set of extractions were mounted under a coverglass in Canada Balsam. These mounts were examined at a magnification of ×100 using a Leica DMLM light microscope with crossed polars and a 1λ compensator plate. Critical examination, at ×400 magnification, of the morphology of isotropic grains showing a negative Becke line in plane-polarised light (Stroiber and Morse, 1994) was used to confirm the presence of tephra shards. Where tephra shards were detected, the subsequent samples spanning 1 cm depth were required to provide material for chemical characterisation of the tephra, as well as to identify more accurately the depth of peak shard occurrence. In this case, therefore, final residues were resuspended in 0.5 cm^3 of distilled water, a single drop of which was examined microscopically to determine relative shard concentration, thus enabling depths of peak occurrence to be identified (Fig. 2).

Four layers of vesiculate cryptotephra (Ranner, in prep.) shards (size range 10–100 μm) were located in this way (Fig. 2). Three of these (S13, 10.94 m; S21, 11.32 m; S30, 11.86 m) were represented by sufficiently large and abundant shards for chemical characterisation by electron microprobe analysis; shards of the fourth (S20, 11.16 m) were extremely rare and it was not studied further. Shards from the occurrence peaks were used for analysis, slides for electron microprobe analysis being prepared using standard techniques (Dugmore *et al.*, 1995). Analyses were performed on the five spectrometer Cameca SX100 electron microprobe microanalyser at the NERC Tephrochronology Analytical Unit, University of Edinburgh, using a standard wavelength dispersive spectrometry (WDS) technique with an accelerating voltage of 20 keV, a beam current of 4 nA and a raster beam with a scan width of 5.0 μm. Calibration was carried out using standards of known composition (pure metals, synthetic oxides and simple silica compounds); at regular intervals throughout each analytical session an andradite ($Ca_3Fe_2Si_3O_{12}$) control sample of known composition was analysed to enable sample measurements to be corrected for variations in machine-operating conditions. Measurements were rejected for individual shards where the oxides total was less than 95% of the shard mass (Dugmore *et al.*, 1995). Results of the electron microprobe analyses are presented in Table 1.

Although examination of biplots, such as those illustrated in Figure 3(a,b), reveals that the three tephra layers are differentiated clearly by their major element oxide composition, all three have high silica and potassium contents, indicating a common silicic/rhyolitic character (Le Maitre *et al.*, 1989). Furthermore, their high potassium content indicates that they are most probably all derived from Icelandic sources (Haflidason *et al.*, 2000). One of them (S21, 11.32 m) can be correlated on the basis of its chemical signature with the

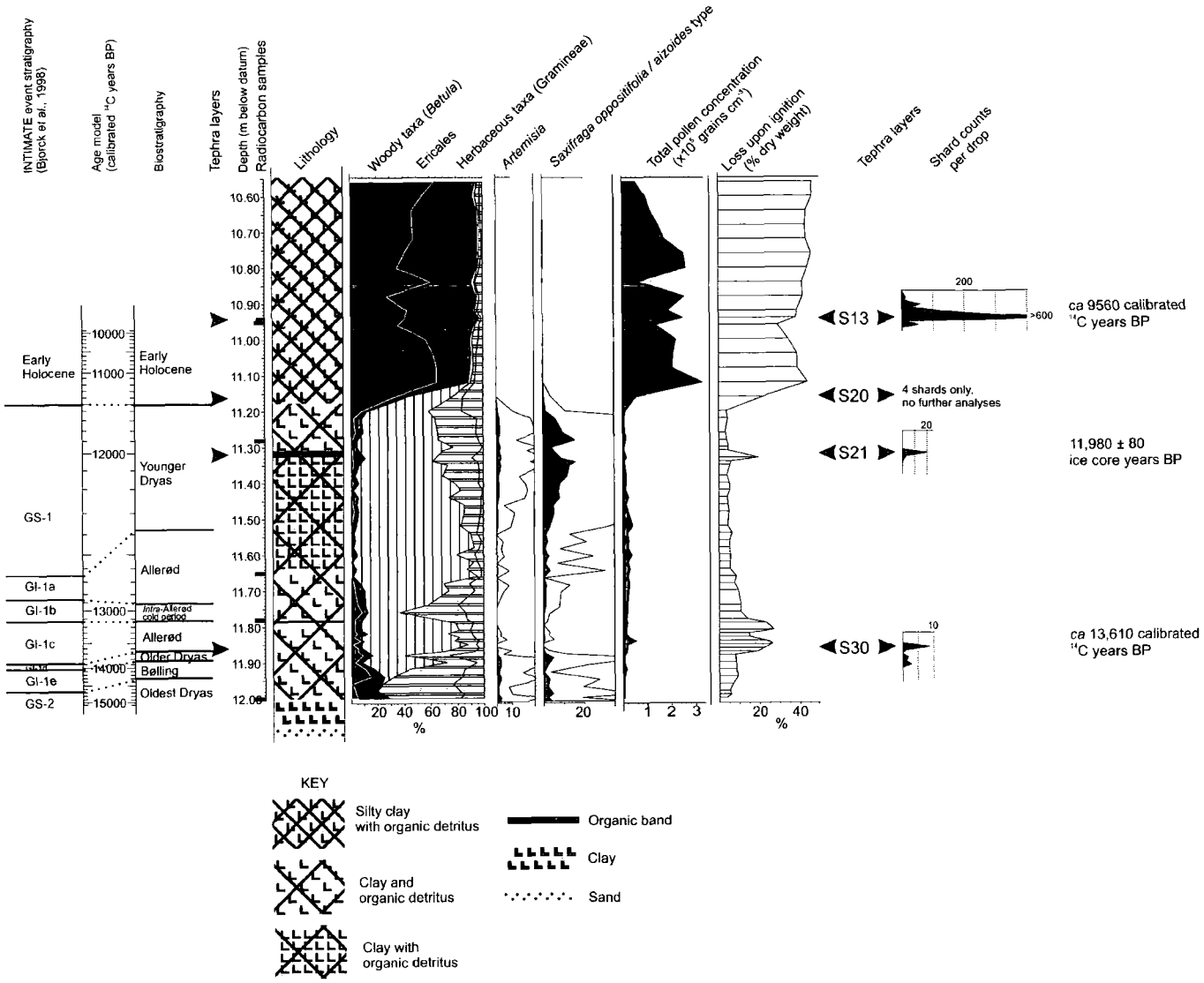

Figure 2 Summary diagram of Lateglacial pollen and sediment stratigraphy. Stratigraphic plot of sediment type, pollen percentages (ΣP = all terrestrial pollen and spores), total pollen and spore concentration, and organic content as estimated by loss in weight upon ignition (550 °C). Also shown are the positions of the radiocarbon samples and cryptotephra layers

already well-known Vedde Ash; a second (S30; 11.86 m) has a Borrobol-like chemistry. Figure 3(c) illustrates these correlations using a ternary plot of potassium, calcium and iron oxides. No match has been found, however, for the third layer identified at Lochan An Druim (S13). This tephra is characterised by a particularly high potassium content. Although its chemical signature is similar to that of some shards of the Lairg B Tephra (Figure 3(d)), the latter is much younger, being of mid-Holocene age (ca. 6000 ^{14}C yr BP: Dugmore *et al.*, 1995). We have named this new tephra the 'An Druim Tephra'.

Chronology

Lochan An Druim lies on the eastern edge of an outcrop of the Durness limestone (Cambrian–Ordovician, 540–500 Ma), hence there are potential problems in radiocarbon dating bulk sediment samples that may incorporate carbonate derived from this source. In the previous study of this site, Birks (1984) obtained radiocarbon age determinations for bulk sediment samples, each spanning ca. 10 cm sediment depth. These ages were consistently older, by as much as 1000 ^{14}C yr, than expected on the basis of the well-known and distinctive features of the pollen stratigraphy to which they related. In this study we have obtained AMS radiocarbon age determinations of terrestrial plant macrofossils wherever possible, each macrofossil sample being obtained from a 1 cm depth sediment slice. In the case of the An Druim Tephra layer (S13, 10.94 m), however, terrestrial plant macrofossils were absent from the adjacent sediments. Our strategy for dating this tephra, therefore, was to obtain an AMS age determination upon a bulk sediment sample from a 1 cm depth slice centred upon the cryptotephra, and also to obtain paired AMS age determinations for terrestrial plant macrofossils and for a bulk sediment sample from the immediately underlying 1 cm depth slice. These paired measurements provide an estimate of the adjustment to be applied to the bulk sediment age obtained for the An Druim Tephra layer. We do not propose that this 'correction' can be applied elsewhere in the stratigraphy, nor to Birks's (1984) bulk sediment ages. However, because the An Druim Tephra is only 1 cm above the paired samples, and from the same sedimentary unit, we believe it is acceptable to use the results of the paired measurements to adjust the bulk sediment age obtained for the

Table 1 Major oxide percentages for shards from the Lochan An Druim sediments

Shard	SiO_2	TiO_2	Al_2O_3	FeO	MnO	MgO	CaO	Na_2O	K_2O	Total
Tephra layer S13 (10.94 m)										
1	72.28	0.18	11.91	2.85	0.06	0.07	0.36	5.34	4.52	97.57
2	70.67	0.16	12.25	3.03	0.07	0.07	0.35	5.65	4.18	96.43
3	70.80	0.15	12.33	2.75	0.08	0.08	0.38	5.39	4.41	96.36
4	71.19	0.16	12.11	2.70	0.13	0.06	0.35	5.34	4.29	96.32
5	70.58	0.09	13.09	2.42	0.15	0.08	0.29	5.35	4.19	96.24
6	71.43	0.13	11.87	2.84	0.08	0.06	0.35	5.07	4.27	96.09
7	70.65	0.17	11.90	2.90	0.07	0.07	0.38	5.36	4.45	95.96
8	70.80	0.17	11.72	2.96	0.08	0.04	0.38	5.37	4.44	95.95
9	71.05	0.16	11.83	2.88	0.10	0.05	0.37	5.09	4.33	95.85
10	70.94	0.16	11.62	2.77	0.12	0.08	0.41	5.46	4.26	95.82
11	70.71	0.12	12.02	2.59	0.12	0.04	0.40	4.84	4.43	95.27
12	70.81	0.17	11.79	2.96	0.00	0.06	0.40	4.88	4.16	95.22
13	70.16	0.17	12.02	2.56	0.07	0.04	0.35	5.17	4.48	95.00
mean	**70.92**	**0.15**	**12.03**	**2.79**	**0.09**	**0.06**	**0.37**	**5.25**	**4.34**	**96.01**
1σ	0.51	0.02	0.37	0.18	0.04	0.01	0.03	0.23	0.12	0.65
Tephra layer S21 (11.32 m)										
1	70.97	0.27	13.48	3.83	0.23	0.23	1.34	4.66	3.47	98.47
2	69.99	0.23	12.99	3.72	0.16	0.18	1.36	5.11	3.53	97.28
3	69.77	0.28	13.21	3.47	0.18	0.24	1.30	5.22	3.55	97.22
4	69.37	0.32	13.29	3.80	0.12	0.19	1.29	5.34	3.31	97.03
5	69.70	0.21	13.06	3.87	0.14	0.21	1.27	4.89	3.40	96.75
6	68.34	0.20	13.26	3.92	0.19	0.21	1.31	4.96	3.45	95.85
7	68.69	0.29	12.81	3.70	0.06	0.21	1.32	5.15	3.42	95.65
8	68.36	0.27	13.12	3.88	0.23	0.20	1.33	4.98	3.28	95.64
9	68.59	0.23	12.93	3.57	0.06	0.22	1.23	5.34	3.37	95.54
10	68.43	0.23	13.00	3.69	0.13	0.23	1.29	5.03	3.37	95.38
11	69.75	0.28	12.95	3.87	0.10	0.23	1.30	3.34	3.16	94.97
mean	**69.27**	**0.26**	**13.10**	**3.76**	**0.14**	**0.21**	**1.30**	**4.91**	**3.39**	**96.34**
1σ	0.85	0.04	0.20	0.14	0.06	0.02	0.04	0.56	0.11	1.07
Tephra layer S30 (11.86 m)										
1	74.59	0.10	12.76	1.37	0.00	0.08	0.73	4.05	3.66	97.34
2	72.93	0.11	12.97	1.20	0.02	0.06	0.82	4.57	3.38	96.06
3	73.45	0.11	12.32	1.49	0.10	0.07	0.75	4.00	3.68	95.97
4	72.88	0.13	12.44	1.51	0.02	0.08	0.76	4.08	3.95	95.85
5	73.95	0.09	12.34	1.37	0.00	0.07	0.74	3.63	3.47	95.66
6	73.30	0.09	12.23	1.40	0.03	0.10	0.77	3.98	3.58	95.47
7	72.52	0.12	12.38	1.48	0.05	0.10	0.76	4.00	3.96	95.38
8	73.08	0.09	11.88	1.51	0.06	0.07	0.75	4.04	3.89	95.37
9	72.65	0.11	12.38	1.51	0.02	0.04	0.77	3.95	3.90	95.34
10	72.74	0.12	12.28	1.40	0.05	0.07	0.72	4.02	3.80	95.20
11	72.56	0.09	12.18	1.53	0.07	0.09	0.73	4.14	3.80	95.20
12	72.65	0.09	12.42	1.46	0.03	0.07	0.75	3.97	3.67	95.10
mean	**73.11**	**0.10**	**12.38**	**1.44**	**0.04**	**0.08**	**0.76**	**4.04**	**3.73**	**95.66**
1σ	0.63	0.02	0.27	0.09	0.03	0.02	0.03	0.21	0.19	0.61

tephra layer. Table 2 gives details of the samples from which radiocarbon age determinations were obtained, as well as the results of these measurements. The results for the paired samples, POZ-6527 (bulk sediment) and POZ-6526 (terrestrial plant macrofossils), indicate that the 'true' radiocarbon age of the bulk sediment sample can be obtained by subtracting a 'correction' of 1330 ^{14}C years. Applying this to the bulk sediment age obtained for the An Druim Tephra (POZ-6525) gives a radiocarbon age of 8590 ± 50 ^{14}C yr BP for this tephra (calibrated age: 9560 cal. yr BP; 2σ range 9488–9633 cal. yr BP).

No direct age determinations were made for the tephras identified as the Vedde Ash and 'Borrobol-like tephra'. Whereas the former is well-defined in a variety of records, and its age well-established, the age of the latter has recently been questioned, with evidence advanced that more than one 'Borrobol-like tephra' may occur in sediments dating from the early part of the Lateglacial interstadial (Davies *et al.*, 2004). In order to estimate the age of the 'Borrobol-like tephra' found at Lochan An Druim we constructed an age–depth model for the Lateglacial–early Holocene section of the sediments at the site. In addition to the AMS age determinations obtained, this model also uses the corrected and calibrated bulk sediment age for the An Druim Tephra (9560 cal. yr BP) and the GRIP ice-core age of the Vedde Ash ($11\,980 \pm 80$ ice-core years: Grönvold *et al.*, 1995). Because the ages determined at 11.28 m (Ua-21242) and 11.65 m (Ua-21241) were not distinguishable with 95% confidence (i.e. their 2σ ranges overlap), a single age of 12 335 cal. yr BP (range 11 746–12 837 cal. yr BP) at 11.465 m was substituted and used for model construction. The model thus used a total of six data

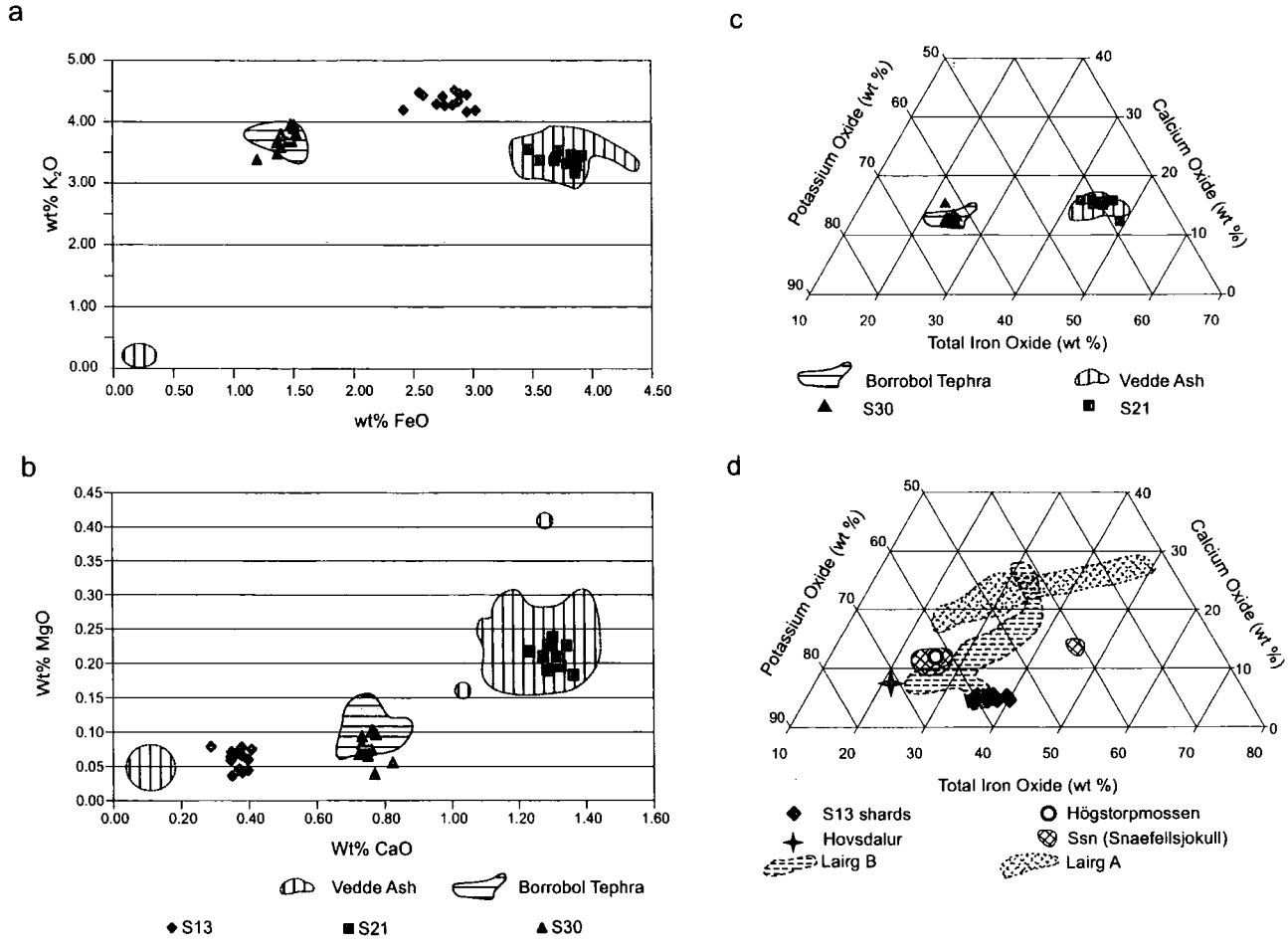

Figure 3 Chemical characteristics of tephras. Two biplots showing the clear separation of the three tephra layers at Lochan An Druim by their major element oxides, also shown are the envelopes for the Vedde Ash (Turney *et al.*, 1997; Wastegård *et al.*, 1998; Björck and Wastegård, 1999; Wastegård *et al.*, 2000b) and Borrobol Tephra (Turney *et al.*, 1997): (a) plot of potassium oxide and iron oxide; (b) plot of magnesium oxide and calcium oxide. Two ternary diagrams showing the relative proportions of the oxides of potassium, calcium and iron in the three tephra layers at Lochan An Druim and various other tephras: (c) S21 and S30 tephras from Lochan An Druim, Vedde Ash (Turney *et al.*, 1997; Wastegård *et al.*, 1998; Björck and Wastegård, 1999; Wastegård *et al.*, 2000b) and Borrobol Tephra (Turney *et al.*, 1997) (data for the latter two from *Tephrabase*: http://www.geo.ed.ac.uk:81/tephra/). (d) An Druim Tephra (S13) and known early Holocene tephras with high potassium content (Ssn (Snæfellsjökull) (Boygle, 1994), Lairg A (Dugmore *et al.*, 1995; Pilcher *et al.*, 1996; Hall and Pilcher, 2002), Lairg B (Dugmore *et al.*, 1995; Pilcher *et al.*, 1996), Högstorpmossen (Björck and Wastegård, 1999) and Hovsdalur (Wastegård, 2002) Tephras (data for the former three from *Tephrabase*: http://www.geo.ed.ac.uk:81/tephra/))

Table 2 Radiocarbon dates

Depth below datum (m)	Laboratory number	Material (dry weight)	^{14}C age (yr BP)	Calibrated age[a] (2σ range; midpoint)
10.935–10.945	POZ-6525	Bulk sediment—organic gyttja (412.3 mg)	9 920 ± 50	11 197–11 364; 11 280
10.945–10.955	POZ-6527	Bulk sediment—organic gyttja (915.4 mg)	10 010 ± 150	11 254–11 694; 11 470
10.945–10.955	POZ-6526	Woody plant fragments (2.3 mg)	8680 ± 50	9538–9781; 9660
11.275–11.285	Ua-21242	Woody plant fragments (8.5 mg)	10 345 ± 100	11 746–12 681; 12 220
11.645–11.655	Ua-21241	Woody plant fragments (12.1 mg)	10 465 ± 75	12 070–12 837; 12 450
11.765–11.775	Ua-21240	Woody plant fragments (9.6 mg)	11 095 ± 75	12 872–13 218; 13 040
11.995–12.005	Ua-21239	Woody plant fragments (10.3 mg)	12 625 ± 100	14 265–15 620; 14 940

[a] Calibrated using CALIB 4.4.1 (Stuiver and Reimer, 1993) with the INTCAL98 dataset (Stuiver *et al.*, 1998).

points. The best-fitting model (Fig. 4) was obtained using a third-order polynomial:

$$y = 12\,778.69x^3 - 439\,890.759x^2 + 5\,049\,058.309x - 19\,311\,069.039 (r^2 = 0.999)$$

Whilst we acknowledge that there are many problems associated with ^{14}C dating the last glacial–interglacial transition (Lowe and Walker, 2000), we note that our estimated age model fits well our interpretation of the pollen stratigraphic information from this site (Fig. 2). We therefore believe that this model can be used to obtain an estimated age for the 'Borrobol-like tephra' found at a depth of 11.86 m in the Lochan An Druim sediments; the age estimated is ca. 13 610 cal. yr BP.

The same model also estimates an age of 8085 cal. yr BP for the prominent pollen concentration minimum in the sample at

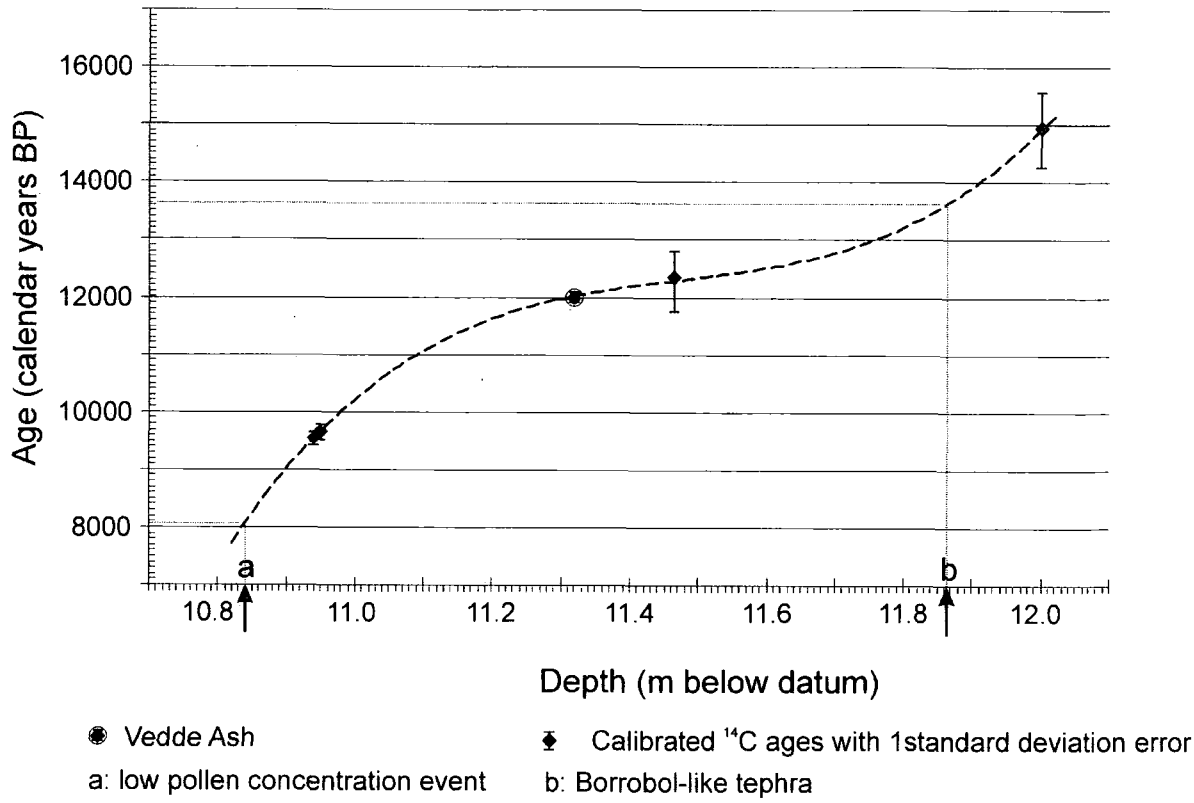

Figure 4 Chronology. Age–depth relationship for the Lateglacial part of the Lochan An Druim stratigraphy

a depth of 10.84 m (Fig. 2); the close correspondence between this age estimate and the prior inference from the palynostratigraphy that this concentration minimum is a likely correlate of the '8200 event' (Alley *et al.*, 1997) adds to our confidence in the age–depth model fitted. This widespread cooling event is recorded in many early-Holocene records (von Grafenstein *et al.*, 1998; Duplessy *et al.*, 2001; Johnsen *et al.*, 2001; Snowball *et al.*, 2002; Paus *et al.*, 2003) and variously dated to between 8000 and 8400 cal. yr BP. At Lochan An Druim the cooling event, the duration of which we estimate as no more than 600 years, was of sufficient magnitude to be reflected clearly in the palynological record.

Discussion

Understanding the complex and rapid environmental changes that took place during the Lateglacial and early Holocene, as the global system moved from a glacial to an interglacial condition, requires improved knowledge of the phase relationships between different components of the global system. Event markers, such as distinct tephra layers, that can be detected in sediment or other records from many localities and/or more than one realm are vital to this effort. Securely dated and chemically characterised tephras, including the so-called cryptotephra layers (Turney *et al.*, 2004) that can be identified in lake sediments, are increasingly important in improving the accuracy and precision that can be attained in correlating records from separate localities. As a contribution to this area of research, three cryptotephra layers identified in the Lateglacial and early Holocene sediments at Lochan An Druim have been chemically characterised, including the newly recorded rhyolitic An Druim Tephra.

Although, as we have shown above, there is some overlap in chemical composition between the An Druim Tephra and the Lairg B Tephra, they differ in age by >2500 ^{14}C yr (An Druim: 8590 ± 50 ^{14}C yr BP; Lairg B: ca. 6000 ^{14}C yr BP). Thus, although it is likely, given its chemical signature, that the An Druim Tephra originated from the same volcanic source as the Lairg B Tephra (Torfajökull in southern Iceland) we propose that the An Druim and Lairg B Tephras reflect distinct volcanic events. Of previously widely recorded early-Holocene tephras not identified from the sediments at Lochan An Druim, the Saksunarvatn Tephra (Grönvold *et al.*, 1995; Birks *et al.*, 1996; Eiriksson *et al.*, 2000) is most similar in age to the An Druim Tephra (9560 cal. yr BP), being dated variously to 9930–10 010 cal. yr BP (Birks *et al.*, 1996) or 10 240 cal. yr BP (Björck *et al.*, 2001). The Saksunarvatn Tephra, however, is basaltic with no rhyolitic component recorded from any of the sites where it has been found to date; thus it not only differs in age from the An Druim Tephra by ca. 500 years, but also is chemically distinct. Three other less widely reported tephras recorded from northwest Europe, however, have high potassium levels broadly comparable to those of the An Druim Tephra. One of these, the Ssn (Snæfellsjökull) Tephra (Boygle, 1994) dates from the period 6000 to 7000 ^{14}C yr BP and thus, like the Lairg B Tephra, is much younger than the An Druim Tephra. The other two, however, are of a similar age to the An Druim Tephra: the rhyolitic Hovsdalur Tephra found in the Faroe Islands (Wastegård, 2002) and dated to 10 500 cal. yr BP; and a tephra represented by just two shards from Högstorpmossen, Sweden (ca. 9000 ^{14}C yr BP; Björck and Wastegård, 1999). Both of these, however, are chemically distinct from the An Druim Tephra when viewed on a ternary plot of potassium, calcium and total iron oxides (Fig. 3d). We thus conclude that the An Druim Tephra is an additional early Holocene tephra layer in the Scottish tephrochronological sequence younger than the widely found Saksunarvatn

Tephra and substantially older than the chemically similar Lairg B Tephra.

The 'Borrobol-like tephra' found at Lochan An Druim (S30) lies in sediments representing the early part of the Allerød interval (GI-1c of Bjorck *et al.*, 1998), the onset of which is marked at this site by a small peak in *Betula*, an increase in Ericales and decreases in *Artemisia* and *Saxifraga oppositifolia/S. aizoides type* (Fig. 2); the age of this tephra is estimated as ca. 13 610 cal. yr BP. Turney *et al.* (1997) in their paper reporting the discovery of the Borrobol Tephra estimated its age to be ca. 12.5 ^{14}C kyr BP on the basis of its stratigraphic position in the Bølling (GI-1e). This age estimate is equivalent to ca. 14 600 cal. yr BP, but was revised by Turney (1998b) on the basis of ^{14}C dating of bulk organic sediment to 14 400 cal. yr BP; it is thus ca. 800–1000 years older than the 'Borrobol-like tephra' found at An Druim. Davies *et al.* (2004) discuss the possibility that at least two chemically identical 'Borrobol-like tephra' layers may have been deposited during the interval between ca. 13 600 and ca. 14 500 cal. yr BP. The evidence they discuss includes the report by Turney (1998b) of the occurrence at the Borrobol site of a low concentration layer of tephra shards, chemically indistinguishable from those of the Borrobol Tephra, some 30 cm above the latter in sediments dating from the early part of the Allerød (GI-1c). The new evidence presented here of a 'Borrobol-like tephra' at An Druim dating from ca. 13 610 cal. yr BP lends further support to the occurrence of a 'Younger Borrobol Tephra' dating from the early Allerød. Until such time as both this and the original Borrobol Tephra are identified and dated in a single stratigraphic profile, however, 'Borrobol-like tephras' will remain of limited value as event markers.

The Vedde Ash is a unique layer, clearly identifiable by its major element chemistry, that was deposited during the Younger Dryas (GS-1 of Bjorck *et al.*, 1998). It has been identified in many deposits, both marine and terrestrial (e.g. Mangerud *et al.*, 1984; Austin *et al.*, 1995; Birks *et al.*, 1996; Lowe and Turney, 1997; Turney, 1998a; Turney *et al.*, 1998; Eiriksson *et al.*, 2000; Wastegård *et al.*, 2000a, 2000b; Bondevik *et al.*, 2001), and is an extremely useful event marker horizon. In the Lochan An Druim pollen stratigraphy the Vedde Ash lies within the peak of *Artemisia* and *Saxifraga oppositifolia/ S. aizoides* type, a short distance below the marked increase in woody taxa (especially *Betula*), that marks the transition to the early Holocene (Fig. 2); this is consistent with deposition during the Younger Dryas as recorded elsewhere.

Locating, characterising and determining the age of cryptotephras such as these in lake sediments offers new opportunities for detailed correlations between records. New techniques, such as the application of laser ablation sampling coupled to ICP-MS analysis (Pearce *et al.*, 1999, 2002, 2004), may in future address the dual challenges of chemically characterising even the extremely small tephra shards of which many of these layers are composed and of 'fingerprinting', using elements present at very low concentrations, tephras such as the Borrobol and Younger Borrobol that are at present indistinguishable using electron microprobe analyses of major oxides.

Acknowledgements We thank Scottish Natural Heritage and Mr J. Clark, Eriboll Lodge, for permission to core at Lochan An Druim in spring 1999. A. L. Huntley, J. P. Huntley, J. R. P. Huntley and V. Kay assisted with the coring. PHR was supported by a University of Durham Millennium Studentship. NERC supported the electron microprobe analyses performed at the University of Edinburgh. Radiocarbon dating was supported using funds from the Royal Society—Wolfson Foundation 'Research Merit Award' held by BH. C. S. M. Turney and S. M. Davies are thanked for their constructive comments on an earlier version of this paper.

References

Alley RB, Mayewski PA, Sowers T, Stuiver M, Taylor KC, Clark PU. 1997. Holocene climatic instability: a prominent widespread event 8200 yr ago. *Geology* **25**: 483–486.

Austin WEN, Bard E, Hunt JB, Kroon D, Peacock JD. 1995. The ^{14}C age of the Icelandic Vedde ash: implications for Younger Dryas marine reservoir age corrections. *Radiocarbon* **37**: 53–62.

Birks HH. 1984. Late-Quaternary pollen and plant macrofossil stratigraphy at Lochan an Druim, north-west Scotland. In *Lake Sediments and Environmental History*, Haworth EY, Lund JWG (eds). University of Minnesota Press: Minneapolis.

Birks HH, Gulliksen S, Haflidi H, Mangerud J. 1996. New radiocarbon dates for the Vedde ash and Saksunarvatn ash from western Norway. *Quaternary Research* **45**: 119–127.

Björck J, Wastegård S. 1999. Climate oscillations and tephrochronology in eastern middle Sweden during the last glacial–interglacial transition. *Journal of Quaternary Science* **14**: 399–410.

Bjorck S, Walker MJC, Cwynar LC, Johnsen S, Knudsen K-L, Lowe JJ, Wohlfarth B, Members I. 1998. An event stratigraphy for the Last Termination in the North Atlantic region based on the Greenland ice-core record: a proposal by the INTIMATE group. *Journal of Quaternary Science* **13**: 283–292.

Björck S, Muscheler R, Kromer B, Andresen CS, Heinemeier J, Johnsen J, Johnsen SJ, Conley D, Koc N, Spurk M, Veski S. 2001. High-resolution analyses of an early Holocene climate event may imply decreased solar forcing as an important climate trigger. *Geology* **29**: 1107–1110.

Bondevik S, Mangerud J, Gulliksen S. 2001. The marine ^{14}C age of the Vedde Ash Bed along the west coast of Norway. *Journal of Quaternary Science* **16**: 3–7.

Boygle JE. 1994. *Tephra in lake sediments: an unambiguous geochronological marker?* PhD thesis, University of Edinburgh.

Chambers FM, Daniell JRG, Hunt JB, Molloy K, O'Connell M. 2004. Tephrostratigraphy of An Loch Mór, Inis Óir, western Ireland: implications for Holocene tephrochronology in the northeastern Atlantic region. *The Holocene* **14**: 703–720.

Daniell J, Hunt J, Chambers F. 2000. *Tephrostratigraphy of An Loch Mòr*: Second Report.

Davies SM, Turney CSM, Lowe JJ. 2001. Identification and significance of a visible, basalt rich Vedde Ash layer in a Late-glacial sequence on the Isle of Skye, Inner Hebrides, Scotland. *Journal of Quaternary Science* **16**: 99–104.

Davies SM, Wastegård S, Wohlfarth B. 2003. Extending the limits of the Borrobol tephra to Scandinavia and detection of new early Holocene tephras. *Quaternary Research* **59**: 345–352.

Davies SM, Wohlfarth B, Wastegård S, Andersson M, Blockley S, Possnert G. 2004. Were there two Borrobol Tephras during the early Lateglacial period: implications for tephrochronology? *Quaternary Science Reviews* **23**: 581–589.

Dugmore A. 1989. Icelandic volcanic ash in Scotland. *Scottish Geographical Magazine* **105**: 168–172.

Dugmore AJ, Larsen G, Newton AJ. 1995. Seven tephra isochrones in Scotland. *The Holocene* **5**: 257–266.

Duplessy J-C, Ivanova E, Murdmaa I, Paterne M, Labeyrie L. 2001. Holocene paleoceanography of the northern Barents Sea and variations of the northward heat transport by the Atlantic Ocean. *Boreas* **30**: 2–16.

Dwyer GS, Cronin TM, Baker PA, Raymo ME, Buzas JS, Corrège T. 1995. North Atlantic deepwater temperature change during Late Pliocene and Late Quaternary climatic cycles. *Science* **270**: 1347–1351.

Eiriksson J, Knudsen KL, Haflidason H, Henriksen P. 2000. Late-glacial and Holocene palaeoceanography of the North Icelandic shelf. *Journal of Quaternary Science* **15**: 23–42.

Gordon JE, Sutherland GG (eds). 1993. *Quaternary of Scotland.* Geological Conservation Review: Vol. 6. Joint Nature Conservation Committee: Peterborough.

Grönvold K, Óskarsson N, Johnsen SJ, Clausen HB, Hammer CU, Bond G, Bard E. 1995. Ash layers from Iceland in the Greenland Grip ice core correlated with oceanic and land sediments. *Earth and Planetary Science Letters* **135**: 149–155.

Haflidason H, Eiriksson J, Van Kreveld S. 2000. The tephrochronology of Iceland and the North Atlantic region during the Middle and Late Quaternary: a review. *Journal of Quaternary Science* **15**: 3–22.

Hall VA. 2003. Assessing the impact of Icelandic volcanism on vegetation systems in the north of Ireland in the fifth and sixth millennia BC. *The Holocene* **13**: 131–138.

Hall VA, Pilcher JR. 2002. Late-Quaternary Icelandic tephras in Ireland and Great Britain: detection, characterization and usefulness. *The Holocene* **12**: 223–230.

Johnsen SJ, Dahl-Jensen D, Gundestrup N, Steffensen JP, Clausen HB, Miller H, Masson-Delmotte V, Sveinbjörnsdottir AE, White J. 2001. Oxygen isotope and palaeotemperature records from six Greenland ice-core stations: Camp Century, Dye-3, GRIP, GISP2, Renland and NorthGRIP. *Journal of Quaternary Science* **16**: 299–307.

Le Maitre RW, Bateman P, Dudek A, Keller J, Lameyre Le Bas MJ, Sabine PA, Schmid R, Sorensen H, Streckeisen A, Woolley AR, Zanettin B. 1989. *A Classification of Igneous Rocks and Glossary of Terms*. Blackwell: Oxford.

Lowe JJ, Turney CM. 1997. Vedde Ash layer discovered in a small lake basin on the Scottish mainland. *Journal of the Geological Society, London* **154**: 605–612.

Lowe JJ, Walker MJC. 2000. Radiocarbon dating of the last glacial–interglacial transition (ca 14–9 ^{14}C ka BP) in terrestrial and marine records: the need for new quality assurance protocols. *Radiocarbon* **42**: 53–68.

Mangerud J, Lie SE, Furnes H, Kristiansen IL, Lomo L. 1984. A Younger Dryas ash bed in western Norway, and its possible correlations with tephra in cores from the Norwegian Sea and the North Atlantic. *Quaternary Research* **21**: 85–104.

Mangerud J, Furnes H, Johansen J. 1986. A 9000-year old ash bed on the Faroe Islands. *Quaternary Research* **21**: 85–104.

Paus A, Svendsen JI, Matiouchkov A. 2003. Late Weichselian (Valdaian) and Holocene vegetation and environmental history of the northern Timan Ridge, European Arctic Russia. *Quaternary Science Reviews* **22**: 2285–2302.

Pearce NJG, Westgate JA, Perkins WT, Eastwood WJ, Shane P. 1999. The application of laser ablation ICP-MS to the analysis of volcanic glass shards from tephra deposits: bulk glass and single shard analysis. *Global and Planetary Change* **21**: 151–171.

Pearce NJG, Eastwood WJ, Westgate JA, Perkins WT. 2002. Trace-element composition of single glass shards in distal Minoan tephra from SW Turkey. *Journal of the Geological Society* **159**: 545–556.

Pearce NJG, Westgate JA, Perkins WT, Preece SJ. 2004. The application of ICP-MS methods to tephrochronological problems. *Applied Geochemistry* **19**: 289–322.

Pilcher JR, Hall VA, McCormac FG. 1996. An outline tephrochronology for the Holocene of the north of Ireland. *Journal of Quaternary Science* **11**: 485–494.

Ranner PH. in prep. *Lateglacial and early Holocene environmental changes along the northwest European continental margin*. PhD thesis, University of Durham.

Rose NL, Golding PNE, Battarbee RW. 1996. Selective concentration and enumeration of tephra shards from lake sediment cores. *Holocene* **6**: 243–246.

Snowball I, Zillen L, Gaillard MJ. 2002. Rapid early-Holocene environmental changes in northern Sweden based on studies of two varved lake-sediment sequences. *Holocene* **12**: 7–16.

Stroiber RE, Morse SA. 1994. *Crystal Identification with the Polarising Microscope*. Chapman & Hall: New York.

Stuiver M, Reimer PJ. 1993. Extended ^{14}C data base and revised CALIB 3.0 ^{14}C age calibration program. *Radiocarbon* **35**: 215–230.

Stuiver M, Reimer PJ, Bard E, Beck JW, Burr GS, Hughen KA, Kromer B, McCormac G, Van der Plicht J, Spurk M. 1998. INTCAL98 radiocarbon age calibration, 24 000–0 cal. BP. *Radiocarbon* **40**: 1041–1083.

Turney CSM. 1998a. Extraction of rhyolitic component of Vedde microtephra from minerogenic lake sediments. *Journal of Paleolimnology* **19**: 199–206.

Turney CSM. 1998b. *Isotope stratigraphy and tephrochronology of the last glacial-interglacial transition (14–9 ka ^{14}C BP) in the British Isles*. PhD thesis, University of London.

Turney CSM, Harkness DD, Lowe JJ. 1997. The use of microtephra horizons to correlate Late-glacial lake sediment successions in Scotland. *Journal of Quaternary Science* **12**: 525–531.

Turney CSM, Harkness DD, Lowe JJ. 1998. Carbon isotope variations and chronology of the last glacial–interglacial transition (14–9 ka BP). *Radiocarbon* **40**: 873–881.

Turney CSM, Lowe JJ, Davies SM, Hall V, Lowe DJ, Wastegård S, Hoek WZ, Alloway B. 2004. Tephrochronology of last termination sequences in Europe: a protocol for improved analytical precision and robust correlation procedures (a joint SCOTAV-INTIMATE proposal). *Journal of Quaternary Science* **19**: 111–120.

van den Bogaard C, Schmincke H-U. 2002. Linking the North Atlantic to central Europe: a high-resolution Holocene tephrochronological record from northern Germany. *Journal of Quaternary Science* **17**: 3–20.

van den Bogaard C, Dorfler W, Glos R, Nadeau M-J, Grootes PM, Erlenkauser H. 2002. Two tephra layers bracketing late Holocene paleoecological changes in northern Germany. *Quaternary Research* **57**: 314–324.

von Grafenstein U, Erlenkeuser H, Muller J, Jouzel J, Johnsen S. 1998. The cold event 8200 years ago documented in oxygen isotope records of precipitation in Europe and Greenland. *Climate Dynamics* **14**: 73–81.

Wastegård S. 2002. Early to middle Holocene silicic tephra horizons from the Katla volcanic system, Iceland: new results from the Faroe Islands. *Journal of Quaternary Science* **17**: 723–730.

Wastegård S, Bjorck S, Possnert G, Wohlfarth B. 1998. Evidence of the occurence of Vedde Ash in Sweden: radiocarbon age estimates. *Journal of Quaternary Science* **13**: 271–274.

Wastegård S, Turney CSM, Lowe JJ, Roberts SJ. 2000a. New discoveries of the Vedde Ash in southern Sweden and Scotland. *Boreas* **29**: 72–78.

Wastegård S, Wohlfarth B, Subetto DA, Sapelko TV. 2000b. Extending the known distribution of the Younger Dryas Vedde Ash into northwestern Russia. *Journal of Quaternary Science* **15**: 581–586.

Wright HE. 1967. A square-rod piston sampler for lake sediments. *Journal of Sedimentology and Petrology* **37**: 975–976.

Appendix II

Data tables for analyses at Lochan An Druim and Nikkupierjav'ri

Contents

Folder: 1 - Lochan An Druim

Files:

LAD-% Loss on Ignition (dry weight).xls

Results and calculations.

LAD-Age-depth Model.xls

Development of model segments and calculations of the dates assigned to each sample.

LAD-Biomes.xls

Systematic biome analysis of pollen percentage data.

LAD-Detrended Correspondence Analysis-output.xls

Output from the detrended correspondence analysis carried out within the Tilia Programme.

LAD-Pollen Data-Final.xls

Pollen count data and presence/absence data for the macrofossils from the pollen washings, for the accepted samples, with the subsequent calculations for percentage data, concentration values, influx data (with mean values) and mean sample resolution.

LAD-Pollen Data-Original.xls

Pollen count data and presence/absence data for the macrofossils from the pollen washings, for all the samples.

LAD-Climate Reconstructions (Direct Analogue) (Northern Hemisphere+Pinus).xls

Data for the reconstructed bioclimate variables derived using the direct analogue approach.

Folder: 2 – Nikkupierjav'ri

Files:

LAD-% Loss on Ignition (dry weight).xls

Results and calculations.

LAD-Age-depth Model.xls

Development of model segments and calculations of the dates assigned to each sample.

LAD-Biomes.xls

Systematic biome analysis of pollen percentage data.

LAD-Detrended Correspondence Analysis-output.xls

Output from the detrended correspondence analysis carried out within the Tilia Programme.

LAD-Pollen Data-Final

Pollen count data and presence/absence data for the macrofossils from the pollen washings, for the accepted samples, with the subsequent calculations for percentage data, concentration values, influx data (with mean values) and mean sample resolution.

LAD-Pollen Data-Original

Pollen count data and presence/absence data for the macrofossils from the pollen washings, for all the samples.

Appendix III

Lochan An Druim: Relative abundance data are displayed for all the taxa with totals (undifferentiated) for the monolete and trilete Pteridophyte spores; taxa have been grouped into arboreal taxa and non-arboreal taxa, terrestrial Pteridophytes and obligate aquatics and plotted against age (cal yrs BP). Pollen sums are specified as follows for selected taxa: Terrestrial Pollen (ΣTP), i.e. Arboreal Pollen minus Pinus (AP) plus Non-Arboreal Pollen (NAP); Terrestrial Pollen and Terrestrial Pteridophyte Spores (ΣTP + ΣPS); Terrestrial Pollen and Aquatic Pollen (including Sphagnum) (ΣTP + ΣAP); Terrestrial Pollen and Indeterminable Pollen (ΣTP + ΣIP).

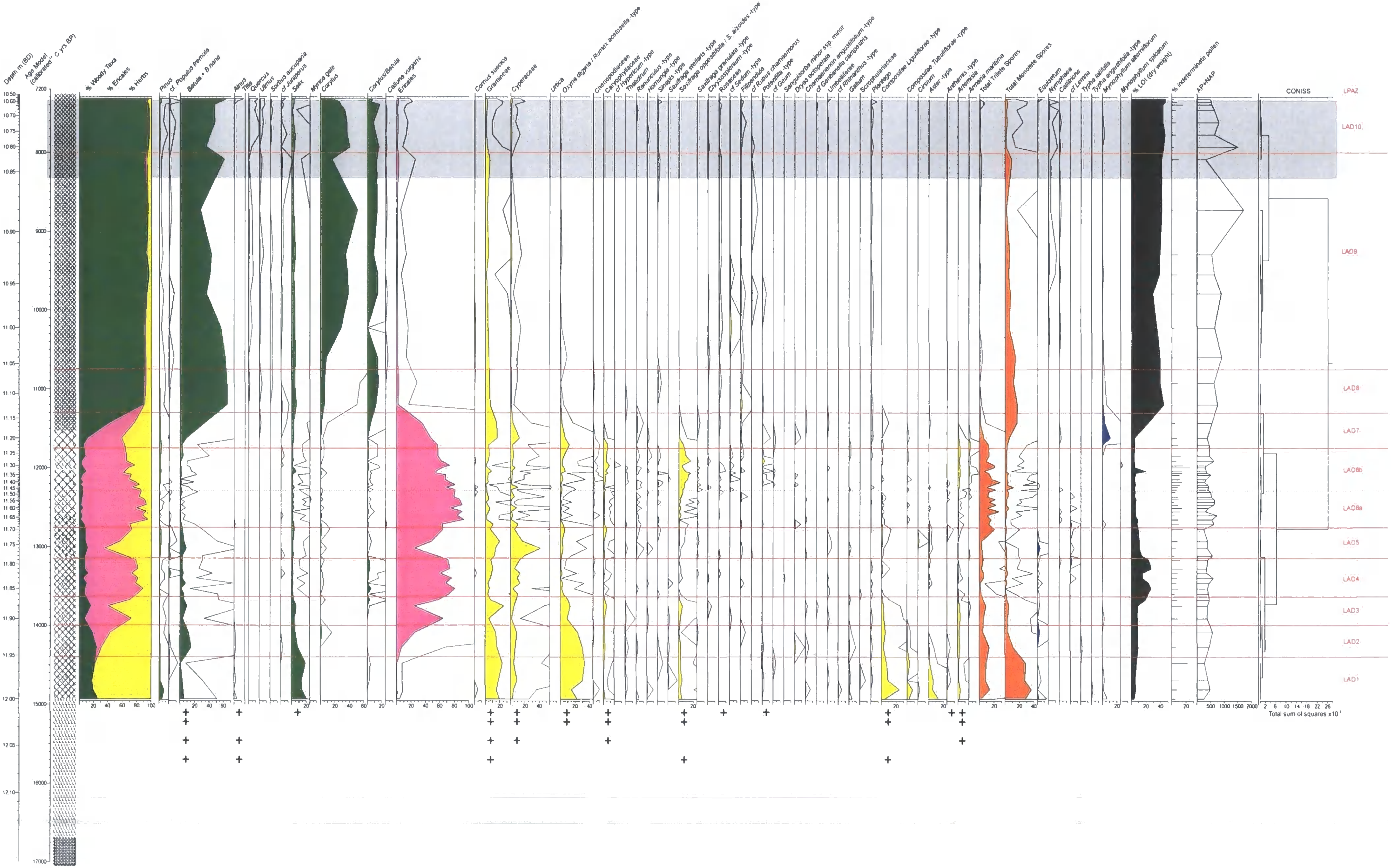

Depth m (BD)
Age Model (calibrated ¹⁴C yrs BP)
% Woody Taxa
% Ericales
% Herbs
Pinus
cf. Populus tremula
Betula + B. nana
Alnus
Tilia
Quercus
Ulmus
Sorbus aucuparia
cf Juniperus
Salix
Myrica gale
Corylus
Corylus/Betula
Calluna vulgaris
Ericales
Cornus suecica
Gramineae
Cyperaceae
Urtica
Oxyria digyna / Rumex acetosella -type
Chenopodiaceae
Caryophyllaceae
cf Hypericum -type
Thalictrum
Ranunculus -type
Hornungia -type
Sinapis -type
Saxifraga stellaris -type
Saxifraga oppositifolia / S. aizoides -type
Saxifraga granulata -type
Chrysosplenium -type
Rosaceae
cf Sedum -type
Filipendula
cf Rubus chamaemorus
Potentilla -type
cf Geum
Sanguisorba minor ssp. minor
Dryas octopetala
Chamaenerion angustifolium -type
cf Gentianella campestris
Umbelliferae
cf Rhinanthus -type
Galium
Scrophulariaceae
Plantago
Compositae Liguliflorae -type
Compositae Tubuliflorae -type
Cirsium
Aster -type
Anthemis -type
Artemisia
Armeria maritima
Total Trilete Spores
Total Monolete Spores
Equisetum
Nymphaea
Callitriche
cf Lemna
Typha latifolia
Typha angustifolia -type
Myriophyllum alterniflorum
Myriophyllum spicatum
% LOI (dry weight)
% indeterminate pollen
AP+NAP
CONISS
LPAZ
LAD10
LAD9
LAD8
LAD7
LAD6b
LAD6a
LAD5
LAD4
LAD3
LAD2
LAD1
Total sum of squares x10⁻³

Appendix IV

Nikkupierjav'ri: Relative abundance data are displayed for all the taxa with totals (undifferentiated) for the monolete and trilete Pteridophyte spores; taxa have been grouped into arboreal taxa and non-arboreal taxa, terrestrial Pteridophytes and obligate aquatics and plotted against age (cal yrs BP). Pollen sums are specified as follows for selected taxa: Terrestrial Pollen (ΣTP), i.e. Arboreal Pollen minus Pinus (AP) plus Non-Arboreal Pollen (NAP); Terrestrial Pollen and Terrestrial Pteridophyte Spores (ΣTP + ΣPS); Terrestrial Pollen and Aquatic Pollen (including Sphagnum) (ΣTP + ΣAP); Terrestrial Pollen and Indeterminable Pollen (ΣTP + ΣIP).

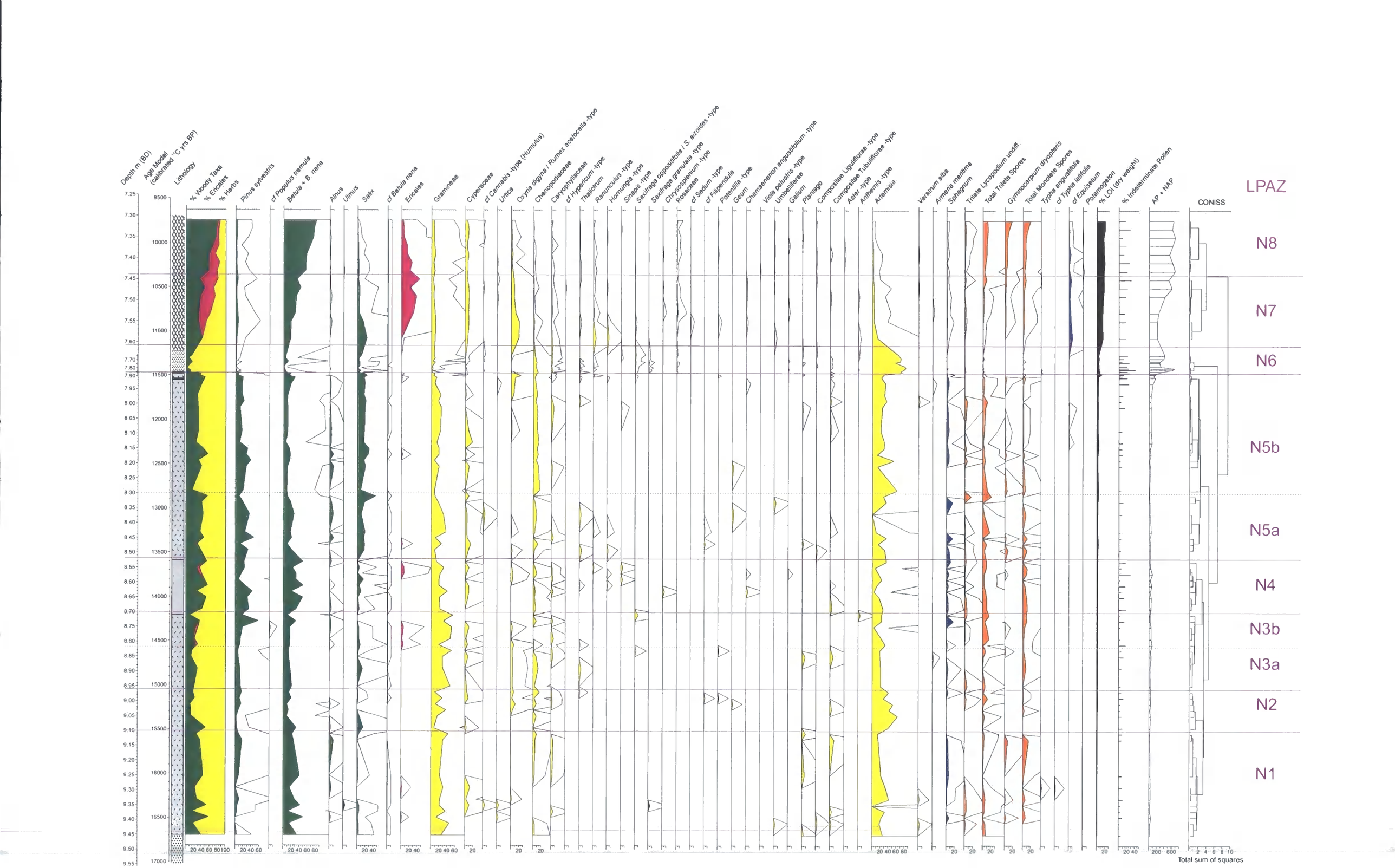
Depth m (BD)
Age Model (calibrated ¹⁴C yrs BP)
Lithology
% Woody Taxa
% Ericales
% Herbs
Pinus sylvestris
cf Populus tremula
Betula + B. nana
Alnus
Ulmus
Salix
cf Betula nana
Ericales
Gramineae
Cyperaceae
cf Cannabis -type (Humulus)
Urtica
Oxyria digyna / Rumex acetocella -type
Chenopodiaceae
Caryophyllaceae
cf Hypericum -type
Thalictrum
Ranunculus -type
Hornungia -type
Sinapis -type
Saxifraga oppositifolia / S. azoides -type
Saxifraga granulata -type
Chrysosplenium -type
Rosaceae
cf Sedum -type
cf Filipendula
Potentilla -type
Geum
Chamaenerion angustifolium -type
Viola palustris -type
Umbelliferae
Galium
Plantago
Compositae Liguliflorae -type
Compositae Tubuliflorae -type
Aster -type
Anthemis -type
Artemisia
Veratrum alba
Armeria maritima
Sphagnum
Trilete Lycopodium undiff.
Total Trilete Spores
Gymnocarpium dryopteris
Total Monolete Spores
Typha angustifolia
cf Typha latifolia
cf Equisetum
Potamogeton
% LOI (dry weight)
% Indeterminate Pollen
AP + NAP
CONISS
LPAZ
N8
N7
N6
N5b
N5a
N4
N3b
N3a
N2
N1
Total sum of squares

References

Aaby, B., and Berglund, B. E. (1986). Characterization of peat and lake deposits. *In* "Handbook of Holocene Palaeoecology and Palaeohydrology." (B. E. Berglund, Ed.), pp. 231-246. John Wiley & Sons, Chichester.

Allen, J. R. M., Watts, W. A., and Huntley, B. (2000). Weichselian palynostratigraphy, palaeovegetation and palaeoenvironment; the record from Lago Grande di Monticchio, southern Italy. *Quaternary International* **73/74,** 91-110.

Alley, R. B. (2003). Palaeoclimatic insights into future climate challenges. *Phil. Trans. R. Soc. Lond. A* **361,** 1831-1848.

Alley, R. B., Anandakrishnan, S., and Jung, P. (2001). Stochastic resonance in the North Atlantic. *Paleoceanography* **16,** 190-198.

Alley, R. B., Mayewski, P. A., Sowers, T., Stuiver, M., Taylor, K. C., and Clark, P. U. (1997). Holocene climatic instability: A prominent widespread event 8200 yr ago. *Geology* **25,** 483-486.

Alm, T. (1993). Øvre Æråsvatn - palynostratigraphy of a 22,000 to 10,000 BP lacustrine record on Andøya, northern Norway. *Boreas* **22,** 171-188.

Alm, T., and Birks, H. H. (1991). Late Weichselian flora and vegetation of Andøya, Northern Norway - macrofossil (seed and fruit) evidence from Nedre Æråsvatn. *Nord. J. Bot.* **11,** 465-475.

Ammann, B., and Lotter, A. F. (1989). Late-Glacial radiocarbon and palynostratigraphy on the Swiss Plateau. *Boreas* **18,** 109-126.

Andersen, B. G. (1979). The deglaciation of Norway 15,000 - 10,000 BP. *Boreas* **8,** 79-87.

Austin, W. E. N., and Kroon, D. (1996). Late glacial sedimentology, Foraminifera and stable isotope stratigraphy of the Hebridean Continental Shelf, northwest Scotland. *In* "Late Quaternary Palaeoceanography of the North Atlantic Margins." (J. T. Andrews, W. E. N. Austin, H. Bergsten, and A. E. Jennings, Eds.), pp. 187-213. Geological Society Special Publications. The Geological Society.

Austin, W. E. N., and Kroon, D. (2001). Deep sea ventilation of the northeastern Atlantic during the last 15,000 years. *Global and Planetary Change* **30,** 13-31.

Ballantyne, C. K., McCarroll, D., Nesje, A., Dahl, S. O., and Stone, J. O. (1998). The Last Ice Sheet in North-west Scotland: Reconstruction and Implications. *Quaternary Science Reviews* **17,** 1149-1184.

Bard, E., Arnold, M., Duprat, J., Moyes, J., and Duplessy, J.-C. (1987). Retreat velocity of the North Atlantic polar front during the last deglaciation determined by accelerator mass spectrometry. *Nature* **328,** 791-794.

Bard, E., Arnold, M., Fairbanks, R. G., and Hamelin, B. (1993). Th-230-U-234 and C-14 ages obtained by mass spectrometry on corals. *Radiocarbon*, 191-199.

Bard, E., Hamelin, B., Arnold, M., Montaggioni, L., Cabioch, G., Faure, G., and Rougerie, F. (1996). Deglacial sea-level record from Tahiti corals and the timing of global meltwater discharge. *Nature* **382,** 241-244.

Bartlein, P. J., Edwards, M. E., Shafer, S. L., and Barker, E. D. (1995). Calibration of radiocarbon ages and the interpretation of paleoenvironmental records. *Quaternary Research* **44,** 417-424.

Bartlein, P. J., Prentice, I. C., and Webb III, T. (1986). Climatic response surfaces from pollen data for some eastern North American taxa. *Journal of Biogeography* **13,** 35-57.

Baumann, K.-H., Lackschewitz, K. S., Mangerud, J., Spielhagen, F., Wolf-welling, T. C. W., Henrich, R., and Kassens, H. (1995). Reflection of Scandinavian Ice Sheet Fluctuations in Norwegian Sea Sediments during the Past 150,000 Years. *Quaternary Research* **43,** 185-197.

Berglund, B. E., Birks, H. J. B., Ralska-Jasiewiczowa, M., and Wright, H. E. (1996). Palaeoecological Events During The Last 15,000 Years, pp. 764. John Wiley & Sons Ltd., Chichester.

Berglund, B. E., and Ralska-Jasiewiczowa, M. (1986). Pollen analysis and pollen diagrams. *In* "Handbook of Holocene Palaeoecology and Palaeohydrology." (B. E. Berglund, Ed.), pp. 455-484. John Wiley & Sons, Chichester.

Birks, C. J. A., and Koc, N. (2002). A high-resolution diatom record of late-Quaternary sea-surface temperatures and oceanographic conditions from the eastern Norwegian Sea. *Boreas* **31,** 323-344.

Birks, H. H. (1984). Late-Quaternary pollen and plant macrofossil stratigraphy at Lochan an Druim, north-west Scotland. *In* "Lake Sediments and Environmental History." (E. Y. Haworth, and J. W. G. Lund, Eds.), pp. 377-405. University of Minnesota Press, Minneapolis.

Birks, H. H., Battarbee, R. W., and Birks, H. J. B. (2000a). The development of the aquatic ecosystem at Kråkenes Lake, wastern Norway, during the late-glacial and early-Holocene - a synthesis. *Journal of Paleolimnology* **23,** 91-114.

Birks, H. H., Battarbee, R. W., and Birks, H. J. B. (2000b). The development of the aquatic ecosystem at Krakenes Lake, western Norway, during the late glacial and early Holocene - a synthesis. *Journal of Paleolimnology* **23,** 91-114.

Birks, H. H., Gulliksen, S., Haflidason, H., and Mangerud, J. (1996). New Radiocarbon Dates for the Vedde Ash and the Saksunarvatn Ash from Western Norway. *Quaternary Research* **45,** 119-127.

Birks, H. H., and Mathewes, R. W. (1978). Studies in the vegetational history of Scotland V. Late Devensian and early Flandrian pollen and macrofossil stratigraphy at Abernethy Forest, Inverness-shire. *New Phytologist* **80,** 455-484.

Birks, H. H., Paus, A., Svendsen, J. I., Alm, T., Mangerud, J., and Landvik, J. Y. (1994). Late Weichselian environmental change in Norway, including Svalbard. *Journal of Quaternary Science* **9,** 133-145.

Birks, H. J. B. (1973). "Past and Present Vegetation of the Isle of Skye. A Palaeoecological Study." University Press, Cambridge.

Birks, H. J. B. (1986). Numerical zonation, comparison and correlation of Quaternary pollen-stratigraphical data. *In* "Handbook od Holocene Palaeoecology and Palaeohydrology." (B. E. Berglund, Ed.), pp. 743-774. John Wiley & Sons, Chichester.

Birks, H. J. B., and Birks, H. H. (1980). "Quaternary Palaeoecology." Edward Arnold (Publishers) Limited, London.

Birks, H. J. B., and West, R. G. (1973). Quaternary Plant Ecology, pp. 326. Blackwell Science Publications, Oxford.

Birks, H. J. B., and Williams, W. (1983). Late-Quaternary vegetational history of the Inner Hebrides. *Proceedings of the Royal Society of Edinburgh* **838,** 269-292.

Birnie, J. F. (2000). Devensian lateglacial palaeoecological changes in Shetland. *Boreas* **29,** 205-218.

Björck, S., Rundgren, M., Ongólfsson, O., and Funder, S. (1997). The Preboreal oscillation around the Nordic Seas: terrestrial and lacustrine responses. *Journal of Quaternary Science* **12,** 455-465.

Björck, S., Walker, J. C., Cwynar, L. C., Johnsen, S., Knudsen, K., Lowe, J. J., Wohlfarth, B., and INTIMATE Members. (1998). An event stratigraphy for the Last Termination in the North Atlantic region based on the Greenland Ice-core record: a proposal by the INTIMATE group. *Journal of Quaternary Science* **13,** 283-292.

Boessenkool, K. P., Brinkhuis, H., Schonfeld, J., and Targarona, J. (2001). North Atlantic sea-surface temperature changes and the climate of western Iberia during the last deglaciation; a marine palynological approach. *Global and Planetary Change* **30,** 33-39.

Bond, G., Broecker, W., Johnsen, S., McManus, J., Labeyrie, L., Jouzel, J., and Bonani, G. (1993). Correlations between climate records from North Atlantic sediments and Greenland ice. *Nature* **365,** 143-147.

Bond, G., Heinrich, H., Broecker, W., Labeyrie, L., McManus, J., Andrews, J., Huon, S., Jantschik, R., Clasen, S., Simet, C., Tedesco, K., Klas, M., Bonani, G., and Ivy,

S. (1992). Evidence for massive discharges in icebergs into the North Atlantic ocean during the last glacial period. *Nature* **360,** 245-249.

Bond, G. C., and Lotti, R. (1995). Iceberg Discharges into the North Atlantic on Millennial Time Scales During the Last Glaciation. *Science* **267,** 1005-1010.

Bowen, D. Q., Phillips, F. M., McCabe, A. M., Knutz, P. C., and Sykes, G. A. (2002). New data for the Last Glacial Maximum in Great Britain and Ireland. *Quaternary Science Reviews* **21,** 89-101.

Boygle, J. (1999). Variability of tephra in lake and catchment sediments, Svínavatn, Iceland. *Global and Planetary Change* **21,** 129-149.

Bradley, R. S. (1999). "Paleoclimatology - Reconstructing Climates of the Quaternary." Academic Press Limited, London.

Brasier, M. D. (1980). "Microfossils." George Allen & Unwin, London.

Broecker, W. S. (1992). The strength of the Nordic heat pump. *In* "The Last Deglaciation: Absolute and Relative Chronologies." (E. Bard, and W. S. Broecker, Eds.), pp. 173-181. NATO ASI. Springer-Verlag, Berlin.

Broecker, W. S., Andree, M., Wolfli, W., Oeschger, H., Bonani, G., Kennett, J. P., and Peteet, D. M. (1988). The chronology of the last glaciation: Implications to the cause of the Younger Dryas event. *Paleoceanography* **3,** 1-19.

Broecker, W. S., and Denton, G. H. (1990). The role of ocean-atmosphere reorganisations in glacial cycles. *Quaternary Science Reviews* **9,** 305-341.

Chapman, M. R., Shackleton, N. J., and Duplessy, J.-C. (2000). Sea surface temperature variability during the last glacial-interglacial cycle: assessing the magnitude and pattern of climate change in the North Atlantic. *Palaeogeography, Palaeoclimatology, Palaeoecology* **157,** 1-25.

Clark, P. U., and Mix, A. C. (2002). Ice sheets and sea level of the Last Glacial Maximum. *Quaternary Science Reviews* **21,** 1-7.

Corner, G. D., Kolka, V. V., Yevzerov, V. Y., and Møller, J. J. (2001). Postglacial relative sea-level change and stratigraphy of raised coastal basins on Kola Peninsula, northwest Russia. *Global and Planetary Change* **31,** 155-177.

Corner, G. D., Yevzerov, V. Y., Kolka, V. V., and Moller, J. (1999). Isolation basin stratigraphy and Holocene relative sea-level change at the Norwegian-Russian border north of Nikel, northwest Russia. *Boreas* **28,** 146-166.

Daniell, J., Hunt, J., and Chambers, F. (2000). Tephrostratigraphy of An Loch Mór: second report. Centre for Environmental Change and Quaternary Research, Geography and Environmental Management Research Unit (GEMRU), C&GCHE Cheltenham, Cheltenham.

Dansgaard, W., Johnsen, S. J., Clausen, H. B., Dahl-Jensen, D., Gundestrup, N. S., Hammer, C. U., Hvidberg, C. S., Steffensen, J. P., Sveinbjörnsdottir, Jouzel, J.,

and Bond, G. (1993). Evidence for general instability of past climate from a 250-kyr ice-core record. *Nature* **364,** 218-220.

Davies, S. M., Branch, N. P., Lowe, J. J., and Turney, C. S. M. (2002). Towards a European tephrochronological framework for Termination 1 and the Early Holocene. *Phil. Trans. R. Soc. Lond. A* **360,** 767-802.

Davies, S. M., Turney, C. S. M., and Lowe, J. J. (2001). Identification and significance of a visible, basalt-rich Vedde Ash layer in a Late-glacial sequence on the Isle of Skye, Inner Hebrides, Scotland. *Journal of Quaternary Science* **16,** 99-104.

Davies, S. M., Wohlfarth, B., Wastegard, S., Andersson, M., Blockley, S., and Possnert, G. (2004). Were there two Borrobol Tephras during the early Lateglacial period: implications for tephrochronology? *Quaternary Science Reviews* **23,** 581-589.

Davis, R. B., and Webb III, T. (1975). The Contemporary Distribution of Pollen in Eastern North America: A Comparison with the vegetation. *Quaternary Research* **5,** 395-434.

Dawson, S., and Smith, D. E. (1997). Holocene relative sea-level changes on the margin of a glacio-isostatically uplifted area: an example from Caithness, Scotland. *The Holocene* **7,** 59-77.

Dean Jr, W. E. (1974). Determination of carbonate and organic matter in calcareous sediments and sedimentary rocks by loss on ignition: Comparison with other methods. *Journal of Sedimentary Petrology* **44,** 242-248.

Denton, G. H., and Hughes, T. J. (1981). The Last Great Ice Sheets. Wiley, New York.

Dickinson, C. I. (1963). "British Seaweeds." Eyre & Spottiswoode, London.

Dugmore, A. J., Larsen, G., and Newton, A. J. (1995). Seven tephra isochrones in Scotland. *The Holocene* **5,** 257-266.

Duigan, C. A., and Birks, H. H. (2000). The late-glacial and early-Holocene palaeoecology of cladoceran microfossil assemblages at Krakenes, western Norway, with a quantitative reconstruction of temperature changes. *Journal of Paleolimnology* **23,** 67-76.

Duplessy, J.-C., Ivanova, E., Murdmaa, I., Paterne, M., and Labeyrie, L. (2001). Holocene palaeoceanography of the northern Barents Sea and variations of the northward heat transport by the Atlantic Ocean. *Boreas* **30,** 2-16.

Eiriksson, J., Knudsen, K. L., Haflidason, H., and Henriksen, P. (2000). Late-glacial and Holocene palaeoceanography of the North Icelandic shelf. *Journal of Quaternary Science* **15,** 23-42.

Eiriksson, J., Larsen, G., Knudsen, K. L., Heinemeier, J., and Simonarson, L. A. (2004). Marine reservoir age variability and water mass distribution in the Iceland Sea. *Quaternary Science Reviews* **23,** 2247-2268.

Elliot, M., Labeyrie, L., and Duplessy, J.-C. (2002). Changes in North Atlantic deep-water formation associated with the Dansgaard-Oeschger temperature oscillations (60-10ka). *Quaternary Science Reviews* **21,** 1153-1165.

Erdtman, G. (1923). Studies in the Micropalaeontology of Postglacial Deposits in Northern Scotland and the Scotch Isles, with especial reference to the history of the woodlands.

Fairbanks, G. (1989). A 17,000 year glacio-eustatic lea level record: influence of glacial melting rates on the Younger Dryas event and deep-ocean circulation. *Nature* **342,** 637-?

Fitter, R., and Manuel, R. (1994). "Lakes, Rivers, Streams and Ponds of Britain and North-west Europe." HarperCollins, Hong Kong.

Fossitt, J. A. (1996). Late Quaternary vegetation history of the Western Isles of Scotland. *New Phytologist* **132,** 171-196.

Fredskild, B. (1985). Holocene pollen records from west Greenland. *In* "Quaternary Environments. Eastern Canadian Arctic, Baffin Island and Western Greenland." (J. T. Andrews, Ed.), pp. 643-681. Allen & Unwin.

Frey, D. G. (1982). Contrasting Strategies of Gamogenesis in Northern and Southern-Populations of Cladocera. *Ecology* **63,** 223-241.

Ganopolski, A., and Rahmstorf, S. (2001). Rapid changes of glacial climate simulated in a coupled climate model. *Nature* **409,** 153-158.

Griffiths, H. I. (2001). Ostracod evolution and extinction - its biostratigraphic value in the European Quaternary. *Quaternary Science Reviews* **20,** 1743-1751.

Grimm, E. C. (1987). CONISS: A fortran 77 program for stratigraphically constrained cluster analysis by the method of incremental sum of squares. *Computers & Geosciences* **13,** 13-35.

Grimm, E. C. (1997). Tilia version 2.0 b5. Illinois State Museum, Springfield.

Grootes, P. M., Stuiver, M., White, J. W. C., Johnsen, S., and Jouzel, J. (1993). Comparison of oxygen isotope records from the GISP2 and GRIP Greenland ice cores. *Nature* **366,** 552-554.

Gulliksen, S., Birks, H. H., Possnert, G., and Mangerud, J. (1998). A calendar age estimate of the younger Dryas-Holocene boundary at Kråkenes, western Norway. *The Holocene* **8,** 249-259.

Haflidason, H., Eiriksson, J., and Van Kreveld, S. (2000). The tephrochronology of Iceland and the North Atlantic region during the Middle and Late Quaternary: a review. *Journal of Quaternary Science* **15,** 3-22.

Haflidason, H., Sejrup, H. P., Kristensen, D. K., and Johnsen, S. (1995). Coupled response of the late glacial climatic shifts of northwest Europe reflected in

Greenland ice cores: Evidence from the northern North Sea. *Geology* **23,** 1059-1062.

Heinrich, H. (1988). Origin and Consequences of Cyclic Ice Rafting in the Northeast Atlantic Ocean during the Past 130,000 Years. *Quaternary Research* **29,** 142-152.

Hicks, S. (2001). The use of annual arboreal pollen deposition values for delimiting tree-lines in the landscape and exploring models of pollen dispersal. *Review of Palaeobotany and Palynology* **117,** 1-29.

Houghton, J. T., Ding, Y., Griggs, D. J., Noguer, N., van der Linden, P. J., Dai, X., Maskell, K., and Johnson, C. A. (2001). IPCC, 2001: Climate Change 2001: The Scientific Basis. Contribution of Working Group 1 to the Third Assessment Report of the Intergovernmental Panel on Climate Change, pp. 881. Cambridge University Press, Cambridge, United Kingdom and New York, NY, USA.

Hubbard, A. (1999). High-resolution modeling of the advance of the younger dryas ice sheet and its climate in Scotland. *Quaternary Research* **52,** 27-43.

Hughen, K. A., Overpeck, J. T., Peterson, L. C., and Trumbore, S. (1996). Rapid climate changes in the tropical Atlantic region during the last deglaciation. *Nature* **380,** 51-54.

Hughen, K. A., Southon, J. R., Lehman, S. J., and Overpeck, J. T. (2000). Synchronous Radiocarbon and Climate Shifts During the Last Deglaciation. *Science* **290,** 1951-1954.

Huntley, B. (1990a). Dissimilarity Mapping between Fossil and Contemporary Pollen Spectra in Europe for the Past 13,000 Years. *Quaternary Research* **33,** 360-367.

Huntley, B. (1990b). European vegetation history: palaeovetation maps from pollen data 13,000 BP to present. *Journal of Quaternary Science* **5,** 103-122.

Huntley, B. (1993). The use of climate response surfaces to reconstruct palaeoclimate from Quaternary pollen and plant macrofossil data. *Phil. Trans. R. Soc. Lond. B* **341,** 215-224.

Huntley, B. (1994). Late-Devensian and Holocene palaeoecology and palaeoenvironments of the Morrone Birkwoods, Aberdeenshire, Scotland. *Journal of Quaternary Science* **9,** 311-336.

Huntley, B. (2001). Reconstructing Past Environments from the Quaternary Palaeovegetation Record. *Biology and Environment: Proceedings of the Royal Irish Academy* **101B,** 3-18.

Huntley, B., and Birks, H. J. B. (1983). "An Atlas of Past and Present Pollen Maps for Europe, 0 - 13,000 Years Ago." Cambridge University Press, Cambridge.

Huntley, B., and Prentice, I. C. (1993). Holocene vegetation and Climates of Europe. *In* "Global Climates Since the Last Glacial Maximum." (H. E. J. Wright, J. E. Kutzbach, T. Webb III, W. F. Ruddiman, F. A. Street-Perrott, and P. J. Bartlein, Eds.), pp. 136-168. University of Minnesota Press, London.

Hyvarinen, H. (1975). Absolute and relative pollen diagrams from northernmost Fennoscandia. *Fennia* **142,** 5-23.

Hyvarinen, H. (1976). Flandrian pollen deposition rates and tree-line history in northern Fennoscandia. *Boreas* **5,** 163-175.

Imbrie, J., Hays, J. D., Martinson, D. G., McIntyre, A., Mix, A. G., Morley, J. J., Pisias, N. G., Prell, W. L., and Shackleton, N. J. (1984). The orbital theory of Pleistocene climate: support from a revised chronology of the marine $\delta^{18}0$ record. *In* "Milankovitch and Climate." (A. L. Berger, J. Imbrie, J. Hays, G. Kukla, and B. Saltzman, Eds.), pp. 269-305. Reidel Publishing Company, Dordrecht.

Isarin, R. F. B., and Bohncke, S. J. P. (1999). Mean July temperatures during the Younger Dryas in northwestern and central Europe as inferred from climate indicator plant species. *Quaternary Research* **51,** 158-173.

Jacobsen, G. L., and Bradshaw, R. H. W. (1981). The selection of sites for paleovegetational studies. *Quaternary Research* **16,** 80-96.

Jakobsson, S. P. (1979). Petrology of recent basalts of the Eastern Volcanic Zone, Iceland. *Acta Naturalia Islandica* **26,** 1-103.

Janssen, C. R. (1976-7). On the reconstruction of past vegetation by pollen analysis: A review. *In* "IV Int. Palynol. Conf." pp. 163-172, Lucknow.

Jensen, C., Kuiper, J. G. J., and Vorren, K. D. (2002). First post-glacial establishment of forest trees: early Holocene vegetation, mollusc settlement and climate dynamics in central Troms, North Norway. *Boreas* **31,** 285-301.

Johnsen, S. J., Clausen, H. B., Dansgaard, W., Fuhrer, K., Gundestrup, N., Hammer, C. U., Iverson, J., Jouzel, J., Stauffer, B., and Stefferson, J. P. (1992). Irregular glacial interstadials recorded in a new Greenland ice core. *Nature* **359,** 311-313.

Johnsen, S. J., Clausen, H. B., Dansgaard, W., Gundestrup, N. S., Hammer, C. U., Andersen, U., Andersen, K. K., Hvidberg, C. S., Dahl-Jensen, D., Steffensen, J. P., Shoji, H., Sveinbjörnsdóttir, A. E., White, J. W. C., Jouzel, J., and D., F. (1997). The d18O record along the Greenland Ice Core Project deep ice core and the problem of possible Eemian climatic instability. *Journal of Geophysical Research* **102,** 26397-26410.

Johnsen, S. J., Dahl-Jensen, D., Gundestrup, N., Steffensen, J. P., Clausen, H. B., Miller, H., Masson-Delmotte, V., Sveinbjörnsdottir, A. E., and White, J. (2001).

Oxygen isotope and palaeotemperature records from six Greenland ice-core stations: Camp Century, Dye-3, GRIP, GISP2, Renland and NorthGRIP. *Journal of Quaternary Science* **16,** 299-307.

Jouzel, J., Alley, R. B., Cuffey, K. M., Dansgaard, W., Grootes, P., Hoffmann, G., Johnsen, S. J., Koster, R. D., Peel, D., Shuman, C. A., Stievenard, M., Stuiver, M., and White, J. (1997). Validity of the temperature reconstruction from water isotopes in ice cores. *Journal of Geophysical Research - Oceans* **102,** 26,471-26,487.

Kaland, P. E., Krzywinski, K., and Stabell, B. (1984). Radiocarbon dating of transitions between marine and lacustrine sediments and their relation to the development of lakes. *Boreas* **13,** 243-258.

Keigwin, L. D., Jones, G. A., and Lehman, S. J. (1991). Deglacial meltwater discharge, North Atlantic deep circulation, and abrupt climate change. *Journal of Geophysical Research* **96,** 16811-16826.

Kitagawa, H., and van der Plicht, J. (2000). Atmospheric radiocarbon calibration beyond 11,900 cal BP from Lake Suigetsu laminated sediments. *Radiocarbon* **42,** 369-380.

Kjemperud, A. (1986). Late Weichselian and Holocene Shoreline Displacement in the Trondheimsfjord Area, Central Norway. *Boreas* **15,** 61-82.

Kleman, J., Hattestrand, C., Borgstrom, I., and Stroeven, A. (1997). Fennoscandian palaeoglaciology reconstructed using a glacial geological inversion model. *Journal of Glaciology* **43,** 283-299.

Koç, N., Jansen, E., and Haflidason, H. (1992). A high-resolution diatom record of the last deglaciation from the SE Norwegian Sea: Documentation of rapid climate changes. *Paleoceanography* **5,** 557-580.

Koç, N., Jansen, E., and Haflidason, H. (1993). Paleoceanographic Reconstructions of Surface Ocean Conditions in the Greenland, Iceland and Norwegian Seas through the Last 14-Ka Based on Diatoms. *Quaternary Science Reviews* **12,** 115-140.

Kristiansen, I. J., Mangerud, J., and Lømo, L. (1988). Late Weichselian/early Holocene pollen and lithostratigraphy in lakes in the Alesund area, western Norway. *Review of Palaeobotany and Palynology* **53,** 185-231.

Kroon, D., Austin, W. E. N., Chapman, M. R., and Ganssen, G. M. (1997). Deglacial surface circulation in the northeastern Atlantic: Temperature and salinity records off NW Scotland on a century scale. *Paleoceanography* **12,** 755-763.

Laberg, J. S., and Vorren, T. O. (1995). Late Weichselian Submarine Debris Flow Deposits on the Bear- Island-Trough-Mouth-Fan. *Marine Geology* **127,** 45-72.

Landvik, J. Y., Bondevik, S., Elverhoi, A., Fjeldskaar, W., Mangerud, J., Salvigsen, O., Siegert, M. J., Svendsen, J. I., and Vorren, T. O. (1998). The last glacial maximum of Svalbard and the Barents Sea area: Ice sheet extent and configuration. *Quaternary Science Reviews* **17,** 43-75.

Laskar, J., Robutel, P., Joutel, F., Gastineau, M., Correia, A. C. M., and Levrard, B. (2004). A long-term numerical solution for the insolation quantities of the Earth. *Astronomy & Astrophysics* **428,** 261-285.

Le Maitre, R. W. (1989). A Classification of Igneous Rocks and Glossary of Terms. Basil Blackwell, Oxford.

Leemans, R., and Cramer, W. (1991). The IIASA climate database for mean monthly values of temperature, precipitation and cloudiness on a terrestrial grid. RR-91-18, IIASA, Laxenburg.

Lehman, S. J., and Keigwin, L. D. (1992). Sudden changes in North Atlantic circulation during the last deglaciation. *Nature* **356,** 757-762.

Lohne, O. S., Bondevik, S., Mangerud, J., and Schrader, H. (2004). Calendar year age estimates of Allerod-Younger Dryas sea-level oscillations at Os, western Norway. *Journal of Quaternary Science* **19,** 443-464.

Long, A. J., Roberts, D. H., and Wright, M. R. (1999). Isolation basin stratigraphy and Holocene relative sea-level change on Arveprinsen Ejland, Disko Bugt, West Greenland. *Journal of Quaternary Science* **14,** 323-345.

Lowe, J. J., Ammann, B., Birks, H. H., Björck, S., Coope, G. R., Cwynar, L., De Beaulieu, J.-L., Mott, R. J., Peteet, D. M., and Walker, M. J. C. (1994). Climatic changes in areas adjacent to the North Atlantic during the last glacial-interglacial transition (14 - 9 ka BP): a contribution to IGCP-253. *Journal of Quaternary Science* **9,** 185-198.

Lowe, J. J., Birks, H. H., Brooks, S. J., Coope, G. R., Harkness, D. D., Mayle, F. E., Sheldrick, C., Turney, C. S. M., and Walker, M. J. C. (1999). The chronology of palaeoenvironmental changes during the last Glacial-Holocene transition: towards an event stratigraphy for the British Isles. *Journal of the Geological Society, London* **156,** 397-410.

Lowe, J. J., and Hoek, W. Z. (2001). Inter-regional correlation of palaeoclimatic records for the Last Glacial-Interglacial Transition: a protocol for improved precision recommended by the INTIMATE project group. *Quaternary Science Reviews* **20,** 1175-1187.

Lowe, J. J., and Turney, C. S. M. (1997). Vedde ash layer discovered in a small lake basin on the Scottish mainland. *Journal of the Geological Society, London* **154,** 605-612.

Lowe, J. J., and Walker, M. C. J. (1997). "Reconstructing Quaternary Environments." Prentice Hall, Harlow, England.

Lowe, J. J., and Walker, M. J. C. (1986). Lateglacial and early Flandrian environmental history of the Isle of Mull, Inner Hebrides, Scotland. *Transactions of the Royal Society of Edinburgh* **77,** 1-20.

Lowe, J. J., and Walker, M. J. C. (2000). Radiocarbon dating of the last glacial - interglacial transition (ca 14-9 14C ka BP) in terrestrial and marine records: The need for new quality assurance protocols. *Radiocarbon* **42,** 53-68.

Mackie, E. A. V., Davies, S. M., Turney, C. S. M., Dobbyn, K., Lowe, J. J., and Hill, P. G. (2002). The use of magnetic separation techniques to detect basaltic microtephra in last glacial-interglacial transition (LGIT; 15-10 ka cal. BP) ssediment sequences in Scotland. *Scottish Journal of Geology* **38,** 21-30.

Mangerud, J. (1991). The Last Interglacial / Glacial Cycle in Northern Europe. *In* "Quaternary Landscapes." (L. C. K. Shane, and E. J. Cushing, Eds.). Belhaven Press, London.

Mangerud, J., Anderson, S. T., Berglund, B. E., and Donner, J. J. (1974). Quaternary stratigraphy of Norden, a proposal for terminology and classification. *Boreas* **3,** 109-127.

Mangerud, J., Furnes, H., and Jóhansen, J. (1986). A 9000 year old ash bed on the Faroe Islands. *Quaternary Research* **26,** 262-265.

Mangerud, J., Jansen, E., and Landvik, J. Y. (1996). Late Cenozoic history of the Scandinavian and Barents Sea ice sheets. *Global and Planetary Change* **12,** 11-26.

Mangerud, J., Lie, S. E., Furnes, H., Kristiansen, I. L., and Lomo, L. (1984). A youger Dryas ash bed in western Norway, and its possible correlations with tephra in cores from the Norwegian Sea and the North Atlantic. *Quaternary Research* **21,** 85-104.

Mann, M. E., Bradley, R. S., and Hughes, M. K. (1998). Global-scale temperature patterns and climate forcing over the past six centuries. *Nature* **392,** 779-787.

Martinson, D. G., Pisias, N. G., Hays, J. D., Imbrie, J., Moore, T. C. J., and Shackleton, N. J. (1987). Age Dating and the Orbital Theory of the Ice Ages: Development of a High-Resolution 0 to 300,000-Year Chronostratigraphy. *Quaternary Research* **27,** 1-29.

McCabe, M., Knight, J., and McCarron, S. (1998). Evidence for Heinrich event 1 in the British Isles. *Journal of Quaternary Science* **13,** 549-568.

McVean, D. N., and Ratcliffe, D. A. (1962). "Plant Communities of the Scottish Highlands." HMSO, London.

Moore, J. A. (1986). "Charophytes of Great Britain and Ireland." Botanical Society of the British Isles, London.

Moore, P. D., Webb, J. A., and Collinson, M. E. (1991). "Pollen Analysis." Blackwell Science Ltd, Oxford.

North Greenland Ice Core Project members. (2004). High-resolution record of Northern Hemisphere climate extending into the last interglacial period. *Nature* **431,** 147-151.

Oskarsson, N., Steinthorsson, S., and Sigvaldason, G. (1985). Iceland geochemical anomaly: origin, volcanotectonic, chemical fractionation and isotope evolution of the crust. *Journal of Geophysical Research* **90,** 10011-10025.

Overpeck, J. T., Webb III, T., and Prentice, I. C. (1985). Quantitative interpretation of fossil pollen spectra: dissimilarity coefficients and the method of modern analogs. *Quaternary Research* **23,** 87-108.

Patience, A. J., and Kroon, D. (1991). Oxygen Isotope Chronostratigraphy. *In* "Quaternary Dating Methods - A User's Guide." (P. L. Smart, and P. D. Frances, Eds.), pp. 199-228. Quaternary Research Association, Cambridge.

Paus, A. (1988). Late Weichselian Vegetation, Climate, and Floral Migration at Sandvikvatn, North Rogaland, Southwestern Norway. *Boreas* **17,** 113-139.

Paus, A. (1989a). Late Weichselian Vegetation, Climate and Floral Migration at Eigebakken, South Rogaland, Southwestern Norway. *Review of Palaeobotany and Palynology* **61,** 177-203.

Paus, A. (1989b). Late Weichselian Vegetation, Climate, and Floral Migration at Liastemmen, North-Rogaland, South-Western Norway. *Journal of Quaternary Science* **4,** 223-242.

Paus, A. (1990). Late Weichselian and Early Holocene Vegetation, Climate, and Floral Migration at Utsira, North-Rogaland, Southwestern Norway. *Norsk Geologisk Tidsskrift* **70,** 135-152.

Paus, A., Svendsen, J. I., and Matiouchkov, A. (2003). Late Weichselian (Valdaian) and Holocene vegetation and environmental history of the northern Timan Ridge, European Arctic Russia. *Quaternary Science Reviews* **22,** 2285-2302.

Pennington, W. (1973). Absolute pollen frequencies in the sediment of lakes of different morphometry. *In* "Quaternary Plant Ecology." (H. J. B. Birks, and R. G. West, Eds.), pp. v-326. blackwell Scientific Publications, Oxford.

Pennington, W. (1977a). Lake Sediments and the Lateglacial Environment in Northern Scotland. *In* "Studies in the Scottish Lateglacial Environment." (J. M. Gray, and J. J. Lowe, Eds.), pp. 119-142. Pergamon Press, Oxford.

Pennington, W. (1977b). The Late Devensian flora and vegetation of Britain. *Philosophical Transactions of the Royal Society of London B* **280,** 247-271.

Pilcher, J. R. (1991). Radiocarbon Dating for the Quaternary Scientist. *Quaternary Proceedings* **1,** 27-33.

Pollard, A. M., Blockley, S. P. E., and Ward, K. R. (2003). Chemical alteration of tephra in the depositional environment: theoretical stability modelling. *Journal of Quaternary Science* **18,** 385-394.

Prentice, C., Bartlein, P. J., and Webb III, T. (1991). Vegetation and climate change in eastern North America since the last glacial maximum. *Ecology* **72,** 2038-2056.

Prentice, H. C. (1981). A Late Weichselian and early Flandrian pollen diagram from Østervatnet, Varanger peninsula, NE Norway. *Boreas* **10,** 53-70.

Prentice, I. C. (1988). Records of vegetation in time and space: the principles of pollen analysis. *In* "Vegetation History." (B. Huntley, and T. I. Webb, Eds.), pp. 17-42. Handbook of vegetation science. Kluwer Academic Publishers, London.

Prentice, I. C., Cramer, W., Harrison, S. P., Leemans, R., Monserud, R. A., and Solomon, A. M. (1992). A global biome model based on plant physiology and dominance, soil properties and climate. *Journal of Biogeography* **19,** 117-134.

Prentice, I. C., Guiot, J., Huntley, B., Jolly, D., and Cheddadi, R. (1996). Reconstructing biomes from palaeoecological data: a general method and its application to European pollen data at 0 and 6 ka. *Climate Dynamics* **12,** 185-194.

Prentice, I. C., and Webb III, T. (1986). Pollen percentages, tree abundances and the Fagerlind effect. *Journal of Quaternary Science* **1,** 35-43.

Ranner, P. H. (2005). "Lateglacial and early Holocene environmental changes along the northwest European Continental margin." University of Durham.

Ranner, P. H., Allen, J. R. M., and Huntley, B. (2005). A new early Holocene cryptotephra from northwest Scotland. *Journal of Quaternary Science* **20,** 201-208.

Reille, M. (1992). "Pollen et spores D'Europe et D'Afrique Du Nord." Laboratoire De Botanique Historique et Palynologie, Marseille.

Reimer, P. J., and Reimer, R. W. (2001). A marine reservoir correction database and on-line interface. *Radiocarbon* **43,** 461-463.

Renssen, H., and Isarin, R. F. B. (2001a). Rapid climatic warming at the end of the last glacial: new perspectives. *Global and Planetary Change* **30,** 155-165.

Renssen, H., and Isarin, R. F. B. (2001b). The two major warming phases of the last deglaciation similar to 14.7 and similar to 11.5 ka cal BP in Europe: climate reconstructions and AGCM experiments. *Global and Planetary Change* **30,** 117-153.

Roberts, J. L. (2003). "The Highland Geology Trail." Luath Press Ltd., Edinburgh.

Rose, H. L., Golding, P. N. E., and Battarbee, R. W. (1996). Selective concentration and enumeration of tephra shards from lake sediment cores. *The Holocene* **6,** 243-246.

Rosenberg, S. A., Walker, I. R., Mathewes, R. W., and Hallett, D. J. (2004). Midge-inferred Holocene climate history of two subalpine lakes in southern British Columbia, Canada. *Holocene* **14,** 258-271.

Ruddiman, W. F., and McIntyre, A. (1981). The North Atlantic Ocean During the Last Deglaciation. *Palaeogeography, Palaeoclimatology, Palaeoecology* **35,** 145-214.

Ruddiman, W. F., Raymo, M. E., Martinson, D. G., Clement, B. M., and Backman, J. (1989). Pleistocene evolution:Northern hemisphere ice sheets and North Atlantic Ocean. *Paleoceanography* **4,** 353-412.

Ruddiman, W. F., Sancetta, C. D., and McIntyre, A. (1977). Glacial/Interglacial response rate of subpolar North Atlantic waters to climatic change: the record in oceanic sediments. *Phil. Trans. R. Soc. Lond. B* **280,** 119-142.

Saarnisto, M. (1986). Annually Laminated lake Sediments. *In* "Handbook of Holocene Palaeoecology and Palaeohydrology." (B. E. Berglund, Ed.), pp. 343-370. John Wiley & Sons, Chichester.

Sarmaja-Korjonen, K. (2003). Chydorid ephippia as indicators of environmental change - biostratigraphical evidence from two lakes in southern Finland. *Holocene* **13,** 691-700.

Sarnthein, M., Kennett, J. P., Allen, J. R. M., Beer, J., Grootes, P., Laj, C., McManus, J., Ramesh, R., and 117, S.-I. W. G. (2002). Decadal-to-millennial-scale climate variability chronology and mechanisms: summary and recommendations. *Quaternary Science Reviews* **21,** 1121-1128.

Sarnthein, M., Winn, K., Jung, J. A., Duplessy, J., Labeyrie, L., Erlenkeuser, H., and Gassen, G. (1994). Changes in east Atlantic deepwater circulation over the last 30,000 years: Eight time slice reconstructions. *Paleoceanography* **9,** 209-267.

Shennan, I. (1999). Global meltwater discharge and the deglacial sea-level record from northwest Scotland. *Journal of Quaternary Science* **14,** 715-719.

Shennan, I., Green, F., Innes, J., Lloyd, J., Rutherford, M., and Walker, K. (1996). Evaluation of rapid relative sea-level changes in north-west Scotland during the last glacial-interglacial transition: Evidence from Ardtoe and other isolation basins. *Journal of Coastal Research* **12,** 862-874.

Shennan, I., Innes, J., Long, A. J., and Zong, Y. Q. (1995). Late Devensian and Holocene relative sea-level changes in northwestern Scotland - new data to test existing models. *Quaternary International* **26,** 97-123.

Shennan, I., Lambeck, K., Horton, B., Innes, J., Lloyd, J., McArthur, J., Purcell, T., and Rutherford, M. (2000). Late Devensian and Holocene records of relative sea-level changes in northwest Scotland and their implications for glacio-hydro-isostatic modelling. *Quaternary Science Reviews* **19,** 1103-1135.

Snowball, I., Zillen, L., and Gaillard, M. J. (2002). Rapid early-Holocene environmental changes in northern Sweden based on studies of two varved lake-sediment sequences. *Holocene* **12,** 7-16.

Snyder, J. A., Forman, S. L., Mode, W. N., and Tarasov, G. A. (1997). Postglacial relative sea-level history: sediment and diatom records of emerged coastal lakes. north-central Kola Peninsula, Russia. *Boreas* **26,** 329-346.

Snyder, J. A., Macdonald, G. M., Forman, S. L., Tarasov, G. A., and Mode, W. N. (2000). Postglacial climate and vegetation history, north-central Kola Peninsula, Russia: pollen and diatom records from Lake Yarnyshnoe-3. *Boreas* **29,** 261-271.

Sollid, J. L., Anderson, S., Hamre, N., Kjeldsen, O., Salvigsen, O., Sturød, S., Tveita, T., and Wilhelmsen, A. (1973). Deglaciation of Finnmark, North Norway. *Norsk Geografisk Tidsskrift* **27,** 233-325.

Strobier, R. E., and Morse, S. A. (1994). "Crystal Identification with the Polarising Microscope." Chapman & Hall, London.

Stuiver, M., and Reimer, P. J. (1993). Extended ^{14}C Data Base and Revised CALIB 3.0 ^{14}C Age Calibration Program. *Radiocarbon* **35,** 215-230.

Stuiver, M., Reimer, P. J., Bard, E., Beck, J. W., Burr, G. S., Hughen, K. A., Kromer, B., McCormac, G., Van der Plicht, J., and Spurk, M. (1998a). INTCAL98 radiocarbon age calibration, 24,000-0 cal BP. *Radiocarbon* **40,** 1041-1083.

Stuiver, M., Reimer, P. J., and Braziunas, T. F. (1998b). High-precision radiocarbon age calibration for terrestrial and marine samples. *Radiocarbon* **40,** 1127-1151.

Sutherland, D. G. (1984). The Quaternary deposits and landforms of Scotland and the neighbouring shelves: a review. *Quaternary Science Reviews* **3,** 157-254.

Tarasov, P. E., Cheddadi, R., Guiot, J., Bottema, S., Peyron, O., Belmonte, J., Ruiz-Sanchez, V., Saadi, F., and Brewer, S. (1998). A Method to determine warm and cool steppe biomes from pollen data; application to the Mediterranean and Kazakhstan regions. *Journal of Quaternary Science* **13,** 335-344.

Taylor, K. C., Lamorey, G. W., Doyle, G. A., Alley, R. B., Grootes, P. M., Mayewski, P. A., White, J. W. C., and Barlow, L. K. (1993). The 'flickering switch' of late Pleistocene climate change. *Nature* **361,** 432-436.

Taylor, K. C., Mayewski, P. A., Alley, R. B., Brook, E. J., Gow, A. J., Grootes, P. M., Meese, D. A., Saltzman, E. S., Severinghaus, B., Twickler, M. S., White, J. W.

C., Whitlow, S., and Zielinski, G. A. (1997). The Holocene-Younger Dryas Transition Recorded at Summit, Greenland. *Science* **278,** 825-827.

Telford, R. J., Heegaard, E., and Birks, H. J. B. (2004). All age-depth models are wrong: but how badly? *Quaternary Science Reviews* **23,** 1-5.

Troels-Smith. (1955). Characterisation of Unconsolidated Sediments. *Geological Survey of Denmark IV Series* **3,** 39-71.

Turney, C. S. M. (1998). Extraction of rhyolitic component of Vedde microtephra from minerogenic lake sediments. *Journal of Palaeolimnology* **19,** 199-206.

Turney, C. S. M., Coope, G. R., Harkness, D. D., Lowe, J. J., and Walker, M. J. C. (2000). Implications for the dating of Wisconsinan (Weichselian) late- glacial events of systematic radiocarbon age differences between terrestrial plant macrofossils from a site in SW Ireland. *Quaternary Research* **53,** 114-121.

Turney, C. S. M., Harkness, D. D., and Lowe, J. J. (1997). The use of microtephra horizons to correlate Late-glacial lake sediment successions in Scotland. *Journal of Quaternary Science* **12,** 525-531.

Tutin, T. G., Burgess, N. A., Chater, A. O., Edmondson, J. R., Heywood, V. H., Moore, D. M., Valentine, D. H., Walters, S. M., Webb, D. A., and Moore, D. M. (1964-1993). "Flora Europaea." University Press, Cambridge.

Ukkonen, P., Lunkka, J. P., Junger, H., and Donner, J. (1999). New radiocarbon dates from Finnish mammoths indicating large ice-free areas in Fennoscandia during the Middle Weichselian. *Journal of Quaternary Science* **14,** 711-714.

van Geel, B., van der Plicht, J., and Renssen, H. (2003). Major Delta C-14 excursions during the late glacial and early Holocene: changes in ocean ventilation or solar forcing of climate change? *Quaternary International* **105,** 71-76.

Vandenberghe, J., Isarin, R. F. B., and Renssen, H. (2001). Rapid climatic warming: palaeo-data analysis and modeling. *Global and Planetary Change* **30,** 1-5.

Vasari, Y., and Vasari, A. (1968). Late- and Post-glacial Macrophytic Vegetation in the Lochs of Northern Scotland. *Acta Botanica Fennica* **80,** 1-120.

Von Grafenstein, U., Erlenkeuser, H., Brauer, A., Jouzel, J., and Johnsen, S. J. (1999). A mid-European decadal isotope-climate record from 15,500 to 5000 years BP. *Science* **284,** 1654-1657.

von Grafenstein, U., Erlenkeuser, H., Muller, J., Jouzel, J., and Johnsen, S. (1998). The cold event 8200 years ago documented in oxygen isotope records of precipitation in Europe and Greenland. *Climate Dynamics* **14,** 73-81.

Vorren, K.-D. (1978). Late and Middle Weichselian stratigraphy of Andøya, north Norway. *Boreas* **7,** 19 - 38.

Vorren, T. O., and Laberg, J. S. (1996). Lateglacial air temperature, oceanographic and ice sheet interactions in the southern Barents Sea region. *In* "Geological

Society Special Publication No. 111." (J. T. Andrews, W. E. N. Austin, H. Bergsten, and A. E. Jennings, Eds.). The Geological Society, London.

Vorren, T. O., and Plassen, V. (2002). Deglaciation and palaeoclimate of the Andfjord-Vågsfjord area, North Norway. *Boreas* **31,** 98-125.

Vorren, T. O., Vorren, K.-D., Alm, T., Gulliksen, S., and Løvlie, R. (1988). The last deglaciation (20,000 to 11,000 BP) on Andøya, northern Norway. *Boreas* **17,** 41-77.

Walker, M. J. C. (2001). Rapid climate change during the last glacial-interglacial transition; implications for stratigraphic subdivision, correlation and dating. *Global and Planetary Change* **30,** 59-72.

Walker, M. J. C., Ballantyne, C. K., Lowe, J. J., and Sutherland, D. G. (1988). A reinterpretation of the Late-glacial environmental history of the Isle of Skye, Inner Hebrides, Scotland. *Journal of Quaternary Science* **3,** 135-146.

Walker, M. J. C., Coope, G. R., and Lowe, J. J. (1993). The Devensian (Weichselian) Late-Glacial Paleoenvironmental Record from Gransmoor, East Yorkshire, England. *Quaternary Science Reviews* **12,** 659-680.

Walker, M. J. C., Coope, G. R., Sheldrick, C., Turney, C. S. M., Lowe, J. J., Blockley, S. P. E., and Harkness, D. D. (2003). Devensian lateglacial environmental changes in Britain: a multi-proxy environmental record from Llanilid, South Wales, UK. *Quaternary Science Reviews* **22,** 475-520.

Walker, M. J. C., and Lowe, J. J. (1990). Reconstructing the environmental history of the last glacial-interglacial transition: evidence from the Isle of Skye, Inner Hebrides, Scotland. *Quaternary Science Reviews* **9,** 15-49.

West, R. G. (2000). "Plant Life of the Quaternary Cold Stages." Cambridge University Press, Cambridge.

Whittaker, A., Cope, J. C. W., Cowie, J. W., Gibbons, W., Hailwood, E. A., House, M. R., Jenkins, D. G., Rawson, P. F., Rushton, A. W. A., Smith, D. G., Thomas, A. T., and Wimbledon, W. A. (1991). A Guide to Stratigraphical Procedure. *Journal of the Geological Society, London* **148,** 813-824.

Whittington, G., Buckland, P., Edwards, K. J., Greenwood, M., Hall, A. M., and Robinson, M. (2003). Multiproxy Devensian Late-glacial and Holocene environmental records at an Atlantic coastal site in Shetland. *Journal of Quaternary Science* **18,** 151-168.

Wohlfarth, B. (1996). The chronology of the Last Ternination: A review of radiocarbon-dated, high-resolution terrestrial stratigraphies. *Quaternary Science Reviews* **15,** 267-284.

Wohlfarth, B., Björck, S., Possnert, G., Lemdahl, G., Brunnberg, L., Ising, J., Olsson, S., and Svensson, N.-O. (1993). AMS dating Swedish varved clays of the last

glacial/interglacial transition and the potential difficulties of calibrating Late Weichselian 'absolute' chronologies. *Boreas* **22,** 113-128.

Wright, H. E. J. (1979). Cores of soft lake sediments. *Boreas* **9,** 107-114.

Zielinski, G. A., Mayewski, P. A., Meeker, L. D., Whitlow, S., and Twickler, M. S. (1996). A 110,000-yr record of explosive volcanism from the GISP2 (Greenland) ice core. *Quaternary Research* **45,** 109-118.

Zolitschka, B., and Negendank, J. F. W. (1999). High-resolution records from European Lakes. *Quaternary Science Reviews* **18,** 885-888.